Dissecting the Interactive Effects of Hypoxia and Kaposi's Sarcoma-Associated Herpesvirus on microRNA and mRNA Transcriptomes

CORALIE VIOLLET

A thesis submitted in partial fulfilment of the requirements for the degree of Doctor of Philosophy in Clinical Medicine

Trinity Term, 2015

Corpus Christi College
Nuffield Department of Clinical Medicine
University of Oxford

Permettez-moi de vous révéler le secret qui m'a conduit à atteindre mon but. Ma force repose uniquement sur ma ténacité.

Let me tell you the secret that has led me to my goal. My strength lies solely in my tenacity.

– Louis Pasteur (1822 – 1895)

Abstract

Kaposi's sarcoma-associated herpesvirus (KSHV) causes several tumours and hyperproliferative disorders. Hypoxia plays an important role in KSHV lifecycle, as hypoxia-inducible factors (HIFs) are involved in the latent/lytic switch and affect other KSHV genes, and as KSHV infection can in turn enhance cellular levels of HIFs. Two KSHV-associated tumours tend to develop in settings of relative hypoxia; Kaposi's sarcoma (KS) often occurs in the lower extremities and primary effusion lymphoma (PEL) exists in pleural effusions. A better knowledge of the pathways that regulate KSHV infection in hypoxia is therefore essential for an improved understanding of viral infection and pathogenesis. MicroRNAs (miRNAs) have been shown to play important roles in regulating the expression of genes in oncogenesis, and herpesviruses, including KSHV, encode for miRNAs.

This thesis describes a multidisciplinary approach toward understanding the mechanisms behind the hypoxia-regulated miRNA-mRNA networks in the context of KSHV infection. The question of miRNA and mRNA regulation through hypoxia, KSHV or both is addressed in this thesis by deep sequencing and gene expression assays as well as various transfection and functional assays. In chronically infected cells compared to uninfected controls, it is demonstrated that the majority of cellular miRNAs whose expression is affected are substantially down-regulated. A third of this down-regulation can be attributed to a single genomic region, 14q32 cluster, where miRNAs are lowly expressed in infected cells. In hypoxia, hsa-miR-210 is the only miRNA to be consistently up-regulated in the KSHV-infected cell lines subjected to deep sequencing in this study. Computational approaches additionally allowed for the investigation of mRNA targets. Inversely correlated miRNA-mRNA target pairs were identified and distributed into canonical pathways and biological networks.

Taken together, these results suggest that miRNAs affected by hypoxic stress and/or viral infection are implicated in the pathogenesis of KSHV-related diseases. It is expected that the outcomes of these studies will change our understanding of how KSHV uses the host RNA silencing machinery to its advantage and how this intersects with the use of the cell's response to hypoxia.

Acknowledgements

First and foremost, I would like to express my deepest appreciation to my supervisors Dr. Robert Yarchoan at the National Institutes of Health (US), Dr. Jiannis Ragoussis at McGill University (Canada), and Prof. Francesco Pezzella at the University of Oxford (UK). I will be forever grateful for their guidance, continued support, and inspiration. There have been surprisingly few difficulties conducting this project across two continents, in two different labs, with three different collaborators, and in what feels like three separate fields: KSHV, Genomics, and Hypoxia.

Furthermore, this D.Phil would not have been possible without the institutional and funding support of the Wellcome Trust and the Intramural Research Program (NIH, NCI).

During my time at Oxford, I was fortunate to work in the friendly, supportive, and stimulating environment of the Wellcome Trust Centre for Human Genetics. I am particularly thankful for the help of Jiannis Ragoussis – who suggested I apply to the Wellcome Trust fellowship – without whom this entire D.Phil would never have seen the light of day. I would also like to offer my thanks and gratitude to all members of the Ragoussis lab for patiently indulging my curiosity in RNA biology and translational research, and for their cheerful encouragement: Drs. Carme Camps, Ana Teixeira, Daniel Wong, Hani Choudhry, and Spyros Oikonomopoulos. It was in the Ragoussis lab that I

learned the art of library prep for microRNA sequencing. I would also like to thank Francesco Pezzella, my Oxford advisor, for his wisdom and support, and particularly for accepting me as his D.Phil student, after being an examiner at the Viva for my transfer of status.

On the other side of the pond, I was fully exposed to the joys of collaboration in the pursuit of great science at the HIV and AIDS Malignancy Branch (HAMB, NIH). There are so many people to whom I owe thanks for their inspiration throughout my time at the NIH. My supervisor, Robert Yarchoan, not only made this whole enterprise possible, but has also been a constant advocate of my success. I am honoured to have been his first D.Phil student and will always be indebted to him for taking me on this adventure. I am thankful for his help navigating what has proven to be a fruitful collaboration in which the tremendous resources of both labs have propelled this project. Furthermore, I would like to thank the members of the HAMB branch for their unending personal support and intellectual stimulation: M.D. Vicky Wang, Drs. Prabha Shrestha, Shewit Tekeste, Joseph Ziegelbauer, Christine Happel, and Philippe Kieffer-Kwon. Finally, I owe Dr. David Davis particular thanks not only for his expertise in KSHV biology and hypoxia, but also for his distinct sense of humour even in the face of trying circumstances. The wisdom, ethic, curiosity, clarity, and endless enthusiasm with which he approaches his work – and life in general – have changed the way I understand and practice scientific research. I am honoured and grateful to have called him my colleague and friend. Thanks for being a role model.

Moreover, NIH and Oxford would *never* have been the same without my classmates, my housemates, my lab neighbours and all-around great friends: Mama-J (Jason Murray), Pikachu (Muktha Natrajan), KP (Kristy Pluchino), Megatron (Michael Tee), and my favourite squirrel Adam Knight. Crucially, Cazzle-Dazzle (Casmir Turnquist) provided not only a raw appreciation

and enthusiasm for science but also emotional support when it was most needed. All of us have followed each other from the UK to the US and have become a small, stable family.

Then there are many more people who had nothing to do with the science per se, but everything to do with making these last few years fun, unforgettable and life-changing: my rowing coaches at the Oxford University Women's Boat Club, Christine Wilson and Natasha Townsend, for changing my outlook on life and giving me the chance to take part in the Boat Race while being a full-time D.Phil student; Christopher Beddor, for his ability to somehow make me forget I am on a timeline, for literally feeding me whenever my lab schedule would go insane, and for enriching my life every day; non-scientist James Graham, for reading the entire Introduction Chapter of this thesis in an airplane from DC to Colorado; Laure, my former piano teacher and "big sister," for always inquiring about the next time I will be in France and when my next publication is going to be; NIH Admin genius Katie Soucy, for taking care of everything and everyone on the NIH-OxCam PhD programme and for truly enjoying helping people; my Master's degree advisors, Federica Calevro and Stefano Colella, for suggesting that I do a six month-research internship at Oxford as part of my Bioengineering degree requirements, which subsequently led to my D.Phil application; and finally, Sonya Hanson, Jenny Brown, Prabha Shrestha, and Matt Jones, for letting me read their theses, and thereby helping me to understand the standards of a doctoral thesis.

The final thanks goes to my mother, Jocelyne, whose unwavering support, unconditional love, countless sacrifices, and dedication to making my life rise have truly made a tremendous difference. I am eternally grateful to her for teaching me how to love life, how to be courageous, how to be independent and strong, but also honest and caring. Thanks for being my personal hero.

Declaration

I, Coralie Viollet, hereby declare that the work on which this thesis is based is my original work and that neither the whole work nor any part of it has been, is being, or will be submitted for another degree in this or any other university. The work is original, except where listed by reference in the text.

SIGNED:…… DATE:……

Table of Contents

List of Figures

List of Tables

List of Abbreviations

AIDS	Acquired Immunodeficiency Syndrome
AGO	Argonaute
AP	Alkaline Phosphatase
ART	Antiretroviral Therapy
αR	Anti-Rat
αRt	Anti-Rabbit
αM	Anti-Mouse
BCA	Bicinchoninic Acid
BCBL	Body Cavity Based Lymphoma
BSA	Bovine Serum Albumin
bp	Base Pairs
β-actin	Beta Actin
cDNA	Complementary DNA
cel	*Caenorhabditis elegans*
CLIP	Cross-Linking Immunoprecipitation
$CoCl_2$	Cobalt Chloride
C-terminal	Carboxyl-terminal
Ctrl	Control

°C	Degrees Centigrade
DDR	DNA damage response
DGCR8	DiGeorge Syndrome Critical Region 8
DNA	Deoxyribonucleic Acid
DNase	Deoxyribonuclease
dme	*Drosophila melanogaster*
DMEM	Dulbecco's Modified Eagle Medium
DMSO	Dimethylsulfoxide
dNTP	Deoxyribonucleotide Triphosphate
dpi	Days Post Infection
dsDNA	Double Stranded DNA
EBV	Epstein-Barr Virus
ECL	Enhanced Chemiluminescence
EDTA	Ethylenediaminetetraacetic acid
EMT	Epithelial to Mesenchymal Transition
ETC	Electron Transport Chain
FBS	Foetal Bovine Serum
FC	Fold Change
FDR	False Discovery Rate
FLICE	Fas-Associated Protein with Death Domain (FADD)-Like Interleukin-1β
FOSL1	FBJ Osteosarcoma Viral (FOS)-Like Antigen 1
FPKM	Fragments Per Million Kilobase of Exon per Million Mapped Reads
gB/H/L/M/N	Glycoprotein B/H/L/M/N

GEO	Gene Expression Omnibus
GαM	Goat Anti-Mouse
GαR	Goat Anti-Rat
GαRt	Goat Anti-Rabbit
GSEA	Gene Set Enrichment Analysis
H_2O	Water
H_2O_2	Hydrogen Peroxide
HAART	Highly Active Antiretroviral Therapy
HBV	Hepatitis B Virus
HHV8	Human Herpesvirus 8
HIF	Hypoxia Inducible Factor
HIV	Human Immunodeficiency Virus
HRE	Hypoxia Response Element
HRM	Hypoxia-Regulated miRNA
HRP	Horseradish Peroxidase
hr	Hour
hrs	Hours
HVS	Herpes Virus Saimiri
hsa	*Homo Sapiens*
IFN	Interferon
IQR	Interquartile Range
IP	Immunoprecipitation
IL	Interleukin

IPA	Ingenuity Pathway Analysis
IRF	Interferon Regulatory Factor
ISCU	Iron-Sulphur Cluster Assembly Enzyme
kb	Kilobase
kbp	Kilobase Pair
KICS	KSHV Inflammation Cytokine Syndrome
KS	Kaposi's Sarcoma
KSHV	Kaposi's Sarcoma-Associated Herpesvirus
LANA	Latency Associated Nuclear Antigen
LDS	Lithium Dodecyl Sulphate
Log_2FC	Log-Transformed Fold Change
LUR	Long Unique Region
MCD	Multicentric Castleman's Disease
MCF7	Michigan Cancer Foundation-7
MHC I	Major Histocompatibility Complex Class I
miRNA	MicroRNA
miRNA-Seq	MicroRNA Sequencing
miRISC	MiRNA-Incorporated RNA-Induced Silencing Complex
miRNP	MiRNA Ribonucleoprotein Complex
mAb	Monoclonal Antibody
mg	Milligram
mL	Millilitre
MM	Multiple Myeloma

mmHg	Millimetre of mercury
MOPS	3-(N-morpholino)propanesulfonic Acid
mRNA	Messenger RNA
mRNA-Seq	Messenger RNA Sequencing
MSigDB	Molecular Signature Database
µL	Microlitre
µM	Micromolar
NaCl	Sodium Chloride
ncRNA	Non-coding RNA
ng	Nanogram
NIH	National Institutes of Health
NF-κB	Nuclear factor kappa-light-chain-enhancer of activated B cells
nM	Nanomolar
NPC	Nuclear Pore Complex
ns	Not Significant
nt	Nucleotide
NT control	No transfection control
N-terminal	Amino terminal
O_2	Oxygen
Opti-MEM	Modified Eagle's Minimum Essential Medium (Reduced Serum)
ORF	Open Reading Frame
P	*P*-value
p53	Tumour Suppressor Protein with Apparent Molecular Mass of 53 kiloDaltons

pAb	Polyclonal Antibody
piRNA	Piwi Interacting RNA
PAGE	Polyacrylamide Gel Electrophoresis
PBS	Phosphate Buffered Saline
PEL	Primary Effusion Lymphoma
PCR	Polymerase Chain Reaction
pmol	Picomole
Poly(A)	Polyadenylate
Pre-miRNA	Precursor microRNA
Pri-miRNA	Primary transcript MicroRNA
pVHL	Von Hippel-Lindau protein
qPCR	Quantitative Real-Time Polymerase Chain Reaction
qRT-PCR	Quantitative Reverse Transcription Polymerase Chain Reaction
rasiRNA	Repeat-Associated Small Interfering RNA
RISC	RNA-Induced Silencing Complex
RIPA	Radioimmunoprecipitation Assay
RNA	Ribonucleic Acid
RNA-Seq	RNA Sequencing
RNAi	RNA interference
RNase	Ribonuclease
ROS	Reactive Oxygen Species
RPM	Revolutions Per Minute
RPMI	Roswell Park Memorial Institute formulation 1640 medium

rRNA	Ribosomal RNA
RT	Reverse Transcription
RTA	Replication and Transcription Activator
scnRNA	Small Scan RNA
SDS	Sodium Dodecyl Sulphate
sec	Seconds
shRNA	Short Hairpin RNA
siRNA	Small Interfering RNA
snoRNA	Small Nucleolar RNA
TBS	Tris-Buffered Saline
TBST	Tris-Buffered Saline plus Tween-20
TR	Terminal Repeat
tRNA	Transfer RNA
UTR	Untranslated Region
UV	Ultraviolet
V	Volt
vs.	Versus
v-cyclin	Viral Cyclin (KSHV homolog of cellular cyclin D protein)
VEGF	Vascular Endothelial Growth Factor
v-FLIP	Viral FLICE inhibitory protein
v-GPCR	Viral G protein couple receptor
v-IRF	Viral Interferon Regulatory Factor
v-IL-6	Viral Interleukin 6

1

Introduction

FIRST stated by Francis Crick in 1956, the central dogma of molecular biology is known as "DNA makes RNA, and RNA makes protein". Without those three essential macromolecules, no living organisms can exist. Since then, the scientific understanding of this flow of genetic information, from DNA through RNA to protein, has made significant progress. Initially, RNA was believed to play three major roles – as a "DNA photocopy" (messenger RNA, or mRNA), as an adaptor molecule between the genetic code and the amino acids of a protein (transfer RNA, or tRNA), and as a structural component of the ribosome (ribosomal RNA, or rRNA). However, RNA was subsequently found to encompass numerous other dimensions. Like DNA, RNA can carry genetic information (RNA viruses). Like enzymes, RNA can catalyze biochemical reactions (ribozymes). Last but not least, like repressor factors, RNA can regulate protein synthesis (RNA interference, or RNAi).

This thesis focuses on a new family of RNAi molecules called microRNAs (miRNAs), which are important negative regulators of eukaryotic gene expression, and their role in

Kaposi's sarcoma-associated herpesvirus (KSHV) pathobiology. In order to put this thesis into context, this chapter covers (1) a review of the key aspects of miRNA biology (2) the background of the cellular understanding of oxygen deprivation (hypoxia), and finally (3) the historical and contemporary studies of KSHV pathogenesis. The chapter then concludes with an overview of the main aims of this thesis.

1.1 MicroRNAs

While microRNAs, abbreviated miRNAs, are one of the more recently discovered RNAs, the understanding of their biogenesis, their regulatory mechanisms, their role in biological processes and human diseases has rapidly evolved due to an efficient combination of high-throughput approaches for miRNA expression analysis and computational bioinformatics methods for miRNA target gene prediction.

1.1.1 Discovery

Found in plants, animals and some viruses, miRNAs are an abundant class of endogenous 18-25 nucleotide (nt) long non-coding RNA molecules that regulate the expression of multiple protein-coding genes. The first miRNA, cel-lin-4, was described in *Caenorhabditis elegans* two decades ago by Victor Ambros and his colleagues (Lee et al. 1993) who discovered that a small RNA had an antisense complementarity to a target mRNA gene involved in larval developmental. Seven years later, the Ruvkun lab reported the discovery of another *C. elegans* miRNA, let-7, that could also silence gene expression post-transcriptionally via base-pairing (Reinhart et al. 2000). Interestingly, let-7 was found to be conserved in many species, including vertebrates (Pasquinelli et al. 2000). Together, these discoveries prompted the scientific community to explore the world of RNA interference, and more specifically, small RNA regulation. There are now

over 2500 mature miRNAs registered in the latest miRNA database miRBase (Version 21, http://www.mirbase.org/) for *Homo sapiens* alone.

1.1.2 Nomenclature

The miRNA nomenclature follows the subsequent rules: (1) a three to four letter prefix is usually assigned to a miRNA to identify its species. For example, cel-miR (cel for *Caenorhabditis elegans*) or hsa-miR (hsa for *Homo sapiens*); (2) when discovered, miRNAs are given a numerical identifier. For example, if the last miRNA discovered is named miR-209, then the next will be named miR-210; (3) in a given organism, miRNA isoforms (isomiRs) with just one or two base difference are given an additional letter to their common numerical suffix (e.g. hsa-miR-210a and hsa-miR-210b in human); (4) if a given miRNA sequence is present in different species, miRNAs are given the same numerical suffix (e.g. hsa-miR-101 and cel-miR-101 for *Homo sapiens* and *C. elegans* respectively); (5) in a given organism, if the same miRNA is encoded by several genes, an additional numerical suffix is added to differentiate their origins (e.g. dme-miR-281-1 and dme-miR-281-2 for *Drosophila melanogaster).*

1.1.3 Classification

MiRNAs, together with small interfering RNAs (siRNAs), Piwi interacting RNAs (piRNAs), repeat-associated small interfering RNAs (rasiRNAs), and small scan RNAs (scnRNAs) are part of a class of RNAs called small non-coding RNAs (small ncRNAs), with a length of up to 30 nucleotides (nt). The list of small ncRNAs is expanding quickly. There are also medium-size ncRNAs (30nt to 200nt) and long ncRNAs (up to 100kb), as shown in **Table 1.1**. Small nuclear RNAs (snRNA), small nucleolar RNAs (snoRNAs) and guide RNAs (gRNAs) are all part of the family of medium-size

ncRNAs, whereas *Xist* and *Tsix* (an antisense regulator of *Xist*) are examples of long ncRNAs (Choudhuri 2010).

1.1.4 Canonical miRNA biogenesis

The genes encoding miRNAs reside in regions of the genome as distinct transcriptional units as well as in clusters of polycistronic units, carrying the information of several miRNAs. Approximately 60% of miRNAs are expressed independently, 15% are expressed in clusters, and 25% are in introns. Most of the miRNA genes are present in areas of the genome associated with known genes (Lagos-Quintana et al. 2001; Lau et al. 2001). The excision and the activation of single-stranded mature miRNAs from precursor transcripts occur through a multiple-step process that is detailed below and depicted in **Figure 1.1.**

- Transcription of miRNA genes:

The genes encoding miRNAs are transcribed by RNA Polymerase II, generating long primary transcripts called pri-miRNAs. Pri-miRNAs include 5' caps and 3' poly(A) tails. Within the primary transcript, the miRNA-encoding portion forms an imperfect stem-loop hairpin structure.

Non-coding RNAs		
Small ncRNAs (~20 - 30nt)	Medium-size ncRNAs (30nt – 200nt)	Long ncRNAs (>200nt and <100kb)
miRNA, siRNA, piRNA, rasiRNA, scnRNA	snRNA, snoRNA, gRNA	*Xist*, *Tsix*

Table 1.1: Non-coding RNA classification.

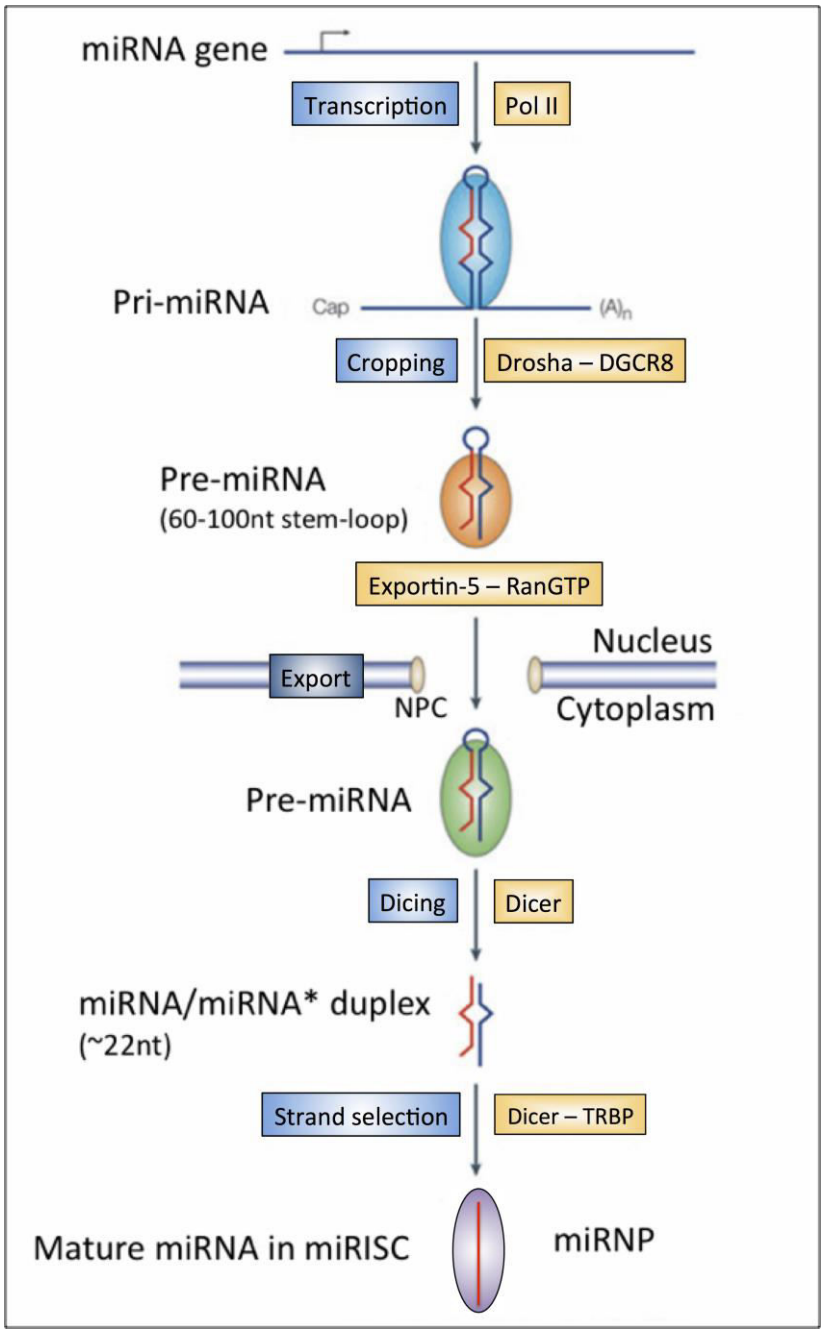

Figure 1.1: MicroRNA biogenesis and activity. NPC: Nuclear pore complex, miRNP: miRNA ribonucleoprotein complex, and miRISC: miRNA-incorporated RNA-induced silencing complex. Image adapted with permission from Kim (2005)**.**

- Hairpin release in the nucleus ('cropping'):

The microprocessor complex composed of the ribonuclease type III enzyme Drosha and the RNA binding protein, DiGeorge syndrome critical region 8 (DGCR8), processes the long primary transcript (pri-miRNA), yielding a hairpin precursor (pre-miRNA) consisting of approximately 70nt (**Figures 1.1** and **1.2**).

- Pre-miRNA export to the cytoplasm:

Exportin-5 (Exp5 or Xpo-5) together with its cofactor Ran (the GTP-bound form) is responsible for the export of pre-miRNA from the nucleus to the cytoplasm.

- Dicer processing ('dicing'):

Once in the cytoplasm, a protein complex containing the Dicer type III RNase that cleaves the miRNA to its mature size further processes the pre-miRNA. The resulting miRNA duplex (miRNA/miRNA*) is composed of two strands, one of which will be the mature miRNA. The other strand, called the passenger strand due to its lower levels in the steady state, is denoted with an asterisk (*) and is usually degraded. In some cases, both strands of the duplex are viable and become functional miRNAs that target different mRNA populations. Dicer processing, or 'dicing', of the pre-miRNA is thought to be coupled with unwinding of this duplex.

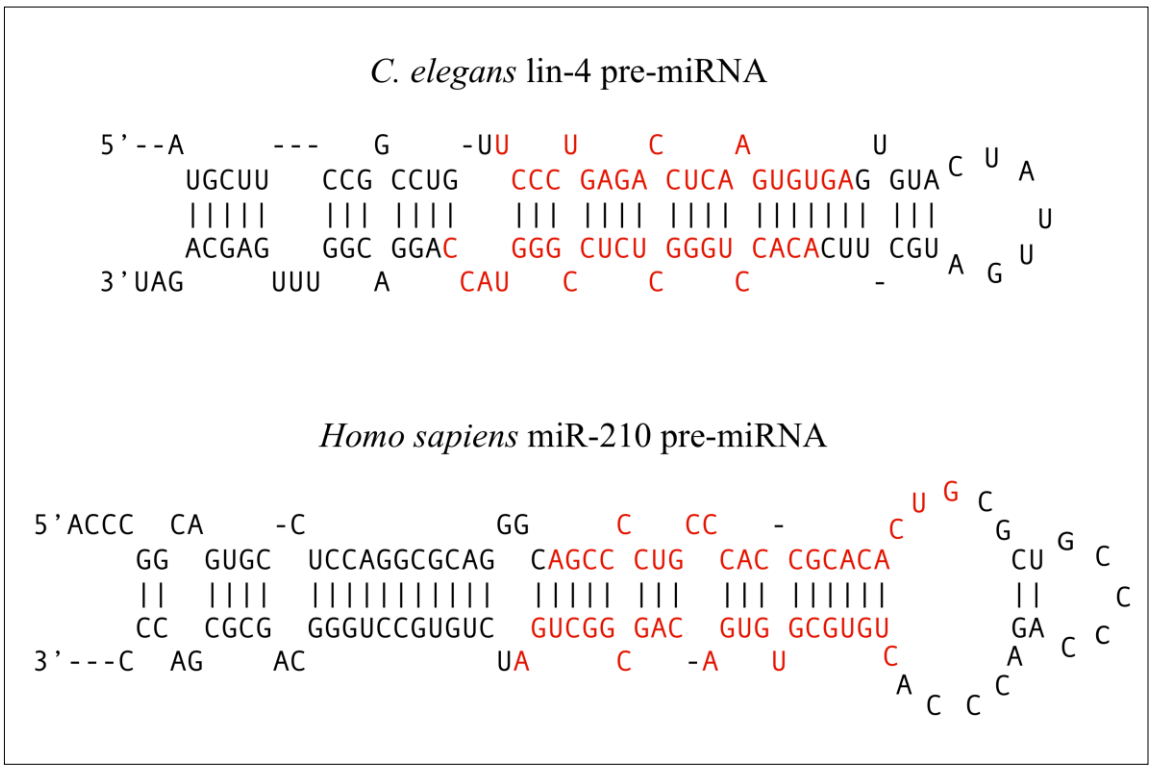

Figure 1.2: Pre-miRNA secondary structures. This illustrates examples of miRNA stem-loops. The mature miRNAs are indicated in red with cel-lin-4-5p at the top and cel-lin-4-3p at the bottom; and hsa-miR-210-3p at the top and hsa-miR-210-5p at the bottom.

- Selection of the active strand by RISC:

Generally, only one strand is incorporated into a final protein complex called RISC (RNA-induced silencing complex), which contains an Argonaute (AGO) family protein (Argonaute 2 for instance in mammals) and many other associated proteins such as the trans-activation response RNA-binding protein, TRBP (Chendrimada et al. 2005). RISC is also referred to as miRNP (microRNA ribonucleoprotein complex) and when a miRNA is incorporated, it may be called "miRISC" (**Figure 1.1**). The selection of the active miRNA strand over its miRNA* counterpart depends on the thermodynamic instability of the miRNA/miRNA* duplex. Several proteins including DICER, AGO,

TRBP and protein-activator of dsRNA-dependent protein kinase (PACT) can sense weaker base-pairing at the 5' terminus relative to the other strand. The strand with the most favourable thermodynamic features will be selected to become the guide strand (Meijer et al. 2014). The position of the stem-loop may also influence strand choice.

1.1.5 Mechanisms of miRNA interference: degradation or translation arrest

MiRNAs bind target sites within the mRNA target sequence. Target sites on mRNA typically contain seven nucleotides and are mostly located in their 3' untranslated regions (UTRs); but target sites have also been found in the coding region or 5' UTR of mRNAs. mRNA target sites match a key feature of recognition within the miRNA called seed region (miRNA nucleotides 2 to 8). The miRNA-mRNA binding involves Watson-Crick base pairing. A single miRNA may have multiple target sites within a single mRNA and may target several mRNAs (up to a few hundred). Therefore, miRNAs regulate a large proportion of mammalian genes.

Once a miRNA binds to its target mRNA sequence, the degree of complementarity between the miRNA and the target mRNA sequence generally determines the fate of the target mRNA – either mRNA decay or translation regulation will be involved, depending on perfect or imperfect base-pairing, respectively. Once incorporated into a RISC, the single-stranded miRNA is poised to regulate the targeted genes by degrading the mRNA transcripts through direct cleavage or by inhibiting protein synthesis. Most plant miRNAs have 100% homology (~20nt) to the mRNA; in this case, the latter is usually directly degraded. By contrast, most animal miRNAs bind with an imperfect homology that typically results in repressing the mRNA translation into a protein.

The detailed mechanisms by which miRNAs regulate translation remain unclear. Regulation may occur either at the translation initiation, at the post-initiation step, or at

both simultaneously (**Figure 1.3**). At the beginning of translation initiation, the elF4F complex recognises the mRNA 5' terminal cap and recruits the 40S ribosomal subunit. elF4F also circularises the mRNA by binding to poly(A)-binding protein 1 (PABP1), a protein associated with the poly(A) tail at the 3' end of the mRNA. The 60S ribosomal subunit is then recruited by elF6 and the elongation may begin at AUG codon of the 5' end (top, **Figure 1.3**).

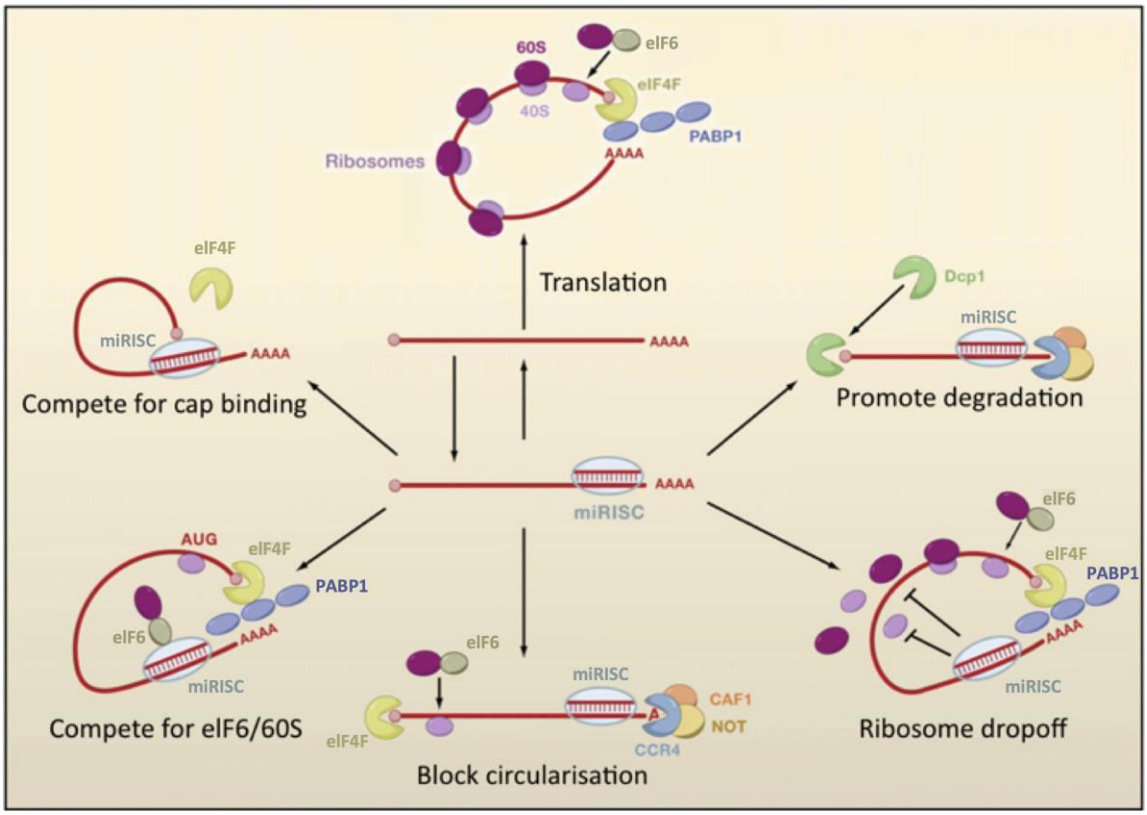

Figure 1.3: Possible mechanisms of miRNA target regulation. Image adapted with permission from Carthew & Sontheimer (2009).

Messenger RNAs that are not repressed recruit initiation factors and ribosomes to form circular structures in order to enhance their own translation. However, when under miRNA repression, mRNAs are inhibited via a variety of biological processes including deadenylation and decapping. miRNA-mediated deadenylation is orchestrated by the CCR4-NOT complex which consists of the proteins CCR4, CAF1 and NOT1 to NOT5. Deadenylation blocks mRNA circularisation and ultimately leads to translational repression. Decapping may occur after deadenylation and involves the eukaryote mRNA decapping protein DCP1, which then promotes mRNA degradation (Behm-Ansmant et al. 2006).

There are different models explaining the overall mechanisms of miRISC-mediated repression (**Figure 1.3**). First, miRISC may act at the initiation level and compete for the mRNA 5' terminal cap to prevent elF4F binding (upper left, **Figure 1.3**). Second, miRISC may prevent the assembly of the two ribosomal subunits by recruiting elF6 (lower left). Third, miRISC may initiate linearization and promote mRNA degradation by inducing deadenylation followed by decapping (bottom and upper right, **Figure 1.3**, respectively). Finally, miRISC may trigger the ribosome drop off after the subunit assembly (lower right, **Figure 1.3**).

A better understanding of the complex gene-silencing mechanisms of miRNA interference has offered insightful guidance for the development of powerful bioinformatic pipelines able to predict miRNA targets as well as new protocols to isolate miRNAs and mRNA targets from miRNPs such as Argonaute co-immunoprecipitation (AGO co-IP).

1.1.6 Cellular functions

The primary function of miRNAs in cells appears to be in gene regulation. There is an ongoing debate about the relative role of miRNAs as compared to transcriptional factors. By virtue of interfering with multiple transcripts, often hundreds, miRNAs have the potential to regulate all cellular mechanisms. Research suggests that as many as one-third of all human genes may be regulated by miRNAs (Lim et al. 2003).

Most miRNAs that have been studied in animals reduce steady state protein levels for the targeted mRNAs. Powerful regulators of gene expression, miRNAs play a role in a range of cellular processes from stem cell differentiation to tumourigenesis and host-pathogen interactions. Evidence has been provided that miRNAs are key regulators in processes such as early development (Reinhart et al. 2000), cell proliferation, cell death, apoptosis, fat metabolism (Brennecke et al. 2003), and cell differentiation (Chen et al. 2004). As such, miRNAs have been linked to a number of diseases including cancer, neurodevelopment diseases and viral infections.

1.1.7 Carcinogenesis and miRNAs

When human miRNAs were initially discovered, it was noted that many were located at fragile sites in the genome or in regions that are commonly amplified or deleted in human cancer, such as chromosome 11 (Calin et al. 2004). Since then, the dysregulation of miRNAs has been shown to frequently be associated with cancer and other complex genetic diseases. Malignant tumours and tumour cell lines were found to have unique widespread dysregulated miRNA expression compared to normal tissues (Lu et al. 2005), suggesting that changes in miRNA expression profiles contribute to tumour formation and that miRNA profiling could help diagnose human cancers. Kumar et al. (2007) also showed that global miRNA loss contributes to tumourgenesis. Endogenous

miRNAs are implicated in diverse fundamental biological processes such as development, cell proliferation, differentiation and apoptosis (Bartel et al. 2004). Accordingly, altered miRNA expression plausibly contributes to human disease, including cancer. The implication of miRNAs in diseases is today supported by evidence from research conducted by human geneticists, biochemists and clinicians. Some bioinformaticians even claim that more than 60% of human protein-coding genes are regulated by miRNAs (Friedman et al. 2009).

A global decrease in miRNA levels has been observed in human cancers, indicating that small RNAs may have an intrinsic function in tumour proliferation. For example, hsa-miR-145, which is down-regulated in lung cancer, targets c-Myc, a strong proto-oncogene (Chen et al. 2010). Additionally, it has been shown that hsa-miR-145 also targets both EGFR (epidermal growth factor receptor) and NUDT1 (nucleoside diphosphate linked moiety X-type motif 1), which promote cell proliferation (Cho et al. 2011). Similarly, Jian et al. (2011) show that several miRNAs (miR-663, miR-107, miR-223) are down-regulated in acute myeloid leukaemia (AML).

However, not all miRNAs are down-regulated in cancer. Some miRNAs promote the development of cancer and those are often up-regulated in cancers and cancer cell lines. For instance, hsa-miR-21 is over-expressed in most tumour types and targets tumour suppressor PDCD4 protein (Programmed Cell Death 4). miR-21 also targets PTEN (Phosphatase and Tension homolog) and reversion-inducing-cystein-rich protein with Kazal motifs (RECK), which contribute to cell growth arrest and metastasis inhibition respectively (Frankel et al. 2008).

Typically, miRNAs targeting tumour suppressor genes function as oncogenes and are called oncogenic miRNAs or oncomiRs. Conversely, miRNAs targeting oncogenes are

typically repressed in cancer. They can be classified as tumour suppressor miRNAs because their induction negatively regulates genes promoting the development of cancer (O'Hara et al. 2009). They may turn out to be potential leads for cancer therapy. It has been generally observed that the development of cancer is associated with either a down-regulation of tumour suppressor miRNAs and/or an up-regulation of oncomiRs, as seen in **Table 1.2**.

1.2 Hypoxia

While gene regulation mechanisms by miRNAs have been well-documented for years, relatively little is known about external factors influencing these important non-coding RNAs. One of the first breakthroughs was reported in 2007 when hypoxia, a microenvironmental factor typical of solid tumours, was shown to affect miRNA expression (Kulshreshtha et al. 2007). This state of widespread low-level oxygenation and its involvements with cancer and miRNAs are described hereafter.

	miRNAs		**miRNA target genes**	
	OncomiRs	Tumour-suppressive miRNAs	OncomiR targets: tumour suppressor genes (cell differentiation, pro-apoptosis…)	Targets of tumour-suppressive miRNAs: oncogenes (cell growth, anti-apoptosis…)
Cancer	↑	↓	↓	↑
Therapy	-	+	+	-

Table 1.2: Example of miRNA regulation in cancer and anti-cancer therapies. Anti-cancer treatments aim at either inhibiting oncomiRs (-) or introducing tumour suppressor miRNAs (+). ↑, up-regulated ; ↓, down-regulated.

1.2.1 Hypoxic response: HIF pathway

Hypoxia describes the state in which the oxygen supply is insufficient. Unusually low oxygen concentrations may affect the whole body (generalised hypoxia), or a region of the body (tissue hypoxia). Generalised hypoxia typically occurs in individuals that climb at high altitude where oxygen becomes scarce. It causes altitude sickness and can potentially lead to fatal complications such as high altitude pulmonary oedema (HAPE) or high altitude cerebral oedema (HACE). Generalised hypoxia can also result from lung disease or anaemia. Tissue hypoxia, on the other hand, occurs locally in the extremities of the body but also during cancer, vascular diseases and pulmonary disorders (Ubbink et al. 1997). In order to cope with this reduction in oxygen tension and create better oxygenation, healthy tissue induces a cascade of molecular and physiological responses including angiogenesis (a process involving growth of new blood vessels from pre-existing vessels), erythropoiesis (a process by which red blood cells are produced), and vascular cellular proliferation (Höckel & Vaupel 2001). When the latter mechanisms to restore normal oxygenation are insufficient, severe or prolonged tissue hypoxia occurs, which ultimately leads to cell death.

At the cellular level, cells respond to fluctuations in oxygen concentration primarily through transcription factors called hypoxia-inducible factors (HIFs). There are two primary players in the HIF pathway, HIF-1 and HIF-2, each a heterodimer composed of an alpha and a beta subunit. These proteins are constantly produced, regardless of oxygen concentration. However, their degradation or accumulation, as well as the suppression or expression of their target genes, are directly correlated with the presence or the absence of oxygen, respectively.

Under normoxia (normal oxygen concentration), HIF-1α undergoes post-translational hydroxylation of two proline residues leading to its rapid degradation by the ubiquitin-proteasome complex (Semenza 2010). Although HIF is constantly produced in the presence of oxygen, it is degraded post-translationally, preventing it from entering the nucleus and triggering the enhanced transcription of its target genes (**Figure 1.4**). Under hypoxia, these cellular degradation mechanisms are suppressed, thereby inducing HIF-1α accumulation in the nucleus. There, HIF-1α dimerises with HIF-1β and binds hypoxic response elements (HREs) that are typically located within the promoter region of genes coding for proteins such as pro-angiogenic growth factor vascular endothelial growth factor (VEGF), erythropoietin (EPO) and glycolytic enzymes (Harris 2002) (**Figure 1.4**). Hence cells under hypoxia promote the expansion of the vascular system, the formation of blood vessels, the switch to an oxygen-independent metabolic pathway (anaerobic glycolysis), and other changes, in order to cope with a lack of oxygen.

Interestingly, the ability to not only adapt but even to benefit from this limit in oxygen diffusion is one of the fundamental characteristics of tumour cells. In fact, it was shown that hypoxia-inducible genes not only mediate the adaptation and behaviour of normal tissues but also help the growth and survival of cancer cells (Pocock 2011). Because hypoxia-inducible genes regulate several biological processes mentioned above, targeting their transcription factor, HIF, represents a potentially new therapeutic strategy to treat cancer.

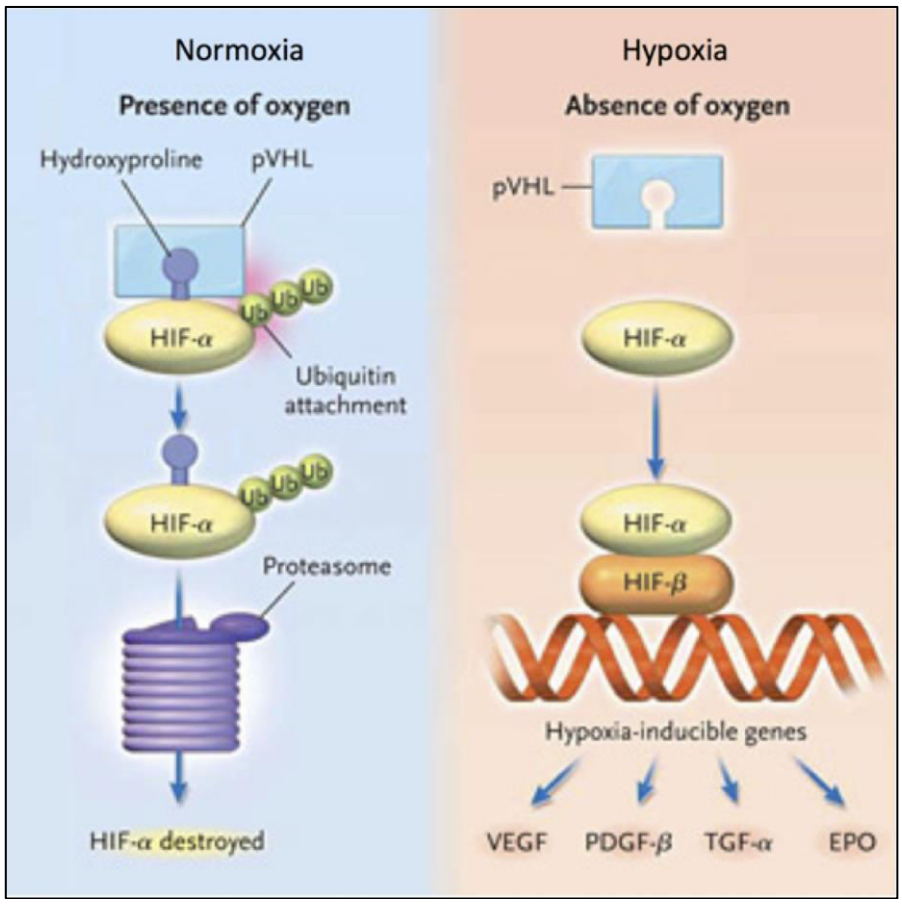

Figure 1.4: Representation of HIF regulation under hypoxic and normoxic conditions. In normoxia, hydroxylation at two proline residues promotes HIF-α association with the von Hippel-Lindau protein (pVHL). This triggers the degradation of HIF via ubiquitin/proteasome pathways. In hypoxia, these processes are suppressed, allowing HIF-α to escape proteolysis, dimerise with HIF-1β, recruit coactivators, and activate transcription via HREs. Platelet-derived growth factor beta (PDGF-β) regulates division and cell growth, while transformation growth factors (TGF-α) control proliferation and cell differentiation. Image adapted with permission from George & Kaelin (2003).

1.2.2 Hypoxia and cancer

Eukaryotic cells depend on a constant supply of oxygen to synthesise energy-rich adenosine triphosphate (ATP) molecules needed for nearly every aspect of normal cellular function. However, many pathological conditions including cardiovascular disease, stroke, and cancer, are associated with depletion of oxygen availability to cells (Simmons 2009).

Tumour hypoxia, for example, occurs when cells proliferate and grow at such a high rate that they starve themselves of oxygen. Whereas normal vasculature is structured with vessels that are organised in a way that ensures adequate oxygen supply, tumour vessels are chaotic, dilated and tortuous (**Figure 1.5**). Therefore, solid tumours contain regions of hypoxia, often surrounding areas of necrosis, because their vasculature cannot adequately supply oxygen and nutrients to all the cells (Höckel & Vaupel 2001). Blood supply in cancer tissues becomes insufficient, leaving regions of the tumour where the oxygen concentration is significantly lower than in healthy tissues. It was observed that oxygen tension in hypoxic tumour areas can be as low as 0mmHg with a mean of 10mmHg, which corresponds to 1.5% of oxygen. In normoxic tissue, oxygen tension varies between 20 and 100mmHg with a mean of 50mmHg, which corresponds to 7% of oxygen (Gabalski et al. 1998).

Tumour hypoxia is therefore an inherent ‘by-product’ of solid tumours. Although hypoxia is a source of stress for both cancer and normal cells, cancer cells often undergo advantageous genetic and adaptive changes that allow them to survive and even proliferate under hypoxic conditions (J Martin Brown & Giaccia 1998). These adaptive processes include variations in cell division, survival, motility, or differentiation. In fact, cancer cells adapt so well to hypoxic stress compared to normal cells that they can show

an increase in tumour angiogenesis, vasculogenesis, metastasis, and genome instability (Liao & Johnson 2007; Kioi et al. 2010; Chang et al. 2011; J Martin Brown & Giaccia 1998; Höckel & Vaupel 2001). Additionally, hypoxic tumour cells exhibit both a decrease in immune reactivity and a resistance to cell death (Yotnda et al. 2010; Erler et al. 2004). Consequently, tumour hypoxia is related to a poorer prognosis in cancer (Harris 2002).

Hypoxia leads to both radiotherapy and chemotherapy resistance via different biological mechanisms. Radioresistance of hypoxic cells is mediated by HIF-1, which has been shown to promote cell survival and regulate vascular radiosensitivity in tumours (Semenza 2004; Moeller et al. 2004). Chemotherapy resistance, on the other hand, is directly due to the nature of a hypoxic tumour (Shannon et al. 2003). Anti-cancer drugs cannot easily reach the site of action due to its tortuous vasculature (**Figure 1.5**).

Remarkably, even in the presence of oxygen, cancer cells maintain anaerobic glycolysis, using glucose to produce lactate instead of pyruvate in aerobic glycolysis. This is known as the Warburg effect, where lactic acid fermentation is used to produce energy, rather than oxidative breakdown of pyruvate (Warburg 1956).

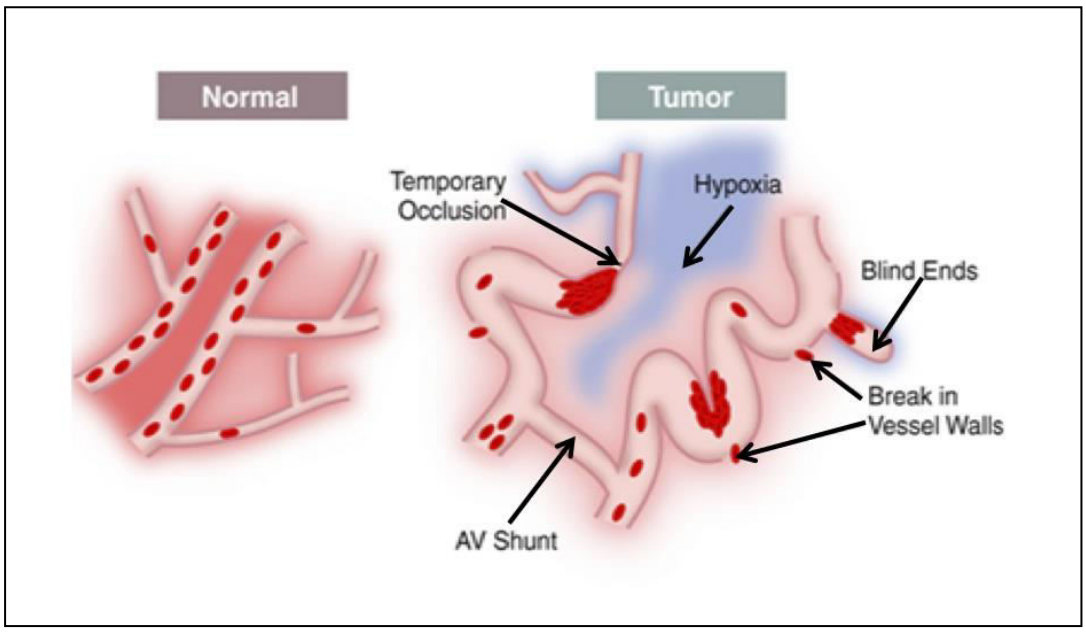

Figure 1.5: Tumour physiology under hypoxia versus normoxia. A tumour clearly lacks the network of blood vessels needed to maintain homogenous oxygen levels throughout the tissue. Image adapted with permission from J M Brown & Giaccia (1998).

1.2.3 Hypoxia-regulated miRNAs

Hypoxia is known to cause changes in the expression of a number of mRNAs, and there is recent evidence that it can also affect miRNAs. Indeed, miRNAs can be induced by hypoxic stress in various cells or cell lines, either through HIF-dependent mechanisms or through other hypoxic pathways. The induction of hypoxia-regulated miRNAs (HRMs) in turn affects target protein levels to 'fine-tune' the hypoxic gene expression pattern (Gorospe et al. 2011). Certain HRMs such as hsa-miR-155, hsa-miR-210 and hsa-miR-373 have enhancer HREs in their promoter region where HIF-1 can bind (Crosby et al. 2009; Kulshreshtha et al. 2007; Bruning et al. 2011). Also, some HRMs can be induced by other hypoxia-response transcription factors. For example hsa-miR-21, a frequently

up-regulated oncomiRs in cancer, is up-regulated by hypoxia-inducible activation protein 1 (AP-1; Fujita et al. 2008) and has been shown to have anti-apoptotic properties in hypoxia (Cheng et al. 2010). On the other hand, certain HRMs such as miR-20b and miR-200b, are down-regulated by hypoxia to enhance the angiogenic response (Cascio et al. 2010; Chan et al. 2011). HRM target genes have been shown to be involved in a number of cellular processes such as apoptosis, invasion, metastasis, glycolysis, and cell migration. Interestingly, a high proportion of hypoxia-regulated miRNAs are associated with cancer (i.e. miR-21). Therefore, matching the changes in target mRNAs in hypoxic cancer to changes in miRNAs may help delineate which miRNAs are cancer-promoting. Also, the inactivation of such hypoxia-induced oncomiRs may represent an encouraging therapeutic strategy for the treatment of some forms of cancer.

One of the only miRNAs consistently up-regulated under hypoxia in a wide variety of human cell lines is miR-210, also known as the "master" miRNA hypoxic marker (Chan et al. 2012). In breast cancer cells, for instance, Camps et al. (2008) reported that hypoxia results in an increased production of miR-210. This over-expression of miR-210 was strongly associated with poor prognosis in breast cancer. It was also shown that miR-210 contains an HRE allowing HIF binding and is therefore a direct downstream target of HIF-1α (Kulshreshtha et al. 2007).

To date, nine miR-210 target genes have been validated experimentally in the literature. They are involved in cellular processes such as apoptosis, angiogenesis inhibition, stem cell biology, cell cycle regulation, DNA damage response (DDR), mitochondrial metabolism and tumour growth inhibition (Huang et al. 2010). Using a combined approach of bioinformatics tools and experimental checks, it was reported that the iron-sulphur cluster scaffold homolog (ISCU) is a miR-210 target and is significantly down-regulated in hypoxic conditions with respect to normoxia. miR-210 binds to the 3' UTR

of the ISCU transcript leading to a decrease in mRNA levels (Favaro et al. 2010; Chan et al. 2009). ISCU is needed to assemble critical components of enzymes that are important for a range of functions in the cell, including energy oxygen-dependent energy production and mitochondrial respiration. It is an important factor of the mitochondrial electron transport chain (ETC) (Tong & Rouault 2006). This metabolic shift between mitochondrial ETC and glycolysis is characteristic of hypoxic cells, as they need to develop ways to produce adenosine triphosphate (ATP) without oxygen. Repressing mitochondrial biogenesis via ISCU is therefore part of the hypoxia-induced miR-210 pathway. Consequently, down-regulation of ISCU by miR-210 is likely to contribute to the tumour cell survival under hypoxic conditions.

Moreover, miR-210 was reported to target the ligand for ephrin-related receptor tyrosine kinase Ephrin-A3 (EFNA3) which plays a role in endothelial cell apoptosis (Fasanaro et al. 2008). Because miR-210 effects range from induction of angiogenesis, cell proliferation, and cancer metastasis, to inhibition of apoptosis and DDR, it is no surprise that its suppression correlates with increased radiosensitivity of hypoxic cancer cells (Yang et al. 2012).

1.3 Kaposi's sarcoma-associated herpesvirus

Kaposi's sarcoma-associated herpesvirus (KSHV) is a tumour virus responsible for several cancers including Kaposi's sarcoma (KS) and primary effusion lymphoma (PEL), both of which tend to develop in settings of relative hypoxia. Moreover, KSHV can modulate cellular HIF and miRNA levels, and it encodes its own set of viral miRNAs. While the previous sections provided an overview of our current understanding of miRNAs and hypoxia, and highlighted how those two entities overlapped, this section focuses on the putative roles of both miRNAs and hypoxia in KSHV biology.

1.3.1 A short history of KSHV biology and oncogenicity

Discovered in 1994 (Chang et al. 1994), KSHV was originally isolated from KS lesions in an AIDS patient. Also known as human herpesvirus 8 (HHV8), it is one of seven known human oncoviruses. Together with Epstein-Barr Virus (EBV), KSHV is part of the γ-herpesvirus family. Specifically, it is a member of the γ2-lymphotropic oncogenic herpesviruses, while EBV belongs to the γ-1 lineage. Its 165kb-long genome shows homologies to both EBV and Herpes virus Saimiri (HVS), another γ2-herpesvirus.

EBV, KSHV's closest human relative, is known to infect the majority (>90%) of the world's population (Thompson & Kurzrock 2004). However, unlike most herpesviruses such as EBV, the seroprevalence of KSHV infection is not as high and varies considerably among countries. While KSHV overall seroprevalence is less than 10% in the United States, northern Europe and Asia, seroprevalence rates increase to more than 40% in many sub-Saharan African countries and Peru (Mesri et al. 2010) (**Figure 1.6**). Therefore, sub-Saharan Africa is a major endemic region for KSHV infection. KSHV

infection is more common in men than in women and some experts think this might be related to hormones. There is a genetic predisposition for certain populations such as Mediterranean males and certain areas of Italy, as well as an increased risk in some African populations regardless of HIV status.

KSHV is a necessary, albeit not sufficient, causative agent of KS and two B-cell tumours, PEL and a type of multicentric Castleman's disease (MCD) (Greene et al. 2007). In addition, KSHV infection has recently been associated with an inflammatory symptom complex called KSHV inflammation cytokine syndrome (KICS), which is characterised by an increase in cytokine production (Uldrick et al. 2010). Interestingly, these KSHV-associated diseases often occur in immunocompromised patients, such as HIV-infected individuals or organ transplant patients.

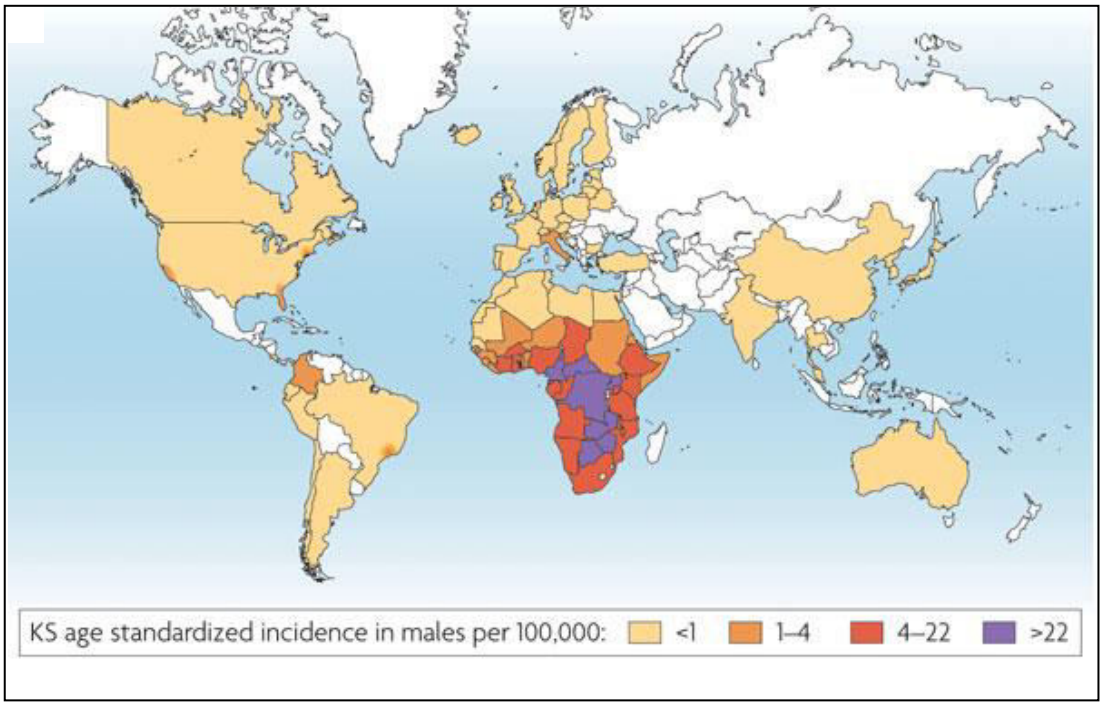

Figure 1.6: Seroprevalence of KSHV. This map represents data derived from the International Agency for Research on Cancer and is adapted with permission from Mesri et al. (2010).

At the onset of the AIDS epidemic in the 1980s, KS, a hypervascular endothelial tumour, was the most common HIV-associated malignancy and it became the fourth most common cancer caused by an infectious agent worldwide (Beral et al. 1990). The epidemiological data for the incidence of KS generally mirrors those of KSHV seroprevalence, shown in **Figure 1.6**, suggesting a strong correlation between viral infection and the development of KS lesions. The contribution of KSHV to the development of KS is supported by strong evidence including the clinical observations that virtually all cases of KS are KSHV positive (Chang et al. 1994; Schulz 1999). Furthermore, KSHV DNA is detectable in peripheral blood mononuclear cells of homosexual men prior to the development of KS (Engels et al. 2003) and antibodies to KSHV antigens can be detected in AIDS patients prior to the KS diagnosis (Davis et al. 1997).

There are four epidemiologic subtypes of KS– classical KS, endemic KS, iatrogenic KS and epidemic KS (Antman & Chang 2000). All of them exhibit the same characteristic purple, brown, red nodules on the skin, oral cavities and/or internal organs such as the gastrointestinal tract, lungs, liver, lymph nodes, etc. If disseminated, KS may become life-threatening. The classical KS subtype affects predominantly older men of Mediterranean, Eastern European, and Middle Eastern descent. Endemic KS, sometimes called African KS, mainly occurs in people from Equatorial Africa. Iatrogenic KS may follow organ transplant surgery in patients on immunosuppressive therapy. Finally, epidemic or AIDS-related KS refers to the KS found in AIDS patients. It is the most common type of KS in the United States and the most frequently reported cancer in many African countries (e.g. Zimbabwe), in part because of the high HIV occurrence and the lack of access to antiretroviral therapy (ART). Fortunately, significant regression of AIDS-related KS can be observed when immunocompromised patients are

administered ART. Sometimes referred to as highly active antiretroviral therapy (HAART) or effective combination ART (cART), it is a cocktail of HIV drugs that can suppress HIV to essentially undetectable levels (Cattelan et al. 2001). cART is a first-line treatment for AIDS-associated KS, and it is believed to work largely through the reconstitution of the immune system. Both KSHV and HIV-1 viral loads decrease upon reception of cART (Wilkinson et al. 2002).

Histologically, there is no distinction between the four subtypes of KS lesions. They are composed of various cell types comprising endothelial cells, fibroblast, inflammatory cells, and smooth muscle cells (Kaaya et al. 1995). KS typically develops in the cutaneous or dermal region of the skin and is characterised by dilated, irregularly shaped blood vessels and proliferating spindle endothelial cells. Research in the area can greatly benefit from the availability of valid KS cell culture model systems; hence there were many attempts to establish immortalized cell lines from KS-derived cells (Nakamura et al. 1988; Roth et al. 1988). Unfortunately, only the KS^{Imm} cell line was successfully isolated thus far but is not widely used (Albini et al. 1997). SLK and KS Y-1 cell lines were originally thought to be of KS origin, when in fact they were a contaminant from renal carcinoma and bladder cancer cell lines, respectively (Stürzl et al. 2013).

Often diagnosed in the course of HIV infection, PEL is the second malignancy causally associated with KSHV and is a type of B-cell non-Hodgkin's lymphoma (NHL). Although rare, PEL is highly aggressive with a median survival rate of 6 months following initial diagnosis (Boulanger, Gérard, et al. 2005; Boulanger, Duprez, et al. 2005). In most cases, PEL cells are co-infected with KSHV and EBV and are located in body cavities, hence its former name body cavity-based lymphoma (BCBL; reviewed in Chen et al. 2007). The degree to which EBV contribute to the disease pathogenesis is unclear. However, it is known that KSHV latent genes drive the development, survival

and maintenance of infected PELs. Indeed, *in vitro* generation of KSHV-negative PEL cells was unsuccessful and inhibition of KSHV latent genes leads to apoptosis or cell cycle arrest (Guasparri et al. 2004; Nishimura et al. 2001). KSHV-infected PEL cells, derived from patient clinical samples, rapidly became a KSHV cell model (Drexler et al. 1998). A distinction can be made between KSHV-positive EBV-negative cell lines such as BCBL-1 or BC-3 cells, and KSHV- and EBV-positive cell lines such as BC-1 or JSC-1 cells.

The third type of KSHV-associated disease, although technically not a lymphoma, is MCD. This lymphoproliferative disorder develops mainly in lymph nodes and spleen. Factors released from infected cells cause hyperactivation of the immune system together with proliferation of B-cells and severe inflammatory symptoms (Judde et al. 2000). Approximately half of all MCD cases are caused by KSHV. However, what triggers the immune activation in the other half remains unknown. If untreated, the survival of patient with KSHV-MCD is about 2 years or less. The general consensus is that KSHV-associated MCD is driven by the activation of cellular cytokines such as interleukin 6 and 10 (IL-6 and IL-10), and lytic genes such as the viral homologue of IL-6 (vIL-6; Parravicini et al. 1997; Aoki et al. 2000; Staskus et al. 1999). Moreover, high levels of KSHV DNA is detected in MCD patients, indicative of active lytic replication (Grandadam et al. 1997). KSHV-infected cells in the mantle zone of affected MCD lymph nodes exhibit significantly more lytic markers than in KS spindle cells and PELs (Parravicini et al. 2000; Katano et al. 2000). Together, these observations suggest that KSHV-positive cells in MCD patients mediate the release of pro-inflammatory cytokines and other lytic factors that in turn promote survival, differentiation and proliferation of B-cells, and thus the development of systemic inflammatory symptoms.

1.3.2 An overview of KSHV gene expression

The linear, double-stranded DNA genome of KSHV is encapsulated in an icosahedral capsid of ~125nm in diameter, which is surrounded by a layer of tegument proteins and a lipid bilayer envelop containing viral glycoproteins. Upon primary infection, KSHV DNA is delivered to the cell nucleus and circularises into an episome. The KSHV genome is not integrated into the human genome but rather remains in the infected nuclei as full viral DNA episome and utilises the host cellular machinery to replicate. The KSHV genome consists of (i) a 140kbp long unique region (LUR) that encodes >90 open reading frames (ORFs), and (ii) a number of GC-rich terminal repeat (TR) elements of 801bp each (Neipel et al. 1998). KSHV genes are involved in signal transduction, immune evasion, inhibition of apoptosis, and cell cycle regulation. Many KSHV ORFs are conserved in α- and β-herpesviruses. However some genes are unique to KSHV and are annotated from K1 to K15, according to their location on the genome (from left to right, **Figure 1.7**). An estimated 25% of KSHV genes are viral homologues of human genes. This is known as "molecular piracy" or "molecular mimicry". KSHV has borrowed many oncoproteins from the host cell, such as interleukin 6, Bcl-2 family protein, cyclin, or G protein coupled receptor. These KSHV genes control cellular growth, angiogenesis, cell replication, escape from the host immune response, and anti-apoptotic pathways.

Like all herpesviruses, KSHV has both latent and lytic cycles. During latency, KSHV expresses only a restricted number of genes associated with partitioning and genome replication. The KSHV latency locus is comprised of four genes within 10kb of each other: the latency associated nuclear antigen (LANA, or ORF73), v-cyclin (ORF72), v-FLIP (K13 or ORF71) and kaposin (K12). Although located outside of the latency locus, v-IRF3 (LANA-2, or ORF10.5) can be detected in certain latent cells (Parravicini et al.

2000). In addition, KSHV encodes 25 viral miRNAs derived from 12 pre-miRNAs (Cai et al. 2005), 10 of which are found in the latency locus between K12 and K13. During the lytic phase, more than 90 viral genes are expressed in a choreographed manner, from immediate-early to early, to late transcripts, which ultimately results in the active replication of the linear KSHV genome and the production of infectious virions (**Figure 1.7**). One of the most important immediate-early ORFs is RTA (ORF50), the replication and transcription activator. RTA plays a major role in KSHV reactivation, while LANA is the main hallmark of KSHV latency. These two important KSHV proteins are discussed in more detail hereafter. Of note, the lytic phase is marked by the high expression of a long non-coding RNA (lncRNA) called polyadenylated nuclear RNA (PAN RNA), which is believed to facilitate the induction of viral gene expression via direct binding to the viral chromosome (Sun et al. 1996; Rossetto & Pari 2012). Also expressed during chronic latent infection in cell culture, PAN RNA has been shown to disrupt the transcription of cellular genes involved in immune response, inflammation and cell cycle.

The 134 kDa LANA protein plays a major role in latency and is ubiquitously expressed in all latently infected cells (Rainbow et al. 1997; Ballestas et al. 1999). It contains three distinct domains: an N-terminal domain rich in serine and proline, a central domain, and a proline-rich C-terminal domain presenting charged and hydrophobic regions. Two LANA proteins can dimerise via their C-terminus. Additionally, the N-terminus of LANA can bind chromosomal DNA and nucleosomes via core histone; this is required for the persistence of the KSHV episome (Shinohara et al. 2002; Barbera et al. 2006). Moreover, both N- and C-terminal domains interact with chromatin-binding protein Methyl-CpG-binding protein (MeCP2), which is critical for LANA's localisation (Matsumura et al. 2010). LANA can both negatively and positively regulate biological

processes in order to drive cell proliferation (Lu et al. 2012). One of the pathways negatively affected by LANA is the central pro-apoptotic p53 pathway. LANA directly interacts with p53 to inhibit its transcriptional activity and its ability to induce apoptotic cell death (Friborg et al. 1999). In addition to p53, LANA also regulates genes that are part of the tumour necrosis factor (TNF) and IFN-γ regulatory networks, leading to survival of latently infected cells and suppressing antiviral responses, respectively (Cloutier & Flamand 2010).

The replication and transcription activator RTA is an immediate-early KSHV gene that governs the transition from latency over to the productive transcriptional programme leading to viral spread. In KSHV biology, RTA is often referred to as the master lytic switch, alone responsible for the induction of the cascade of cellular and viral responses. Targeting its own promoter via a positive feedback loop, RTA also binds RTA-responsive element (RRE) within other downstream lytic genes including K1, K2 (vIL-6), K3, and v-IRF1 (Song et al. 2003). Interestingly, LANA has been shown to inhibit RTA-mediated autoactivation as well as RTA-mediated KSHV replication and virion production (Lan et al. 2004). This shows that the latent-lytic switch is tightly controlled and highly dependent on external stimuli responsible for RTA up-regulation, such as oxidative stress, hypoxia, inflammatory cytokines, or secondary infection by bacteria and viruses.

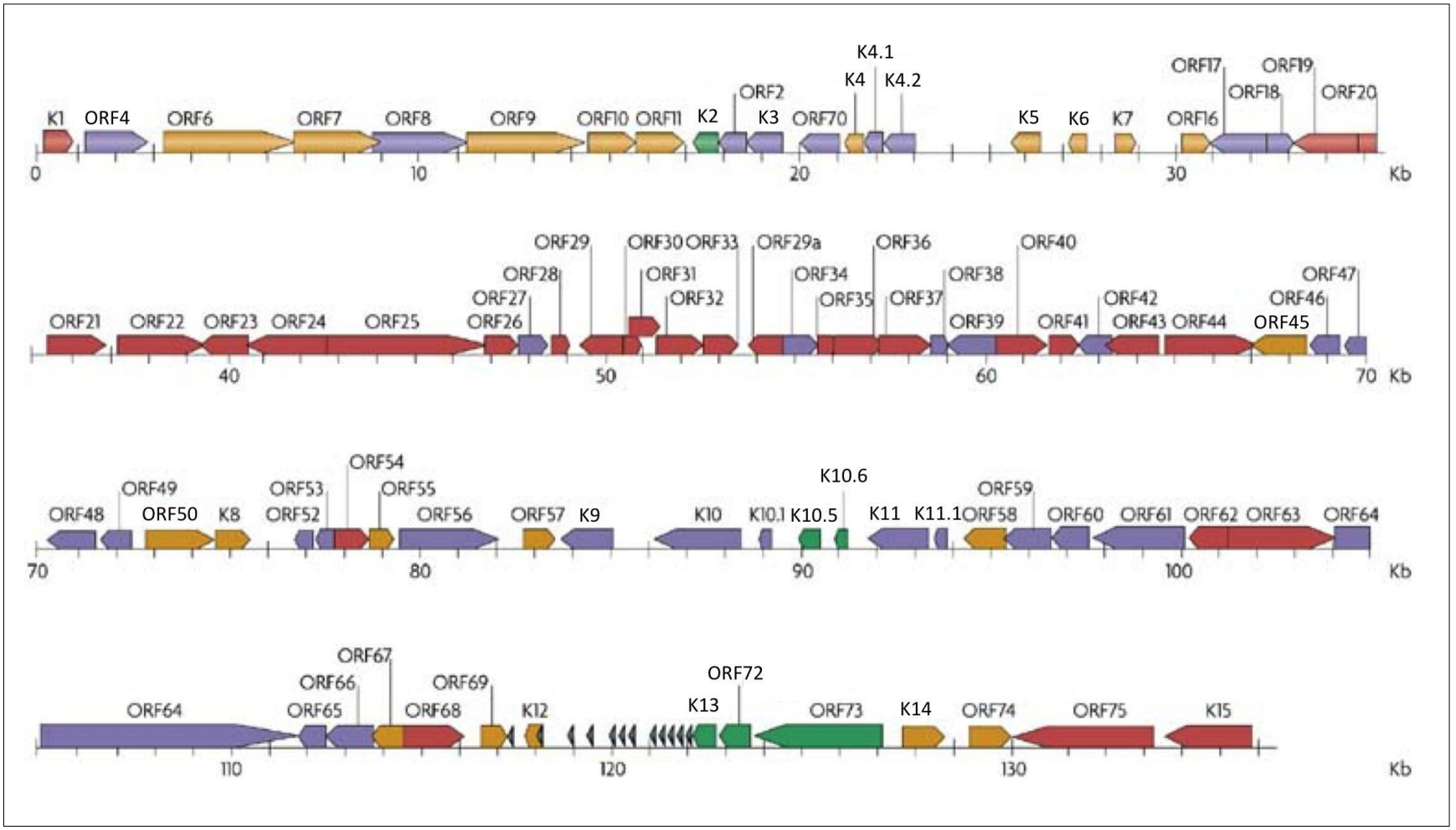

Figure 1.7: KSHV Genome. This map displays 75 ORFs and 21 distinct KSHV-specific genes (K genes). Genes belonging to the latent programme are indicated in green, while genes belonging to the immediate-early, early and late lytic programme are indicated in purple, orange, red, respectively. Image adapted with permission from Coscoy (2007).

1.3.3 KSHV miRNAs

Being non-immunogenic, virally encoded miRNAs are potentially attractive tools for viruses to both avoid detection by the immune system and interfere with the host machinery. A decade after the discovery of KSHV in 1994, Pfeffer et al. (2004) discovered that KSHV encodes its own miRNAs. Thus far, 12 pre-miRNAs have been characterised; they are called 'KSHV-miR-K12' because they are located in the vicinity of Kaposin (K12 gene). Ten pre-miRNAs are located within the intron of K12 (i.e. between K12 and K13), while the remaining two, KSHV-miR-K12-12 and -10 are located within the ORF and 3'UTR of K12, and are expressed in a different transcript. KSHV miRNAs are numbered from 1 to 12, and are ordered from left to right on the KSHV genome, as follows: miR-K12-12, -10, -9, -8, -7, -11, -6, -5, -4, -3, -2 and -1 (**Figure 1.8**).

KSHV miRNAs are not all equally expressed. miR-K12-10 and -12 are expressed during both latency and lytic replication while the rest, miR-K12-1 to -9 and -11, are expressed solely during latency (Pfeffer et al. 2005; Cai & Cullen 2006). Taken together, they yield the production of 25 mature KHSV miRNAs whose individual expression varies from one cell line to another. For example, three different PEL lines, BCBL-1, BC-1 and BC-3, express these miRNAs in significantly different levels (Cai et al. 2005). Some miRNAs including miR-K12-1, -3, -8, -10, -11, and -12, are highly conserved, while others, such as miR-K12-2, -4, -5, -6, -7, and -9 show significant sequence disparities, which could alter their processing and function, although this postulate demands further investigation (Marshall et al. 2007).

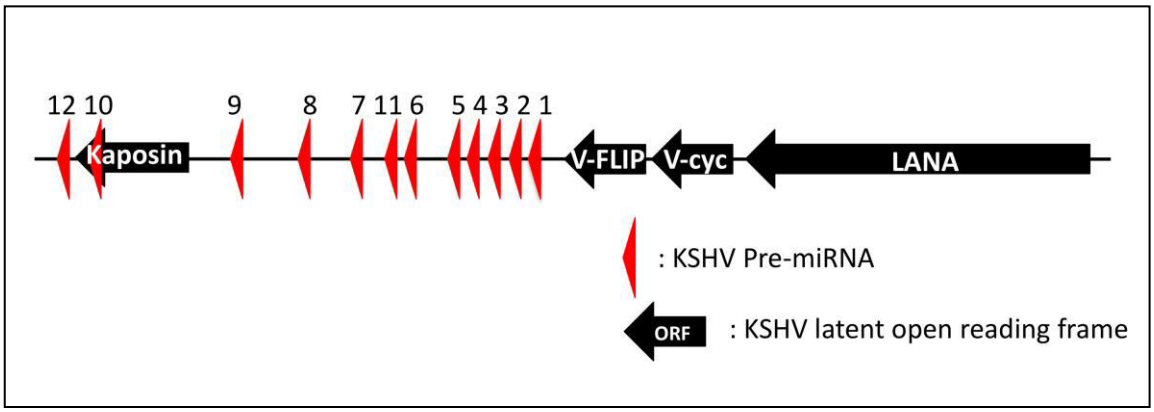

Figure 1.8: KSHV latency locus. This schematic of KSHV major latency locus illustrates the open reading frames (ORFs) of Kaposin, v-FLIP, v-cyclin and LANA (black arrows) and the 12 pre-miRNAs (red arrows).

Following their discovery, putative functions for KSHV miRNAs have rapidly immerged thanks to bioinformatics, miRNA target prediction tools, and genome-wide analysis of candidate cellular targets. Using photoactivable-ribonucleoside-enhanced crosslinking and immunoprecipitation (PAR-CLIP), more than 2000 potential cellular targets have been identified (Gottwein et al. 2011; Samols et al. 2007) and KSHV miRNAs have been shown to regulate both host and viral gene expressions in order to maintain latency (Lu et al. 2010), induce angiogenesis (Samols et al. 2007) and evade the immune system (**Table 1.3**; Nachmani et al. 2009).

One of the KSHV miRNAs in particular, miR-K12-11, has been the focus of much scrutiny. Its homology to cellular oncomiR miR-155 was reported in 2007 (Gottwein et al. 2007). Its role in KSHV cell entry was later established by a study showing that miR-K12-11-mediated repression of BACH-1 leading to the up-regulation of xCT, a fusion entry receptor for KSHV (Qin et al. 2010). In addition, miR-K12-11 targets a transcriptional regulator of IL-6, C/EBPβ, and induces both splenic B-cell expansion and KSHV-associated lymphomagenesis (Boss et al. 2011). Furthermore, miRNAs miR-

K12-7 and 9 have been shown to play a role in the latent/lytic switch by targeting RTA and preventing lytic reactivation (Lin et al. 2011; Bellare & Ganem 2009). In addition, miR-K12-5 has also been shown to prevent apoptosis via repression of BCL-2-associated factor (BCLAF1; **Table 1.3**; Ziegelbauer et al. 2009).

While numerous studies have investigated the roles of KSHV miRNAs, the exact mechanisms governing the regulation of KSHV miRNA expression remain unclear. Cellular miRNAs, as well as viral miRNAs, are quick responders and therefore have the ability to react rapidly to microenvironmental changes such as oxidative or hypoxic stress. However, it is not known if either of those microenvironmental changes affects KSHV miRNAs.

Functions	KSHV miRNAs	Validated targets
KSHV entry	miR-K12-1	—
	miR-K12-9	—
	miR-K12-11	BACH-1
Induction of reactive nitrogen species (RNS)	miR-K12-1, 9 and 11	—
Endothelial cell reprogramming	miR-K12-6 and 11	MAF
KSHV gene expression	miR-K12-7	RTA
	miR-K12-9	RTA/BCLAF1
	miR-K12-4	Rbl2
	miR-K12-1	IκBα
	miR-K12-3	Nuclear factor I/B
	miR-K12-5	BCLAF1
	miR-K12-11	IKKε
	miR-K12-10 and 12	—
Cytokine secretion	miR-K12-3 and 7	—
	miR-K12-11	C/EBPβ
	miR-K12-10	TWEAKR
Immune escape	miR-K12-7	MICB
Cell survival	miR-K12-10	TWEAKR
	miR-K12-1	p21

Table 1.3: Putative functions and targets of KSHV miRNAs. Table adapted with permission from Qin et al. (2012).

1.3.4 The relevance of hypoxia in KSHV life cycle

Hypoxia and HIFs play an important role in KSHV pathogenesis. Several KSHV proteins are indeed known to it induce or otherwise affect HIF. KSHV-encoded G protein-coupled receptor (v-GPCR) is an IL-8 chemokine receptor homologue expressed during the lytic cycle and induces several signalling pathways including angiogenesis via indirect stimulation of HIF-1α and its target gene, VEGF (Sodhi et al. 2000). Viral interferon regulatory factor 3 (v-IRF3) also promotes HIF-1α stability, thereby inducing VEGF and angiogenesis (Shin et al. 2008). Additionally, not only can LANA act as an inhibitor of HIF-1α suppressor proteins pVHL and p53, but it can also trigger HIF-1α accumulation in the nucleus (Cai et al. 2006; Cai et al. 2007), even in normoxic conditions. It is worth mentioning that other KSHV proteins, such as vIL-6 and K1, can also stimulate tumour growth and angiogenesis via HIF-independent mechanisms (**Figure 1.9**; Aoki et al. 2011; Wang 2004).

Remarkably, hypoxia can in turn activate lytic and latent KSHV genes such as LANA and RTA via hypoxic response elements (HREs) located within their 3'UTR (Veeranna et al. 2012; Cai et al. 2006). In PEL cells, a whole lytic gene cluster in the KSHV genome, ORF34 through 37, is up-regulated by hypoxia via functional HREs (Haque et al. 2006). This is consistent with the observation that HIFs up-regulate both latent and lytic KSHV genes. Therefore, the presence of HIFs in lesions may have implications for the pathogenesis of KSHV-associated diseases PEL and KS. Both disorders tend to develop in settings of relative hypoxia, and HIF-1α is up-regulated in HIV-associated KS lesions (Long et al. 2009).

Despite hypoxia being such an important feature of KS and PEL pathogenesis, no study has investigated the effects of KSHV infection on the hypoxic pathway, and vice versa,

through miRNA regulation. Hence this thesis is focused on understanding the underlying miRNA-mediated mechanisms between hypoxia and KSHV pathogenesis.

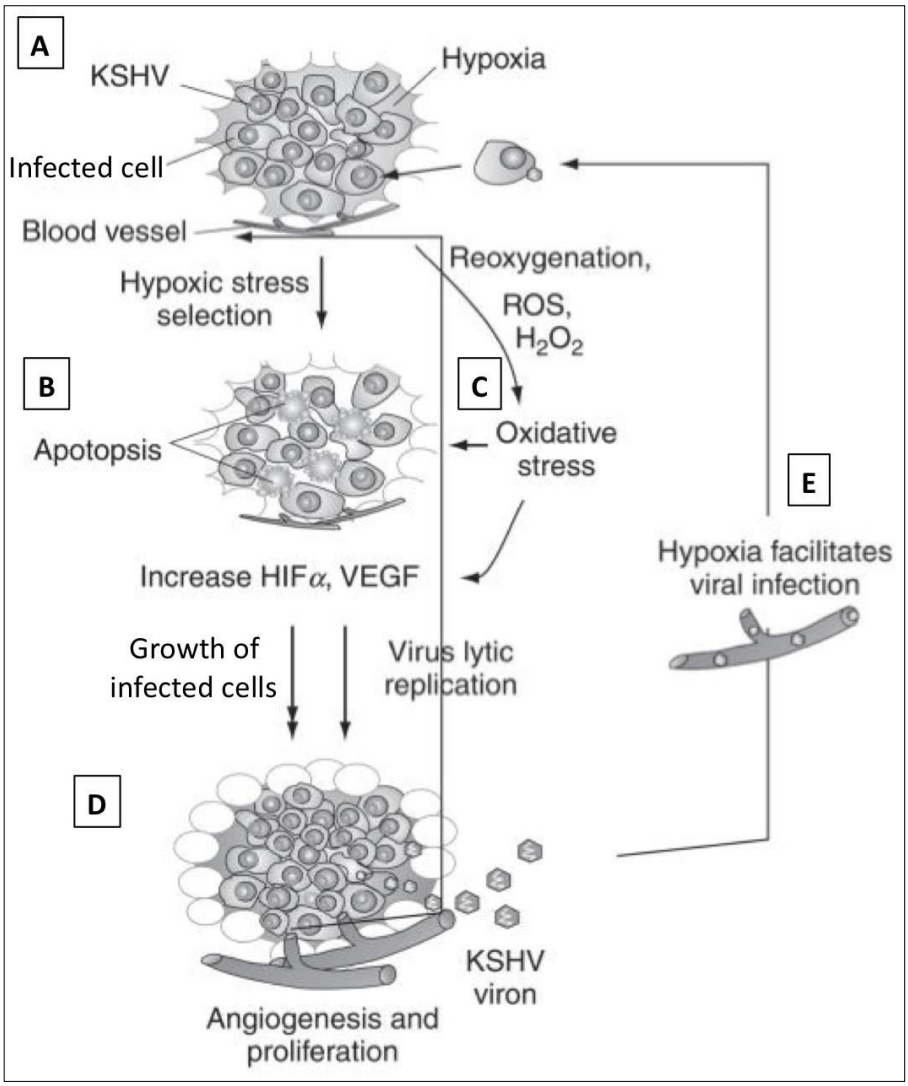

Figure 1.9: Development of KSHV-related malignancy under microenvironmental stress. **(A)** Hypoxia is induced by the proliferation of KSHV-infected cells. **(B)** Apoptosis and mutations occur under hypoxic stress inducing an increase in HIF-α and VEGF levels, while **(C)** reoxygenation and overproduction of ROS induce oxidative stress. **(D)** Combined oxidative and hypoxic stress induces the survival of malignant cells and KSHV lytic replication, which promote angiogenesis and tumour progression. **(E)** KSHV is reactivated from latency due to microenvironmental stresses and produces new virion particles. Image adapted with permission from Cai et al. (2010).

1.3.5 KSHV entry into target cells

KSHV infects a wide variety of human cell types including B cells, endothelial cells, epithelial cells, fibroblasts, monocytes and keratinocytes (Ganem 2007). Initial attachment of the virion and internalisation into target cells are critical steps in any viral infection. Multiple interactions are required for an efficient attachment of the envelope proteins on KSHV virions to the host cell, and viral entry. Heparin sulphate is one of the host cell surface receptors KSHV binds to and is a common target receptor for many herpesviruses. At least two envelope proteins, glycoprotein B (gB) and K8.1, mediate KSHV's binding to heparin sulphate, although others (gH/gL and gM/gN) have been shown to also play a role in the attachment and entry of KSHV into host cells (Spear & Longnecker 2003; Akula, Pramod, et al. 2001). Besides heparin sulphate, ephrin type A-receptor 2 (EPHA2) has recently been identified as another target receptor essential for KSHV entry into endothelial and epithelial cells, and it is likely to bind KSHV glycoproteins H and L (Hahn et al. 2012; Chakraborty et al. 2012). In addition to heparin sulphate and EphA2, xCT has been shown to enable KSHV-cell fusion and viral entry and is coincidently up-regulated by KSHV-encoded miRNAs (Kaleeba & Berger 2006; Qin et al. 2010). Notably, hypoxia also up-regulates the cell-surface expression of xCT in glioma cells although it remains unclear if hypoxic induction has an effect on KSHV uptake via xCT up-regulation.

Regarding internalisation, KSHV utilises a combination of two endocytic pathways that varies depending on the cell type: clathrin-mediated endocytosis, which has been shown to occur in embryonic kidney epithelial cells (HEK-293; Akula, Wang, et al. 2001) and human foreskin fibroblast cells (HFF; Akula et al. 2003); and actin-dependent macropinocytosis in human microvascular dermal endothelial cells (HMVEC-d) and human umbilical vein endothelial cells (HUVEC; Raghu et al. 2009).

Macropinocytosis is typically associated with the uptake of solutes from the extracellular milieu and vesicles are formed by the cell surface rufflings. Similarly to KSHV, HIV-1 entry into macrophages is mediated by macropinocytosis (Maréchal et al. 2001). Interestingly, β-amyloid (Aβ) fibrils are known to stimulate the uptake of HIV-1 (Wojtowicz et al. 2002) but it has not been described if that was through a macropinocytic mechanism at that point. Seven years later, Mandrekar et al. (2009) reported that macropinocytosis is the mechanism used by microglia, brain's tissue macrophages, to internalise β-amyloid peptide (Aβ). Recently, Daniels et al. described how an engineered peptide, p27, enhances HIV infection (Daniels et al. 2014). Further studies are needed to draw conclusions regarding p27's ability to induce KSHV uptake via macropinocytosis.

Within 8hrs of entry into primary endothelial cells, each KSHV virion releases its double stranded viral DNA genome into the cell nucleus for it to be circularised. The production of virions and lysis of most host cells occur within 72hrs post-infection. By 8dpi (days post infection), lytic replication usually comes to a halt, leaving latently infected cells (Dezube et al. 2002). Of note, this model might not be reflective of KSHV-infected B-cells.

1.4 Thesis aims

Background summary

Over the last two decades, KSHV pathogenesis has been extensively studied and crucial discoveries in the fields of cellular as well as virus-encoded miRNAs and hypoxic regulation have been made (**Sections 1.1** and **1.2**). There is compelling evidence that KSHV uses the cell's response to hypoxia to its advantage (**Section 1.3**). While it is clear that (i) hypoxia-induced angiogenesis is instrumental to the survival and proliferation of KSHV infected cells and (ii) some cellular miRNAs are induced by hypoxia, the functional relationship between miRNAs and KSHV infection, especially in the context of hypoxia, has not been explored.

Specifically, there is very little information regarding the regulation of cellular miRNAs by KSHV, hypoxia or both, the regulation of viral miRNAs by external stimuli such as hypoxic stress, and how these miRNAs may contribute to KSHV pathogenesis. Broadly put, this thesis project focuses on the interplay between three major axes: KSHV, miRNAs and hypoxia.

Hypothesis

This thesis will address the hypothesis that dysregulation of miRNAs due to hypoxia, KSHV infection or the interaction of the two processes, plays a significant role in KSHV pathogenesis. Consequently, the overall goal of the research set out in this thesis is to understand how KSHV uses the host miRNA silencing machinery to its advantage and how this intersects with its use of the cell's response to hypoxia.

Aims

This thesis aims to address the miRNA-mediated mechanisms associated with KSHV infection and/or hypoxia induction by:

1. Profiling the cellular miRNA and mRNA responses to KSHV infection
2. Evaluating the interplay between KSHV infection and the hypoxic cellular response.
3. Examining the role of hypoxia-regulated miRNAs in KHSV-infected B-cells.
4. Assessing the response of KSHV miRNAs to external stimuli.

This thesis does not only address miRNA dysregulation, but also relates it to the mRNA target changes in order to decipher the relevant miRNA-mRNA pairs that have the greatest impact on KSHV pathogenesis. In the subsequent chapters, after an explanation of the materials and methods (**Chapter 2**), these goals are pursued by first profiling the differential expression of cellular miRNAs and mRNAs in response to KSHV infection (**Chapter 3**), profiling the differential expression of miRNAs and mRNAs in response to hypoxic induction using an infected/uninfected KSHV cell model (**Chapter 4**), investigating the cellular response to hypoxia in chronically infected B-cells (**Chapter 5**), and lastly evaluating how KSHV miRNAs may be influenced by external stimuli, such as hypoxia, oxidative stress or drug treatment (**Chapter 6**). This thesis finally provides an overall summary and discussion of the reported findings (**Chapter 7**).

2

Materials and methods

THIS chapter is a collection of the materials and methods used in experiments conducted either in the laboratory of Dr. Robert Yarchoan at the National Cancer Institute of the U.S. National Institutes of Health, or in the laboratory of Dr. Jiannis Ragoussis at the Nuffield Department of Medicine of the University of Oxford, now at McGill University in Canada.

2.1 Reagents, suppliers and instruments

Tissue culture flasks, plates and dishes were obtained from Corning (Tewksbury, MA, USA). Unless otherwise stated, any additional reagents not provided by a standard kit were supplied from Sigma-Aldrich (UK and USA). The principal instrumentation has been divided by lab location as follows.

RAGOUSSIS LAB, NUFFIELD DEPARTMENT OF MEDICINE, UNIVERSITY OF OXFORD

- Microfuge 22R [Beckman Coulter]
- IQ5 iCycler™ Multicolor Real-Time PCR detection system instrument [Bio-Rad Laboratories]
- CFX96 Real-Time System C1000 thermal cycler [Bio-Rad laboratories]
- 2100 Bioanalyzer microfluidics-based platform [Agilent Technologies]
- Dark reader blue light transilluminator [Clare Chemicals]
- PowerPac™ HC high-current power supply
- NanoDrop spectrophotometer ND-1000 [NanoDrop Technologies]
- QuBit® Fluorometric Quantitation device [Life Technoogies]
- Countess® automated cell counter [Invitrogen]
- Stackable incubator shakers Innova® 44 [New Brunswick Scientific]
- LabGard® ES NY-425 class II, type A2 biosafety cabinet [NuAire]
- Air-jacketed CO_2 incubators, model 5.3A and 8.5A [VWR Laboratories]
- Invivo2 hypoxia workstation [Ruskinn Technology]
- LSF151 under-counter Laboratory freezer [Lec Medical]
- Forma™ -86°C ultra-low temperature freezer [Thermo Scientific]

YARCHOAN LAB, NATIONAL CANCER INSTITUTE, NATIONAL INSTITUTES OF HEALTH

- Microfuge 18 centrifuge [Beckman Coulter]
- Sorvall™ Legend XTR refrigerated centrifuge [Beckman Coulter]
- T100™ thermal cycler [Bio-Rad Laboratories]
- Vortex-Genie 2 variable speed laboratory mixer [Daigger Laboratories]
- StepOnePlus Real-Time PCR systems [Applied Biosystems]
- Gyrotory shaker model G2 [New Brunswick Scientific]

- Eclipse T1 microscope system [Nikon] with QImaging Retiga 4000R Fast 1394 digital camera features [QImaging]
- PowerEase® 300W power supply [Life Technologies]
- iBlot® blotting system [Invitrogen]
- Sorvall™ Legend Micro 17R microcentrifuge [Thermo Scientific]
- NanoDrop spectrophotometer ND-1000 [NanoDrop Technologies]
- SpectraMax® 190 UV-Vis microplate spectrophotometer [Molecular Devices]
- Odyssey® CLx infrared imaging system with the Image Studio™ software [Li-Cor Biosciences]
- Class II, type B1 biosafety cabinet [NuAire]
- Heracell™ 150 CO_2 incubator [Thermo Scientific]
- Forma™ Laboratory pharmacy freezer [Thermo Scientific]
- K series Cryostorage system with Kryos controller [Taylor-Wharton]
- Forma™ -86°C ultra-low temperature freezer [Thermo Scientific]

2.2 Cell culture methods

2.2.1 Cell lines

Human epithelial SLK and SLKK cells (also known as SLK+rKSHV.219) (Ziegelbauer et al. 2009; Vieira & O'Hearn 2004; Herndier et al. 1994; Stürzl et al. 2013) were a gift from Dr. Don Ganem (UCSF, CA, USA). Cells were expanded on receipt, frozen in liquid nitrogen, and stored until used in the experiments described.

PEL-derived KSHV-infected BC-3 and BCBL-1 cells were previously described (Arvanitakis et al. 1996; Renne et al. 1996) and were, for the purposes of this thesis, obtained from cryogenic storage of the Yarchoan Lab at the National Cancer Institute, NIH (National Institutes of Health AIDS Research and Reagent Program, Rockville, MD). Vero cells were either cultured uninfected as a control, or infected with puromycin-resistant rKSHV.219. They were transfected with a doxycycline inducible plasmid encoding for KSHV lytic protein RTA. All cell lines were originally obtained from the American Type Culture Collection (ATCC) (Manassas, VA, USA) and are described in **Table 2.1**.

rKSHV.219 differs from wild type KSHV in that green and red fluorescent proteins are expressed from a strong cellular promoter, elongation factor 1α, and a KSHV lytic PAN promoter, respectively. It also contains a puromycin resistance gene as a selectable marker (Vieira & O'Hearn 2004).

SLKK cells containing the rKSHV.219 were found to grow slower than SLK cells, probably due to the presence of puromycin in the growth media to select for cells expressing the viral episome.

2.2.2 Cell maintenance

All experiments were established in a minimum of three independent cell cultures at 37°C in humidified 5% CO_2, unless otherwise stated.

Adherent cells were maintained in Dulbecco's Modified Eagle Medium (DMEM, Gibco, Carlsbad, CA, USA) supplemented with 10% v/v foetal bovine serum (Sigma-Aldrich, St Louis, Missouri, USA) and 1% Penicillin/streptomycin/glutamine solution (Gibco). When confluent (~80%), adherent cells were rinsed with sterile PBS, detached using

0.25% trypsin-EDTA (Gibco), centrifuged at 1500rpm for 5 minutes, resuspended in 10mL DMEM (Gibco) and diluted into a new container 10x to 20x depending on the cell type and the experiment conducted at the time. Additionally, KSHV-positive SLK (known as SLKK) cells were periodically grown under selection with 10μg/mL puromycin to maintain the viral episome.

Suspension cells were maintained in RPMI 1640 medium (Gibco) supplemented with 10% v/v foetal bovine serum (Sigma-Aldrich) and 1% Penicillin/streptomycin/glutamine solution (Gibco) (**Table 2.1**). Cells were split every 5 to 7 days depending on the cell type.

2.2.3 Cell counting

Cells were counted before being plated or resuspended for experiments that required a specific cell concentration such as hypoxic treatment, oxidative stress, prior RNA extraction for RNA-Seq analysis, transfection experiments, or pomalidomide treatment. Cells were washed and trypisinized (if adherent cells), centrifuged and resuspended in the adequate cell culture medium. An equal volume of cell suspension and trypan blue was mixed to reach a total of 20 μL that was then loaded onto a disposable Countess chamber slide (Invitrogen, Life Technologies, Carlsbad, CA, USA). The device then takes 16 live pictures, process the live and dead cells and averages the number of cells in order to provide the total cell concentration per mL, the live cell concentration per mL, the dead cell concentration per mL and the viability (as a percentage of live cells to total cells).

Cell line	Organism	Tissue	Morphology	Culture Properties	Disease	Lytic replication inducibility	Culture medium
SLK	Homo sapiens	Kidney:skin	Epithelial	Adherent	Clear cell carcinoma	no	DMEM complete
SLKK	Homo sapiens	Kidney:skin	Epithelial	Adherent	Clear cell carcinoma infected by recombinant puromycin-resistant rKSHV.219	no	DMEM complete + 10µg/mL puromycin
iSLK.219	Homo sapiens	Kidney:skin	Epithelial	Adherent	Clear cell carcinoma infected by recombinant puromycin-resistant rKSHV.219	RTA inducible using 2µg/mL doxycycline	DMEM complete + 1µg/mL puromycin + 250µg/mL G418 (Geneticin)
Vero	Cercopithecus aethiops	Kidney	Epithelial	Adherent	Normal	no	DMEM complete
Vero + KSHV	Cercopithecus aethiops	Kidney	Epithelial	Adherent	infected by recombinant puromycin-resistant rKSHV.219	no	DMEM complete + 10ug/mL puromycin
Vero/RTA + KSHV	Cercopithecus aethiops	Kidney	Epithelial	Adherent	infected by recombinant puromycin-resistant rKSHV.219	RTA inducible using 2µg/mL doxycycline	DMEM complete + 10µg/mL puromycin + 800µg/mL G418 (Geneticin)
BCBL-1	Homo sapiens	B lymphoblast	Lymphoblast	Suspension	Body cavity based lymphoma infected by WT KSHV	TPA or 0.5mM butyrate	RPMI compete
BC-3	Homo sapiens	B lymphoblast	Lymphoblast	Suspension	Body cavity based lymphoma infected by WT KSHV	TPA or 0.5mM butyrate	RPMI compete

Table 2.1: Cell line characteristics. WT : wild type, rKSHV.219 : recombinant KSHV.219, TPA : 12-O-tetradecanoylphorbol-13-acetate.

2.2.4 Cryogenic preservation, storage and thawing of cells

For research purposes, cell lines were frozen and stored away in a liquid nitrogen tank (approximately -150°C) at the Wellcome Trust Centre for Human Genetics at the University of Oxford, or at the National Cancer Institute at the NIH. 2mL cryogenic tubes were used for long-term storage (1 million cells per vial). After cell counting, cells were resuspended in freezing medium (FBS+10% dimethyl sulfoxide) and aliquoted into labelled vials that were gradually frozen, first for an hour on dry ice, then for an hour at -80°C, and finally in the cryogenic storage. To retrieve cells from long-term storage, vials were rapidly thawed in a 37°C water bath, slowly diluted in 48mL medium (either DMEM or RPMI 1640), centrifuged for 5 minutes at 1000rpm and resuspended in 10mL medium. In the case of SLKK cells, 10μg/mL puromycin was added to the medium which would slow growth slightly. Cells were then incubated in a T25 flask and typically reached confluence within a week of being thawed.

2.2.5 Hypoxic treatment

Exposure of cell cultures to hypoxia (1% O_2) was undertaken in either an $InVivo_2$ Hypoxia Work Station (Ruskinn Technology, UK). This was undertaken in parallel with cells maintained in normoxic conditions (21% O_2). As an alternative way to induce HIF, cobalt chloride ($CoCl_2$) was added to the growth medium (100μM final concentration) to trigger HIF-1α accumulation. $CoCl_2$-treated cells were then incubated in normoxic conditions. All cells were harvested for protein and RNA 24hrs post-treatment. All experiments were done at least in triplicate from independent cell cultures.

Hypoxia induces lytic replication in KSHV-infected B-cells BCBL-1 (Davis 2001), but not in SLKK cells where latency is under tight control.

2.2.6 Oxidative stress treatment

The day prior to oxidative stress treatment, BCBL-1 or BC-3 cells were plated at $4x10^5$cells/mL. 25μM hydrogen peroxide (H_2O_2) was used to treat cells. PBS was used for the untreated controls. Cells were harvested for protein and RNA at various time points unless specified otherwise (e.g. 3hrs, 6hrs, 9hrs, 12hrs, 24hrs or 48hrs post-treatment).

2.2.7 Pomalidomide treatment

Stocks of immunomodulatory agent pomalidomide (Celgene Corporation) were dissolved in DMSO and used to treat BCBL-1 cells at varying final concentrations: e.g. 0.1μM, 1μM, 5μM and 10μM. Vehicle controls (DMSO) were used as a negative control for normalisation. Cells were incubated for 72hrs before being harvested for protein and RNA.

2.2.8 *De novo* infection of SLK cells by KSHV

KSHV was harvested from BCBL-1 cultures 6 days after induction with valproic acid and purified by centrifugation. The day prior to *de novo* KSHV infection, SLK cells were plated at $1x10^5$ cells per well in a 6 well-plate to obtain 50% confluence. Cells were incubated for 6hrs at 37°C with DMEM containing 2% FBS, wild-type KSHV, and 8 μg/mL Polybrene (Hexadimetrhine bromide; Sigma-Aldrich). After incubation, cells were washed twice with PBS and normal growth medium was changed every other day throughout the course of infection. Cell lysates and RNA were harvested at various time points including 3 days post-infection (3dpi) and 5 days post-infection (5dpi).

2.2.9 Transfection of miR-210 mimics and anti-miR-210 inhibitors

SLK and SLKK cells were seeded at a concentration of ~2.5x10^4 to 2.8x10^4 cells per well in a 96-well plate in DMEM medium with 10% FBS containing no antibiotics; this allowed cells to achieve 70%-80% confluence the following day. The culture medium was then removed and the cells were transfected with the miRNA mimics (i.e. miR-210), miRNA inhibitors (i.e. anti-miR-210) or negative control ('scramble') (Dharmacon, Lafayette, CO, USA) at 2nM and 10nM final concentration, using Lipofectamine 2000 (0.4µL per well) (Invitrogen). Lipofectamine is a routinely used transfection reagent that allows the negatively charged membrane to interact with the liposome/nucleic acid complex. The miRNA transfection experiments were performed in 50µL Opti-MEM medium (Invitrogen). Five hours post-transfection, the medium was supplemented with 50µL Opti-MEM with 20% FBS (10% final concentration) and the cells were incubated overnight at 37°C/5% CO_2 for RNA isolation.

2.2.10 Transfection of miRNA mimics (miR-708-5-p, miR-409-3p and miR-409-5p)

The day prior to transfection, SLK and SLKK cells were plated at 1x10^5 cells per well in a 6 well-plate to obtain 50% confluence. The control scramble sequence (Negative control #1, Cat. No. 4464051, Ambion, Life Technologies) and the double-stranded miRNA mirVana mimics for miR-708-5p, miR-409-5p and miR-409-3p (assay ID MC11161, MC13028, and MC12446, respectively; Ambion, Life Technologies) were transfected at a final concentration of 10nM using DharmaFECT 1 (Dharmacon, GE Healthcare, Lafayette, CO) according to manufacturer's protocol. Briefly, DharmaFECT 1 and Opti-MEM (1:50 v/v ratio) were incubated at room temperature for 10 minutes. Separately, Opti-MEM and 10pmol of miRNA mimics or miR-scramble were also incubated at room temperature for 10 minutes. 400µL of these two mixtures (1:1 v/v

ratio) were then incubated at room temperature for 20 minutes and subsequently added to the cells with 1.6mL of DMEM containing 10% FBS. Cells were harvested for RNA 48hrs after transfection.

2.3 DNA methods

2.3.1 DNA extraction and quality control

Genomic DNA was isolated from cells using the PureLink Genomic DNA Mini kit (Invitrogen) following the manufacturer's instruction. DNA concentration and integrity were determined after isolation using a Nandrop-ND-1000 spectrophotometer (Thermo Fisher Scientific, Waltham, MA, USA). All samples were stored at -20°C.

2.3.2 Primer design

Primers for DNA amplification were designed using NCBI (http://www.ncbi.nlm.nih.gov/) to retrieve the gene sequence (Genome database) and Primer3Plus (http://primer3plus.com/) to generate the primers (standard settings). Forward and reverse primer sequences were then checked for specificity against the human genome assembly GRCh37/hg19 using UCSC In-silico PCR tool (www.noncode.org/cgi-bin/hgPcr). Reverse Phase Cartridge (RPC) purified custom-made oligonucleotides were then synthesised by either Lofstrand Labs Limited (USA) when at the NIH, or by Metabion (Germany) when at the University of Oxford.

2.3.3 Polymerase chain reaction

Eight individual regions of the 14q32 genomic locus were probed using a set of custom-designed primers at 10μM (**Table 2.2**) and AmpliTaq Gold 360 Master Mix (Applied

Biosystems). DNA amplifications were performed in a final volume of 25µL containing 100ng of DNA template. The cycling conditions were as follows: 10 minutes at 95°C, 35 cycles of amplification at 95°C for 30 seconds, 60°C for 30 seconds and 72°C for 1 minute, followed by 7 minutes at 72°C.

2.3.4 DNA gel electrophoresis

The final PCR products were mixed with 6X orange DNA loading dye (Thermo Fisher Scientific) and introduced into the wells of an agarose gel together with 5µL of a 100bp or 1kb ladder (NEB) depending on the size of the DNA fragments. The DNA samples were electrophoresed on a 1-2% agarose gel in Tris-Borate-EDTA (TBE) at 100V for up to 50 min, then stained with ethidium bromide and visualize under ultraviolet (UV) light.

Region	Primer names	Amplicon size	Sequence (Forward and Reverse)
1	Upstream DLK1	394bp	TGGGAGCTCAAGGTCAGTCT
			AAAAGTAGGGAAGCACCCGT
2	DLK1	403bp	CCATCAACACAACGTTCAGG
			TCTCTGATGATGGAGACCCC
3	Methylation Region	469bp	ACCACCTTAGATGCCGTGTC
			TGCTCAGCTCTGTCTCCTGA
4	MEG3	365bp	GGATGCTGAGATTCGGGATA
			TAGGAACACAACGGGACACA
5	RTL1	494bp	AAGTTCGCCCAAGAGCACTA
			TCGCTGTGATCACTGTCTCC
6	miRNA Cluster	547bp	TCCTTGGAGAGTGTGAGGCT
			CCTACCCTCAAAAGGGCTTC
7	DIO3	475bp	TGTTTCCTGTCCCTGGTAGG
			ACACTCACCAAATGGCCTTC
8	Downstream DIO3	431bp	AGGGGAACAACAGTGTGGAG
			TGGAGCTGGGAGAAGACACT

Table 2.2: Primer sequences for PCR amplification of the 14q32 region. Eight individual regions (~450bp) of the genomic DNA at 14q32 were probed using these custom-designed primers. Columns identify the primer name, direction, sequence as well as amplicon size.

2.4 RNA methods

2.4.1 Total RNA extraction and quality control

Total RNA was extracted from cells using miRVana miRNA isolation kit (Ambion, Life Technologies, Carlsbad, CA, USA) according to manufacturer instructions. RNA abundance and integrity were determined after isolation using a Nanodrop-ND-1000 spectrophotometer (Thermo Fisher Scientific) and an Agilent 2100 Bioanalyzer (Agilent Technologies, Santa Clara, CA, USA), respectively. Only total RNA samples with RNA integrity number (RIN) >9 were further used for RNA-Sequencing and small RNA-Sequencing. All samples were stored at -80°C.

2.4.2 Primer design

Primers for quantitative real-time PCR were designed using NCBI to retrieve the mRNA Fasta sequence (Genome database). Whenever possible, primers were generated by Primer3Plus so that they span the exon-exon boundary to avoid DNA amplification. Forward and reverse primer sequences were then checked for specificity against the human genome assembly GRCh37/hg19 using UCSC *In silico* PCR tool (www.noncode.org/cgi-bin/hgPcr). Additionally, primer specificity was assured by the quality of the melting curve profiles at the end of the qPCR (a single sharp dissociation peak). Reverse Phase Cartridge (RPC) purified custom-made oligonucleotides were synthesised by either Lofstrand Labs Limited (USA) when at the NIH, or by Metabion (Germany) when at the University of Oxford.

2.4.3 Reverse transcription

2.4.3.1 Messenger RNA

For gene expression, cDNA synthesis was performed on total RNA (RIN >9) using the Superscript II reverse transcriptase kit, 0.5mM dNTP set and 50ng/µL random hexamer (Invitrogen). cDNA products were stored at -20°C for further measurements.

2.4.3.2 MicroRNA

For miRNA expression, cDNA synthesis was performed on total RNA (RIN >9) using TaqMan MicroRNA reverse transcription kit (Applied Biosystems) and the following Reverse Transcription microRNA assays (**Table 2.3**). cDNA products were stored at -20°C for further measurements.

2.4.4 Quantitative real-time polymerase chain reaction (qPCR)

2.4.4.1 Messenger RNA

qPCR was performed using the FastStart Universal SYBR Green/ROX master mix (Roche Applied Science, Mannheim, Germany) and cDNA templates diluted 1:8 in nuclease-free water. Thermal conditions included an enzyme activation step (95°C for 10 minutes), 40 cycles of amplification at 95°C for 15 seconds and 60°C for 1 minute, and melting curve analysis following instrument standard instructions. The 18S or RPL11 transcript levels were used as endogenous control to normalise expression of the genes of interest (**Table 2.4**). All qPCR reactions were performed on a StepOnePlus real-time PCR system (Applied Biosystems). Each experiment was performed in triplicate. Change in mRNA expression was determined based on the delta Ct method (Livak & Schmittgen 2001).

miRNA	RT and qPCR Assay number
miR-193b-3p	002367
miR-210-3p	000512
miR-224-5p	002099
miR-409-5p	002331
miR-409-3p	002332
miR-410-3p	001274
miR-708-3p	002342
miR-708-5p	002341
miR-3614-5p	461775
let-7c	000379
RNU43	001095
kshv-miR-K12-1-5p	197204_mat
kshv-miR-K12-2-5p	197192_mat
kshv-miR-K12-3-5p	008316
kshv-miR-K12-4-3p	197240_mat
kshv-miR-K12-6-3p	008459
kshv-miR-K12-7-3p	243633_mat
kshv-miR-K12-8-3p	241994_mat
kshv-miR-K12-10a-3p	008504
kshv-miR-K12-11-3p	008562

Table 2.3: Single tube Taqman miRNA assays for reverse transcription and qPCR.

Gene	Primer sequence (Forward and Reverse)
VEGF	CCTTGCTGCTCTACCTCCAC
	AGCTGCGCTGATAGACATCC
ISCU	AATGGGTGAAAGGAAAGACG
	GCTCCTTGGCGATATCTGTG
LANA	CGCGAATACCGCTATGTACTCA
	GGAACGCGCCTCATACGA
RPL11	CTTTGGCATCCGGAGAAAT
	TCCAAGATTTCTTCTGCCTTG
18S	GCCCGAAGCGTTTACTTTGA
	TCCATTATTCCTAGCTGCGGTATC
EFNA3	GTGCCCAAGCTTGAGAAGAG
	GCGGACACAGATGTATGGTG
FGB	AATTACTGTGGCCTACCAGGTGAATA
	AAGCTGGCTAATTTTATCATTTCCA
ANG	TGGGCGTTTTGTTGTTGGTCTTC
	CGTTTCTGAACCCCGCTGTGG
CASP2	TTGCCGAAGATGAGACTGC
	GCGTTCACCTTAACCAGCA
MDM2	GCAGTGAATCTACAGGGACGC
	ATCCTGATCCAACCAATCACC
LIF	GGCCCGGACACCCATAGACG
	CCACGCGCCATCCAGGTAAA
H19	GGCTCCCAGAACCCACAAC
	GGGTTTTGTGTCCGGATTCA

Table 2.4: Primer sequences used for qRT-PCR.

2.4.4.2 MicroRNA

6-carboxyfluorescein(FAM)-based qPCR was performed using the Taqman Universal Master Mix II (no UNG) (Applied Biosystems), cDNA miRNA templates, and qPCR miRNA primers (Ambion, Life Technologies, **Table 2.3**) following the manufacturer's instructions. Each PCR reaction contained 1.33µL of reverse transcription product, 7.67µL nuclease-free H_2O, 10µL TaqMan Fast Universal PCR Master Mix, and 1µL TaqMan MicroRNA Assay (20X) primer.

qPCR reactions were performed on the IQ5 Multicolor Real-Time PCR Detection System instrument (iCycler, Bio-Rad), the CFX96 Real-Time System C1000 Thermal Cycler (Bio-Rad), or the StepOnePlus real-time PCR system (Applied Biosystems) as follows: enzyme activation step at 95°C for 10 minutes, 40 cycles of amplification at 95°C for 15 seconds followed by 60°C for 1 minute. Reference snoRNA RNU43 was used as endogenous control to normalise expression. Each experiment was performed in triplicate. Change in miRNA expression was determined based on the delta Ct method (Livak & Schmittgen 2001).

$\Delta\Delta Ct_{(i)} = (Ct, miRNA - Ct, RNU43)_{Hypoxia\ (i)} - (Ct, miRNA - Ct, RNU43)_{Normoxia}$

For experiment (i), "Hypoxia (i)" is the mean of the instrument Ct triplicate results for hypoxic sample (i) internal reference RNU43 and the miRNA of interest; and "Normoxia" is the mean Ct of the 6 raw results for all normoxic control samples of the experiment. The relative expression levels are then calculated from these normalised Ct values:

- Relative expression $_{miRNA} = 2^{-\Delta\Delta Ct}$
- Results were considered significant at $P \leq 0.05$.

2.4.5 Preparation of polyadenylated mRNA libraries for deep sequencing

Total RNA samples used for RNA-Sequencing were treated with Turbo DNA-free DNase I and Dynabeads (both from Ambion, Life Technologies) to deplete samples from the residual DNA and to isolate the polyadenylated mRNA transcriptome, respectively. Poly(A) enriched RNA libraries were then prepared with the ScriptSeq v2 RNA-Seq kit (Epicentre, Madison, Wisconsin, USA). The final concentration and size distribution of the RNA libraries were measured using a Nanodrop-ND-1000 spectrophotometer (Thermo Fisher Scientific), and running a DNA 100 chip on an Agilent 2100 Bioanalyzer (Agilent Technologies). Finally, a total of 18 polyadenylated mRNA libraries (hypoxic and normoxic SLK, hypoxic and normoxic SLKK, and hypoxic and normoxic BCBL-1 samples; n=3) were sequenced using the Illumina HiSeq platform at the Wellcome Trust Centre for Human Genetics (University of Oxford).

2.4.6 Preparation of miRNA libraries for deep sequencing

Small RNA libraries were constructed as previously described (Camps et al. 2014) using the TruSeq RNA Sample Prep kit (Illumina inc., San Diego, California, USA). Briefly, after running 2μg of total RNA in a 15% urea-TBE gel (Invitrogen, Life technologies, Carlsbad, California, USA) for 1hr at 200V, the 20 to 30nt RNA fraction was excised and eluted in 0.3M NaCl. Following separation of the elute from the gel debris using a Spin-X-column (Thermo Fisher Scientific), the small RNA samples were precipitated in 100% ethanol and 1mg/mL glycogen, incubated at -80°C for 30 minutes, centrifuged at 14,000rpm for 25 minutes, washed with 75% ethanol, air dried and resuspended in RNase-free water. Illumina TruSeq libraries were then prepared according to the manufacturer's protocol and the final RNA library concentration was measured by a Qubit 2.0 fluorometer using Qubit dsDNA HS Assay kit (Life Technologies). The size of

the products contained in the libraries were verified using a high sensitivity DNA chip and an Agilent 2100 Bioanalyzer (Agilent Technologies). Finally, a total of 18 miRNA libraries (hypoxic and normoxic SLK, hypoxic and normoxic SLKK, and hypoxic and normoxic BCBL-1 samples, n=3 each) were sequenced using the Illumina HiSeq platform at the Wellcome Trust Centre for Human Genetics (University of Oxford).

2.4.7 Illumina Solexa mRNA-Seq analysis

For mRNA sequencing, adapter sequences were trimmed using the Fastx toolkit. Reads were aligned against two target genomes, human (hg19) and KSHV (Genbank accession number NC_009333.1) using TopHat (Trapnell et al. 2009) to generate spliced alignments. Transcripts were assembled using Cufflinks and Cuffdiff (Trapnell et al. 2010) in order to reveal differentially expressed genes. The significance of mRNA fold changes was determined using the cut-off of an adjusted *P*-value lower than 0.05, based on the Benjamini and Hochberg multiple testing correction. Dr. Martin Reczko contributed to the raw sequencing analysis presented in this thesis. R suite software (http://www.R-project.org) was used for statistical analyses, heatmaps and scatter plots. Raw mRNA data for normoxic SLK and SLKK experiments are available on the NCBI Gene Expression Omnibus (GEO) database under the series accession identifier GSE62830.

2.4.8 Small RNA-Seq analysis

For small RNA sequencing, reads were aligned against known miRNAs from miRbase (version 19.0) using the software package SHRIMP (Rumble et al. 2009) (http://compbio.cs.toronto.edu/shrimp/README) with miRNA specific settings (-o 1 -n 2 -r 30% -h 50% --local -Q --qv-offset 32 --sam). As paired-end sequencing, reads were aligned separately covering the mature miRNA both on the forward and reverse read and

the obtained number of matches were averaged. The match counts were normalised and tested for differential expression using the edgeR package (McCarthy et al. 2012) with default settings. In order to visualize miRNA-Seq profiles, sequencing reads were converted to bedGraph format using BEDtools. The output files were then uploaded and displayed using the UCSC Genome Browser (http://www.genome.ucsc.edu). R suite software (http://www.R-project.org) was used for statistical analyses, heatmaps and scatter plots. Raw miRNA data for normoxic SLK and SLKK experiments are available on the NCBI Gene Expression Omnibus (GEO) database under the series accession identifier GSE62830 (http://www.ncbi.nlm.nih.gov/geo/query/acc.cgi?token=gdkpceecbrcxhaj&acc=GSE62830).

2.5 Protein methods

2.5.1 Protein extraction

At the end of an incubation period, adherent cells were rinsed with cold, sterile PBS twice. Suspension cells were centrifuged, and resuspended in cold, sterile PBS twice. All cells were then lysed and nuclear/cytoplasmic extracts were prepared using either the NE-PER Nuclear and Cytoplasmic Extraction reagents kit with 1X halt-protease inhibitors cocktail (both Pierce, Waltham, MA, USA) and EDTA. Alternatively, whole cell lysates were prepared using radioimmunoprecipitation assay RIPA buffer [0.1% sodium deoxycolate, 25mM Tris-HCl (pH 7.5)] (Millipore, Billerica, MA, USA) with 1X halt-protease inhibitors cocktail (Pierce). Protein extracts were stored at -80°C.

2.5.2 Protein quantification

Protein concentrations were determined using a bicinchoninic acid (BCA) colorimetric assay (Pierce). For calibration purposes, bovine serum albumin (BSA) was serially diluted and used to generate a standard curve. Only standard curves with $R^2 \geq 0.98$ were selected. Flat-bottom, transparent 96-well plates were used for the assay. While protein extractions were thawing on ice, BCA working reagent was prepared using a (1:50) mixture of BCA solution B and BCA solution A (v/v). Nine wells were used for the assay calibration using varying concentrations of BSA (0mg/mL, 50mg/mL, 150mg/mL, 250mg/mL, 500mg/mL, 750mg/mL, 1000mg/mL, 1500mg/mL, and 2000mg/mL). 5µL of BSA or cell lysates were added to the well and 95µL of BCA working reagent was added using a multi-channel pipette. After homogenisation, the plate was incubated at 37°C for 30 minutes. The plate was then read by a SpectraMax 190 spectrophotometer at 562nm (Molecular Devices, Sunnyvale, CA, USA) using the SoftMaxPro software. Absorbance values were recorded and adjusted against the BSA standards by least-squares linear regression.

2.5.3 Antibodies

Primary antibodies and secondary antibodies used in experiments are listed hereafter in **Tables 2.5** and **2.6**, together with antibody dilutions, host species, sources and developing methods. Optimisation for antibody dilution and blocking buffers were routinely made.

Primary antibody				
Description	**Host**	**Source**	**Dilution**	**Molecular Weights**
Anti-LANA, mAb	Rat	Leica Biosystems	1:5000	130-135kDa
Anti-LANA Clone 13B10, mAb	Mouse	Leica Biosystems	1:2000	130-135kDa
Anti-HIF-1α, mAb	Mouse	BD Biosciences	1:1000	93kDa
β-actin Clone AC-74, mAb	Mouse	Sigma-Aldrich	1:10,000	42kDa
Anti-HIF-2α, pAb	Rabbit	Novus Biologicals	1:1000	96kDa

Table 2.5: Primary antibody usage. mAb: monoclonal antibody; pAb: polyclonal antibody. The molecular weight of LANA and the apparent molecular weight on the gel system used in this thesis are different. The apparent molecular weight of LANA is between 98kDa and 191kDa.

Secondary antibody			
Description	**Source**	**Dilution**	**Developing methods**
αM AP conjugate	Promega	1:10,000	Colorimetric
αR AP conjugate	Promega	1:10,000	Colorimetric
αRt AP conjugate	Promega	1:10,000	Colorimetric
αM HRP conjugate	Promega	1:10,000	ECL
αR HRP conjugate	Promega	1:10,000	ECL
αRt HRP conjugate	Promega	1:10,000	ECL
GαM IRDye 800CW (green)	Li-Cor	1:10,000	Li-Cor scanner
GαM IRDye 680CW (red)	Li-Cor	1:10,000	Li-Cor infrared scanner
GαR IRDye 800CW (green)	Li-Cor	1:10,000	Li-Cor infrared scanner
GαR IRDye 680CW (red)	Li-Cor	1:10,000	Li-Cor infrared scanner
GαRt IRDye 800CW (red)	Li-Cor	1:10,000	Li-Cor infrared scanner
GαRt IRDye 680CW (green)	Li-Cor	1:10,000	Li-Cor infrared scanner

Table 2.6: Secondary antibody usage. AP: alkaline phosphatase; HRP: horseradish peroxidase; αR: anti-rat; αRt: anti-rabbit; αM: anti-mouse; GαM: goat anti-mouse; GαR: goat anti-rat; GαRt: goat anti-rabbit.

2.5.4 Western immunoblot

Ten µg to 30µg of protein were mixed with warm 2X lithium dodecyl sulfate (LDS) such that the LDS to sample ratio was 1:4 (v/v). Samples were denatured for 5 minutes at 95°C and subjected to SDS-PAGE (4–12% NuPAGE Bis-Tris) with 1X MOPS running buffer diluted with dH_2O. Approximately 200µL of antioxidant (NuPAGE) was added to the buffer in the inner chamber of the electrophoresis unit. A voltage of 200V was applied until the bromophenol blue loading dye had reached the bottom of the gel (~1hr). The gel cassette was then disassembled and the gel was left in 1X transfer buffer, 10% Methanol, and 1:10,000 antioxidant mixture for 20 minutes (all NuPAGE). The gel was then transferred onto a nitrocellulose membrane by an iBlot apparatus for 8 minutes (all Invitrogen). The membrane was blocked with either 5% w/v nonfat dry milk in 1X TBST (10mM Tris-Hcl, pH 80, 150mM NaCl, and 0.05% Tween 20) or 1:1 (v/v) Odyssey blocking buffer and TBST (Li-Cor Biosciences, Lincoln, NE, USA) overnight at 4°C. Blots were incubated with the appropriate primary and secondary antibodies for varying lengths of time; being washed twice with TBS or TBST in between incubations. Typically, secondary antibody incubations were carried out in TBST or in a 1:1 (v/v) mixture of Odyssey blocking buffer and TBST, for no more than an hour at room temperature.

Over the course of this thesis, several methods were used to develop immunnoblots so protein bands could be visualised: horseradish peroxidase (HRP)-based enhanced chemiluminescence (ECL), alkaline phosphatase (AP)-based colorimetry, or infrared (IR)-based scanning. For ECL, the working solution was prepared using a stable peroxide solution and a lumino/enhancer solution in equal parts provided by the SuperSignal West chemiluminescent kit (Pierce). The HRP substrate mixture was then added to the membrane and incubated for 5 minutes in the dark to obtain either pico- of

femtogram-level detection. Autoradiography film was finally exposed to the membrane and protein bands were visualised. For the colorimetric method, a mixture of 5-bromo-4-chloro-3-indolyl-phosphate (BCIP) and nitro blue tetrazolium (NBT) was used as AP substrate (Western Blue stabilized substrate for alkaline phosphatase, Promega). Typically, the blot was allowed to develop for 15 minutes before being scanned. For the IR-based scanning method, the blot was rinsed twice and stored in TBS away from the light at 4°C. Scanning was performed using the Li-Cor Odyssey CLx imaging system coupled with the Image Studio software. Images were later adjusted for contrast and intensity. Of those three different types of developing methods, the Li-Cor system came out on top with an easy experimental set up which does not require additional substrate incubation and allows for accurate, normalised quantitation. Additionally, a blot can be simultaneously imaged using both the red (680nm) and green (800nm) channels, which means that two antibodies can be detected at once and no further blot stripping is required.

2.6 Statistical methods

2.6.1 Gene Set Enrichment Analysis (GSEA)

GSEA (Subramanian et al. 2005) was performed by the JAVA program using the c3 collection of Molecular Signature Database, MSigDB (http://www.broadinstitute.org/gsea/msigdb/index.jsp). Briefly, 221 miRNA families are each linked to a separate gene set consisting of putative targets containing a complementary 3'-UTR miRNA binding motif. The input gene list was generated by our mRNA-Seq differential expression analysis and was tested for enrichment in targets belonging to individual miRNA target genesets. A *P*-value and a false discovery rate

(FDR), estimating the statistical significance of enrichment, were calculated for each miRNA gene set.

2.6.2 Ingenuity Pathway Analysis (IPA)

Pathway analysis and inverse correlations between expression levels of differentially expressed miRNAs and their respective target mRNAs were analysed using Ingenuity Pathway Analysis (IPA, Ingenuity Systems, Redwood City, CA, USA; www.ingenuity.com). This *in silico* analysis software reveals enrichment for molecular networks and signalling pathways. IPA combines different target prediction algorithms such as TargetScan, TarBase, miRecords and the Ingenuity Knowledge Base, to provide medium to high confidence predictions and experimentally observed interactions. Importantly, the tool 'MicroRNA Target Filter' allowed for the integration of miRNAs with mRNA targets that were both differentially expressed. Inverse expression pairing between miRNA and mRNA expression levels was implemented to refine the analysis. Further filtering options were applied such as a confidence parameter.

2.6.3 t-Test

All experiments were performed at least in triplicate biological replicates, and in some cases (qPCR) in triplicate technical replicates, unless otherwise specified. Error bars represent the standard deviation for these replicates. *P*-values were computed using a two-tailed student's t-Test.

3

Profiling the cellular miRNA and mRNA responses to KSHV infection

3.1 Introduction

Studying how Kaposi's sarcoma-associated herpesvirus (KSHV) infection affect cellular miRNA expression is important in understanding the way the virus manipulates the host cells, as well as the cellular responses to KSHV. However, the mechanisms of this regulation have not been fully explored, in part because of the lack of KSVH infected/uninfected cell models. This chapter addresses promising avenues for evaluating effects of KSHV infection on the host cell, both at the miRNA level, and the mRNA level, using the SLK/SLKK model.

3.1.1 Gene expression profiling of KSHV infected cells to date

As with other chronic viruses, infection with KSHV results in a number of changes in the host cells. Many of these are mediated by KSHV to evade the innate and adaptive immune responses, prevent cell cycle arrest, inhibit apoptosis, modulate cellular signalling pathways, and facilitate lifelong infection in the host. Conversely, other changes occur as a result of the host defence response to viral infection.

The human genome encodes thousands of miRNAs (Kozomara & Griffiths-Jones 2011). A limited number of viruses, including KSHV, also encode their own miRNAs (Pfeffer et al. 2004). Similar to other herpesviruses, KSHV expresses 12 viral precursor miRNAs (pre-miRNAs) located within the latency-associated region and these yield 25 mature miRNAs known to play a role in viral pathogenesis (Samols et al. 2007; Gottwein & Cullen 2008). Being non-immunogenic, virally encoded miRNAs are potentially attractive tools for viruses as they can interfere with the host machinery without being detected by the host immune system.

In addition, a number of KSHV-encoded proteins can effect substantial changes in host cell gene expression, either by directly acting on one or more steps in protein expression, or by indirect mechanisms (e.g. cell signalling pathways). In particular, KSHV proteins expressed during viral latency, such as latency-associated nuclear antigen (LANA) or viral FLICE inhibitory protein (v-FLIP), can directly induce changes in expression of certain mRNAs or miRNAs to facilitate the latent infection. These changes in cellular miRNA expression can in turn affect the expression of target genes. In addition, changes in cellular miRNAs may occur as part of the host response to viral infection.

Transcriptome profiling techniques such as RNA-sequencing and microarrays have been used to study PEL cells, which are a valuable model system for latent KSHV infection

(Gottwein et al. 2011). However, a limitation of this approach is the lack of otherwise identical uninfected control lines. To bypass this restriction, differential expression studies using microarrays or high-throughput sequencing techniques have explored other KSHV infection models, such as KS lesion samples and normal skin tissues (Catrina Ene et al. 2014; O'Hara et al. 2009; Wu et al. 2014), mock and KSHV-infected primary lymphatic endothelial cells (T.-Y. Chang et al. 2011; Lagos et al. 2010), or the human epithelial SLK/SLKK (SLK+rKSHV.219) model (Abend et al. 2012; Arias et al. 2014; Vieira & O'Hearn 2004).

3.1.2 Approach to investigate miRNA-mRNA changes in KSHV infected cells

Although previous studies have provided useful insights into KSHV infection and disease pathogenesis, to date there has been no report of a next-generation sequencing study combining both mRNA and miRNA expression profiles in KSHV-infected and uninfected control cells. Here, this chapter presents the outcome of a comprehensive analysis comprised of both small RNA-sequencing and poly(A) enriched mRNA-sequencing in latently infected SLKK cells and uninfected control SLK cells. While these cells are derived from renal cancer and differ somewhat from the principal target cells in KSHV malignancies, advantages of this cell system are that SLKK cells can be compared to an uninfected counterpart and also that they have very low levels of spontaneous lytic KSHV replication. Thus the results reported here focus on changes induced by latent infection, rather than those induced by an acute host response or expression of lytic KSHV genes.

Furthermore, the combined analysis of miRNA and mRNA differential expression of SLK and SLKK cells has enabled the identification of a number of viral-induced miRNA changes that were associated with expected inverse changes in the predicted

target mRNAs, suggesting that miRNAs were mediating many of these changes. This chapter further investigates the functions and pathways in which those miRNA-mRNA pairs were involved and highlights their potential role in pathogen-influenced mechanisms. Overall, these findings provide evidence for a broad posttranscriptional regulatory network of miRNAs and their mRNA targets that will deepen the understanding of KSHV effects on the host cellular machinery and may inform further studies of specific miRNA-mRNA interactions in KSHV-infected cells.

3.2 Comparison of miRNA expression profiles reveals more down-regulated than up-regulated cellular miRNAs in KSHV-infected cells

Differential analysis was performed on the cellular miRNA expression levels between the small RNA libraries of non-infected and KSHV-infected cell cultures. For the purpose of this analysis, thresholds of ≥2 times fold change (FC) in expression ($\log_2$ FC ≤-1 and ≥1) and a *P*-value ≤0.05 were applied. Overall, 153 human mature miRNAs were found significantly altered by KSHV infection in SLKK vs. SLK cells (**Figure 3.1 A-B**). Interestingly, there were substantially more suppressed than induced miRNAs: 111 vs. 42 respectively. In terms of expression fold change, this tendency was also apparent amongst the miRNAs with the greatest changes, which extended to an 11-fold down-regulation but only to a 4-fold up-regulation in $\log_2$ scale (**Figure 3.2 A**).

Amongst the most dysregulated miRNAs that were expressed in relatively high amounts (threshold of mean miR count >10), miR-224-5p (-11 $\log_2$ FC), miR-452-5p and miR-887 (both -9 $\log_2$ FC), were significantly down-regulated, whereas the greatest relative induction was seen for miR-708-5p/3p and 3614-5p (all ~2 $\log_2$ FC) (**Figure 3.3**). It is noteworthy that 42 of the 111 miRNAs that were observed to be repressed by KSHV

infection are located in the same genomic region, the 14q32 miRNA cluster (**Figure 3.4**). For example, 14q32 miRNAs, miR-410, and miR-409-5p/3p, were significantly repressed -6 $\log_2$ FC upon KSHV infection (**Figures 3.2A** and **3.3**). Of note, while both arms of the miR-409 stem-loop were down-regulated, miR-409-3p had a higher relative abundance than miR-409-5p. Interestingly, there has been a previous report of frequent loss of 14q32 in PEL cell lines (Luan et al. 2010), which suggests that down-regulation of this region at the DNA level may be beneficial for the survival of KSHV-infected cells. To test whether SLKK cells were missing 14q32 DNA, eight individual regions of the genomic DNA of SLK and SLKK cells were interrogated by PCR (**Figure 3.5**). It was found that all tested portions of the 14q32 cluster were present in uninfected as well as KSHV-infected cells, suggesting post-transcriptional mechanisms lead to the substantial down-regulation of 14q32 miRNAs.

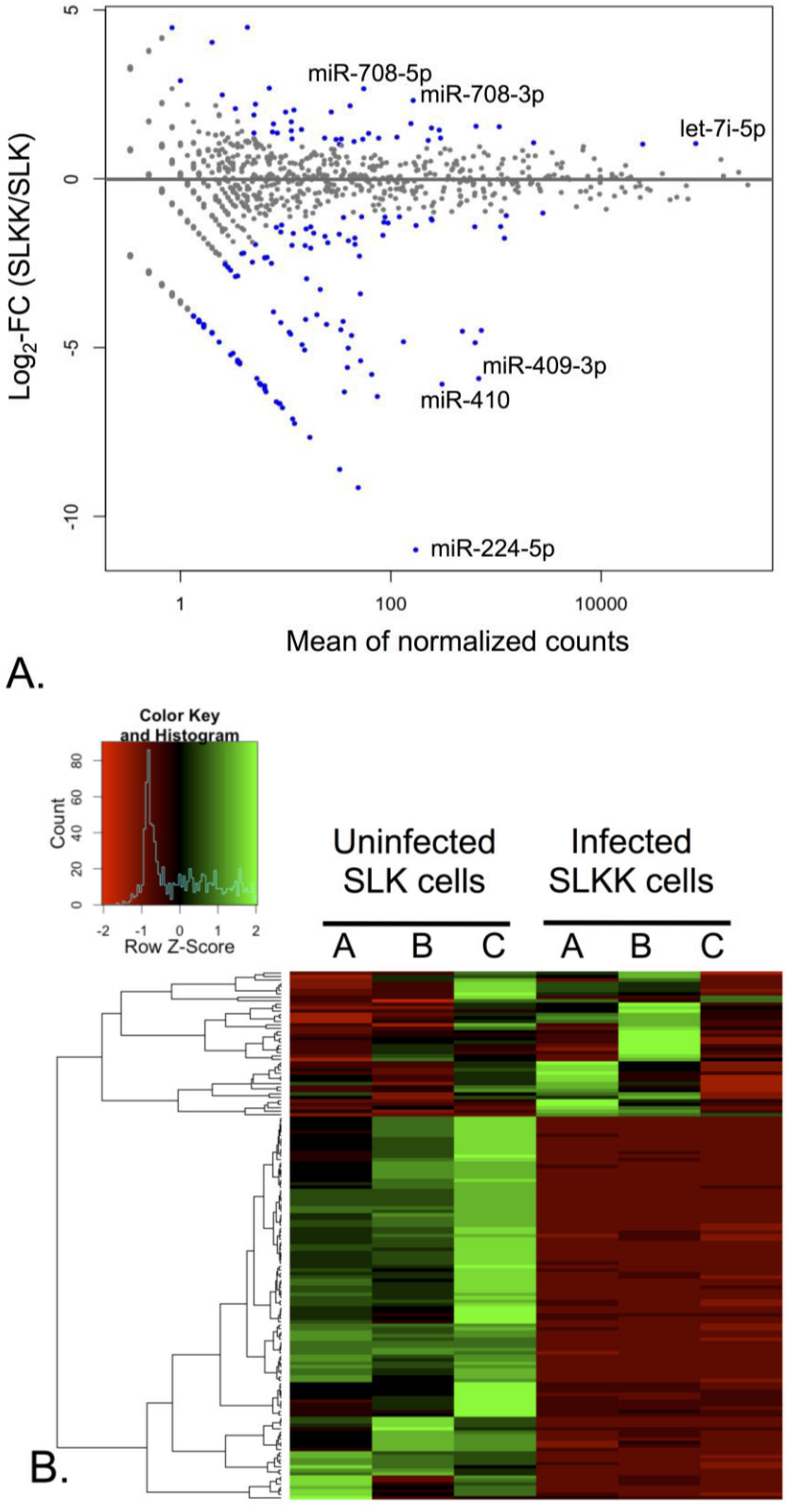

Figure 3.1: Expression of miRNAs in the analysed small RNA libraries

Figure 3.1: Expression of miRNAs in the analysed small RNA libraries.

A. Scatterplot of the transcriptome of KSHV-infected versus uninfected cells. The X-axis represents the average of the normalised miR read counts across all samples. The Y-axis represents the log-transformed expression fold change between SLKK and SLK cells. Blue dots are differentially expressed genes with a $P \leq 0.05$, while grey dots are those with a $P > 0.05$.

B. Heatmap of miRNA changes between SLK and SLKK cells in the six individual replicates (three SLK and three SLKK). Presented is the relative expression of 153 significantly deregulated cellular miRNAs in KSHV-positive vs. KSHV-negative cells (P-value ≤ 0.05, $\log_2$ FC ≤ -1 or ≥ 1). Using uncentered Pearson correlation as the distance metric, an unsupervised hierarchical heatmap was generated, with each row representing a miRNA and each column representing a biological replicate. Red, black and green denote low, median and high relative miRNA expression, respectively.

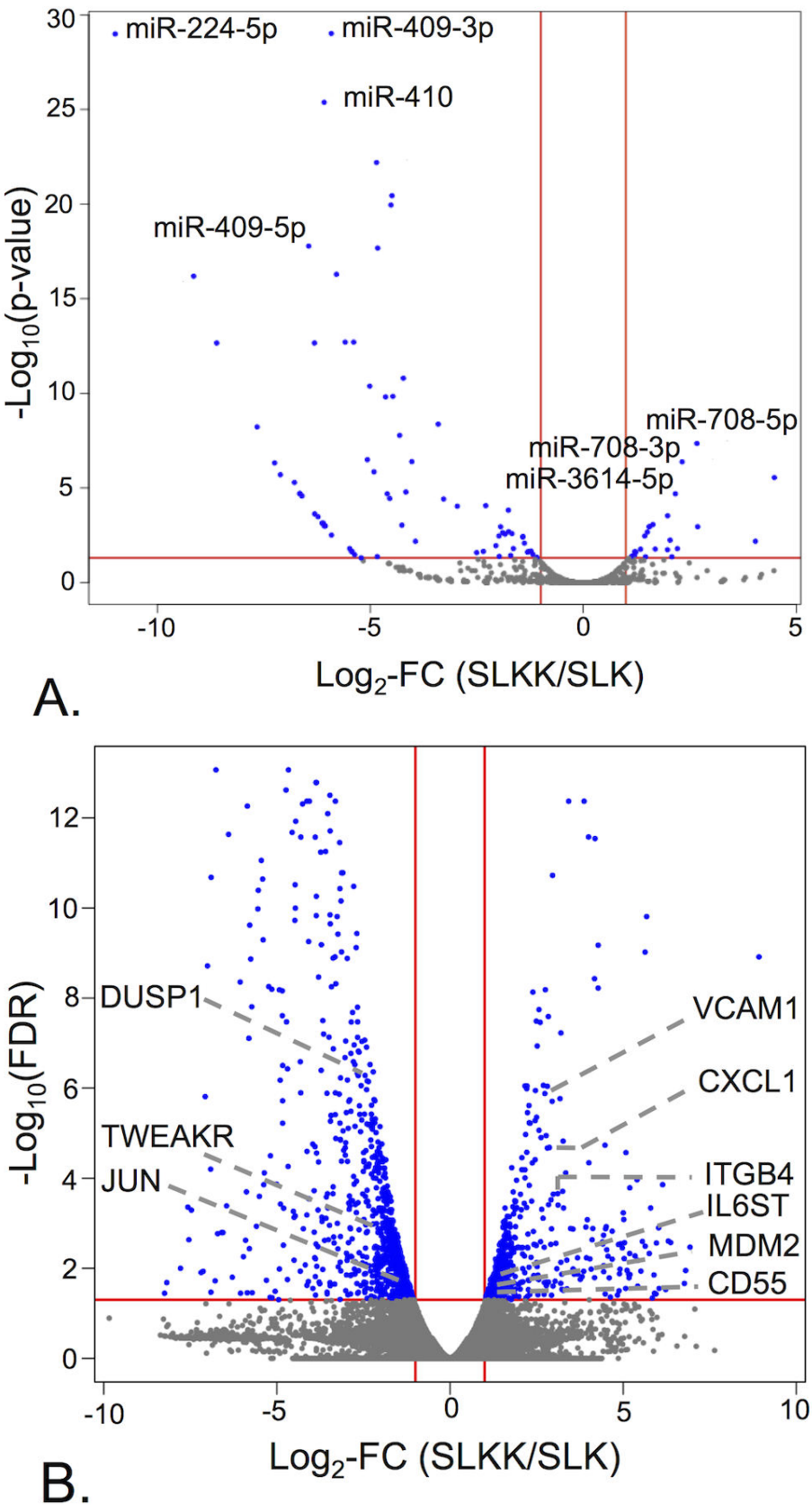

Figure 3.2: Volcano plots of miRNA and mRNA differential expression.

Figure 3.2: Volcano plots of miRNA and mRNA differential expression.

A. Volcano plot of differentially expressed human mature miRNAs in KSHV-infected vs. uninfected cells. Vertical red lines indicate the threshold for a relative expression fold change (FC) of 2 or -2 compared to uninfected controls. The horizontal red line represents the threshold of a 0.05 *P*-value. Thus, the blue points lying in the top right and top left sectors are significantly up-regulated and down-regulated, respectively, in KSHV-positive vs. KSHV-negative cells ($P \leq 0.05$, FC ≤ -2 or ≥ 2). Selected miRNAs that have been validated by qRT-PCR are labelled. Individual data points that are not significant ($P > 0.05$) are shown in grey.

B. Volcano plot of differentially expressed mRNAs in KSHV-infected vs. uninfected cells. The plot is depicted as in **Figure 3.2A**, with vertical and horizontal red lines similarly representing the thresholds of a fold change of 2 or -2, and of a false-discovery rate (FDR) of 0.05, respectively.

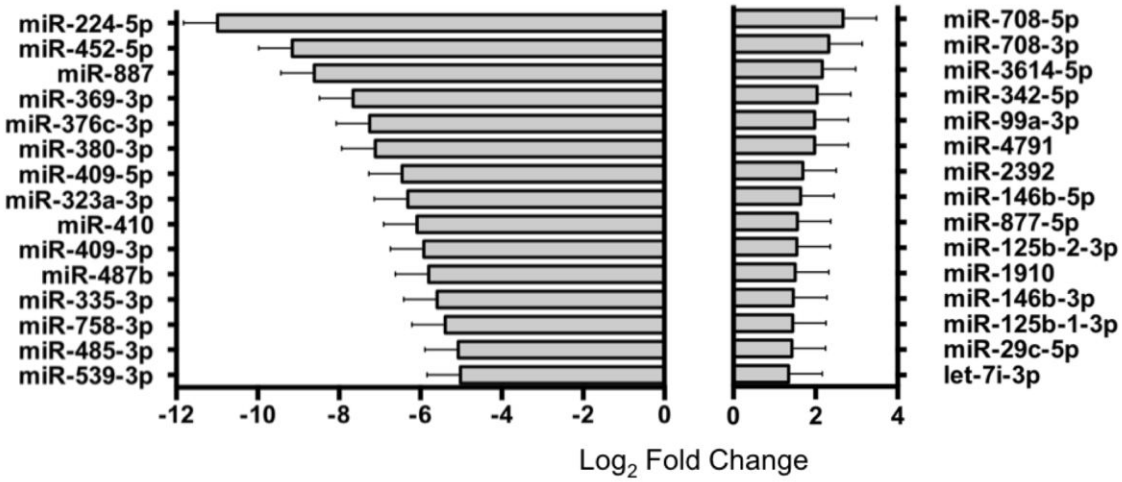

Figure 3.3: Top 15 repressed and induced miRNAs in KSHV-positive vs. uninfected cells. Bars below and above the y-axis show the top 15 repressed and induced miRNAs, respectively, in KSHV-positive cells compared to uninfected controls ($P \leq 0.05$). Presented here are only the medium to highly expressed miRNAs (an average miR count of 10 or more across all replicates; i.e. threshold of miR counts sum higher than 60).

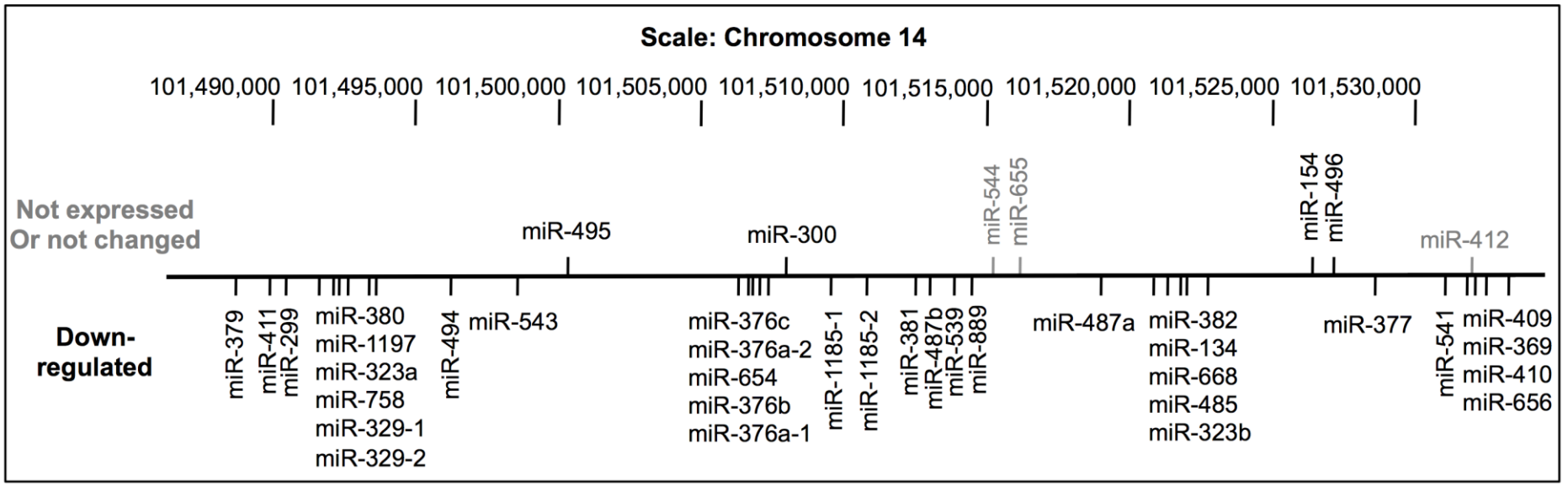

Figure 3.4: Genomic map of the cluster of miRNAs at the 14q32 locus.

The miRNA cluster B of the 14q32 imprinted region is illustrated here. 34 out of 41 (83%) miRNAs from the 14q32 miRNA cluster have at least one arm that is down-regulated. Also, counting the 3p and 5p arms separately, 42 out of 111 (38%) miRNAs that are down-regulated by KSHV infection are located within this miRNA cluster. Below the line, in black are miRNAs that are significantly down-regulated by at least -1 $\log_2$ FC ($P \leq 0.05$). miRNAs above the line in grey are not significantly altered by KSHV infection. Those above the line in black are not expressed in the SLK/SLKK cell model.

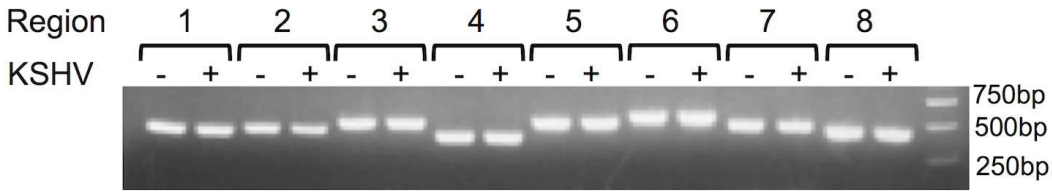

Region #	Location	Chromosome coordinates (chromosome 14)	Amplicon size
1	Pre cluster Upstream of DLK1	100,684,998 – 100,685,391	394bp
2	DLK1	100,730,840 – 100,731,242	403bp
3	Methylated region	100,792,696 – 100,793,164	469bp
4	MEG3	100,853,033 – 100,853,397	365bp
5	RTL1	100,882,975 – 100,883,468	494bp
6	miRNA Cluster	101,065,175 – 101,065,721	547bp
7	DIO3	101,562,907 – 101,563,381	475bp
8	Post cluster Downstream of DIO3	101,623,210 – 101,623,640	431bp

Figure 3.5: DNA presence across the 14q32 cluster. Several regions of the genomic DNA of KSHV-infected and uninfected samples were interrogated. This qualitative assessment shows that all regions were present in both infected and uninfected samples.

3.3 mRNA-Seq analysis of SLKK cells

In parallel with these miRNA studies by deep sequencing, the global changes in gene expression associated with chronic latent KSHV infection was investigated in order to assess the effects of the miRNA changes on their predicted targets. The cellular mRNA expression levels of the poly(A) enriched RNA libraries of non-infected SLK cells were compared to those of infected SLKK cells. In all, 1,570 cellular genes, ~5% of all expressed genes, were significantly altered with either ≤-1 or ≥1 $\log_2$ FC (linear FC ≥2) and an adjusted *P*-value (FDR) ≤0.05 (**Figures 3.2 B** and **3.6 A-B**). This included 980 repressed and 590 up-regulated mRNAs.

Some of these differentially expressed genes have been previously reported to be associated with KSHV infection. For example, in concordance with previous findings, DUSP1, JUN, PLAUR and TWEAKR (TNFRSF12A) were repressed whereas MDM2, CD55, CXCL1, IL6ST and ITGB4 were induced by KSHV infection (Abend et al. 2010; Carroll et al. 2004; Q. Chang et al. 2011; Ueda et al. 2011). Also, KSHV infection induced VCAM-1 (3 $\log_2$ FC), which is a vascular endothelial marker that has been linked to tumour angiogenesis and oncogenesis (Ding et al. 2003) (**Figure 3.2 B**).

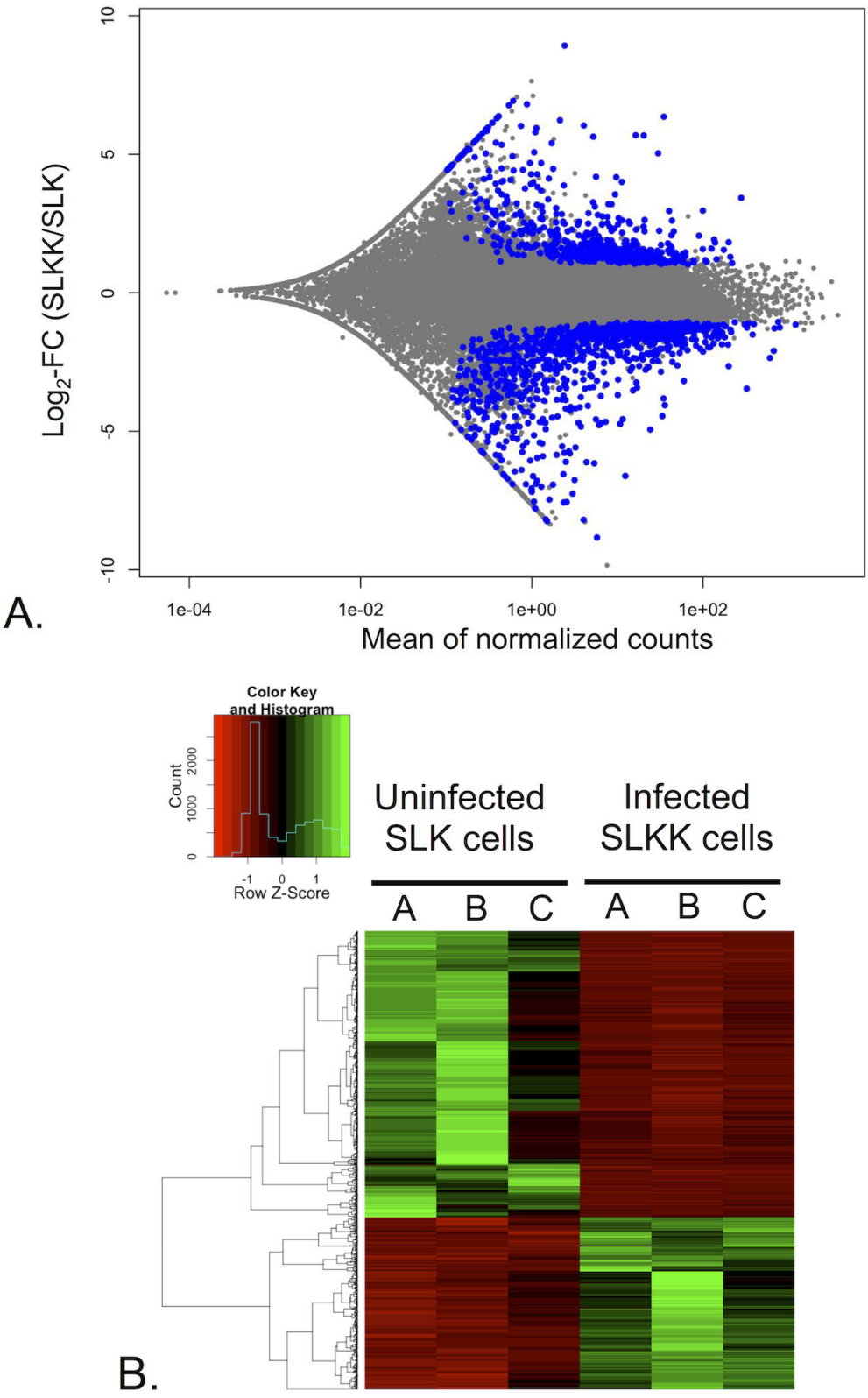

Figure 3.6: Expression of mRNAs in the poly(A) enriched RNA libraries.

Figure 3.6: Expression of mRNAs in the poly(A) enriched RNA libraries.

A. Scatterplot of the transcriptome of KSHV-infected versus uninfected cells. The X-axis represents the average of the normalised read counts across all samples. The Y-axis represents the log_2-transformed expression fold change between SLKK and SLK cells. Blue dots are differentially expressed genes with a FDR $\leq$0.05, while grey dots are those with a FDR >0.05.

B. Heatmap of mRNA changes between SLK and SLKK cells in the six individual replicates (three SLK and three SLKK). Presented is the relative expression of 1,570 significantly deregulated cellular mRNAs in KSHV-positive vs. KSHV-negative cells (FDR $\leq$0.05, log_2 FC $\leq$-1 or $\geq$1). Using uncentered Pearson correlation as the distance metric, an unsupervised hierarchical heatmap was generated, with each row representing a mRNA and each column representing a biological replicate. Red, black and green denote low, median and high relative miRNA expression, respectively.

3.4 Validation of miRNA differential expression patterns by Taqman assay

To validate the results observed in our miRNA sequencing data, Taqman assays (qRT-PCR) were performed on several human miRNAs, with a focus on those with the greatest fold changes. Amongst the most significantly down-regulated miRNAs with high read counts were miR-224-5p, miR-410, miR-409-3p and -5p, whilst the most up-regulated miRNAs were miR-3614-5p, miR-708-3p and -5p. Because of the prominence of the miRNA repression, the differential expression of miR-212-3p, a miRNA that was less strikingly down-regulated, was also verified. Additionally, the expression of miR-210 was verified by qRT-PCR. This miRNA is of particular interest because it is a HIF-inducible miRNA and because KSHV infection increases HIF levels (Carroll et al. 2006). The levels of miR-210 by miRNA-Sequencing were slightly increased during KSHV infection, although the change did not achieve the experimental significance cut-off (FC =0.65 and P =0.13). **Figure 3.7A** shows the $\log_2$-transformed expression fold change of these miRNAs between SLKK and SLK cells, assessed by both miRNA-Sequencing and Taqman assay. The differential expression of all nine miRNAs tested by Taqman assay was significant and consistent with our sequencing data. Pearson correlation coefficient (r) between the two measurement methods of the selected miRNAs indicates strong and significant positive correlation (r=0.98, $P < 10^{-5}$).

The relative expression of the four most down-regulated miRNAs seen in latently infected SLKK cells, three of which belong to the 14q32 cluster, was also examined following *de novo* KSHV infection of SLK cells. At five days post infection (5dpi), we found that two of these four miRNAs (miR-224-5p and miR-409-3p) were similarly down-regulated (n=3) (**Figure 3.7B**). Also, miR-409-5p showed a trend for down-regulation, while miR-410 did not significantly change. A lower KSHV episome copy

number in the *de novo* infected SLK cells as compared to SLKK cells could account for these changes. These results provide additional evidence that a proportion of the miRNA changes in SLKK vs. SLK cells are in response to viral infection. These results also suggest that some of the changes may only be observed in cells latently infected for a period of time.

3.5 Investigation of miRNA target regulation

In an effort to correlate the expression levels of miRNAs to their respective target genes, the expression of known and predicted target mRNAs for three miRNAs were validated by Taqman assay (miR-409-3p, miR-409-5p, and miR-708-5p). miR-409-3p, a miRNA down-regulated in our sequencing data, is known to target fibrinogen beta (FGB) and pro-metastasis gene radixin (RDX) (Fort et al. 2010; Zheng et al. 2012). The other arm, miR-409-5p, which is also down-regulated in SLKK vs. SLK cells, is predicted to target p53-inhibitor MDM2, according to Ingenuity Pathway Analysis (IPA). Our mRNA sequencing analysis indicated an induction of FGB, MDM2 and RDX (P = $8.6x10^{-9}$, $2.1x10^{-3}$, $1.6x10^{-3}$, respectively). This was also consistent with our qRT-PCR validation results showing a ~2 log_2-fold induction for these three genes (**Figure 3.8A**).

Moreover, miR-708-5p, which was found up-regulated ~3 log_2 FC by miRNA-Sequencing and ~2 log_2 FC by qRT-PCR, is known to target pro-apoptotic protease caspase-2 (CASP2) (Song et al. 2013). Consistent with this, the qRT-PCR data demonstrated a small but significant reduction in CASP2 levels in KSHV-infected SLKK cells compared to control SLK cells. According to TargetScan, miR-708-5p is also predicted to bind the 3'UTR of leukaemia inhibitory factor LIF mRNA and indeed LIF was found significantly down-regulated by qRT-PCR (**Figure 3.8A**). The strong reproducibility between both the miRNA-Seq and mRNA-Seq, and the qRT-PCR

analyses provides evidence that the RNA-Seq was very robustly analysed and enabled a valid assessment of the miRNA and gene expression profiles.

In order to further investigate whether the changes in mRNA targets in SLKK cells could be a result of differential miRNA expression, transfection assays were carried out to re-express miRNAs that were decreased in either SLKK cells (miR-409-3p and -5p) or SLK cells (miR-708-5p), as compared to their counterparts. Transfection of miR-409-3p in SLKK cells led to a decrease in two of its known targets, fibrinogen beta and radixin. Additionally, transfection of miR-409-5p in SLKK cells led to a significant decrease in the expression of its predicted target, the p53-inhibitor MDM2. This is the first report providing experimental evidence that miR-409-5p targets MDM2. Finally, transfection of miR-708-5p in SLK cells resulted in a dramatic (80%) decrease in its target, caspase-2; it also led to the significant decrease of predicted target LIF (~40%). This provides evidence that the up-regulation of miR-708-5p in SLKK cells is likely causing the observed down-regulation of caspase-2 (**Figure 3.8B**).

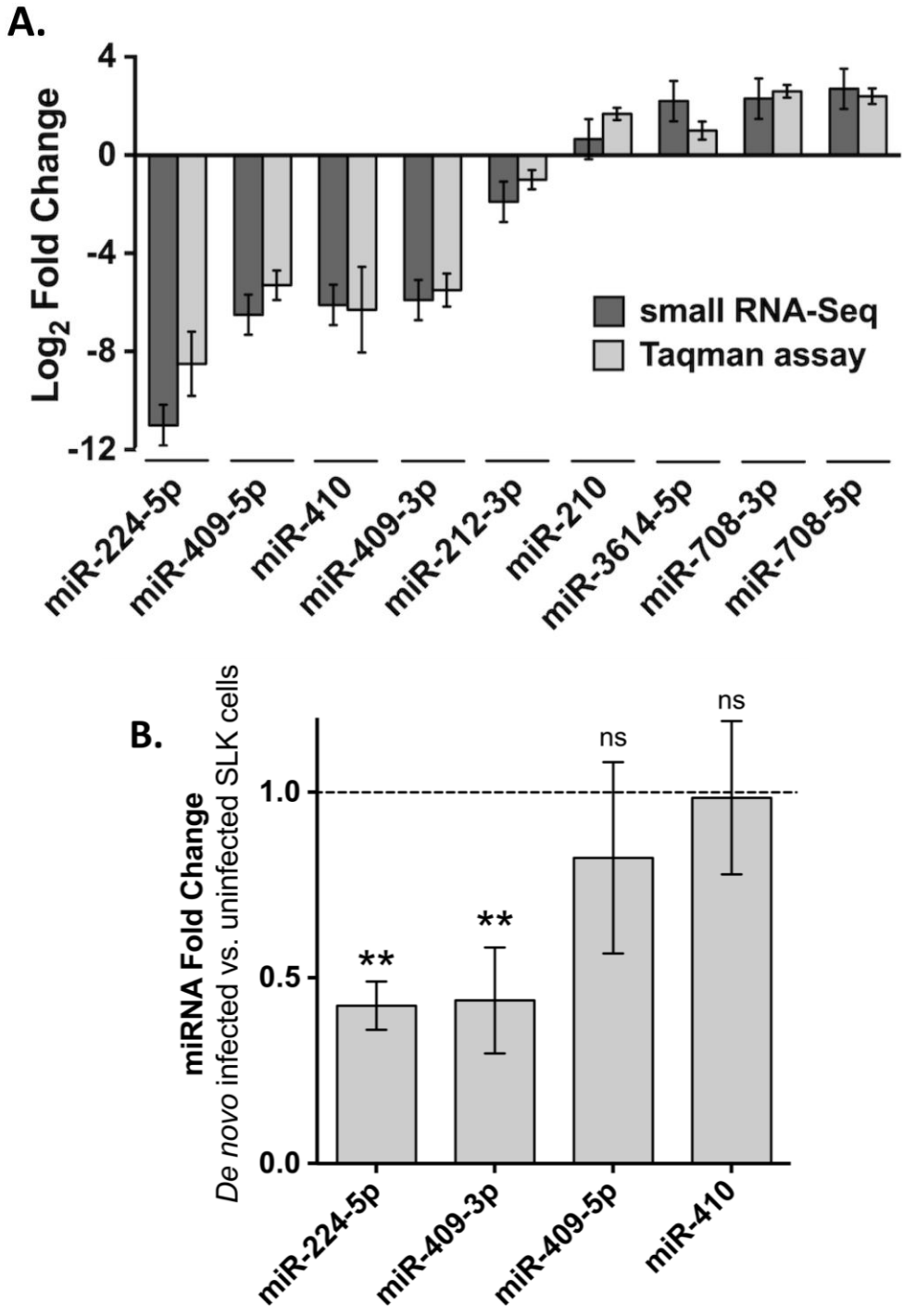

Figure 3.7: Analysis of miRNA expression in latent and *de novo* KSHV-infected cells.

Figure 3.7: Analysis of miRNA expression in latent and *de novo* KSHV-infected cells.

A. Data represent the average log_2-transformed fold change of expression between latently infected SLKK cells and uninfected SLK cells, measured either by small RNA sequencing (black bars) or Taqman assay (grey bars). All the changes are significant ($P \leq 0.05$) except that of miR-210 detected by miRNA-Seq.

B. Effects of *de novo* KSHV infection on miRNAs seen down-regulated in the SLK/SLKK model. SLK cells were exposed to KSHV and after five days, changes in specific miRNAs were assessed by Taqman assay. The dotted line indicates the normalised level of these miRNAs in uninfected SLK cells. *P*-values were calculated using Student t-test. ** indicates $P \leq 0.01$. ns: not significant.

Expression levels of mature miRNAs were evaluated using the comparative Ct methods (2-deltaCt). Transcript levels of RNU43 were used for sample normalisation. Bars depict the mean of three independent experiments; error bars reflect the standard deviation of the log_2 FC ratios.

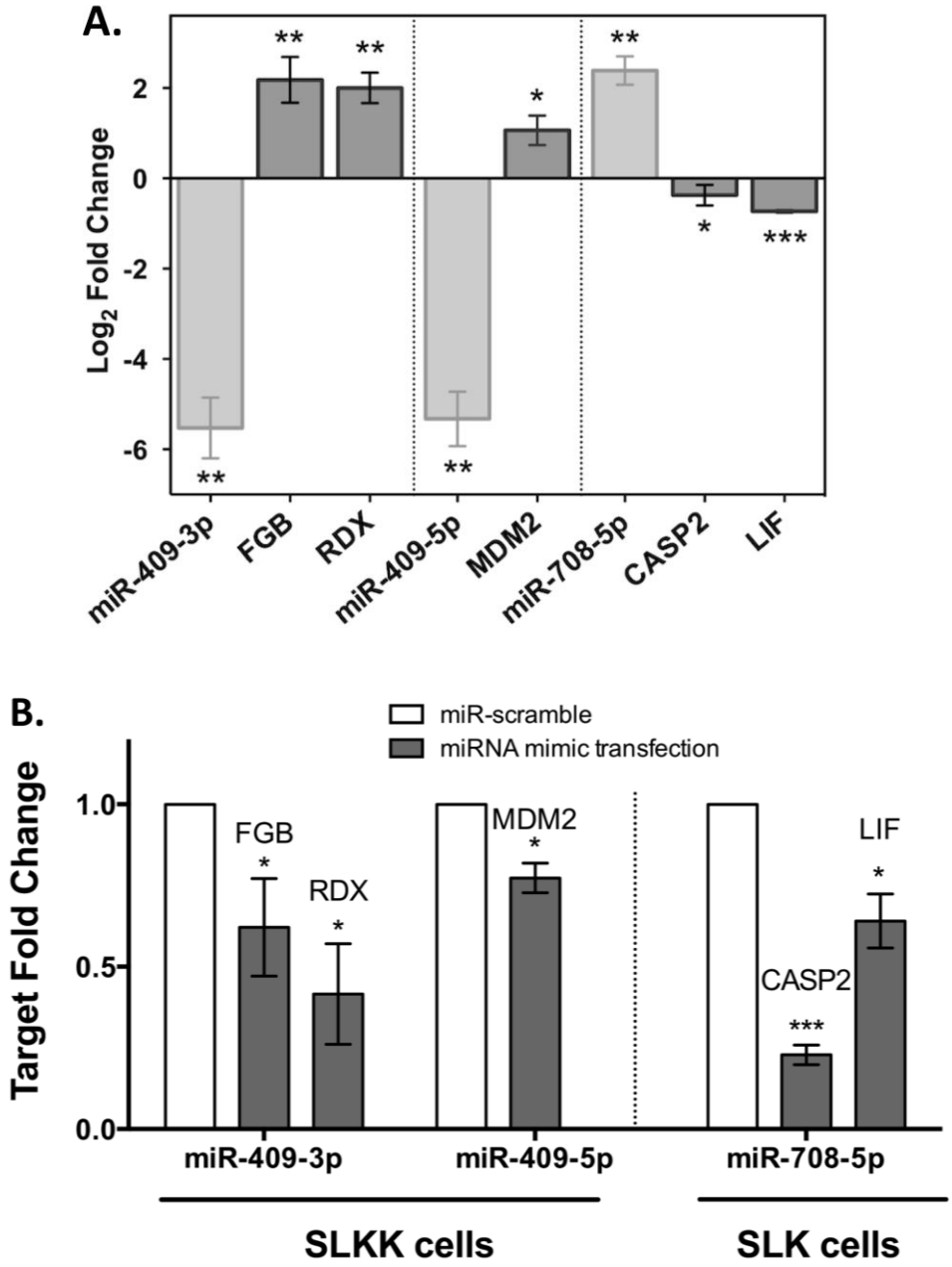

Figure 3.8: Differential expression of miRNA and their known or predicted mRNA targets.

Figure 3.8: Differential expression of miRNA and their known or predicted mRNA targets.

A. miRNA expression in latently infected SLKK cells compared to uninfected SLK cells and the mRNA expression of their corresponding targets (Taqman and qRT-PCR assays). miRNAs and mRNAs are shown in light and dark grey, respectively. miR-409-3p targets fibrinogen beta (FGB) and radixin (RDX). miR-409-5p is predicted to target MDM2. miR-708-5p targets caspase-2 (CASP2) and is predicted to target leukemia inhibitor factor (LIF). *P*-values were calculated using Student t-test. *, ** and *** indicate $P < 0.05$, 0.01 and 0.001, respectively.

B. Effect of miRNA transfection on target regulation. Scramble control (miR-scramble) and miRNA mimics for miR-409-3p, miR-409-5p and miR-708-5p were transfected in either SLK or SLKK cells. Quantitative real-time polymerase chain reaction revealed the target expression for these miRNAs and the relative value is presented as the mean ± standard deviation based on 3 independent experiments. Statistical analysis and its representation are as in **Figure 3.8A**.

3.6 Two integrated miRNA and mRNA analyses show post-transcriptional regulatory networks relevant to KSHV pathogenesis

A number of factors can lead to the changes observed at the mRNA level in virus-infected cells. However, because of the inverse relationship between the miRNA and the mRNA changes, it was hypothesised that at least some of the changes in mRNA expression levels in infected cells may be caused by the differentially expressed miRNAs. It was further hypothesised that these miRNA-mRNA pairs may play a role in KSHV infection or in the cellular response to chronic virus infection, and also in the pathogenesis of KSHV-related diseases.

3.6.1 Gene Set Enrichment Analysis

To formally explore this hypothesis, MSigDB, a function of Gene Set Enrichment Analysis (GSEA), was used to investigate the enrichment of the differentially expressed genes in targets belonging to distinct miRNA families. A miRNA family is determined by its seed region, a 6-8 nucleotide sequence that is located at the 5' end of the miRNA and is able to bind target mRNA, promoting its degradation. Using RNA-Seq data, both up-regulated and down-regulated genes were identified in the SLK/SLKK model. The GSEA output miRNA list was then compared to the miRNA-Seq data and selected for those miRNAs whose up-regulation is associated with the observed target down-regulation and then those whose down-regulation was associated with target up-regulation. This analysis enabled the pairing of four up-regulated miRNAs with 74 down-regulated targets and 17 down-regulated miRNAs with 195 up-regulated targets overall (**Table 3.1**). These findings support the hypothesis that some of the changes in gene expression from cells latently infected with KSHV are caused by reciprocal expression changes in the miRNA that target those genes.

3.6.2 Ingenuity Pathway Analysis

A complementary approach for integration of miRNA and mRNA datasets is to use Ingenuity Pathway Analysis (IPA), which has an extensive collection of both known and predicted targets. IPA gathers comprehensive miRNA targeting information by combining multiple target prediction tools (TargetScan, miRecord and TarBase). **Figure 3.9** summarises the IPA data mining process using both sequencing datasets. Because miRNAs are known to effect relatively small changes in target mRNA expression and because changes induced by poorly expressed miRNAs might be particularly hard to detect at the target level, the results reported here focused on the medium to highly expressed miRNAs that were significantly affected by KSHV infection. To do this, a threshold of 60 was applied to the total miR read count across all replicates (n=6), preventing any bias between the two experimental conditions (infected vs. uninfected) and hence corresponding to an average cut-off of 10 reads per replicate.

Of the 153 differentially expressed miRNAs, 89 met this average read count cut-off. IPA then identified 50 of these 89 miRNAs that had either predicted or validated targets (a total of 12,964 targets). Of these 50 miRNAs, 48 had targets in the list of differentially expressed mRNAs generated by the sequencing analysis, for a total of 1,117 targets (linear FC $\geq$2 and FDR $\leq$0.05). Interestingly, each of the 48 miRNAs targeted at least one gene that was affected in the expected direction. In total, the differential expression of 814 out of 1,117 (73%) of those target genes was inversely correlated to that of their respective miRNAs, suggesting that at least part of the differential mRNA expression was in fact a result of changes in miRNA expression.

To adopt a conservative approach, the dataset was further filtered using experimentally observed or highly predicted target correlations. After this filter, 45 miRNAs targeting

480 mRNAs remained, with each paired interaction being inversely correlated (**Table 3.2**). Of these, eight miRNAs were paired with 34 target genes that had been experimentally determined (**Table 3.3**), and 17 miRNAs had targets directly involved in pathogen-influenced signalling pathways (**Figure 3.10**). It was calculated that a third of IPA miRNA filter results overlapped with those of MSigDB. However, two third of the MSigDB matched IPA analysis, confirming the effectiveness of the IPA analysis.

Using these 480 differentially expressed mRNAs as input, pathway analysis revealed an enrichment in several signalling pathways that could be relevant to KSHV infection or disease pathogenesis, such as "regulation of the epithelial-to-mesenchymal (EMT) transition pathway", "IL-8 signalling", "clathrin-mediated endocytosis signalling" and "Wnt/β-catenin signalling" (**Table 3.4**). Of note, EMT plays a central role in cancer progression and is promoted by KSHV through Notch-induced ZEB1, a transcription factor up-regulated in this study (Gasperini et al. 2012). Also, the Wnt/β-catenin pathway, which regulates tumour development and cell proliferation, is altered by latency-associated nuclear antigen LANA, a major KSHV latency protein suggesting multiple viral mechanisms that achieve the same result (Fujimuro et al. 2003). Finally, the enrichment of the interleukin-8 signalling pathway is noteworthy in that KSHV ORF74, which plays a key role in KS pathogenesis, is a constitutively active viral homologue to the interleukin-8 receptor. Altogether, these findings further support the role of miRNAs and their transcript targets in KSHV pathogenesis and/or the response to cells to chronic viral infection.

miRNA	Target Sequence	Putative target genes (T)	Genes in Overlap (O)	Ratio O/T	*P*-value	FDR
Up-regulated miRNAs/Down-regulated targets						
miR-29c-3p	TGGTGCT	521	33	0.0663	$1.40x10^{-8}$	$3.09x10^{-7}$
let-7i-5p	CTACCTC	391	25	0.0639	$6.53x10^{-7}$	$6.87x10^{-6}$
miR-326	CCCAGAG	155	13	0.0839	$1.94x10^{-5}$	$1.07x10^{-4}$
miR-503-5p	CGCTGCT	24	3	0.125	$1.24x10^{-2}$	$2.75x10^{-2}$
Down-regulated miRNAs/Up-regulated targets						
miR-203a-3p	CATTTCA	287	29	0.1010	$4.07x10^{-19}$	$8.99x10^{-17}$
miR-148a-3p	TGCACTG	304	22	0.0724	$7.03x10^{-12}$	$1.41x10^{-10}$
miR-212-3p	GACTGTT	161	13	0.0807	$3.91x10^{-8}$	$2.88x10^{-7}$
miR-369-3p	GTATTAT	207	14	0.0676	$1.09x10^{-7}$	$7.55x10^{-7}$
miR-128-3p	CACTGTG	337	17	0.0504	$3.38x10^{-7}$	$2.02x10^{-6}$
miR-377-3p	TGTGTGA	200	13	0.0650	$4.88x10^{-7}$	$2.70x10^{-6}$
miR-452-5p	GAGACTG	94	9	0.0957	$1.17x10^{-6}$	$5.63x10^{-6}$
miR-323a-3p	TAATGTG	160	11	0.0688	$2.14x10^{-6}$	$9.85x10^{-6}$
miR-380-3p	ATTACAT	102	9	0.0882	$2.33x10^{-6}$	$1.05x10^{-5}$
miR-381-3p	CTTGTAT	206	11	0.0534	$2.36x10^{-5}$	$8.83x10^{-5}$
miR-7-5p	GTCTTCC	169	9	0.0533	$1.31x10^{-4}$	$4.21x10^{-4}$
miR-485-3p	TGTATGA	153	8	0.0523	$3.49x10^{-4}$	$9.88x10^{-4}$
miR-224-5p	GTGACTT	158	8	0.0506	$4.32x10^{-4}$	$1.19x10^{-3}$
miR-409-3p	AACATTC	142	7	0.0493	$1.14x10^{-3}$	$2.90x10^{-3}$
miR-205-5p	ATGAAGG	157	7	0.0446	$2.03x10^{-3}$	$4.73x10^{-3}$
miR-134-5p	CAGTCAC	52	4	0.0769	$2.74x10^{-3}$	$6.18x10^{-3}$
miR-299-3p	CCCACAT	54	4	0.0741	$3.14x10^{-3}$	$6.94x10^{-3}$

Table 3.1: miRNAs predicted to target differentially expressed mRNAs using GSEA.

Table 3.1: miRNAs predicted to target differentially expressed mRNAs using GSEA.

Using a list of differentially expressed mRNAs from RNA-Seq, GSEA predicted which miRNAs would be upstream inhibitors using the Molecular Signatures Pathways Database (MSigDB). The overlap between the MSigDB output and the miRNA-Seq data highlighted 21 miRNAs that were differentially expressed in SLKK compared to SLK cells. Columns identify their names, the target sequence used to identify base complementarity with the input mRNA, the total number of putative target genes for a given miRNA, the number of putative targets that overlap with the input mRNA list, the percentage ratio between the overlap and the total number of putative targets, and its associated *P*-value and false discovery rate (FDR), correcting for multiple hypothesis testing.

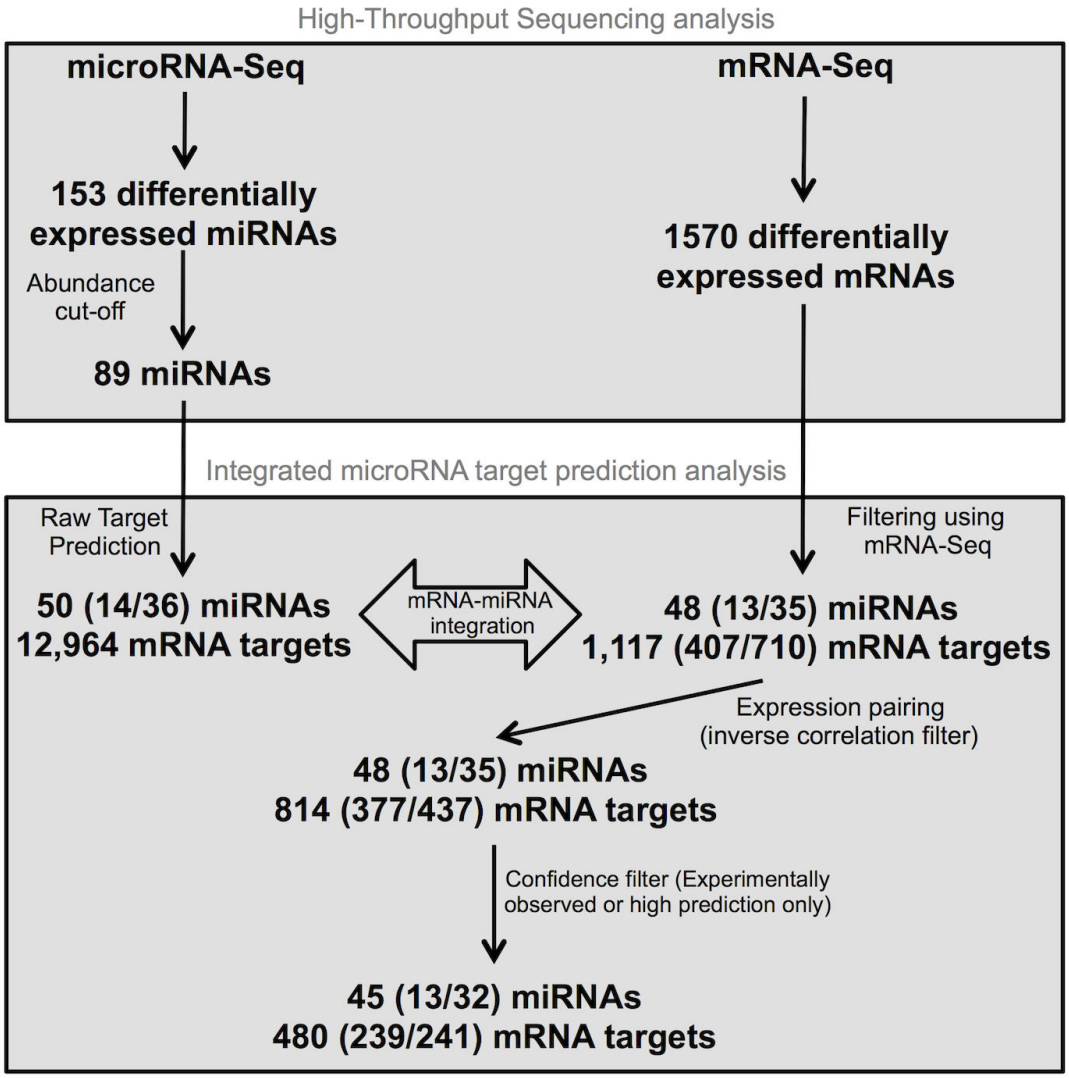

Figure 3.9: Workflow of integrated miRNA-mRNA association analysis using IPA. This experimental workflow shows the various filters used to associate miRNA-Seq and mRNA-Seq data. Numbers are presented as Total differentially expressed miRNAs or mRNAs (Up-regulated/Down-regulated).

miRNA	Log_2 Fold Change	# Target gene	Name of top 5 target genes
Up-regulated miRNAs/Down-regulated targets			
miR-708-5p	2.67	17	FOXN3, RGL1, POU6F1, RNF150, PAPPA
miR-3614-5p	2.16	2	FOXN3, MERTK
miR-342-5p	2.04	37	VANGL2, NR4A1, KIF21B, GNG4, ITPRIP
miR-146b-5p	1.64	19	NRIP3, SDK1, ZNF90, SYT1, KCNIP3
miR-877-5p	1.56	2	SUSD5, PNPO
miR-146b-3p	1.46	12	VANGL2, TSKU, CYFIP2, ASB6, ZNF488
miR-29c-3p	1.23	81	NAV2, C1orf21, FOXN3, GPR37, DUSP2
miR-3664-3p	1.21	7	SPOCK1, PNMA2, CD6, CBX6, FAM109A
miR-3152-5p	1.18	6	SRSF8, CTNNA2, CSPG5, PPARGC1A, SLITRK4
miR-503-5p	1.17	20	C1orf21, KIF5C, MOB3B, APLN, MYOM3
miR-4745-5p	1.10	13	FBXL7, LONRF2, ST6GALNAC3, MOB3B, GAREM
let-7i-5p	1.04	86	C1orf21, FOXN3, TRHDE, LIN28B, PDGFB
miR-21-3p	1.03	4	LIN28B, SHC3, ANO5, FAM117A
Down-regulated miRNAs/Up-regulated targets			
miR-224-5p	-10.99	23	SLCO2B1, FGB, CAST, RNF144B, DPP8
miR-452-5p	-9.15	4	FAM8A1, STAM2, MTMR6, PNN
miR-376c-3p	-7.25	6	TGFBR3, FHDC1, SLC7A11, SECISBP2L, TBC1D12
miR-380-3p	-7.11	1	LPP
miR-409-5p	-6.45	4	FAM102B, TBC1D15, MDM2, SRSF11
miR-323a-3p	-6.31	1	KIAA1430
miR-758-3p	-5.39	14	C2CD4A, NTM, RAB27B, NUDT12, NCOA3
miR-485-3p	-5.07	3	GOLGA8A/GOLGA8B, UBA6, ZMYM4
miR-381-3p	-4.86	53	ID4, SLCO2B1, PTGFR, UNC5C, ICK
miR-411-5p	-4.52	2	NR3C1, RYBP

miR-654-3p	-4.49	2	GMFB, ZNF91
miR-323b-3p	-4.47	3	SPAST, EIF1AX, SMIM13
miR-133a	-4.23	33	HAPLN1, ID4, NDRG1, PLXNA2, ARRB1
miR-654-5p	-4.03	8	LZTS1, UNC5C, FAM8A1, PDGFRB, STK38
miR-369-5p	-4.17	1	ID4
miR-485-5p	-3.28	13	NTM, MLLT3,ZMF527, PLEKHA5, UPF2
miR-299-3p	-2.96	4	TCF4, SLC16A7, SP4, ITGAV
miR-205-5p	-2.29	27	GATA3, GSE1, AXIN2, UNC5C, SECISBP2L
miR-3173-5p	-2.05	4	ADAMTS15, STC2, PEAK1, SKP1
miR-1914-5p	-1.97	3	SKIDA1, GLS, PAQR8
miR-212-3p	-1.89	21	HAPLN1, BTG2, ENPP4, CTDSPL2, KDM7A
miR-129-5p	-1.84	21	NTM, GSE1, ARRDC3, TCF4, CTDSPL2
miR-2355-5p	-1.64	10	CDH1, PLXNA2, LIMA1, ELF3, BTG2
miR-148a-3p	-1.61	45	SPTLC3, ADAMTS15, SKIDA1, ARRDC3, SLC7A11
miR-4786-5p	-1.49	5	PLEKHA5, SNRNP48, TRIM59, COG6, SSR1
miR-149-5p	-1.42	14	ID4, CD34, SORT1, MCTP2, PAQR5
miR-625-5p	-1.31	13	RUNX3, PLCB2, SPN, ARRB1, AXIN2
miR-450a-5p	-1.23	1	DUSP10
miR-548h-5p	-1.15	2	EDIL3, SMAD5
miR-4677-3p	-1.13	1	RPS27L
miR-196b-5p	-1.09	14	TGFBR3, DCDC2, FAM102B, PTPRG, BLOC1S6
miR-128-3p	-1.02	49	HAPLN1, TGFBR3, SLC35F3, DTX4, NEDD4

Table 3.2: Ingenuity analysis predicts inversely correlated miRNA-mRNA target pairs.

Table 3.2: Ingenuity analysis predicts inversely correlated miRNA-mRNA target pairs.

Using lists of differentially expressed miRNAs and mRNAs as input for the Ingenuity Pathway Analysis (IPA), it was found that 45 differentially expressed miRNAs target 480 mRNAs (medium and high confidence). Only mRNAs and miRNAs with opposite differential expression are shown in this table. Columns identify the miRNA name, its log-transformed expression fold change between SLKK and SLK cells, the number of identified targets, and the five or less most differentially expressed targets. In bold are miRNA prediction overlapping with GSEA analysis (**Table 3.1**).

miRNA	Known Target	Reference
Up-regulated miRNAs/Down-regulated targets		
let-7i-5p	ATAD3B, BCL2L1, CCND1, CDIPT, DUSP23, FAM105A, F2, GAK, GPR56, GYS1, MARS2, POLD2, POM121/POM121C, RHOB, RHOG, TAGLN	Selbach et al., 2009 (Nature)
miR-29c-3p	COL1A1, DUSP2, GPR37, KLF4, LOXL2, MAPRE2, MYBL2, TGFB3	Li et al., 2009 (J Biol Chem)
miR-146b-5p	IRAK2, NOVA1, PTGES2, SYT1	Hou et al. 2009 (J Immunol)
miR-503-5p	CCND1	Jiang et al., 2009 (BMC Cancer)
miR-485-5p	MDM2	Ratoviski et al., 2014 (Cell Cycle)
Down-regulated miRNAs/Up-regulated targets		
miR-129-5p	TNPO1	Dyrskjot et al., 2009 (Cancer Res)
miR-205-5p	ZEB1	Gregory et al., 2008 (Nat Cell Biology)
miR-409-3p	FGB, RDX	Fort et al. 2010 (Blood)

Table 3.3: miRNA-mRNA pairs found inversely correlated and validated in the literature This table shows the association between miRNAs and mRNA targets that were dysregulated in SLKK cells compared to SLK cells. Only the miRNA-mRNA pairs experimentally validated in the literature are shown here. The majority of the targets were identified through IPA-integrated TarBase v5.0 and others through independent literature searches.

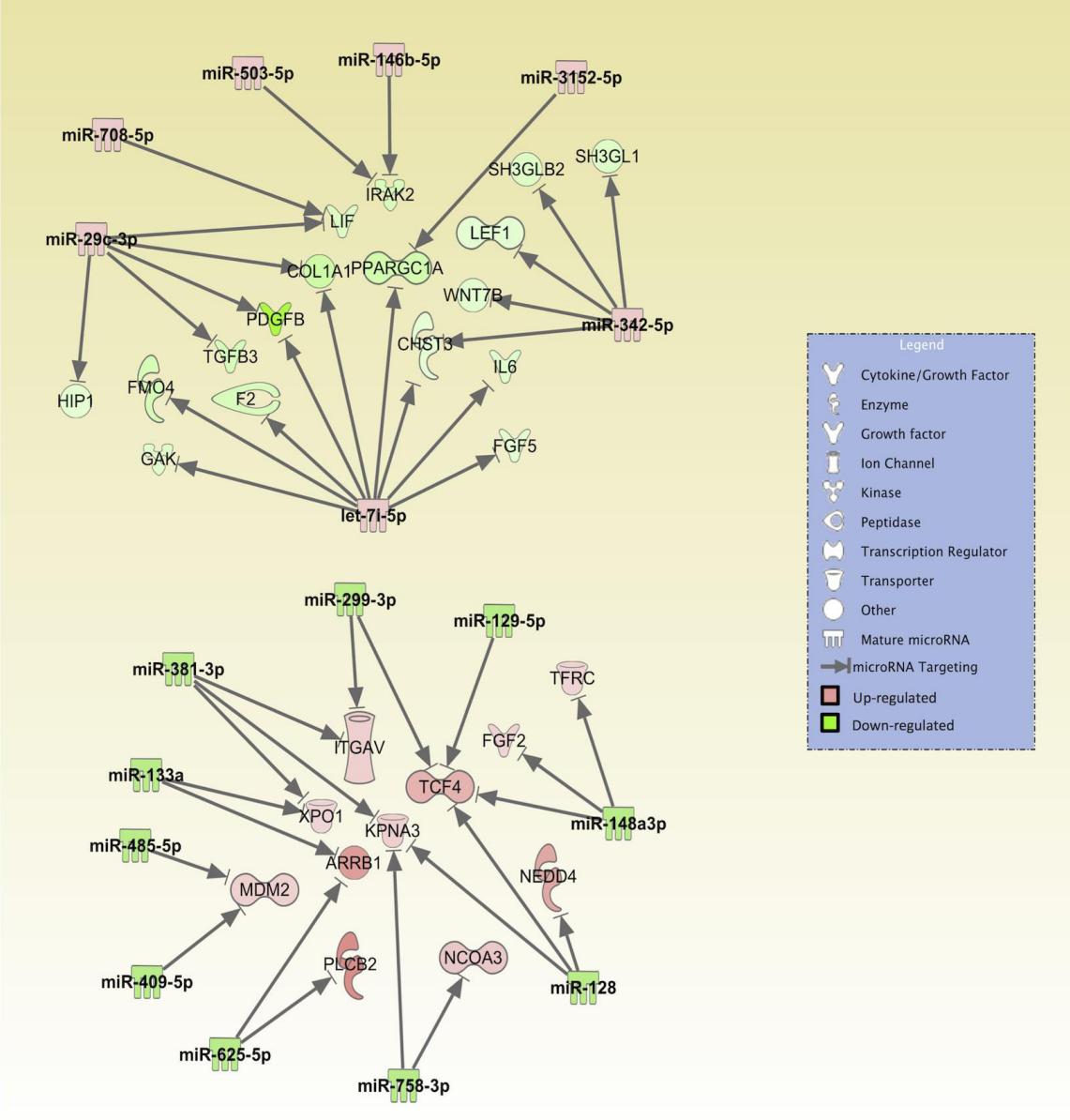

Figure 3.10: Implications of miRNA-mRNA pairs in pathogen-influenced signalling. A total of 17 miRNAs and 28 mRNA targets are involved in the super pathway entitled "Pathogen-influenced signalling". Only target that are experimentally validated or predicted with a high confidence threshold are presented here. The top part shows the up-regulated miRNAs and down-regulated targets. The bottom part shows the down-regulated miRNAs and up-regulated target. The intensity of colours represents the extent of the up-regulation or down-regulation, in red and green respectively.

Ingenuity Canonical Pathways	*P*-value	Ratio (% of genes in pathway)	Dysregulated target gene	Dysregulated miRNA
Regulation of the Epithelial-to-Mesenchymal Transition Pathway	2.5 x 10^{-3}	12/182 (6.6%)	**CDH1**, **FGF2**, FGF5, FGFRL1, **ID2**, LEF1, **PARD6B**, **PDGFRB**, **TCF4**, TGFB3, WNT7B, **ZEB1**	**let-7i-5p**, **miR-29c-3p**, miR-128, miR-129-5p, miR-148a-3p, miR-196b-5p, miR-205-5p, miR-299-3p, **miR-342-5p**, miR-381-3p, miR-654-5p, miR-2355-5p
IL-8 Signalling	7.39 x 10^{-3}	11/183 (6.0%)	BCL2L1, CCND1, **CDH1**, GNG2, GNG4, HBEGF, IRAK2, **ITGAV**, **PLCB2**, RHOB, RHOG	**let-7i-5p**, **miR-29c-3p**, miR-146b-5p, miR-299-3p, **miR-342-5p**, miR-381-3p, **miR-503-5p**, miR-625-5p, miR-2355-5p
Clathrin-mediated Endocytosis Signalling	7.68 x 10^{-3}	11/184 (6.0%)	**ARRB1**, F2, **FGF2**, FGF5, GAK, HIP1, **MDM2**, PDGFB, SH3GL1, SH3GLB2, **TFRC**	**let-7i-5p**, **miR-29c-3p**, miR-133a, miR-148a-3p, **miR-342-5p**, miR-409-5p, miR-485-5p, miR-625-5p, miR-654-5p,
Wnt/β-catenin Signalling	1.02 x 10^{-2}	10/166 (6.0%)	**AXIN2**, CCND1, **CDH1**, KREMEN1, LEF1, **MDM2**, **TCF4**, TGFB3, **TGFBR3**, WNT7B	**let-7i-5p**, **miR-29c-3p**, miR-128, miR-129-5p, **miR-146b-3p**, miR-148a-3p, miR-196b-5p, miR-205-5p, miR-299-3p, miR-376c-3p, **miR-342-5p**, miR-409-5p, miR-485-5p, **miR-503-5p**, miR-625-5p

Table 3.4: Canonical pathways affected by differentially expressed miRNA-mRNA pairs. The 480 differentially expressed genes targeted by miRNAs between SLKK and SLK cells were used as input for the Ingenuity pathway analysis (IPA). Here, four of the top ten enriched pathways were highlighted for their relevance to KSHV pathogenesis. Columns identify the pathway name, its associated *P*-value, the ratio between dysregulated genes and genes in the pathway, and which dysregulated target genes or miRNAs are involved. Genes or miRNAs in bold and normal font were found up-regulated and down-regulated, respectively, by chronic KSHV infection.

3.7 Conclusions and future directions

In this study, next-generation sequencing was used to survey both mRNA and miRNA expression profiles in SLKK cells latently infected with KSHV as compared with the uninfected SLK cells. This helped determine the degree to which changes in gene expression profiles could plausibly be attributed to changes in miRNA expression profiles. Looking at the broad trends in differential miRNA profiles, the majority of miRNAs that met the selection criteria (linear FC $\geq$2 and $P \leq$0.05) were down-regulated in the KSHV-infected cells. This is consistent with previous reports that lymphatic endothelial cells infected with KSHV and primary B-cells infected with Epstein-Barr virus (EBV) show a substantially higher number of down-regulated than up-regulated miRNAs (Godshalk et al. 2008; Wu et al. 2011). One possible explanation was that KSHV-encoded miRNAs were produced at such a high level that they competitively interfered with the processing of the cellular miRNAs. However, in the SLKK cells, viral miRNAs made up only ~9% of the total miRNA fraction, suggesting that this was not the principal mechanism (see **Chapter 6** for details on viral miRNAs). Considering alternative explanations, other viruses have been shown to globally reduce cellular miRNA levels by the saturation of exportin-5 (XPO5), which is involved in the transit of pre-miRNA to the cytoplasm (Bennasser et al. 2011), and it is possible that this may be occurring in KSHV-infected cells.

An unexpected finding was that more than a third of the significantly down-regulated miRNAs were located within 50kb of each other at the 14q32 miRNA cluster, which has previously been linked to cancer development. In fact, some of the 14q32 miRNAs that were easily detectable in the uninfected cells were undetectable in the KSHV-infected cells. Indeed, the down-regulation of 14q32 miRNAs miR-409-3p, miR-409-5p, and

miR-410 was further validated by Taqman assays. A substantial down-regulation of 14q32 miRNAs has similarly been observed in PEL cell lines including BCBL-1, BC-1 and BC-3 (Gottwein et al. 2011). Because of the extent of the down-regulation in the current study, a deletion of this region at the DNA level might have occurred through genomic DNA loss for example. It has been reported that 14q32 deletion is the most frequent chromosomal loss (63%) in a number of PEL cell lines and primary cases of PEL (Luan et al. 2010). In SLKK cells however, DNA was present in each of the eight regions that were probed, suggesting that repression of 14q32 miRNAs was probably not due to chromosomal loss or epigenetic silencing at the DNA level, such as DNA methylation or histone modifications, but rather to post-transcriptional mechanisms. Also, the observation that 14q32 miRNAs are down-regulated in the setting of KSHV infection and that it can occur either through chromosomal deletions or through other mechanisms suggests that down-regulation of these miRNAs are advantageous for survival of KSHV-infected cells.

A key goal of this study was to identify miRNA changes induced by KSHV infection that were associated with the inverse changes in their mRNA targets. However, miRNA changes are not the only factors that can modulate mRNA; KSHV-encoded proteins, as well as manifestations of the host response, can also affect cellular mRNA expression through mechanisms other than the miRNA silencing machinery. Nonetheless, the current analysis provides evidence to suggest that a substantial proportion of the observed mRNA changes were caused by miRNA dysregulation. An extensive list of strongly correlated miRNA-mRNA pairs was compiled. Of 48 miRNAs whose level met the cut-off criteria for modulation, there were predicted or experimentally determined targets that were also modulated in the SLKK cells, for a total of 1,117 targets. Of these, 73% (814 targets) were modulated in the direction predicted by the miRNA change.

These modulated mRNAs include 36 mRNAs that had been previously reported as known targets for nine miRNAs dysregulated in SLKK vs. SLK cells. Transfection assays of three miRNAs that were decreased in SLK or SLKK cells were carried out and changes in five of their respective target mRNAs, including two novel targets (LIF for miR-708-5p and MDM2 for miR-409-5p) were quantified. In each case, transfecting the miRNA resulted in the predicted decrease of its target gene(s). Moreover, changes in some of these mRNAs would benefit KSHV infection. For example, a decrease in proapoptotic caspase-2, a miR-708-5p target, would favour the maintenance of KSHV latent infection (Moore 2007). Taken together, these results are thus consistent with the hypothesis that changes in miRNAs are driving at least some of these mRNA changes. Furthermore, these results provide some additional confidence in the use of paired miRNA-Seq and mRNA-Seq in the SLK/SLKK system to identify mRNA targets that may be relevant to KSHV pathogenesis. However, it is unlikely that all of the changes in any given mRNA target are directly and uniquely caused by a specific miRNA, as biological systems are often redundant.

It is worth keeping in mind that miRNA dysregulation could result from KSHV infection itself, but also be due to a host response to this infection, or to the crosstalk between the two. Interestingly, there was relatively little overlap between the miRNA changes observed here in latently-infected cells and those reported to occur in the first few hours after *de novo* KSHV infection, which would be expected to predominantly reflect the antiviral innate immune response (Lagos et al. 2010). This suggests that the findings reported here are largely related to the effects of long-term KSHV latency.

Looking at the miRNAs overexpressed here in SLKK cells, previous reports provide evidence linking certain miRNA changes to a direct effect of latent KSHV infection. For example, miR-146b has been shown to be induced by STAT3 (Xiang et al. 2014), which

is phosphorylated in cells with latent KSHV infection (Punjabi et al. 2007). miR-146b in turn can down-regulate Toll-like receptors and other aspects of the immune response to pathogens and it may thus help KSHV evade immunity (Taganov et al. 2006). Moreover, a STAT3 knock-down study showed that STAT3 induces miR-21-3p and miR-29c-5p, which were found up-regulated in SLKK cells; and STAT3 represses miR-2276, which was found down-regulated in the current study (Zhang et al. 2014). Also, while the change in miR-210 was not sufficient to meet the original *P*-value miRNA-Seq threshold, it was nonetheless found significantly up-regulated based on the Taqman assay. KSHV LANA has been shown to up-regulate hypoxia-inducible factor (HIF) (Cai et al. 2006), a direct inducer of miR-210 (Huang et al. 2009; Fasanaro et al. 2008), so the increase in miR-210 was predicted based on this mechanism. How various cellular miRNAs are controlled by KSHV and the potential role that KSHV proteins may have at the post-transcriptional level are important questions that remain to be explored in the future.

Looking further at individual miRNAs dysregulated in SLKK cells and their target mRNAs, several stand out as potentially important in KSHV infection. For example, compared to SLK cells, SLKK cells manifested an increase in miR-708-5p along with a significant down-regulation of pro-apoptotic protease caspase-2 (CASP2). Through its induction of apoptosis, CASP2 can have an important anti-viral effect, and inhibition of its activity can thus promote KSHV infection. Also, miRNAs miR-485-5p and miR-409-5p are down-regulated in KSHV-infected cells and this directly correlates with the up-regulation of their predicted target, MDM2, which mediates the degradation of p53 (Brooks & Gu 2006; Stommel & Wahl 2005), an inducer of apoptosis. By this mechanism, MDM2 may suppress virus-induced apoptosis, thereby increasing the survival of KSHV-infected cells.

Two other down-regulated miRNAs, miR-299-3p and miR-381-3p, are predicted to suppress expression of integrin αV (ITGAV) (**Table 3.4** and **Figure 3.10**), which was in turn up-regulated in SLKK cells. ITGAV has been shown to enhance the ability of KSHV-infected cells to infect new cells through binding to the extracellular matrix (Dyson et al. 2008). Interestingly, miR-409-5p, miR-299-3p, and miR-381-3p are all located in the 14q32 cluster that is broadly down-regulated in SLKK cells as well as PEL cells (Luan et al. 2010). Of note, ITGAV is one of the two components of the $\alpha_V\beta_3$ integrin, a cellular receptor mediating entry of several viruses, including EBV and KSHV (Garrigues et al. 2008; Dorner et al. 2010). Similarly, HIV-1 has been shown to up-regulated ITGAV in human T lymphocytes (Weeks et al. 1991).While it might seem counterintuitive for viruses to up-regulate entry receptor proteins once a cell is already infected, studies have demonstrated that KSHV infected cells, for example, can be infected with human herpesvirus 6, human cytomegalovirus and HIV-1 leading to lytic replication hence promoting KS progression (Lu et al. 2005; Vieira et al. 2001). In addition, EBV and KSHV typically coexist in PELs (Epstein 2001; Chang et al. 1994; Cesarman et al. 1995). It is therefore possible that KSHV mediates an indirect up-regulation of ITGAV via down-regulation of cellular miRNAs. Further target validation assays and mechanistic studies would be necessary to determine if the up-regulation of ITGAV aids in co-infection of KSHV infected cells. These results certainly provide new insights into the complex interplay between KSHV infection and host miRNA-mediated gene regulation. This opens up areas of research that can lead to a deeper understanding of viral oncogenesis.

In this study, pathway analysis tools were used to identify some of the most affected pathways. Overall, 45 miRNAs matched 480 paired mRNA targets that were either experimentally determined or highly predicted and whose changes inversely correlated

with the mRNA changes. Of these, 17 miRNAs and 28 putative mRNA targets have been previously identified as being involved in pathogen-related signalling (**Figure 3.10**). Several fundamental pathways were significantly enriched in the 480 mRNA targets. These include the regulation of the epithelial-to-mesenchymal transition (EMT) pathway, IL-8 signalling, clathrin-mediated endocytosis signalling and Wnt/β-catenin signalling (**Table 3.4**).

SLK and SLKK cells were used in the current studies because they provided the ability to compare KSHV-infected and uninfected cells and because of the tight control of KSHV latency in these cells. Experimentally derived from a KS biopsy, the uninfected SLK cell line had endothelial features resembling those of KS and was thought to be a KS cell model in part because it can be stably and latently infected by KSHV (Herndier et al. 1994; Vieira & O'Hearn 2004). However, it was later shown to be indistinguishable from Caki-1, a clear-cell renal-cell carcinoma line of epithelial origin (Stürzl et al. 2013). Nonetheless, it remains a valuable model to study KSHV genetic regulation and host effects from latent KSHV infection (Arias et al. 2014). A number of changes observed here have also been observed in other studies of miRNA or mRNA expression in KSHV-infected cells.

In summary, deep sequencing was used to examine the small RNAs and mRNAs expressed by SLKK and SLK cells, and a number of miRNA-target mRNA pairs that play a significant role in KSHV pathogenesis or KSHV-induced diseases were successfully identified. Of note, the majority of cellular miRNAs that were significantly altered by KSHV were down-regulated, including most members of the 14q32 miRNA cluster, a genomic locus linked to cancer. This is the first comparative study simultaneously analysing and correlating changes at the miRNA and mRNA level in cells with latent KSHV infection and uninfected cells. This survey can help inform

additional studies to better understand the mechanisms responsible for the specific changes observed and their role in the establishment of KSHV infection, the host response to this infection, and the pathogenesis of KSHV-induced tumours.

Publication arising from data presented in this Chapter:

Viollet, Coralie, David A. Davis, Martin Reczko, Joseph M. Ziegelbauer, Francesco Pezzella, Jiannis Ragoussis, and Robert Yarchoan. 2015. "Next-Generation Sequencing Analysis Reveals Differential Expression Profiles of MiRNA-mRNA Target Pairs in KSHV-Infected Cells." Plos One 10 (5): e0126439. doi:10.1371/journal.pone.0126439.

4

Evaluating the interplay between KSHV infection and the hypoxic cellular response

DESPITE a wide interest in hypoxia and its influence on KSHV, the interplay between this microenvironment and viral infection remains poorly characterised. Specifically, cellular stress can be induced by hypoxia, yet how miRNAs of KSHV-infected cells respond to hypoxia is unclear.

In the preceding chapter, the effects of infection on cells were determined by comparing miRNA and mRNA expression profiles of infected and uninfected cells. This chapter addresses how hypoxia affects mRNA and miRNA global expression profiles and to what extent this response compares to KSHV infection.

4.1 Introduction

While numerous studies have examined the role of hypoxia in cancer and how hypoxia confers a survival and growth advantage to cancer cells, its role in viral pathogenesis is still not well defined. Of note, the induction of hypoxia-inducible factor (HIF)-1 has been shown to be a general response in infections with human pathogens such as bacteria, viruses, fungi and protozoa (Werth et al. 2010). However, the pathways regulated by HIF in KSHV-associated malignancies have yet to be completely characterised. In this chapter, the interplay between hypoxia and KSHV infection were investigated by looking at miRNA and mRNA expression profiles.

4.1.1 Hypoxia-regulated miRNAs in KSHV pathogenesis

KSHV-induced diseases, primary effusion lymphoma (PEL) and Kaposi's sarcoma (KS), preferentially develop in settings of relatively low oxygen concentrations (i.e. lower extremities) (Sternbach and Varon 1995). Hypoxic stress can not only increase KSHV reactivation (Davis 2001) but also induce the most abundant latent viral protein, LANA (Veeranna et al. 2012). LANA induces nuclear accumulation of HIF-1α during latent KSHV infection (Carroll et al. 2006). Additionally, viral IFN regulatory factor 3 (v-IRF3), another important latent viral protein, can stabilise HIF-1α, thereby promoting angiogenesis via elevated vascular endothelial growth factor (VEGF) levels (Shin et al. 2008). This is consistent with the observation that HIF-1α is highly expressed in KSHV-associated lesions.

Moreover, several studies have shown that hypoxia can alter miRNA expression profiles. In particular, miR-210 is a universal responder to hypoxia and specifically HIF-1α in a variety of cell lines, and it promotes adaptation to hypoxia as well as cell survival.

However, whether or not KSHV regulation of HIF affects hypoxia-regulated miRNAs (HRMs), including miR-210, is unknown. In the previous chapter, it was highlighted that there was a small but statistically significant up-regulation of miR-210 in cells infected with KSHV compared to uninfected controls even in the normoxic setting. Up-regulation of miR-210 has also been reported in patients suffering from other chronic viral infections such as hepatitis B (HBV; Song et al. 2014). Notably, miR-210 directly targets the pre-S1 region of HBV (HBVPS1) to suppress the production of HBV surface antigene (HBsAg) and HBV virion, hence contributing to viral dormancy and persistent chronic infection (G. Zhang et al. 2010). Additionally, EBV infection has been shown to consistently up-regulate miR-210 levels compared to mock infection controls in human peripheral blood cells (Lu et al. 2008). While these findings support further investigation of hypoxia-regulated miRNAs (HRMs) such as miR-210, and their role in pathogen infection, there has been no published study evaluating the global miRNA response to hypoxia in infected cells.

4.1.2 Next-generation sequencing of miRNAs and mRNAs as a useful approach for addressing the interplay between infection and hypoxia

To better understand the role of HRMs in KSHV pathogenesis, it is important to take a closer look at the involvement of miRNAs in this biological system. However, if data is only collected on miRNA expression, it is of limited utility as *in silico* mRNA target identification remains difficult, and requires extensive validation at the mRNA level. Instead, a dual analysis of miRNA and mRNA expression allows for a direct cross-comparison between miRNA differential profiles and correlations with the effects on putative targets. This allows for an accurate assessment of miRNA-mRNA target expression pairing in the context of hypoxic stress and KSHV infection. While other studies of miRNA expression have been conducted in KSHV infected cells, the reported

findings only address the normoxic context and never directly correlate the effects of hypoxia on miRNAs with their mRNA targets within the same cells.

Using next-generation sequencing, this chapter (i) compares the cellular response to hypoxia, to the cellular response to KSHV infection using the SLK/SLKK model and (ii) determines to what extent the hypoxic response in SLKK cells compares with that of uninfected SLK cells, and to what extent the two responses overlap.

4.2 Hypoxic response in uninfected SLK cells

Studying how SLK cells respond to hypoxia in the absence of KSHV infection is necessary to provide a baseline for future analyses as it can be compared to both the cellular response to KSHV infection (**Section 4.3**) and the hypoxic response in the presence of KSHV (**Section 4.4** and **4.5**).

4.2.1 miRNA response to hypoxia in SLK cells

Next-generation sequencing was performed on miRNA libraries from hypoxic and normoxic uninfected SLK samples in triplicate. Differential expression was subsequently determined and a total of 112 out of 1,378 miRNAs were found significantly dysregulated in hypoxia compared to normoxia ($P \leq 0.05$, FC ≤ -2 or ≥ 2; **Figure 4.1**, top left and right quadrants). Perhaps the most striking observation was that of the 112 dysregulated miRNAs in response to hypoxia, the majority (88%) were down-regulated. Of those 112 HRMs, 47 were expressed with an average miR count greater than 1 and allowed for a clear cluster between the triplicate hypoxic and normoxic samples (**Figure 4.2**). Ten (21%) of the 47 HRMs were up-regulated, while 37 (79%) were down-regulated by hypoxia. This down-regulation could be due to the fact that key

proteins of the miRNA biogenesis, Dicer and Drosha, can be down-regulated in hypoxia, hence preventing miRNA processing (Rupaimoole et al. 2014). However, neither Dicer nor Drosha were significantly down-regulated in this study.

After a stringent selection based on read abundance and significance ($P \leq 0.05$, average miR count of ten or more across all replicates), the 15 most abundant HRMs in SLK cells were determined. Of these 15, three were up-regulated while 12 were down-regulated (**Figure 4.3**). As previously described for other cell types (Pulkkinen et al. 2008; Chan et al. 2012; Fasanaro et al. 2008), miR-210 was potently up-regulated by hypoxia in SLK cells; this was validated by Taqman assay as being significantly up-regulated 15-fold by hypoxia in SLK cells (**Figure 4.4**). By comparison, in the MCF7 breast cancer cell line, miR-210 is up-regulated 3-fold by hypoxia (Camps et al. 2014). Additionally, miR-146a was induced by hypoxia in SLK cells (2-fold) and is another well-known HRM that has been shown to inhibit NF-κB-mediated inflammatory response (Taganov et al. 2006). Another miRNA identified as being induced by hypoxia in SLK cells was miR-5001-3p. This miRNA has not been previously described and is therefore a novel HRM. The remaining 12 miRNAs including miR-6723-5p, miR-222-5p and miR-4484 were all down-regulated.

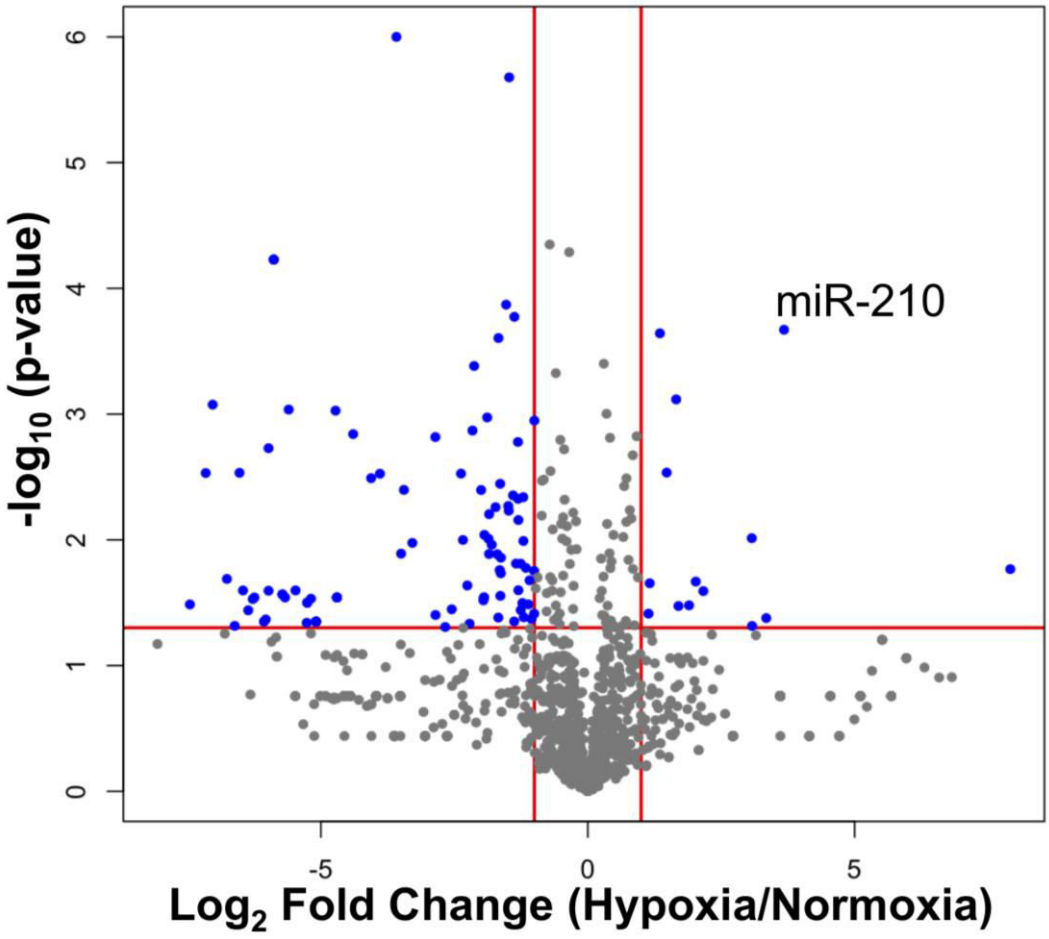

Figure 4.1: Volcano plot of miRNA differential expression in hypoxic vs. normoxic SLK cells. Vertical red lines indicate the threshold for a relative expression fold change (FC) of 2 or -2 compared to normoxic controls. The horizontal red line represents the threshold of a 0.05 *P*-value. Thus, the blue points lying in the top right and top left sectors are significantly up-regulated and down-regulated, respectively, in hypoxic vs. normoxic SLK cells ($P \leq 0.05$, linear FC ≤ -2 or ≥ 2).

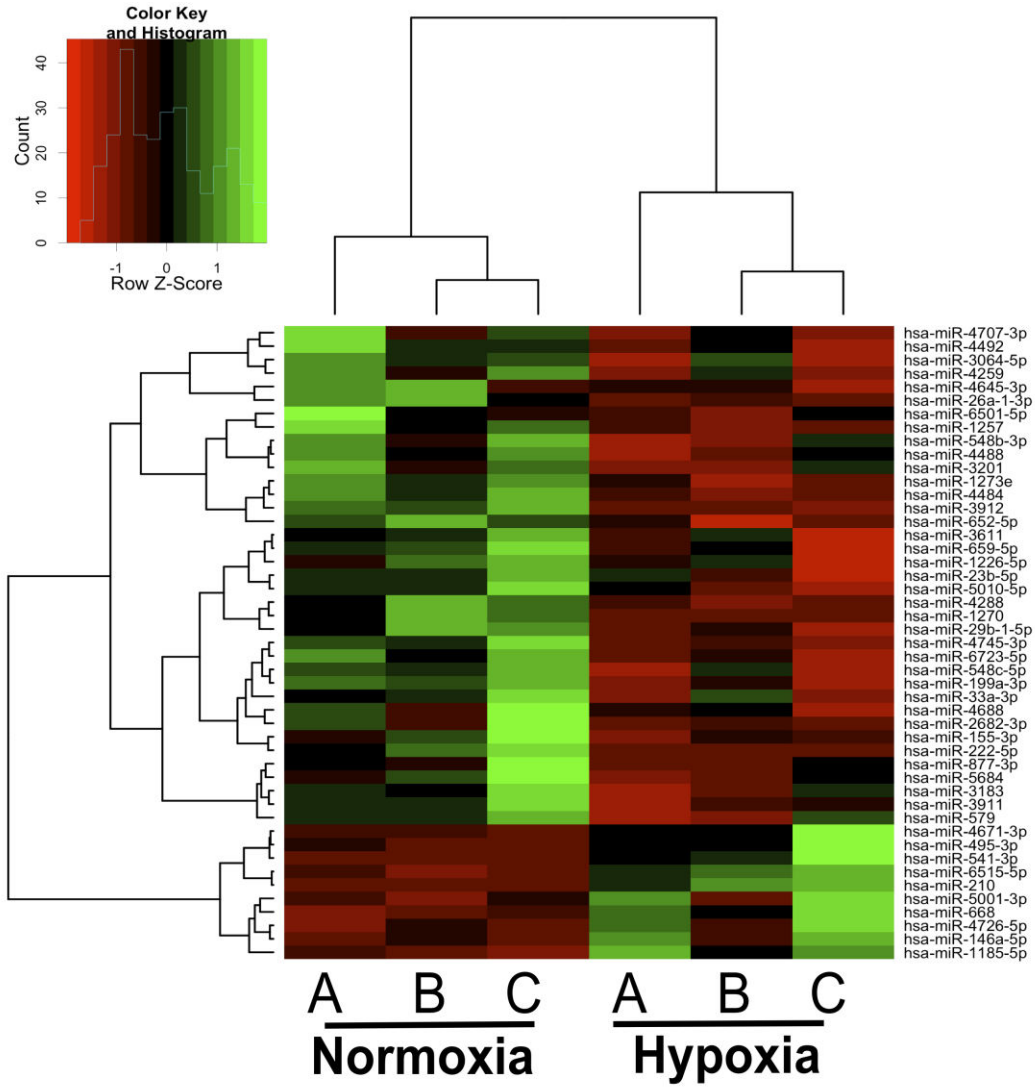

Figure 4.2: Expression of miRNAs in the analysed small RNA libraries. Heatmap of miRNA changes between hypoxic and normoxic SLK cells in the six individual replicates (three normoxic and three hypoxic SLK samples). Presented is the relative expression of 47 significantly dysregulated cellular miRNAs in hypoxic vs. normoxic uninfected cells (*P*-value ≤0.05, $\log_2$ FC ≤-1 or ≥1, average miR count ≥1). Using uncentered Pearson correlation as the distance metric, an unsupervised hierarchical heatmap was generated, with each row representing a miRNA and each column representing a biological replicate. Red, black and green denote low, median and high relative miRNA expression, respectively.

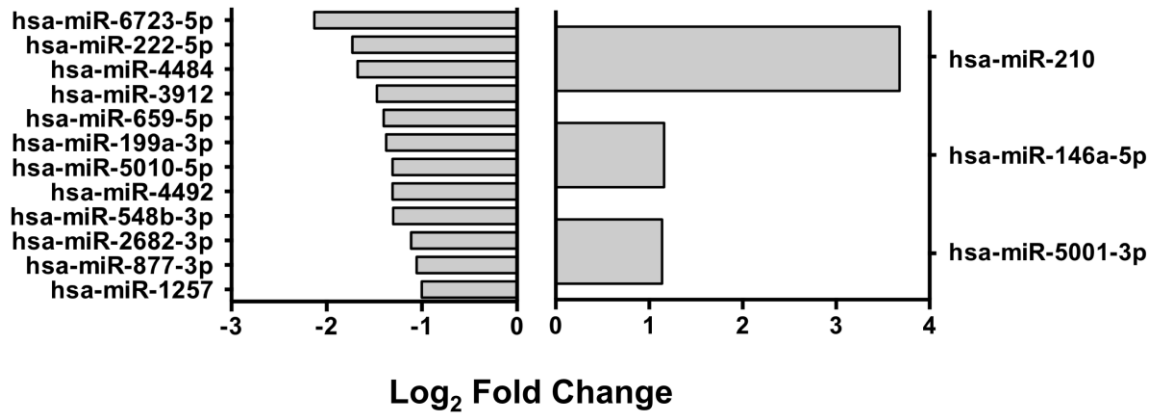

Figure 4.3: Top 15 repressed and induced miRNAs in hypoxic vs. normoxic uninfected cells. Bars below and above the y-axis show the 15 most abundant miRNAs repressed and induced, respectively, in hypoxia compared to normoxia in SLK cells. Data were considered significant when $P \leq 0.05$, an average miR count of 10 or more across all replicates (i.e. threshold of miR counts sum higher than 60).

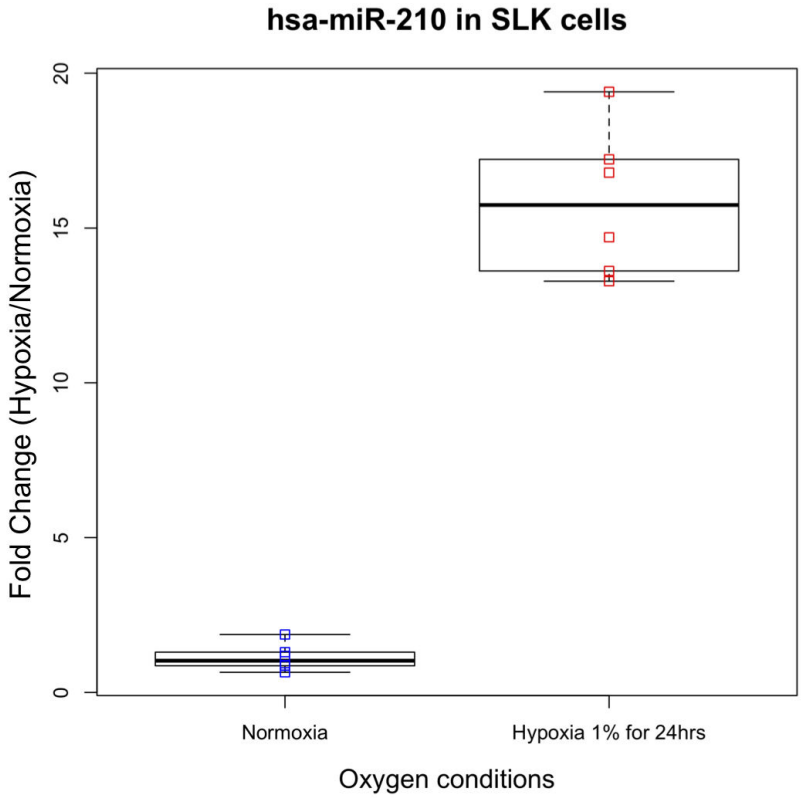

Figure 4.4: miR-210 differential expression in hypoxic vs. normoxic SLK cells. This plot represents the fold difference in miR-210 expression between hypoxia and normoxia in SLK cells, measured by Taqman assays (n=6). Small endogenous RNA, RNU43, was used for internal normalisation. Hypoxic samples were normalised to normoxic samples. This plot was generated using R and the rectangular box shows the interquartile range (IQR), from the 1st quartile (25th percentile) to the 3rd quartile (75th percentile). It includes the 2nd quartile (median) of miR-210 relative expression change. The whiskers correspond to the minimum and maximum values.

4.2.2 mRNA response to hypoxia in SLK cells

The same SLK normoxic and hypoxic samples that were analysed for small RNA-Seq were also sequenced for mRNA. As in **Chapter 3**, the goal was to use this data to pair differentially expressed miRNAs with their inversely expressed targets. Out of a total of 30,808 mRNAs analysed, 545 were differentially expressed (i.e. increased or decreased) in hypoxic vs. normoxic SLK cells (**Figure 4.5**). Among the up-regulated genes, there were a number that have been described previously to be increased in hypoxia. For example, BNIP3, BNIP3L, IGFBP3, PLOD2 and STC2 have all been reported to be up-regulated by HIF-1α (Bellot et al. 2009; Sowter et al. 2001; Natsuizaka et al. 2012; Gilkes et al. 2013; Law and Wong 2010a). Moreover, ARRDC3 was one of the most up-regulated genes in this dataset (5.4 $\log_2$ FC) and it has been recently linked to hypoxia in three tumour cell lines (Olbryt et al. 2014). Similarly, Olbryt et al. found that ARRDC3 was the most hypoxia-induced gene in melanoma, ovarian cancer and prostate cancer cell lines. Additionally, the expression of VEGF, known HIF-1 target gene known to be up-regulated in hypoxia (Wang et al. 2005), was assessed by qRT-PCR in hypoxic and normoxic SLK cells. It was found that VEGF was up-regulated ~2.5-fold by hypoxia (**Figure 4.6**). Taken together, these results provide confidence that the cells were responding to the hypoxic treatments.

Surprisingly, FOSB and WNT7B, that were both down-regulated by hypoxia in SLK cells, were reported to be up-regulated in other studies (Bosco et al. 2006; Qu et al. 2013). FOSB has transcription regulatory activities and is a component of the AP-1 complex (Herdegen and Leah 1998), which is involved in the transactivation of hypoxia-inducible genes (Laderoute et al. 2002). WNT7B plays a role in vasculogenesis and

mediates hypoxia-induced angiogenesis (Shu et al. 2002). The down-regulation of these two genes may be specific to SLK hypoxic cells.

Ingenuity Pathway Analysis (IPA) was used to analyse the large number of dysregulated genes in hypoxic compared to normoxic SLK cells, in order to identify pathways altered by hypoxia (**Figure 4.7**). Among the top 15 most significantly modulated pathways were four cancer signalling pathways, as well as the Wnt/β-catenin signalling, the neuregulin signalling, prostanoid biosynthesis, and the epithelial-mesenchymal transition pathway. These eight pathways are all known to be altered by hypoxia (Harris 2002; Shalinsky, McNamara, and Agrawal 1989; Thiery et al. 2009; Semenza 2012; Mazumdar et al. 2010). Specifically, HIF-1α has been shown to modulate the Wnt/β-catenin signalling in embryonic stem cells and primary cells (Mazumdar et al. 2010), while in turn the Wnt/β-catenin signalling can increase the activity of HIF-1α (Qi Zhang et al. 2013). Neuregulins comprise a family of epidermal growth factor (EGF)-like proteins involved in cell-cell signalling. They are induced by intermittent hypoxia in rat vascular smooth muscle cells, hence promoting cell proliferation (Kyotani et al. 2013).

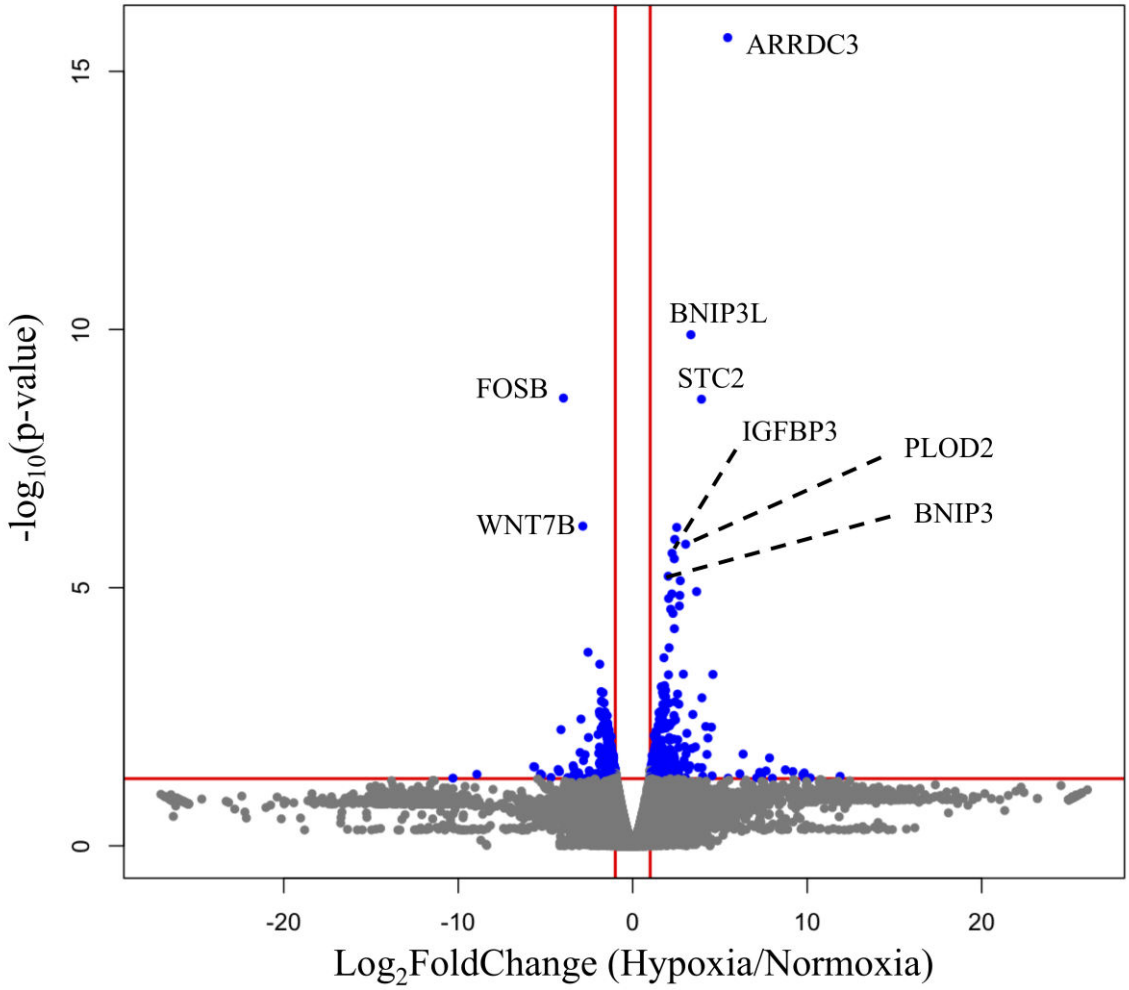

Figure 4.5: Volcano plot of mRNA differential expression in hypoxic vs. normoxic SLK cells. The plot is depicted as in **Figure 4.1**, with vertical and horizontal red lines similarly representing the thresholds of a fold change of 2 or -2, and of a *P*-value of 0.05, respectively.

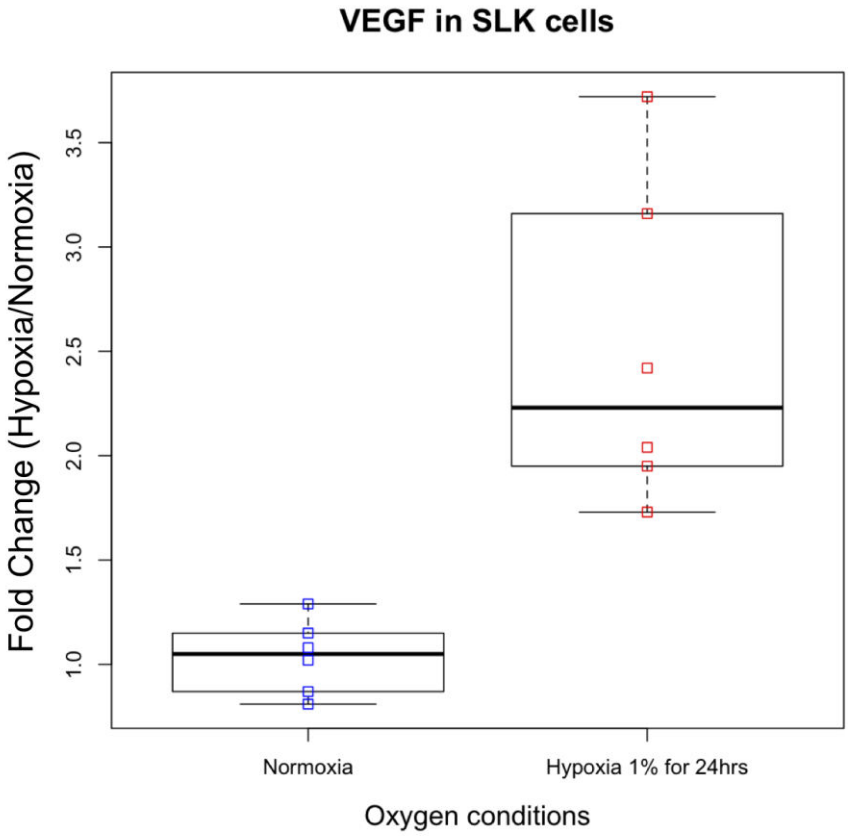

Figure 4.6: VEGF differential expression in hypoxic vs. normoxic SLK cells. This plot represents the fold difference in VEGF expression between hypoxia and normoxia in SLK cells, measured by Taqman assays (n=6). Small endogenous RNA, RNU43, was used for internal normalisation. Hypoxic samples were normalised to normoxic samples. This plot was generated using R and the rectangular box shows the interquartile range (IQR), from the 1st quartile (25th percentile) to the 3rd quartile (75th percentile). It includes the 2nd quartile (median) of VEGF relative expression change. The whiskers correspond to the minimum and maximum values.

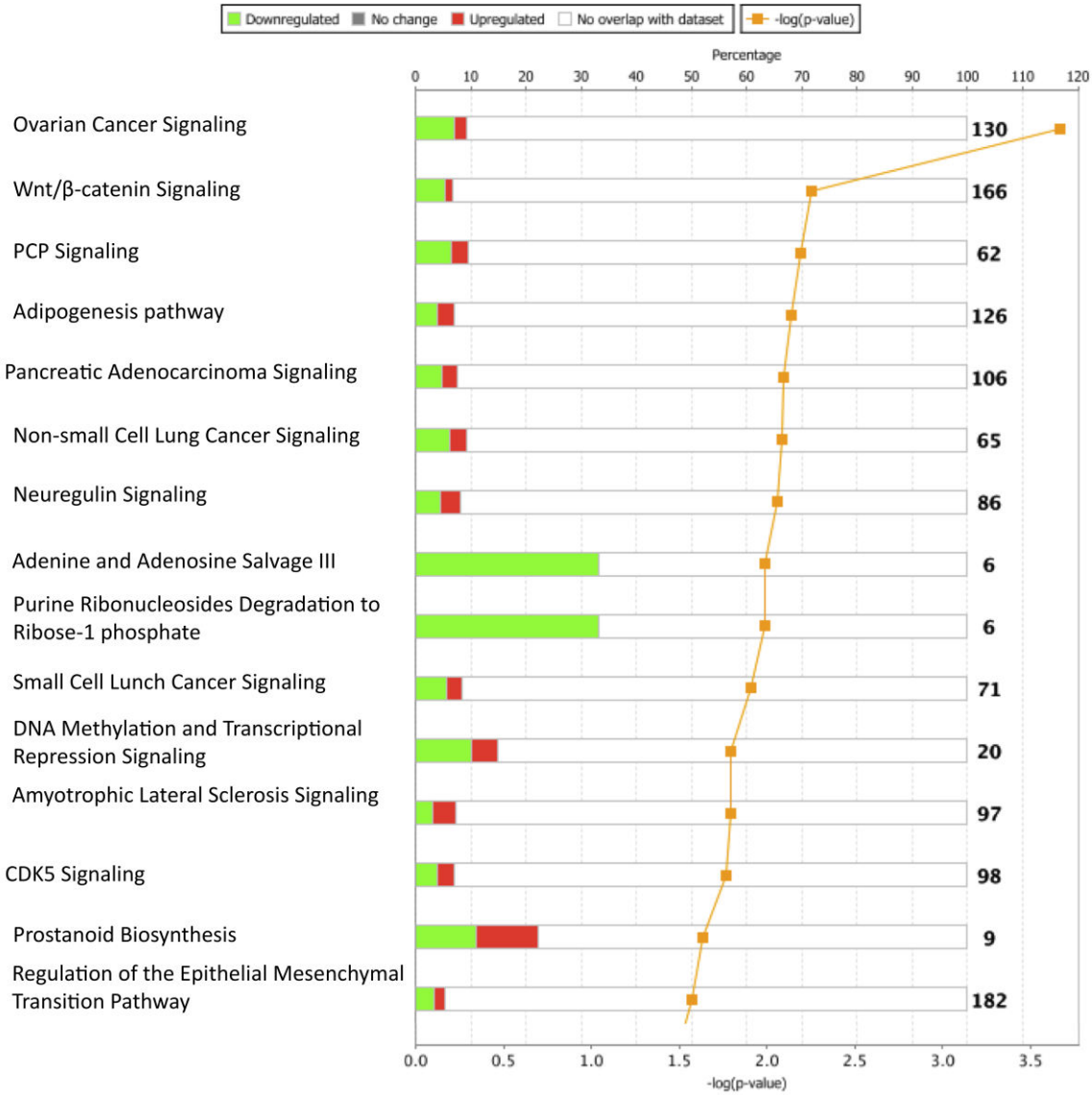

Figure 4.7: Top 15 pathways altered by hypoxia in SLK cells. A list of differentially expressed mRNAs was used as input for Ingenuity Pathway Analysis, generating pathways altered by hypoxia in uninfected SLK cells. The 15 pathways that are most significantly altered are illustrated here. The yellow line reflects the significance ($P \leq 0.05$ when $-\log(P\text{-value}) > 1.3$). The percentage of down-regulated and up-regulated genes in a given pathway is depicted in green and red, respectively.

4.2.3 Inverse correlation of miRNA and mRNA target expression in hypoxic SLK cells

As in **Chapter 3**, an integrated approach was used to correlate miRNA and mRNA differential profiles of the RNA-Seq data. In SLK cells under hypoxia, the IPA microRNA Filter analysis revealed that 65% (278 out of 426 mRNAs) of the predicted miRNA targets were inversely correlated to miRNA expression (up-regulated miRNA and down-regulated target mRNA, or down-regulated miRNA and up-regulated target mRNA). This suggests that more than half of the changes occurring in the mRNA targets under hypoxic stress could be attributed to the miRNA regulation. This percentage is similar to that (73%) which was obtained when miRNAs and mRNA targets were inversely correlated between SLK and SLKK cells.

IPA analysis paired 35 miRNAs to 108 mRNA targets (high confidence prediction or experimentally observed results; **Figure 4.8**). Specifically, eight miRNAs that are up-regulated by hypoxia are predicted to target 43 down-regulated mRNAs. Conversely, 27 miRNAs are down-regulated by hypoxia while 65 of their targets are up-regulated. These miRNA-mRNA pairs are listed in **Table 4.1**. Notably, miR-210 is associated to homeobox A1 (HOXA1), a well-described target of miR-210 (Huang et al. 2009), and CLUH, a predicted target recently identified as a regulator of mitochondrial biogenesis (Gao et al. 2014).

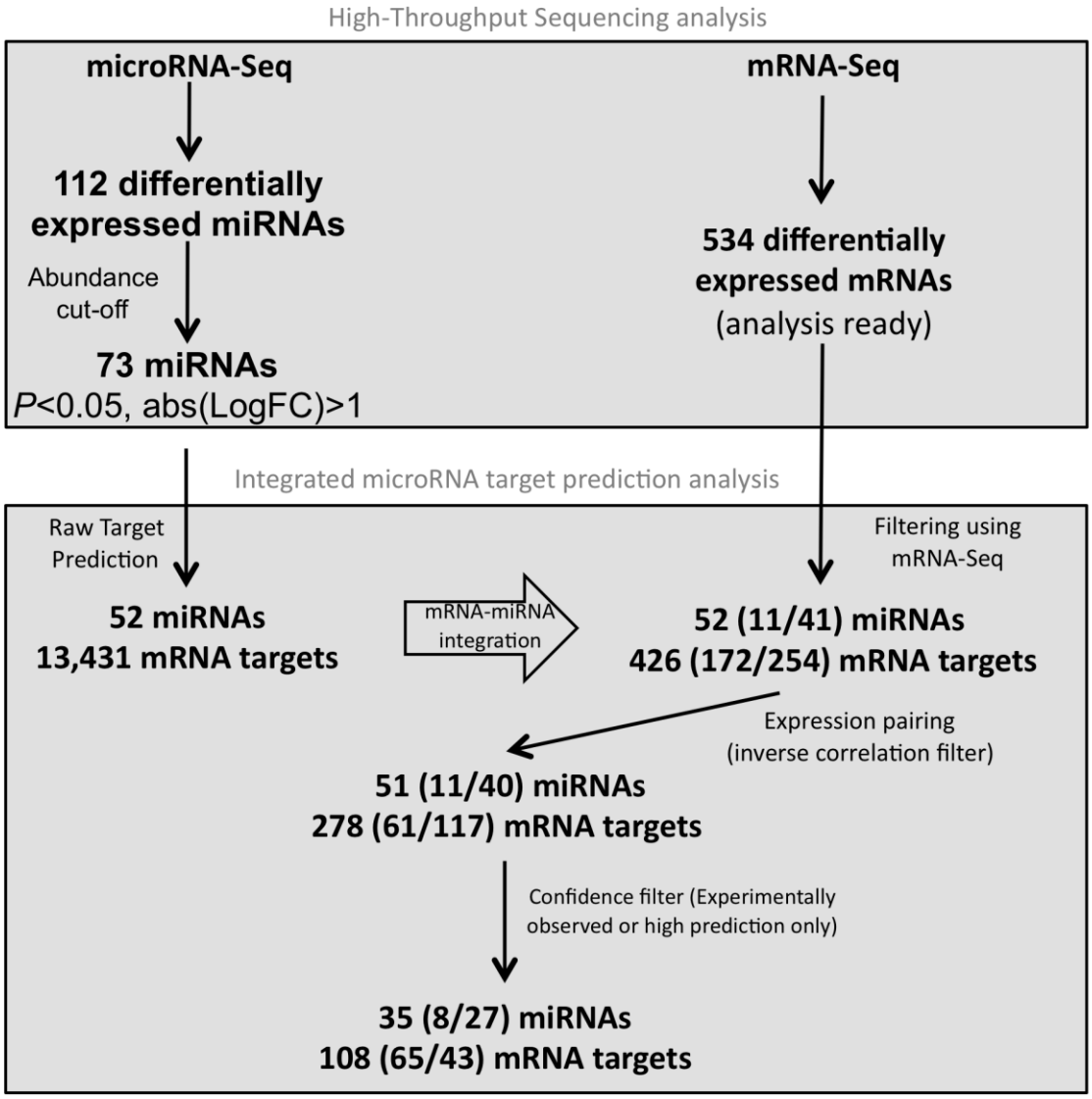

Figure 4.8: Workflow of integrated miRNA-mRNA association analysis using IPA. This experimental workflow shows the various filters used to associate miRNA-Seq and mRNA-Seq data from hypoxic and normoxic SLK cells. Numbers are presented as Total differentially expressed miRNAs or mRNAs (Up-regulated/Down-regulated).

miRNA	Log_2 Fold Change	# Target genes	Top 5 target genes
Up-regulated miRNAs/Down-regulated targets			
miR-541-3p	7.9	15	BCL9L, MAST3, SPRYD4, HMGA1, VDR
miR-210	3.7	2	**HOXA1**, CLUH
miR-4671-3p	3.1	2	FOSL1, ZNF213
miR-4734	3.1	3	TMEM104, ANKRD52, CLUH
miR-4726-5p	2.2	10	SLC25A22, PYCRL, MAPKAPK3, PTGES, WNT7B
miR-495-3p	1.9	10	ZNF697, PSME3, MIDN, SOX9, GPR3
miR-1185-5p	1.7	2	BCAM, SH3RF2
miR-146a-5p	1.2	3	**PA2G4**, SMYD5, SSTR1
Down-regulated miRNAs/Up-regulated targets			
miR-4458	-7.5	20	**PTGS2**, YPEL2, CTHRC1, KLHL24, KLHL31
miR-548ar-3p	-7.2	2	PAG1, HPS2
miR-4793-3p	-7.0	2	ERRFI1, SLC38A2
miR-1270	-4.7	1	POLI
miR-548d-3p	-4.1	1	ZNF468
miR-663b	-3.9	4	SLC2A1, KDM7A, CLIC4, C1QL1
miR-4749-3p	-3.6	4	CD109, IPMK, KLF12, TNFAIP8
miR-1291	-3.5	1	PCMTD1
miR-4747-3p	-3.3	1	POLI
miR-4707-3p	-2.3	4	WSB1, PPP1R3B, KIAA1715, APOL1
miR-3130-3p	-2.0	1	SLC7A11
miR-2278	-1.9	2	PDP1, ZNF33B
miR-4467	-1.8	1	RTN4R
miR-1273e	-1.8	3	FBXL3, ZC3H6, ZNF468
miR-3201	-1.7	2	ITGA2, BNIP3L

miR-3911	-1.6	4	TES, IKBIP, EDN1, PTPRB
miR-3064-5p	-1.6	1	TXNIP
miR-4507	-1.6	2	ZBTB1, CCNG2
miR-4488	-1.5	3	GAL3ST1, NDRG1, C1QL1
miR-3136-5p	-1.5	4	SHOC2, ALG10B, IPMK, AHR
miR-4688	-1.4	2	CDK19, TBL1XR1
miR-199a-3p	-1.4	3	ITGB8, **PTGS2**, RNGTT
hsa-miR-5010-5p	-1.3	3	HK2, EDN1, STC1
hsa-miR-4492	-1.3	5	PJA2, TBL1XR1, PFKFB4, ZNF395, C1QL1
hsa-miR-766-3p	-1.3	3	TGFBR1, ZNF468, ERRFI1
hsa-miR-3175	-1.2	2	SLC2A1, AK4
hsa-miR-1257	-1.0	1	ZNF468

Table 4.1: Ingenuity analysis predicts inversely correlated miRNA-mRNA target pairs. Using lists of differentially expressed miRNAs and mRNAs as input for the Ingenuity Pathway Analysis (IPA), it was found that 35 differentially expressed miRNAs target 108 mRNAs (high confidence and experimentally observed results). Only mRNAs and miRNAs with inverse differential expression are shown in this table. Columns identify the miRNA name, its log-transformed expression fold change between hypoxic and normoxic SLK cells, the number of identified targets, and the five or less most differentially expressed targets. In bold are miRNAs and mRNA targets that have been previously reported in the literature.

4.3 Link between the cellular response to hypoxia and KSHV infection

The responses of SLK cells undergoing infection or hypoxic stress were compared at both the miRNA and the mRNA levels.

4.3.1 Comparative mRNA expression profiling analysis

Cells latently infected with KSHV have been shown to increase HIF-1α activity in normoxia (Carroll et al. 2006), suggesting that viral infection may, to some extent, mimic the hypoxic response. This up-regulation of HIF is mediated by protein-protein interactions with LANA (Cai et al. 2007), stabilization via v-IRF3 (Shin et al. 2008) and transcriptional activation through v-GPCR (Sodhi et al. 2000). Also, hypoxia has been shown to induce lytic replication in B-cells (Davis 2001; Cai et al. 2006). Here, RNA-Seq was used on normoxic SLK cells, hypoxic SLK cells, and normoxic SLKK cells to assess the similarities and differences in mRNA gene expression between KSHV infection and hypoxia.

Figure 4.9 illustrates the overlap of mRNAs found down-regulated by KSHV infection and hypoxia. Remarkably, more than a third (~37%) of the genes down-regulated by hypoxia were also down-regulated by KSHV. By contrast, out of a total of 742 genes down-regulated by KSHV, 122 (~16%) were similarly down-regulated by hypoxia. These results suggest that KSHV infection triggers a greater change than the hypoxic response but that the cellular response to KSHV presence mimics a significant part of the hypoxic response. On the other hand, genes up-regulated by both KSHV and hypoxia are in much fewer numbers as compared to the down-regulated genes (**Figure 4.10**). Nonetheless, the overlap comprised 41 genes, which represent ~20% of the hypoxia up-regulated genes. Of interest, these 41 included nuclear enriched abundant transcript 1

(NEAT1), integrin alpha 5 (ITGAV) and baculoviral IAP repeat-containing 3 (BIRC3). Interestingly, BIRC3, also known as cIAP-2, is an antiapoptotic gene that was previously found to be up-regulated by KSHV latent protein K15 (Brinkmann et al. 2007). It interferes with the activation of caspases and is a down-stream target gene of NF-κB, which is essential to KSHV-infected cells (Keller et al. 2006; Beyaert, Heyninck, and Van Huffel 2000). Additionally, BIRC3 is a known hypoxia-responsive gene that may play a role in conferring apoptosis resistance under hypoxia (Hu et al. 2003). Previously, NEAT1, a host long non-coding RNA involved in nuclear paraspeckle formation, has been shown to increase 5 to 10 fold in human cell lines infected with HIV-1 and to regulate HIV replication (Quan Zhang et al. 2013). However, this is the first time NEAT1 has been described up-regulated in KSHV-infected cells. Of additional relevance, HIF-2α has recently been shown to activate NEAT1 aiding in cancer cell survival (Choudhry et al. 2014), and thus NEAT1 may also play a role in promoting the survival of KSHV-infected cells. Finally, ITGAV was also found up-regulated by hypoxia in SLK cells, consistent with previous findings showing that α_V integrins were induced by hypoxia (Suzuma et al. 1998). Since ITGAV and integrin β_3 form the viral receptor $\alpha_V\beta_3$–integrin which has been shown to mediate KSHV entry (Garrigues et al. 2008), it is plausible that hypoxia may promote KSHV infection via up-regulation of ITGAV. Moreover, ITGAV may also contribute to the vascular development – a feature of KSHV-associated diseases – through fibronectin matrix assembly (Wierzbicka-Patynowski and Schwarzbauer 2003; van der Flier et al. 2010).

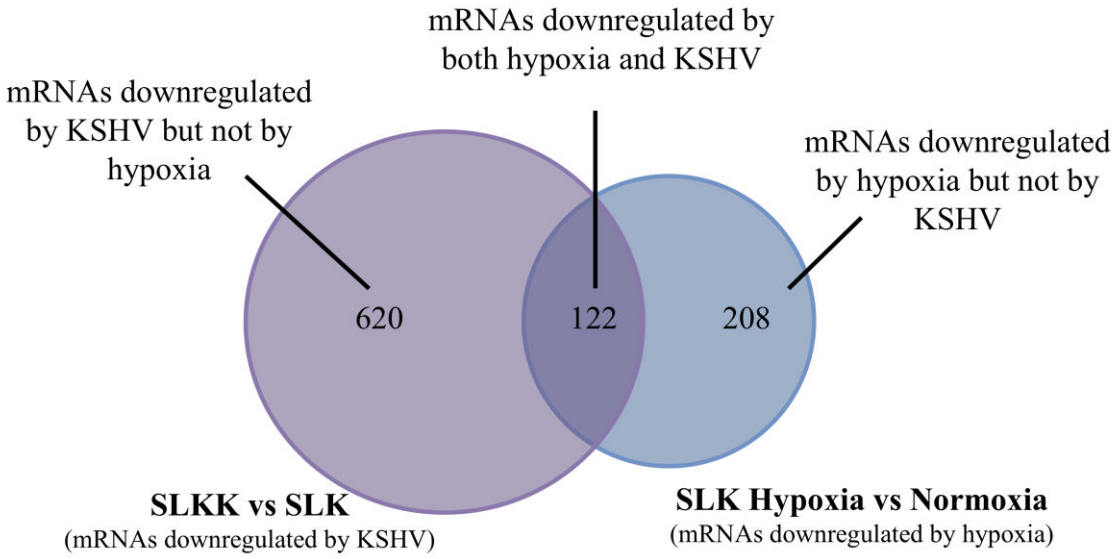

Figure 4.9: Venn diagram showing the overlap of mRNAs down-regulated by hypoxia and KSHV.

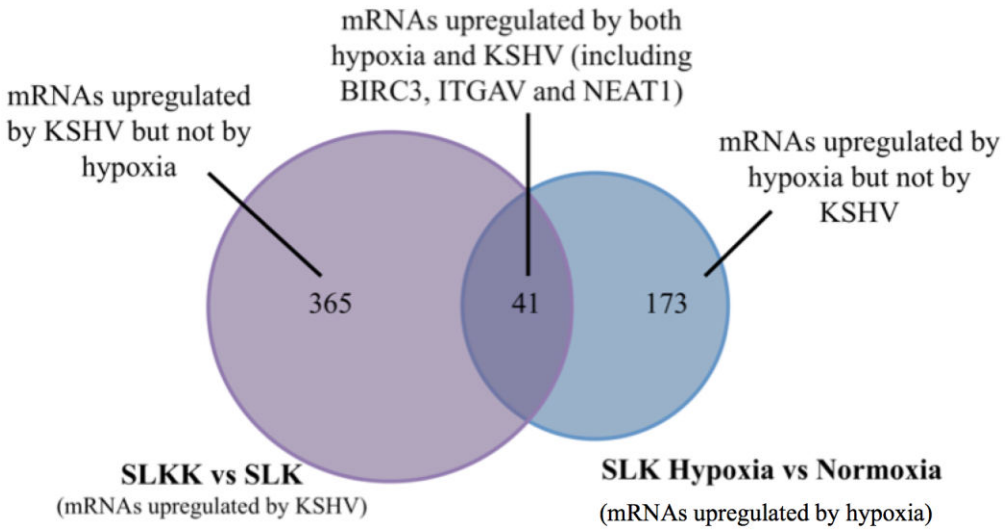

Figure 4.10: Venn diagram showing the overlap of mRNAs up-regulated by hypoxia or KSHV.

4.3.2 Comparative miRNA expression profiling analysis

A similar comparison was carried out on the data obtained from the small RNA-Seq differential analysis (and Taqman analysis in regard to miR-210). There were ten dysregulated miRNAs that overlapped between hypoxia and KSHV infection (**Figure 4.11**). Of these ten, miR-4671-3p and miR-210 were up-regulated, while the other eight were down-regulated – the most abundant included miR-548b-3p and miR-1270. The other up-regulated miRNA in common, miR-4671-3p, is predicted to down-regulate FOSL1 and ZNF213 (**Table 4.1**). Suggested to be a transcription factor, ZNF213 is a zinc finger protein of unknown function (X. Chen et al. 1999). FOSL1 is an oncogenic transcription factor involved in cellular proliferation, vasculogenesis and angiogenesis (Evellin et al. 2013). It belongs to the Fos protein family which dimerises with the Jun protein family (c-Jun, JunB, and JunD) to form the AP-1 complex induced in hypoxia (Verde et al. 2014). TargetScan predicted that miR-4671-3p could bind the 3'UTR of FOSL1 via an 8mer site that is conserved among many species. An 8mer site comprises the miRNA seed region as well as an extra 'A' and is the strongest type of binding seed-match site (**Figure 4.12**).

Although miR-210 did not make the significance threshold of the small RNA-Seq analysis between infected SLKK and uninfected SLK cells (P =0.09), the previous chapter highlighted that it was up-regulated by KSHV using Taqman qPCR assays. Therefore, besides miR-4671-3p, miR-210 is also a common feature of the cellular response between KSHV infection and hypoxic stress.

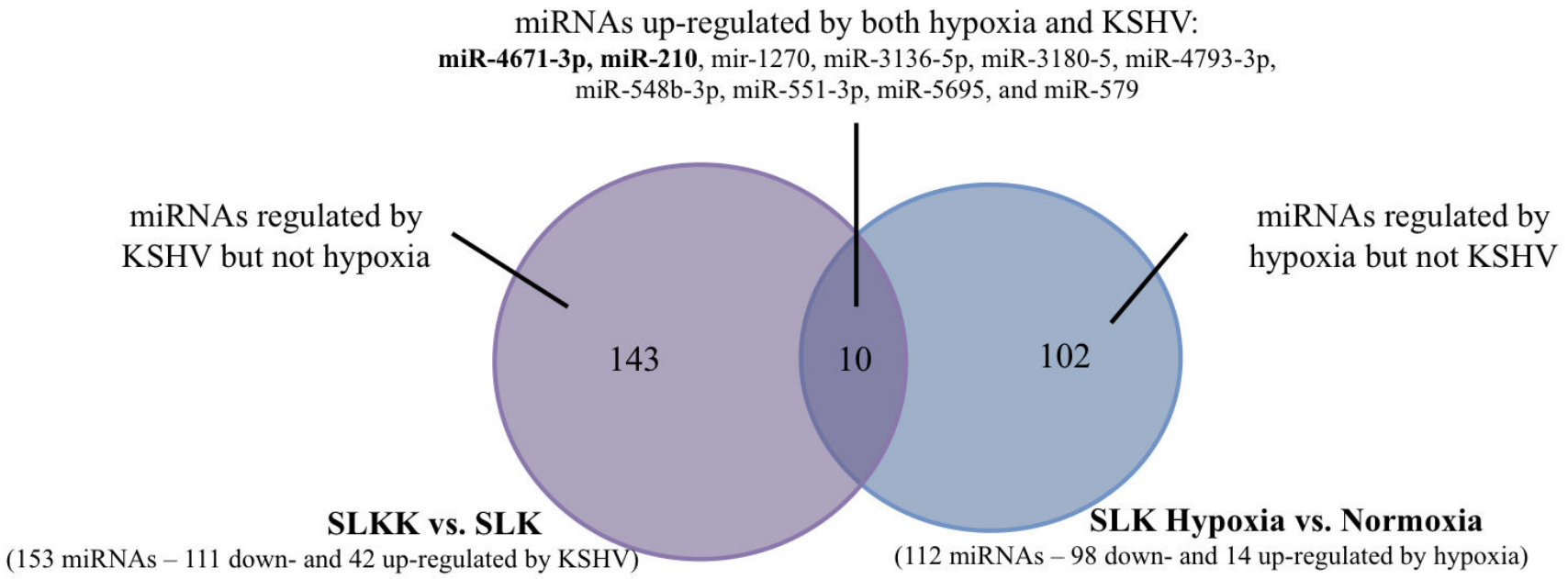

Figure 4.11: Venn diagram showing the overlap of differentially expressed miRNAs between KSHV infection and hypoxic response. Indicated in bold and normal font are the miRNAs found up-regulated and down-regulated, respectively, by both hypoxia and KSHV infection.

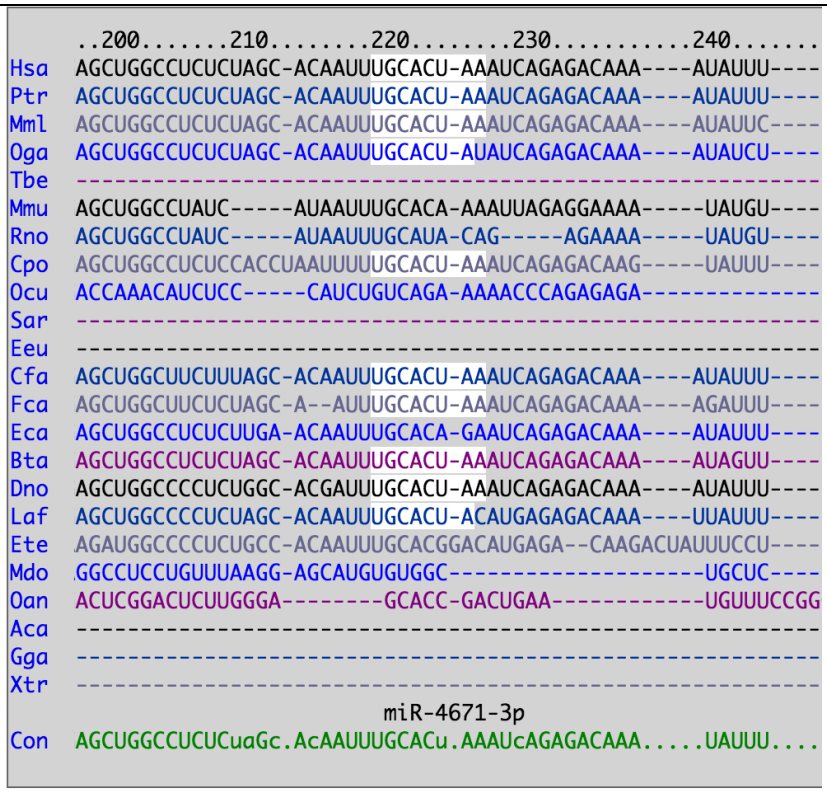

	Duplex Structure	Position	Seed match
FOSL1 3'UTR	5'. . .CUCUCUAGCACAAUUUGCACUAA. . .	220-227	8mer
hsa-miR-4671-3p	3' UCUGGUUUCUGAUACGUGAUU		

Figure 4.12: miR-4671-3p interaction with target FOSL1 3'UTR. This illustrates the conserved binding site (highlighted) between hsa-miR-4671-3p and the 3'UTR region of FOSL1, a putative target predicted by TargetScan. The seed region is predicted to be an 8mer, which is defined as an exact match between FOSL1 mRNA and the mature miRNA from position 2 to 8 (the seed + position 8) followed by an 'A'.

4.4 Hypoxic response in KSHV-infected SLKK cells

As of now, neither the mRNA nor the miRNA cellular responses to hypoxia have been investigated in any kind of pathogen-infected cells using next-generation sequencing. Here, SLKK cells, which are SLK cells stably infected with latent KSHV, were exposed to 1% O_2 for 24hrs and both miRNA and mRNA genome-wide expression profiles were analysed.

4.4.1 miRNA expression profiling of normoxic and hypoxic SLKK cells

Differential analysis between hypoxic and normoxic SLKK cells reveals that, among the 79 miRNAs that are dysregulated by hypoxia, miR-210 is once again the most significantly up-regulated miRNA ($P = 2x10^{-4}$ and $\log_2$ FC =3.7; **Figure 4.13**). Of these 79 HRMs, 72 made the abundance cut-off (average miR count ≥1), which allowed for the unbiased, unsupervised clustering of hypoxic vs. normoxic SLKK samples (**Figure 4.14**). Of these 72 miRNAs, 51 were down-regulated, while 21 were up-regulated, including miR-210 and miR-193a-5p. Of note, the expression of miR-193a-5p increased by 3 fold in hypoxia (P =0.025). Since it has never been reported that miR-193a-5p is modulated in hypoxia, miR-193a-5p can be considered a novel HRM.

The 15 most abundant HRMs were selected using a threshold of 10 for the average miR count (**Figure 4.15**). Of these, miR-210, miR-193a-5p and miR-139-5p were up-regulated while miR-16-1-3p was the top down-regulated miRNA. miR-139-5p had been shown to be induced 4 fold upon hypoxia in pulmonary artery smooth muscle cells (Wu et al. 2011). By contrast, down-regulation of miR-16 has been reported to induce VEGF expression (Dejean et al. 2011).

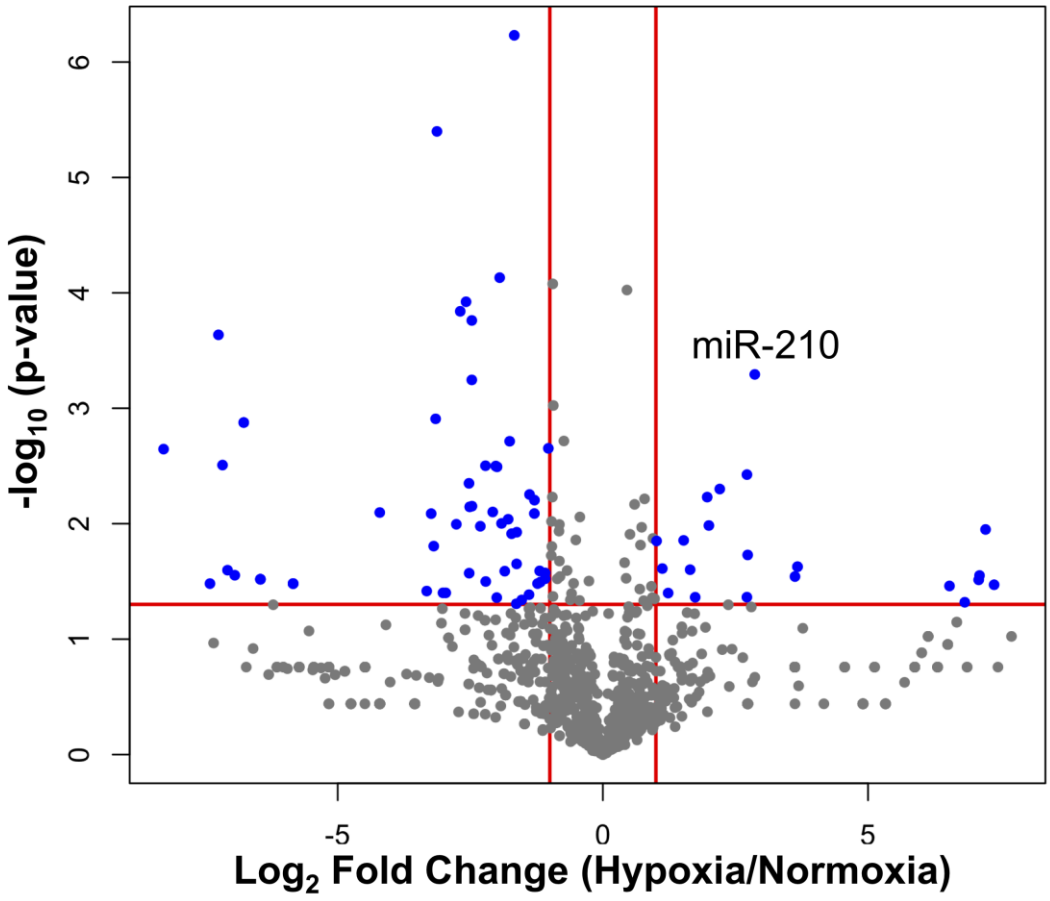

Figure 4.13: Volcano plot of miRNA differential expression in hypoxic vs. normoxic infected SLKK cells. The plot is depicted as in **Figure 4.1**, with vertical and horizontal red lines similarly representing the thresholds of a fold change of 2 or -2, and of a *P*-value of 0.05, respectively.

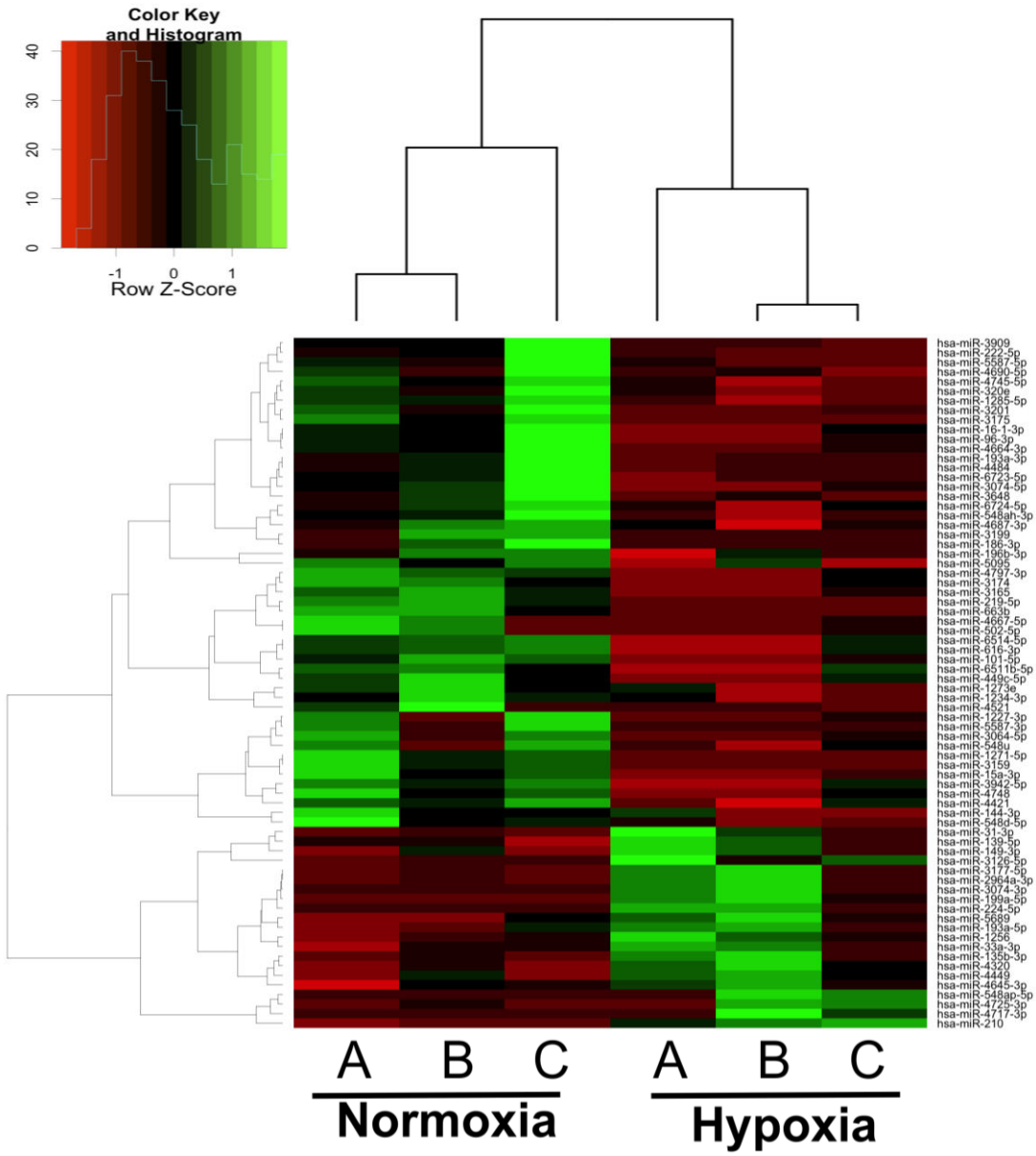

Figure 4.14: Expression of miRNAs in the analysed small RNA libraries. Heatmap of miRNA changes between hypoxic and normoxic SLKK cells in the six individual replicates (three normoxic and three hypoxic SLKK samples). Presented is the relative expression of 72 significantly deregulated cellular miRNAs in hypoxic vs. normoxic infected cells (*P*-value ≤0.05, $\log_2$ FC ≤-1 or ≥-1, average miR count ≥1). The plot is depicted as in **Figure 4.2**, with each row representing a miRNA and each column representing a biological replicate. Red, black and green denote low, median and high relative miRNA expression, respectively.

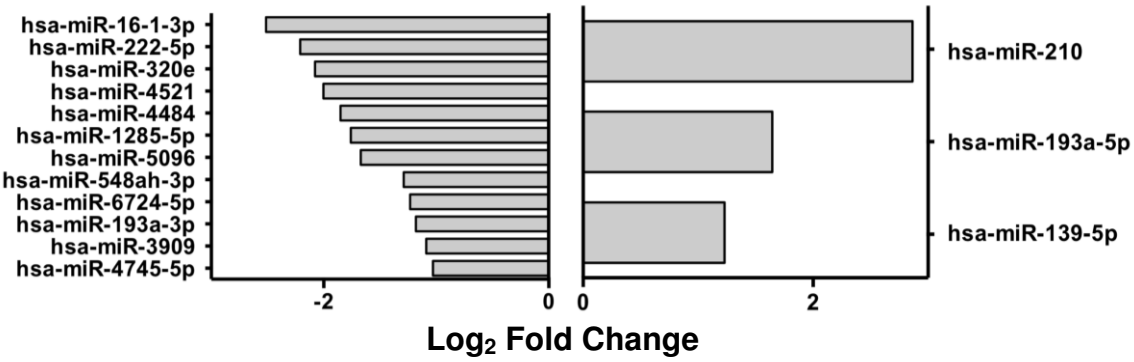

Figure 4.15: Top 15 repressed and induced miRNAs in hypoxic vs. normoxic infected SLKK cells. Bars below and above the y-axis show the 15 most abundant miRNAs repressed and induced, respectively, in hypoxia compared to normoxia in BCBL-1 cells. Data were considered significant when $P \leq 0.05$, an average miR count of 10 or more across all replicates (i.e. threshold of miR counts sum higher than 60).

4.4.2 A detailed study of miR-210 regulation by hypoxia and KSHV

Numerous studies have demonstrated that there is an association between KSHV pathogenesis and hypoxia. KS lesions arise in areas of hypoxia, exhibit elevated levels of HIFs, as well as enhanced angiogenic markers akin to the cellular response to hypoxia. Because miR-210 is the most consistent miRNA increased in response to hypoxia, an investigation of its potential role in KSHV pathogenesis was undertaken.

The relative expression of miR-210 was evaluated by Taqman assay in four different conditions: normoxic SLK cells, normoxic SLKK cells, hypoxic SLK cells and hypoxic SLKK cells (each n=3). Normalising to normoxic SLK samples, it became apparent that infection alone could indeed increase miR-210 levels (**Figure 4.16**). There was a strong induction of miR-210 in hypoxic SLK cells (15-20 fold increase). Based on this observation, it was hypothesised that an increase in miR-210 in KSHV infected cells, either in normoxia or in hypoxia, may help promote cellular alterations that favour infected cells. ISCU, a mitochondrial iron sulphur scaffold protein, is a miR-210 target important in cellular metabolism. In MCF7 cells, it has been shown that miR-210-mediated down-regulation of ISCU causes a shift to glycolysis, an enhanced cell survival, and an increase in iron uptake required for cell growth (Favaro et al. 2010).

To investigate whether ISCU is down-regulated by miR-210, transfection of miRNA mimics and inhibitors was performed in SLKK cells, either in normoxia or in hypoxia (**Figure 4.17**). The experiment was carried out in duplicate wells of a 6-well plate, using a no transfection control and a neutral miRNA mimic called Scramble. In hypoxia, miR-210 is expected to be induced by HIF-1α and therefore the transfection of a miR-210

inhibitor in hypoxia should knock-down miR-210 levels. Inversely, in normoxia, the transfection of miR-210 should mimic a hypoxic induction and induce miR-210 levels.

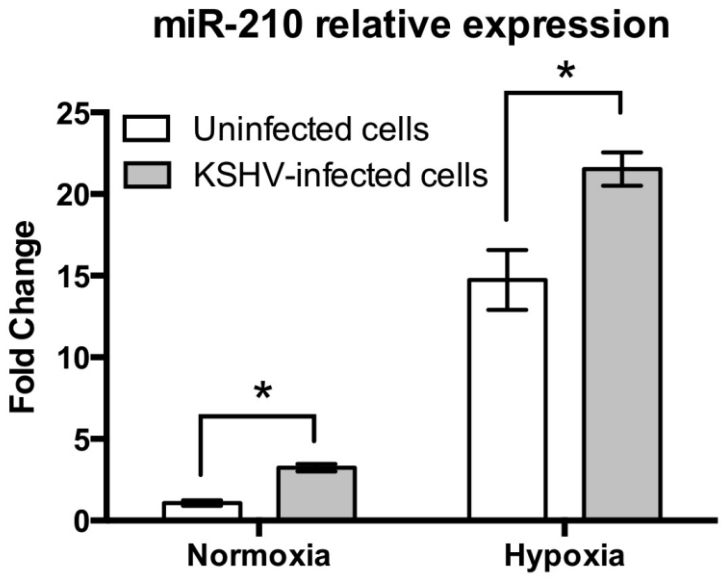

Figure 4.16: Taqman assays validate miR-210 up-regulation both in infected vs. uninfected cells, and in hypoxia vs. normoxia. Data represent the expression fold change between normoxic SLKK vs. SLK cells, and between hypoxic SLKK vs. SLK cells. Bars depict the mean of at least three independent experiments; error bars reflect the standard deviation of the mean. *, $P \leq 0.05$.

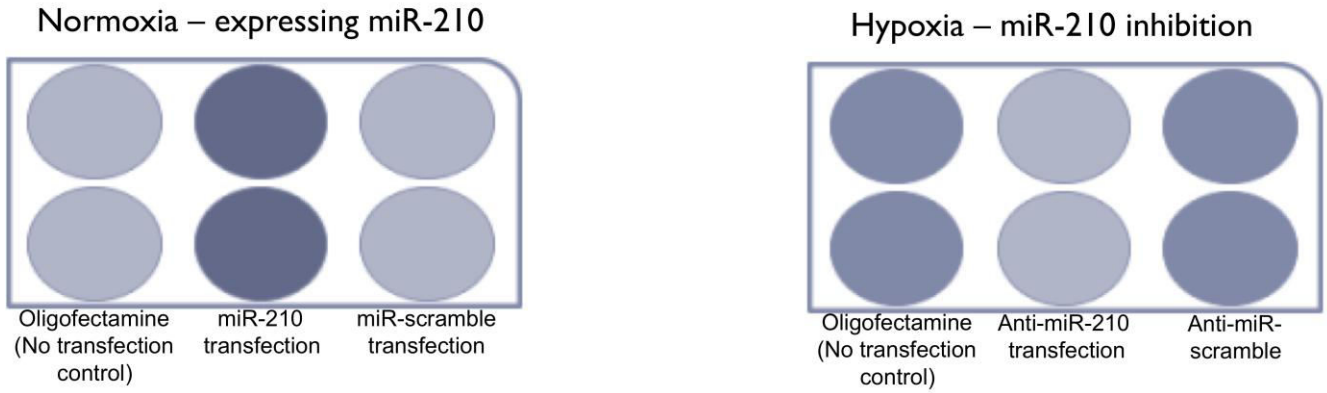

Experimental conditions	Tested effects	Expected results	Internal controls in this condition
Oligofectamine samples under hypoxia vs. normoxia	Hypoxia exposure	• miR-210 ↑ • miR-210 targets ↓	Oligofectamine-only under normoxia
miR-210 mimic vs. miR-scramble under normoxia	miR-210 expression	• miR-210 ↑ • miR-210 targets ↓	miR-scramble under normoxia
Anti-miR-scramble vs. anti-miR-210 under hypoxia	miR-210 inhibition	• miR-210 ↓ • miR-210 targets ↑	Anti-miR-scramble under hypoxia

Figure 4.17: Workflow of mimic-antimiR transfection experiment. This figure shows the experimental workflow of over-expression of miR-210 in normoxic SLKK cells, and inhibition of miR-210 in hypoxic SLKK cells, using the appropriate transfection controls (scrambles) and no transfection controls. The experimental conditions, tested effects, expected results, as well as the internal controls are detailed in this table.

Figure 4.18 shows miR-210 relative expression in this experiment. The no transfection control (Oligofectamine only) and the miRNA mimic control (Scramble) expressed miR-210 in similar amounts. The transfection of SLKK cells with miR-210 mimics increased its relative expression 12-fold (**Figure 4.18**). In comparison, the no transfection control and miRNA control (anti-Scramble) in hypoxia increased miR-210 expression ~5 to 6 fold. Finally, miR-210 expression when miR-210 inhibitors (anti-210) were transfected was similar to its normoxic levels. This data allowed for a further analysis of the effects of miR-210 on ISCU expression.

To test if SLKK cells responded to miR-210 fluctuations similarly, the levels of miR-210 target, ISCU, were evaluated by qRT-PCR (**Figure 4.19**). ISCU was found significantly down-regulated when miR-210 mimics were transfected in normoxia, whereas it was up-regulated when miR-210 inhibitors were transfected in hypoxia, confirming published findings (Favaro et al. 2010). These results confirm that ISCU is a target of miR-210 in KSHV-positive SLKK cells and that miR-210-mediated repression of ISCU may function to mediate cell survival.

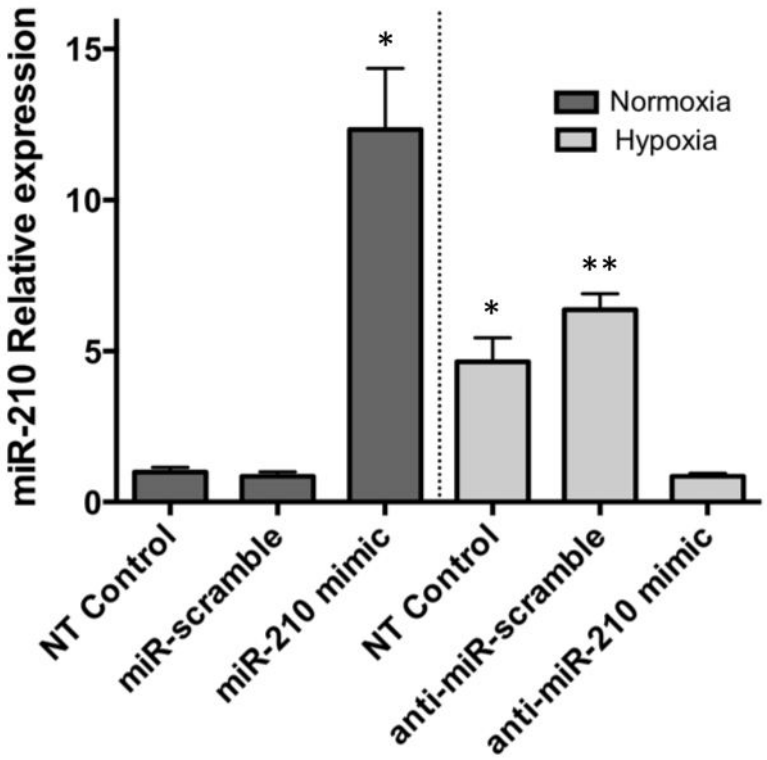

Figure 4.18: Validation of miR-210 expression in transfected SLKK samples using Taqman assays. Bars depict the mean of three independent experiments (expressed as the relative expression compared to normoxic NT controls); error bars reflect the standard deviation of the mean. NT: No Transfection.

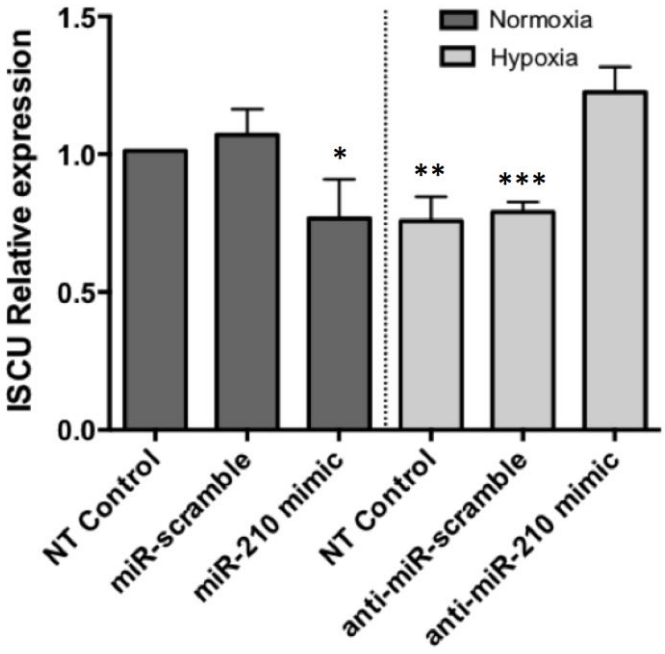

Figure 4.19: ISCU relative expression in transfected SLKK samples measured by qRT-PCR. Bars depict the mean of three independent experiments (expressed as the relative expression compared to normoxic NT controls); error bars reflect the standard deviation of the mean. NT: No Transfection.

4.4.3 mRNA profiling of normoxic and hypoxic SLKK cells

In order to correlate the changes in miRNA levels and their potential target mRNAs, deep sequencing of mRNA libraries of hypoxic and normoxic SLKK cells was performed (each n=3). Differential analysis using Cufflinks showed that 445 out of 30,808 genes (1.4%) were differentially expressed (in blue in **Figure 4.20**). Of interest, N-Myc downstream regulated 1 (NDRG1) was the most significantly up-regulated gene. NDRG1 expression has been shown to be increased by a variety of environmental stresses, including hypoxia, in either normal or tumour cells (P. Zhang, Tchou-Wong, and Costa 2007; B. Chen, Nelson, and Sadovsky 2006; Angst et al. 2006). Interestingly, up-regulation of stanniocalcin-2 (STC2) by hypoxia was very similar in SLK cells and SLKK cells, with a 3.9 and 3.8 $\log_2$ FC increase, respectively. STC2 promotes cell proliferation, epithelial-mesenchymal transition (EMT) and invasiveness in hypoxia; traits that likely promote viral persistence and malignant progression (Law and Wong 2010a; Law and Wong 2010b). In order to confirm that hypoxic induction occurred in the SLKK cells, quantitative real time PCR was undertaken to determine the expression of vascular endothelial growth factor (VEGF) in hypoxia. **Figure 4.21** shows the ~5 fold induction of VEGF upon hypoxia exposure, which is consistent with previous studies showing that VEGF is a potent HIF-1 target gene (Forsythe et al. 1996).

Host genes encoding two miRNAs, miR-210 and miR-675, were also found significantly up-regulated by hypoxia. The promoter region of miR-210 host gene, MIR210HG, has at least two functional HIF-1α binding sites (Hypoxia-response elements, HREs) (Cicchillitti et al. 2012). Therefore, the up-regulation of MIR210HG at the mRNA level is expected. miR-675 is derived from H19-MIR675 which is an antiapoptotic non-coding RNA inducible by hypoxia (Matouk et al. 2007). H19-derived miR-675 regulates COL2A1, a cartilage matrix gene (Dudek et al. 2010). Taqman assay was undertaken to

investigate the expression of miRNAs arising from H19-MIR675, miR-675 and miR-675*. However, no significant changes (P >0.05) were observed in miR-675* or miR-675 levels (**Figure 4.22**).

Ingenuity Pathway Analysis (IPA) was used to identify molecular networks that are disrupted by hypoxic stress in SLKK cells. The top 15 most significantly altered pathways are illustrated in **Figure 4.23**. They included pathways typically altered by hypoxia such as a number of cancer signalling pathways, glycolysis, Wnt/β-catenin signalling, IL-8 signalling, and retinoic acid receptor (RAR) activation (Mazumdar et al. 2010; Fernández-Martínez et al. 2011; Maxwell et al. 2007). Additionally, atherosclerosis signalling and coagulation system were the top dysregulated pathways in hypoxic vs. normoxic SLKK cells. Atherosclerosis is a vascular disease characterised by the narrowing and hardening of arteries due to the accumulation of plaques made of fat cholesterol and calcium. Furthermore, by promoting lipid accumulation, angiogenesis and ATP depletion, hypoxia is known to play a role in atherosclerosis and accelerate its progression (Hultén and Levin 2009; Nakano et al. 2005).

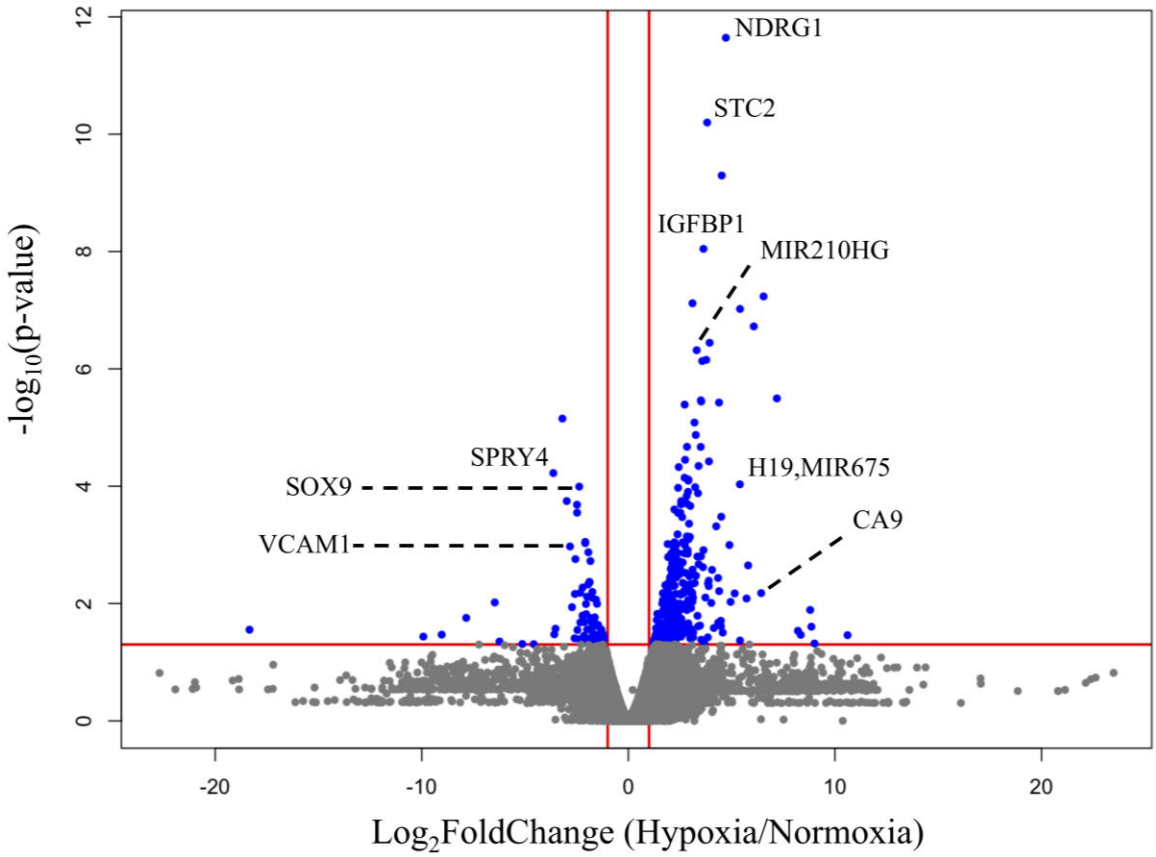

Figure 4.20: Volcano plot of mRNA differential expression in hypoxic vs. normoxic infected SLKK cells. The plot is depicted as in **Figure 4.1**, with vertical and horizontal red lines similarly representing the thresholds of a fold change of 2 or -2, and of a *P*-value of 0.05, respectively.

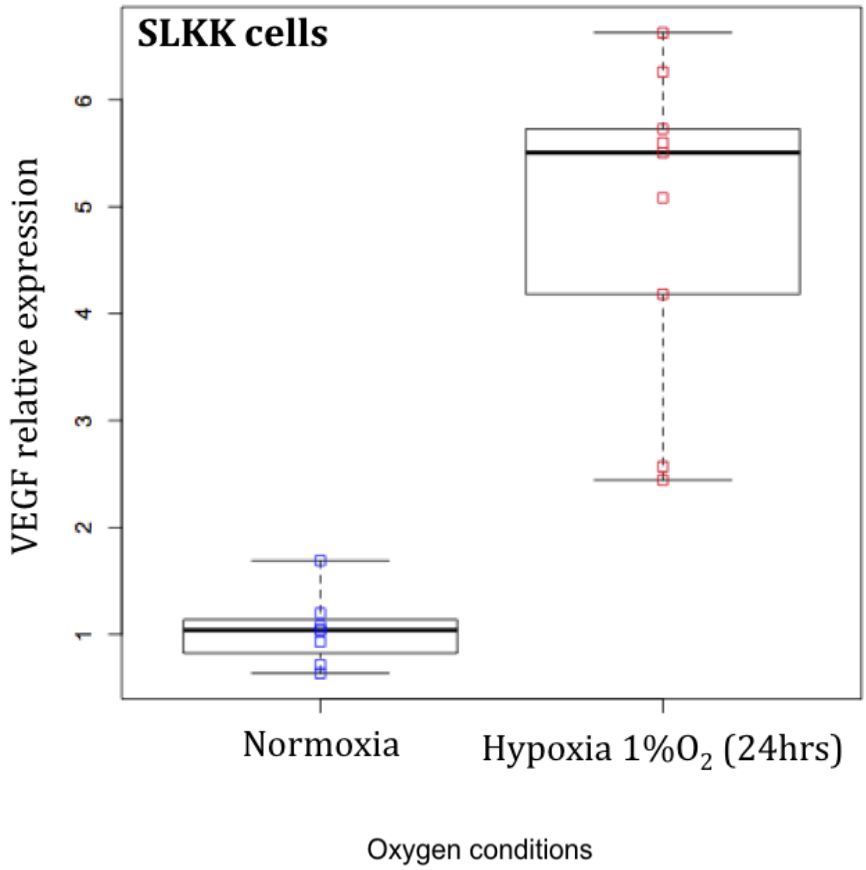

Figure 4.21: VEGF differential expression in hypoxic vs. normoxic SLKK cells. This plot represents the fold difference in VEGF expression between hypoxia and normoxia in SLKK cells, measured by qRT-PCR assays (n=9). Hypoxic samples were normalised to normoxic samples. This plot was generated using R and the rectangular box shows the interquartile range (IQR), from the 1st quartile (25th percentile) to the 3rd quartile (75th percentile). It includes the 2nd quartile (median) of VEGF relative expression change. The whiskers correspond to the minimum and maximum values.

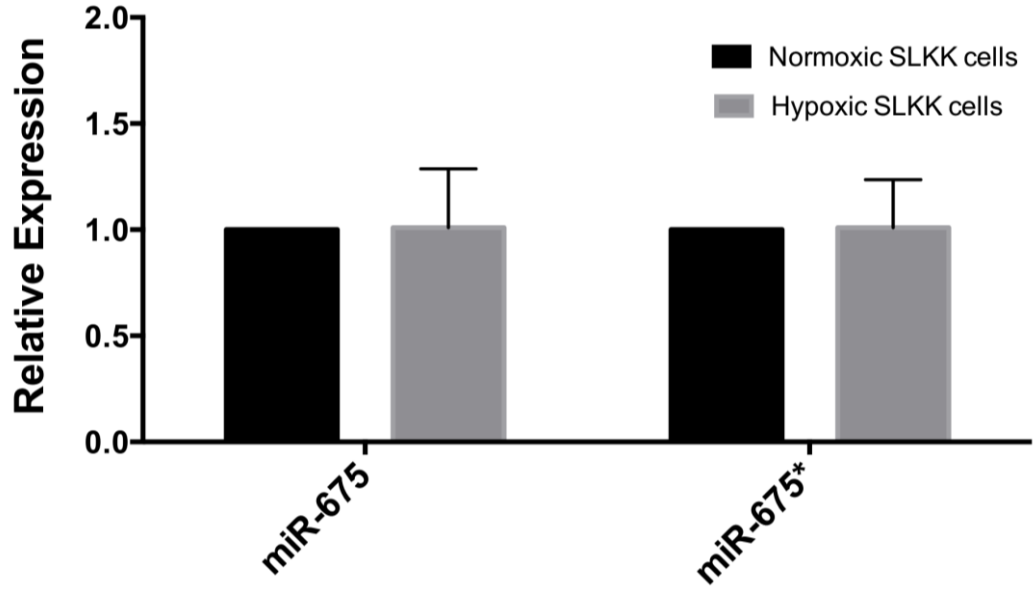

Figure 4.22: Expression levels of H19-derived miRNAs in SLKK cells under hypoxia and normoxia. Expression levels of miR-675 and miR-675* were quantified 24hrs after exposure to 1% O_2 in comparison to 24% O_2 (n=3). Gene expression values were normalised to housekeeping snoRNA RNU43. Shown are mean and standard deviation. No significant change was observed.

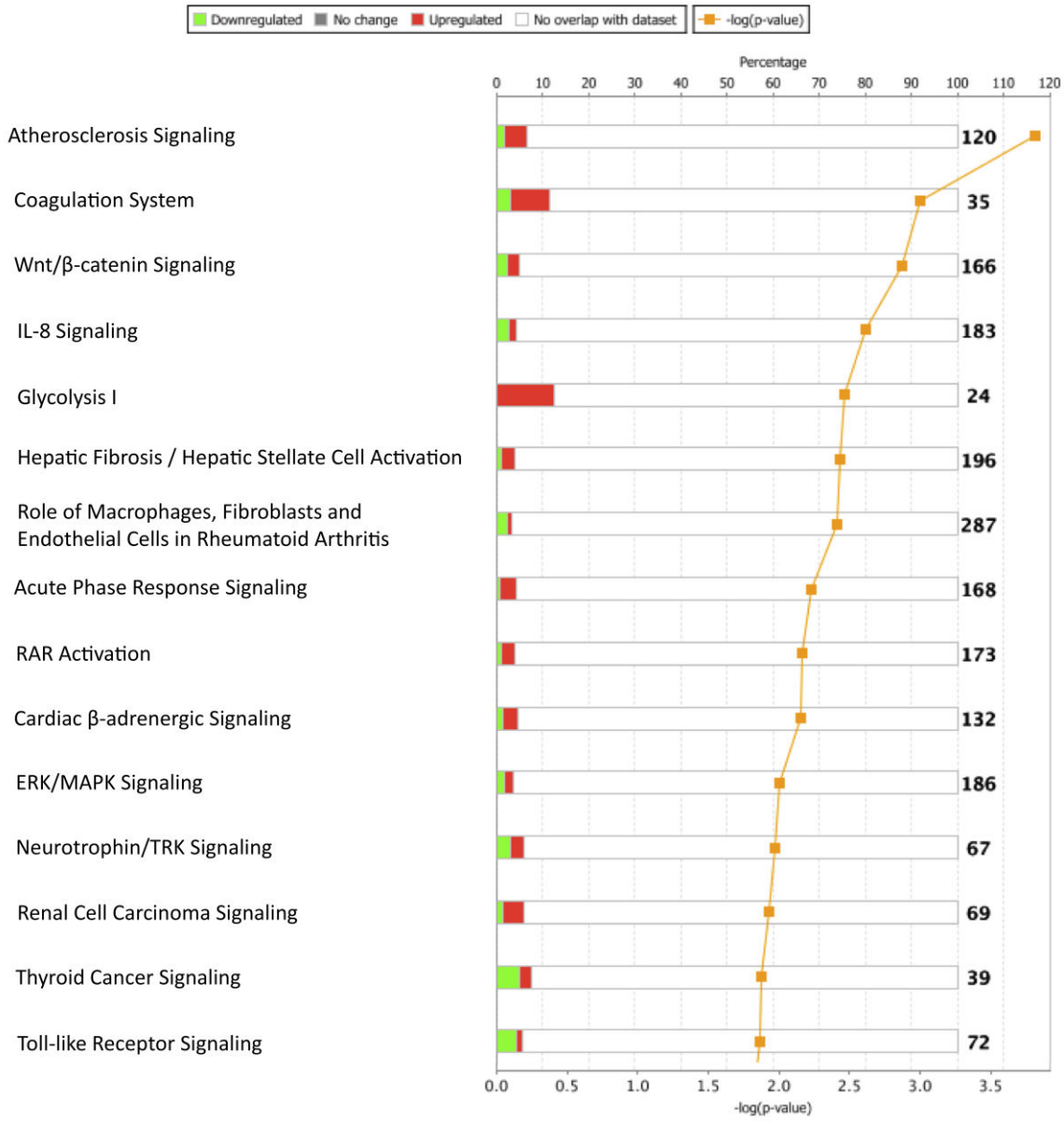

Figure 4.23: Top 15 pathways altered by hypoxia in SLKK cells. A list of differentially expressed mRNAs in SLKK cells was used for Ingenuity Pathway Analysis. The 25 pathways that were most significantly altered by hypoxia are presented here. The yellow line reflects the significance ($P \leq 0.05$ corresponds to $-\log(P\text{-value}) > 1.3$). For any given pathway, the percentage of down-regulated and up-regulated genes are depicted in green and red, respectively. The total number of genes in each pathway is indicated in bold on the right hand side.

4.4.4 Integrated miRNA-mRNA analysis in hypoxic and normoxic SLKK cells

Merging the small RNA-Seq with mRNA-Seq differential analyses, IPA paired 53 miRNAs with 176 mRNA targets, and a remarkable 82% (145 mRNAs) of these targets were concordant under hypoxia (either up-regulated miRNA and down-regulated target, or down-regulated miRNA and up-regulated target; **Figure 4.24**). Of these, 32 HRMs and 67 mRNA targets were paired with a high level of confidence or for being experimentally observed in the literature. **Table 4.2** lists the seven up-regulated miRNAs and their 43 down-regulated targets, as well as the 25 down-regulated miRNAs and their 54 targets. Of note, miR-224-5p is up-regulated in hypoxia and is predicted to down-regulate pentraxin 3 (PTX3), also known as TNF-inducible gene 14 (log_2FC =-1.7). PTX3 is known to play a dual role in both protecting cells against pathogens and controlling autoimmunity.

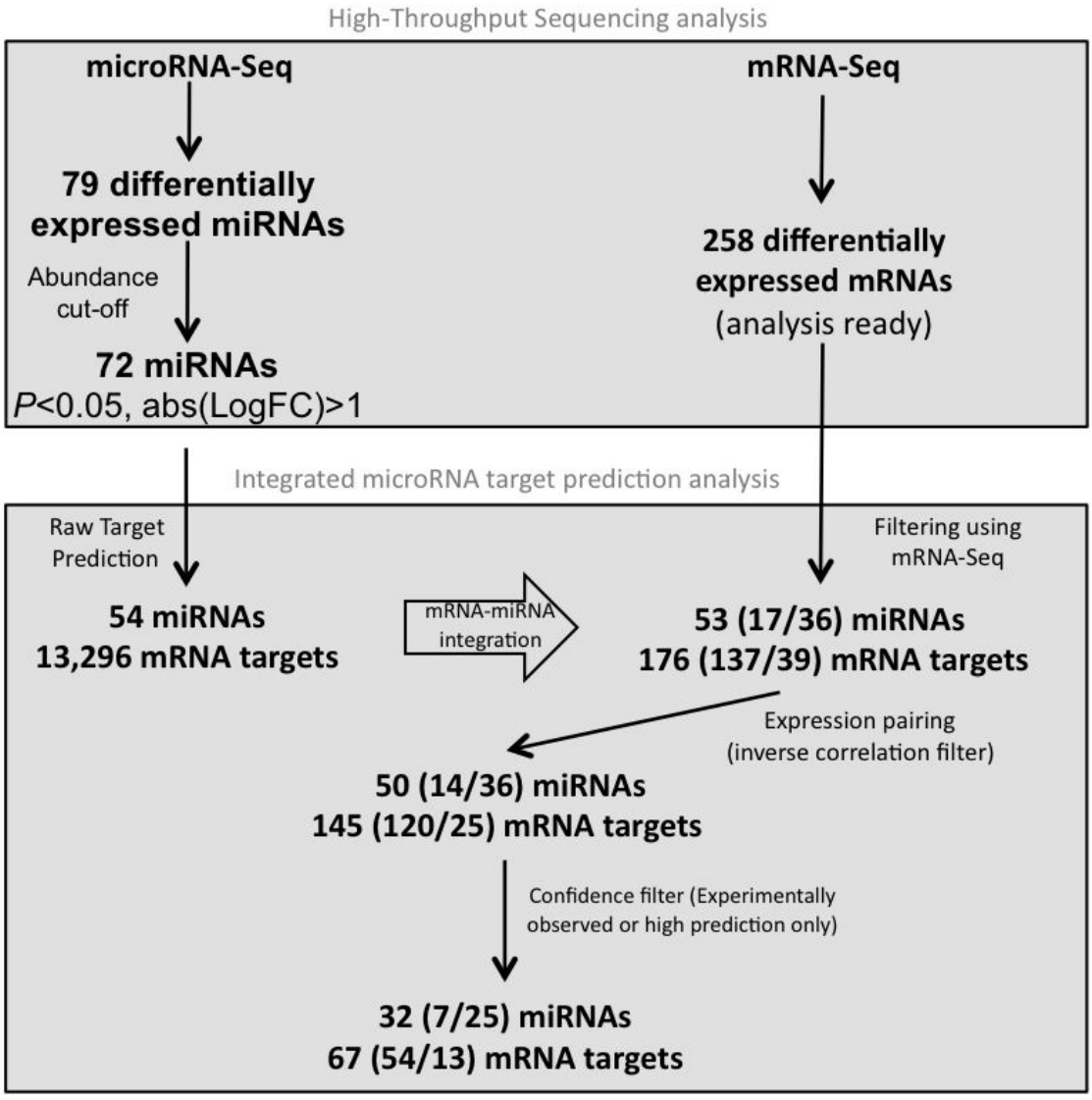

Figure 4.24: Workflow of integrated miRNA-mRNA association analysis using IPA. This experimental workflow shows the various filters used to associate miRNA-Seq and mRNA-Seq data from hypoxic and normoxic SLKK cells. Numbers are presented as Total differentially expressed miRNAs or mRNAs (Up-regulated/Down-regulated).

miRNA	Log_2 Fold Change	# Target genes	Top 5 target genes
Up-regulated miRNAs/Down-regulated targets			
miR-224-5p	7.4	1	PTX3
miR-199a-5p	2.16	2	WNT7B, PPARGC1A
miR-4717-3p	6.8	2	CLDN1, ARHGAP18
miR-4725-3p	2.7	1	SPRY4
miR-149-3p	1.7	3	SPRY4, SOX9, ATP6V0D2
miR-139-5p	1.2	5	FOS, PPARGC1A, PPARGC1B, TMCC3, ZNF697
miR-3126-5p	1.0	2	EMP1, WNT7B
Down-regulated miRNAs/Up-regulated targets			
miR-663b	-8.3	3	C1QL1, KDM4B, SLC2A1
miR-219-5p	-7.2	1	PNRC1
miR-3175	-7.1	5	CDK5R2, PDE6G, SLC2A1, SYNPO, COL1A1
miR-3199	-7.1	4	APOL1, RAB26, ARID5B, TBC1D3
miR-1271-5p	-6.8	15	UNC13C, ARRDC3, STC2, NDRG1, CDK18
miR-3201	-4.2	1	BNIP3L
miR-1227-3p	-3.3	1	PNRC1
miR-4664-3p	-3.2	1	CDK5R2
miR-3064-5p	-3.2	3	ANXA8, LMCD1, TXNIP
miR-502-5p	-3.0	3	ANKZF1, RAB20, SLC12A3
miR-4667-5p	-3.0	2	CSPG4, PFKFB4
miR-4748	-2.2	1	ZP1
miR-320e	-2.1	2	CYP26A1, SPTLC3
miR-616-3p	-2.0	1	TNFSF14
hsa-miR-449c-5p	-1.9	2	IGFBP1, WISP2
hsa-miR-5095	-1.8	3	HILPDA, RAB42, TNFSF14

hsa-miR-144-3p	-1.6	8	EFNB3, CCNG2, PNRC1, DUSP1, PPFIA4
hsa-miR-4690-5p	-1.6	1	SNX33
hsa-miR-1234-3p	-1.6	2	CSPG4, SOWAHD
hsa-miR-1273e	-1.5	1	SERPINB9
hsa-miR-4421	-1.4		C4orf3
hsa-miR-4687-3p	-1.3		C10orf10
hsa-miR-3648	-1.2	2	SECTM1, STC2
hsa-miR-3909	-1.1	2	ARID5B, MXI1
hsa-miR-4745-5p	-1.0	2	KDM4B, C17orf103

Table 4.2: Ingenuity analysis predicts inversely correlated miRNA-mRNA target pairs. Using lists of differentially expressed miRNAs and mRNAs as input for the Ingenuity Pathway Analysis (IPA), it was found that 32 differentially expressed miRNAs target 67 mRNAs (high confidence and experimentally observed results). Only mRNAs and miRNAs with opposite differential expression are shown in this table. Columns identify the miRNA name, its log-transformed expression fold change between hypoxic and normoxic SLKK cells, the number of identified targets, and the five or less most differentially expressed targets.

4.5 Comparison of the hypoxic response between infected and uninfected cells

Section 4.2 and **4.4** compiled the differential expression analyses of miRNA-Seq and mRNA-Seq data of hypoxia vs. normoxia SLK and SLKK cells. This section is investigating the similarities and dissimilarities in the cellular response to hypoxia between infected and uninfected cells. This will reveal the effects of KSHV infection on key mRNAs and miRNAs involved in the hypoxic response as it relates to viral infection.

4.5.1 Comparative miRNA expression profiling analysis

Looking at the overall hypoxic response in both SLK and SLKK cell lines, only 17 miRNAs were similarly up- or down-regulated (**Table 4.3**). There were fewer miRNAs up-regulated by hypoxia than were down-regulated. The overlap for the up-regulated miRNAs comprised miR-210, miR-193b-5p, miR-503-5p and miR-3074-3p (**Figure 4.25**). Based on an examination of the literature, this is the first time that miR-503-5p was found up-regulated by hypoxia; hence it is a novel hypoxia-inducible miRNAs. There were 13 miRNAs down-regulated by hypoxia in both SLK and SLKK cell lines (**Figure 4.26**). Of these 13, miR-222-5p had been previously reported down-regulated by hypoxia in MCF7 cells (Camps et al. 2014). However, a miRNA that has never been reported down-regulated by hypoxia is miR-636 (**Table 4.3**). It has been suggested that miR-636 could be a tumour suppressor miRNA as one of its putative target is Ras (Jang et al. 2013).

miRNAs	SLK		SLKK	
	FPKM N vs. H	Log_2FC	FPKM N vs. H	Log_2FC
Down-regulated miRNAs				
hsa-miR-100-3p	32.7 vs. 18.0	-0.86	75.2 vs. 38.4	-0.97
hsa-miR-1273e	2.8 vs. 0.8	-1.80	3.3 vs. 1.1	-1.53
hsa-miR-222-5p	226.2 vs. 68.2	-1.73	318.1 vs. 68.8	-2.21
hsa-miR-29a-5p	33.9 vs. 24.6	-0.46	48.4 vs. 24.8	-0.96
hsa-miR-3064-5p	2.1 vs. 0.7	-1.63	3.2 vs. 0.3	-3.19
hsa-miR-3175	1.0 vs. 0.4	-1.20	1.4 vs. 0.0	-7.17
hsa-miR-3201	3.7 vs. 1.2	-1.65	6.4 vs. 0.3	-4.21
hsa-miR-4484	20.2 vs. 6.3	-1.67	16.0 vs. 4.4	-1.85
hsa-miR-4664-3p	4.0 vs. 2.9	-0.46	4.3 vs. 0.5	-3.24
hsa-miR-5585-3p	8.1 vs. 4.9	-0.71	12.4 vs. 6.8	-0.86
hsa-miR-636	16.5 vs. 9.3	-0.83	21.8 vs. 11.3	-0.94
hsa-miR-663b	1.8 vs. 0.1	-3.90	3.1 vs. 0.0	-8.28
hsa-miR-6723-5p	13.5 vs. 3.1	-2.13	7.3 vs. 1.5	-2.31
Up-regulated miRNAs				
hsa-miR-210	93.7 vs. 1199.7	3.68	147.2 vs. 1071.4	2.86
hsa-miR-3074-3p	0.2 vs. 1.7	3.34	0.0 vs. 1.4	7.10
hsa-miR-193b-5p	89.5 vs. 142.1	0.67	116.9 vs. 176.9	0.60
hsa-mir-503-5p	24.1 vs. 33.8	0.49	51.0 vs. 72.7	0.51

Table 4.3: HRMs dysregulated in both SLK and SLKK cells. This table details the read count (FPKM values) of miRNAs responding similarly to hypoxia in infected and uninfected cells. miRNA names in bold indicate novel HRMs. FPKM: fragments per kilobase of exon per million mapped reads. N vs. H: Normoxia versus Hypoxia. Log-transformed fold changes were calculated adding 0.01 to both normoxic and hypoxia FPKM values, in order to correct for nil denominators.

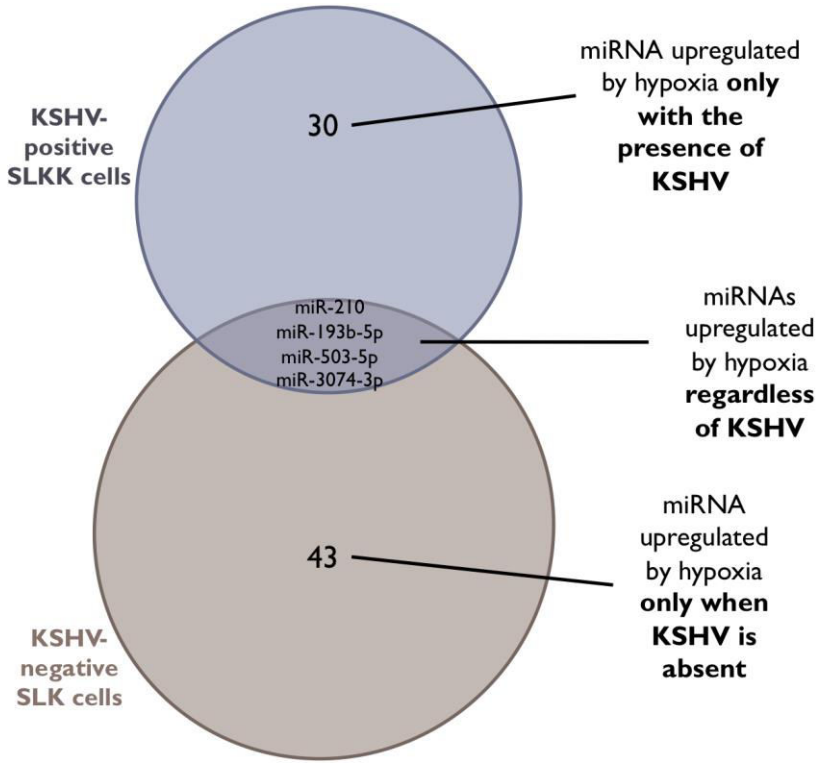

Figure 4.25: Venn diagram showing the overlap of miRNAs up-regulated by hypoxia between uninfected and infected cells.

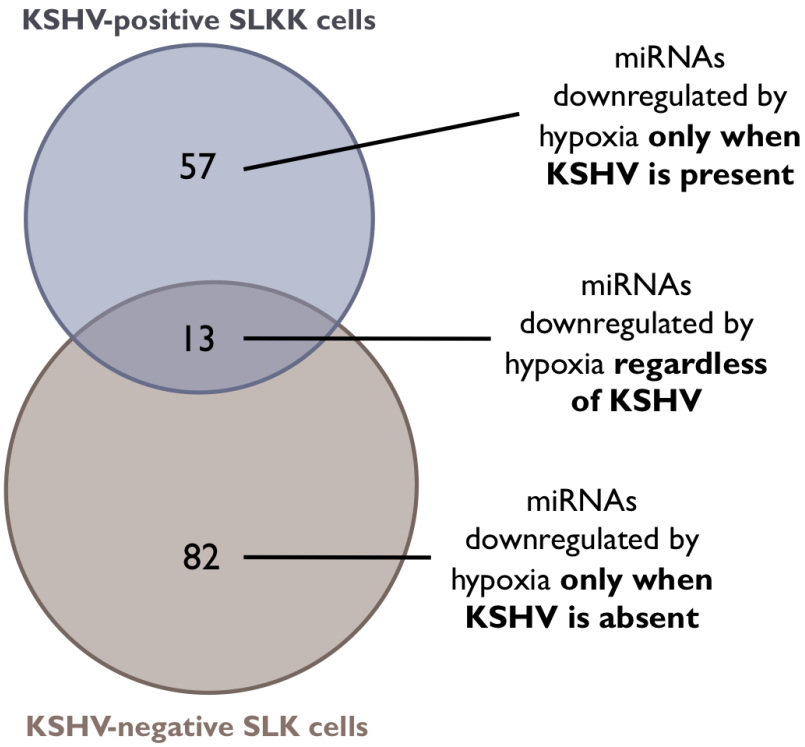

Figure 4.26: Venn diagram showing the overlap of miRNAs down-regulated by hypoxia between uninfected and infected cells.

4.5.2 Comparative mRNA expression profiling analysis

When looking at mRNA expression changes due to hypoxia in SLKK and SLK cells, it was found that 65 mRNAs, including key hypoxic genes, such as BNIP3, LOX, VCAM-1, IGFBP3, PLOD2, and miR-210 host gene (MIR210HG), responded in a similar manner. VCAM-1 was one of the significantly down-regulated mRNAs with -1.4 and -2.8 $\log_2$ FC in SLK and SLKK cells respectively (**Figure 4.27**). This is consistent with the fact that hypoxia has been reported to reduce VCAM-1 expression (Cartee et al. 2012; Rajashekhar et al. 2005). **Figure 4.28** shows an even distribution in the number of up-regulated genes between the infected and uninfected cell lines, with almost a quarter overlapping. Among the 51 up-regulated mRNAs, BNIP3, a pro-apoptotic gene known for being one of the most hypoxia-responsive genes (Guo et al. 2001; Caro 2001), had its mRNA levels increased 4 fold due to hypoxia, in both infected and uninfected cell lines. MIR210HG, host gene for miR-210, was also one of the responders in common between the two cell lines. As pointed out in **Section 4.4**, the gene encoding for miR-210 exhibits at least two functional HREs allowing direct binding with HIF-1α, which explains this up-regulation at the mRNA level in both cell lines.

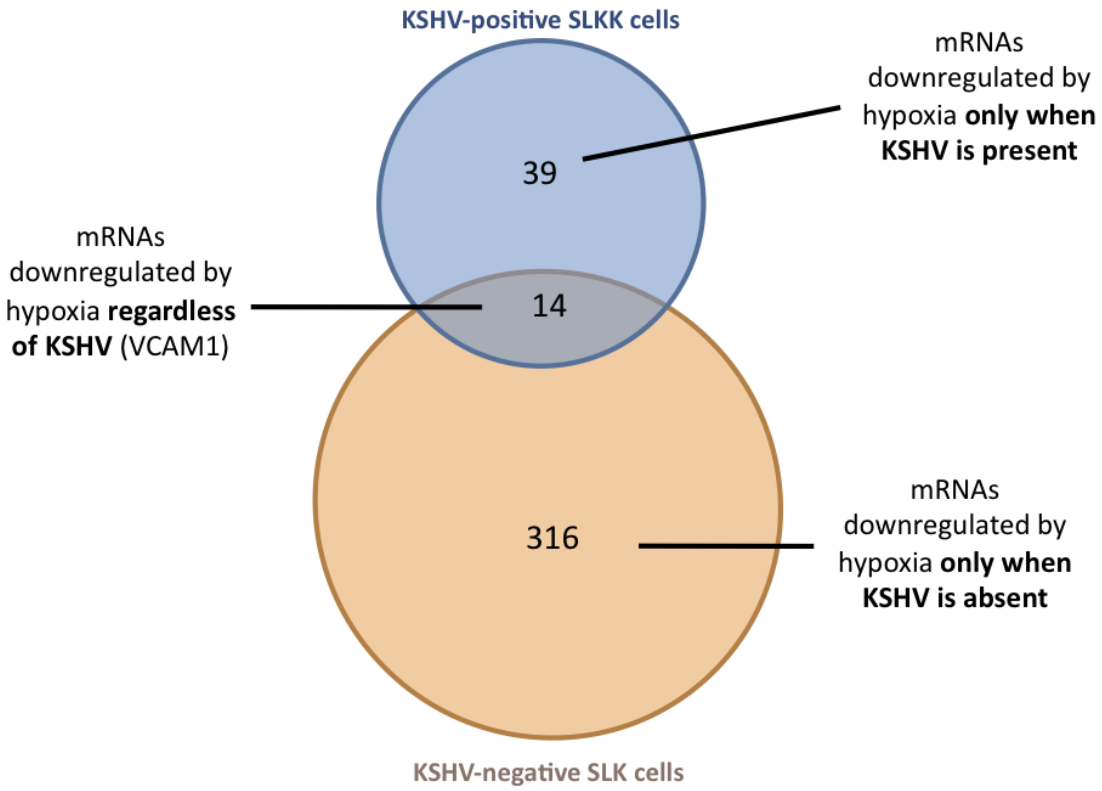

Figure 4.27: Venn diagram showing the overlap of mRNAs down-regulated by hypoxia between uninfected and infected cells.

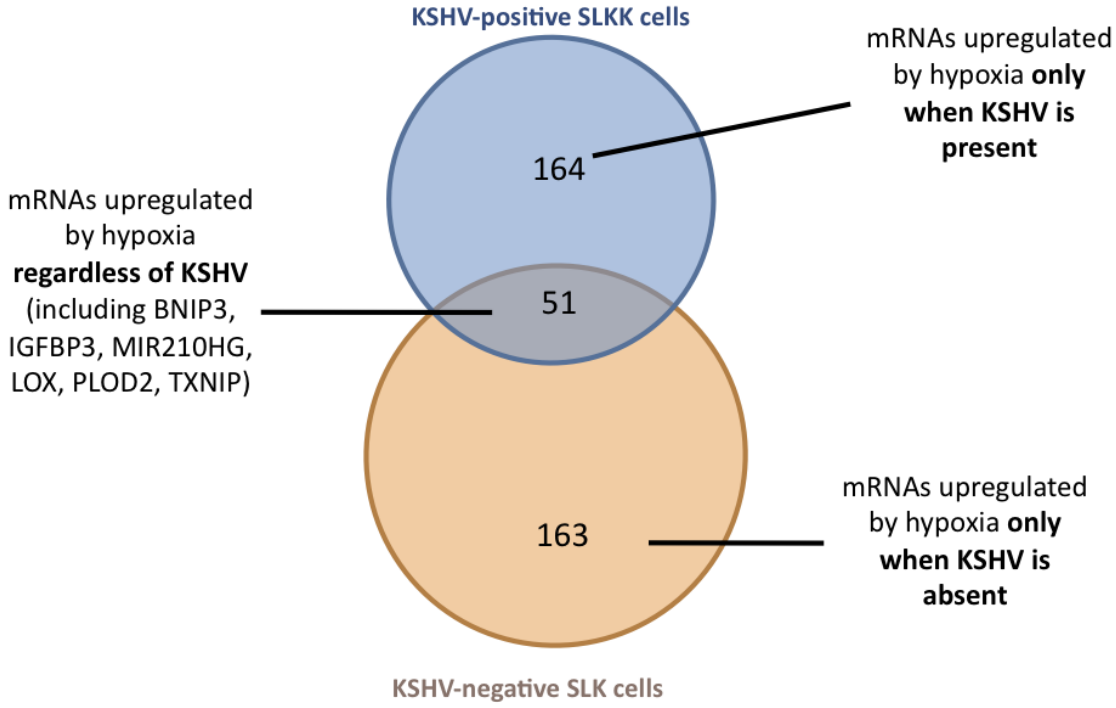

Figure 4.28: Venn diagram showing the overlap of mRNAs up-regulated by hypoxia between uninfected and infected cells.

4.6 Conclusions and future directions

Oxygen deprivation and KSHV infection have certain similarities in the ways they modulate cellular gene expression. The main shared feature is HIF-1 induction in both systems (Semenza 2007; Cai et al. 2007; Carroll et al. 2006; Sternbach and Varon 1995). A recent review from Cuninghame et al. pointed out that several oncogenic viruses, including KSHV, EBV, HPV, HBV/HCV, and human T-cell lymphotrophic virus (HTLV-1), increased cellular HIF-1 levels (Cuninghame, Jackson, and Zehbe 2014), encouraging further investigation into the link between chronic viral infection, viral oncogenesis, and HIF-1. This work, in part, assessed the extent to which hypoxic and KSHV infection led to similar changes at the miRNA and the mRNA levels and it identified the unique changes in each.

It was found that both hypoxia and KSHV infection caused significant dysregulation of miRNAs in the SLK cells, and that both stresses let to an overall decrease in many miRNAs (88% due to hypoxia, and 73% due to KSHV). However, of those dysregulated miRNAs, only a small subset responded similarly in both cases. This demonstrates that KSHV infection dramatically changes overall miRNA expression while at the same time maintaining or enhancing some changes that favour the virus. Of note, miR-210 and miR-4671-3p were both up-regulated by hypoxia and infection. Although miR-210 is clearly a hypoxia-inducible miRNA, its induction by KSHV infection was also observed. It is postulated that the increase in miR-210 in infected cells was indirectly due to the previously documented up-regulation of HIF-1 by KSHV. miR-4671-3p was up-regulated by both hypoxia and KSHV and is predicted to target and down-regulate FOSL1, an oncogenic transcription factor. Further work should be focused on clarifying whether FOSL1 is indeed a target of miR-4671-3p. Finally, taking a closer look at those

miRNAs that were affected in inverse directions by hypoxia and KSHV infection, miR-100-3p was identified as a KSHV-inducible but hypoxia-repressed miRNA. Interestingly, miR-100 has been shown to be decreased in hypoxia which would lead to an increase in its target FGFR3, a fibroblast growth factor receptor involved in maintaining cell viability (Blick et al. 2013). Further investigation would be required to determine whether KSHV infection might trigger the host cell to down-regulate FGFR3 via miR-100, in an attempt to cause cell growth arrest under certain conditions.

Additionally, it was learned that some mRNAs were similarly dysregulated by hypoxia and KSHV infection. However, unlike the miRNA responses where both stresses led to a relatively small overlap in differential expression profiles, the mRNA response to KSHV infection reconstitutes a third of the hypoxic response. This remarkable overlap suggests that KSHV substantially induces changes associated with hypoxia, indicating that such changes may augment the establishment of a viral persistent latent infection. In particular, genes such as BIRC3, ITGAV and NEAT1 were up-regulated by both hypoxia and KSHV infection. BIRC3 is of interest as it can promote the survival of cells under hypoxic stress or viral infection. Indeed, the product of this gene disturbs caspase activation hence inhibiting apoptosis. Interestingly, BIRC3 is known to be induced by hypoxia and KSHV (Hu et al. 2003; Brinkmann et al. 2007), and it has been reported to be up-regulated by the bacterial pathogen *Helicobacter pylori* (Castaño-Rodríguez et al. 2014; Li et al. 2011).

The second part of this chapter investigated the similarities and differences of the hypoxic response between the SLK and the SLKK cell lines. Previously reported hypoxia-inducible miRNAs and genes such as miR-210, miR-193b-5p, BNIP3, IGFBP3, LOX, PLOD2 and TXNIP were found significantly up-regulated by low oxygen tension in both infected and uninfected cells (Baker et al. 2008; Bellot et al. 2009; Natsuizaka et

al. 2012; Erler et al. 2009; Gilkes et al. 2013; Pulkkinen et al. 2008). Interestingly, there were some newly identified HRMs in both SLK and SLKK cells. For instance, miR-5001-3p was significantly up-regulated in hypoxic vs. normoxic SLK cells, while the up-regulation of miR-193a-5p in SLKK cells was novel. Future work should be focused on understanding the extent to which these miRNAs and respective targets benefit the virus and cells undergoing hypoxic stress.

5

Examining the role of hypoxia-regulated miRNAs in KSHV-infected B-cells

INVESTIGATING the effects of hypoxia on the SLK/SLKK model provided useful insights into the similarities and differences in hypoxic responses in the presence or the absence of KSHV. This chapter focuses on the role of hypoxia in the $KSHV^{+}/EBV^{-}$ BCBL-1 cell line, which is a well-established cell model for primary effusion lymphoma (PEL). Here, the miRNAs and putative target genes that are dysregulated by hypoxia are thoroughly examined and cross-compared to previous results in this thesis as well as known published results.

5.1 Introduction

5.1.1 BCBL-1 cells as a valuable PEL model for the study of the effects of hypoxia

Also known as body-cavity-based lymphoma (BCBL), primary effusion lymphoma (PEL) is a KSHV-associated disease that is characterised by the development of lymphoma. This often occurs through an abnormal accumulation of fluid in the pleural cavity, the space between the two membranes (pleurae) of the lungs, the peritoneal space, or other similar cavities. There is no vascular supply within the pleural space, and pleural effusions usually exhibit a relatively low oxygen concentration (Dobyns 1999). In 1996, Renne et al. established a body-cavity-based lymphoma cell line from a seropositive patient (Renne et al. 1996). The cell line harbours KSHV but lacks EBV, and has been extensively used ever since as a model for PEL.

BCBL-1 cells have previously been utilised as a model to study the effects of hypoxia on KSHV lytic activation and other viral parameters. For example, hypoxia induces lytic replication of KSHV via RTA in BCBL-1 cells (Davis 2001; Haque et al. 2003). More recently, it was learned that hypoxia up-regulates latency-associated nuclear antigen (LANA) levels through HIF activation of the LANA promoter (Veeranna et al. 2012).

As of yet however, no published studies have examined cellular genome-wide mRNA or miRNA expression profiles in any KSHV-infected cells exposed to hypoxia. The previous chapter addressed the interactive effects of hypoxia and KSHV latent infection in the SLK/SLKK model. The BCBL-1 cell line is an extremely useful model as it is a KS tumour that arises in a hypoxic environment (Dobyns 1999). Using BCBL-1 cells, the goal of this chapter is to (i) describe the miRNA and the mRNA response to hypoxia

in BCBL-1 cells, (ii) identify miRNA-mRNA pairs that are inversely expressed in hypoxia, and (iii) investigate the potential role of those pairs in KSHV pathogenesis.

5.1.2 RNA-Seq of miRNA and mRNA enriched libraries from BCBL-1 cells, an approach to studying hypoxic stress in PEL

Next-generation sequencing is a useful approach for the global study of hypoxia-regulated miRNAs (HRMs) and their target mRNAs. Here, the integration of these differentially expressed datasets in BCBL-1 cells provides a valuable platform for future analyses in PEL. BCBL-1 cells were incubated at 1% oxygen for 24hrs. The expression profiles of miRNAs and mRNAs were then assessed using small RNA sequencing (Illumina), mRNA-enriched RNA sequencing (Epicentre), real time reverse transcription PCR, Taqman assays, and pathway analysis.

5.2 Hypoxic stress alters miRNA expression in KSHV-infected B-cells

5.2.1 Small RNA-Seq reveals differentially expressed miRNAs in hypoxic versus normoxic BCBL-1 cells

Out of a total of 1,378 human mature miRNAs, 126 miRNAs (9%) were significantly altered upon exposure to hypoxia in BCBL-1 cells ($P \leq 0.05$, FC ≤ -2 or ≥ 2; **Figure 5.1**, top left and right sectors). Of these, the majority (105 miRNAs, 83%) were down-regulated, while 21 (17%) were up-regulated by hypoxia. After filtering for miRNAs with an average miR count of 1 or more, 91 miRNAs with differential expression remained, including 18 induced and 73 repressed by hypoxia. Out of these 91 HRMs ($P \leq 0.05$, FC ≤ -2 or ≥ 2, average miR count ≥ 1), the 30 most significant miRNAs were selected based on *P*-values and these were used in the unbiased clustering of hypoxic vs.

normoxic samples (**Figure 5.2**). There were comprised of 22 down-regulated miRNAs, including miR-4454 and miR-181b-3p, and eight up-regulated miRNAs, including miR-210 and miR-3135b.

5.2.2 Validation of hypoxia-regulated miRNAs by Taqman assays in BCBL-1 cells

In order to validate miRNAs from BCBL-1 cells that were found differentially expressed in the small RNA-Seq analysis by Taqman assays, miRNAs were first filtered based on their abundance levels in BCBL-1 cells. A subset of highly abundant miRNAs was then selected using miR read counts (average sum miR read count ≥10 across all six replicates, $P \leq 0.05$, FC ≤-2 or ≥2). **Figure 5.3** illustrates the top 15 most abundant miRNAs whose expression was significantly altered. They are comprised of five up-regulated and ten down-regulated miRNAs. Based on *P*-values and reads thresholds, seven miRNAs were further selected for validation using Taqman assays. Four up-regulated miRNAs, miR-210, miR-1246, miR-3135b, and miR-4286, were investigated for hypoxic induction, while the expression fold changes of three down-regulated miRNAs, miR-181b-3p, miR-181a-3p, and miR-4800-3p, were determined. **Figure 5.4** shows the differential expression of these miRNAs in hypoxic vs. normoxic BCBL-1 cells (n=3). Of the seven miRNAs tested, five showed a similar dysregulation to that seen using small RNA-Seq analysis, while the remaining two (miR-4800-3p and miR-4286) were not found significantly changed upon hypoxia exposure.

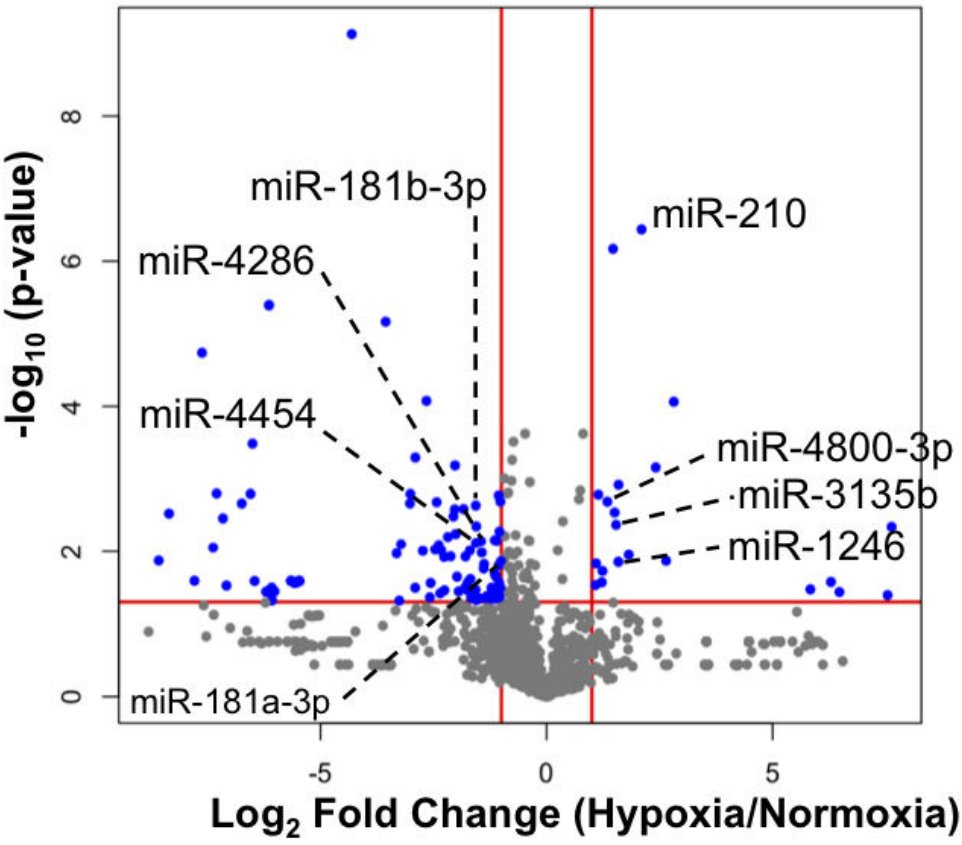

Figure 5.1: Volcano plot of miRNA differential expression in hypoxic vs. normoxic BCBL-1 cells. Vertical red lines indicate the threshold for a relative expression fold change (FC) of 2 or -2 compared to normoxic controls. The horizontal red line represents the threshold of a 0.05 *P*-value. Thus, the blue points lying in the top right and top left sectors are significantly up-regulated and down-regulated by 2 fold or more, respectively, in hypoxic vs. normoxic BCBL-1 cells ($P \leq 0.05$, FC ≤ -2 or ≥ 2).

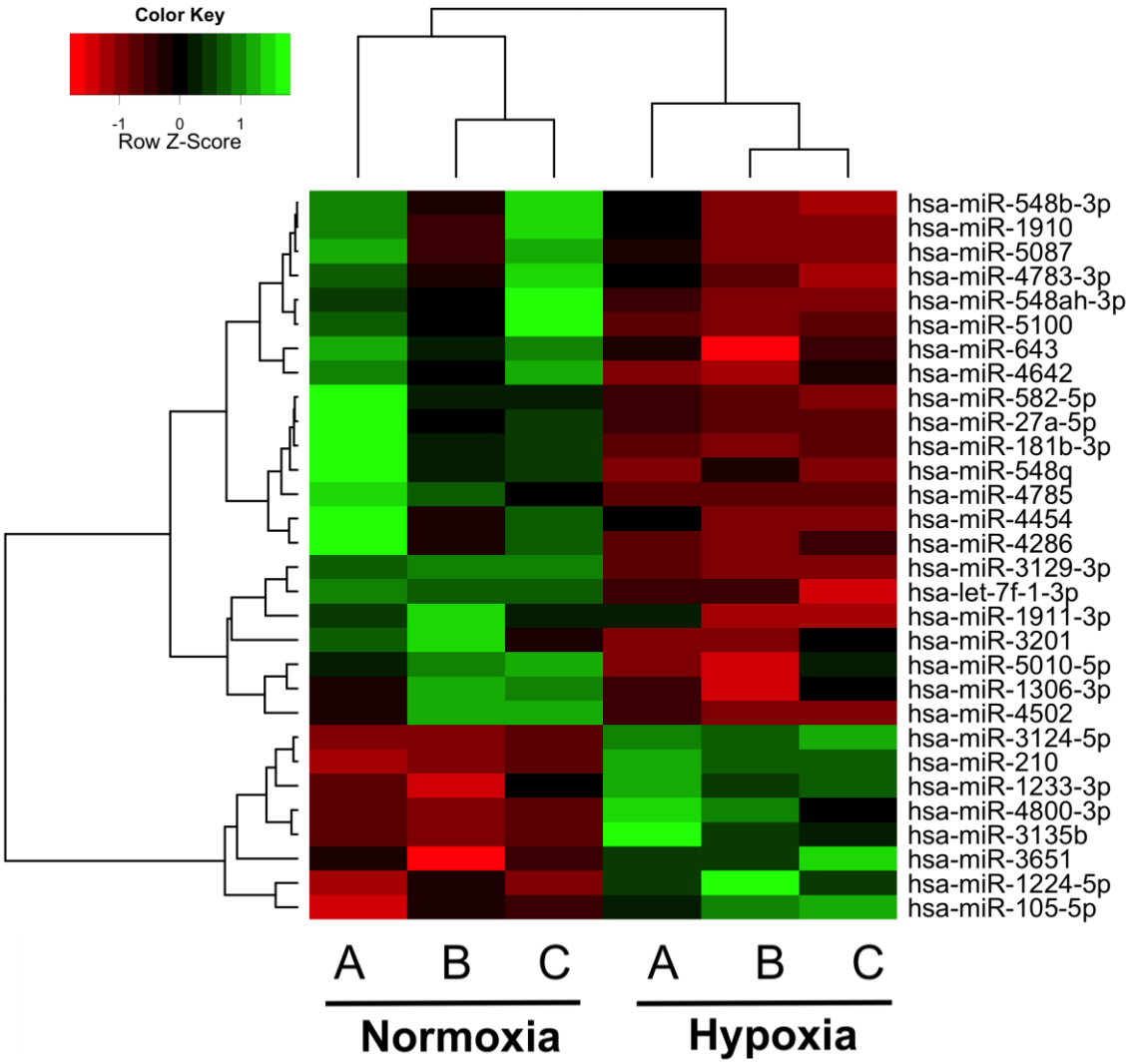

Figure 5.2: Expression of the top 30 differentially expressed miRNAs in hypoxic vs. normoxic BCBL-1 cells. Heatmap of miRNA changes between hypoxic and normoxic BCBL-1 cells in the six individual replicates (three normoxic and three hypoxic BCBL-1 samples). Presented is the relative expression of the 30 most significantly dysregulated miRNAs in hypoxic vs. normoxic KSHV-positive BCBL-1 cells ($P \leq 0.05$, log-transformed fold change greater than 1 and lower than -1, average miR count ≥ 1). Using uncentered Pearson correlation as the distance metric, an unsupervised hierarchical heatmap was generated, with each row representing a miRNA and each column representing a biological replicate. Red, black and green denote low, median and high relative miRNA expression, respectively.

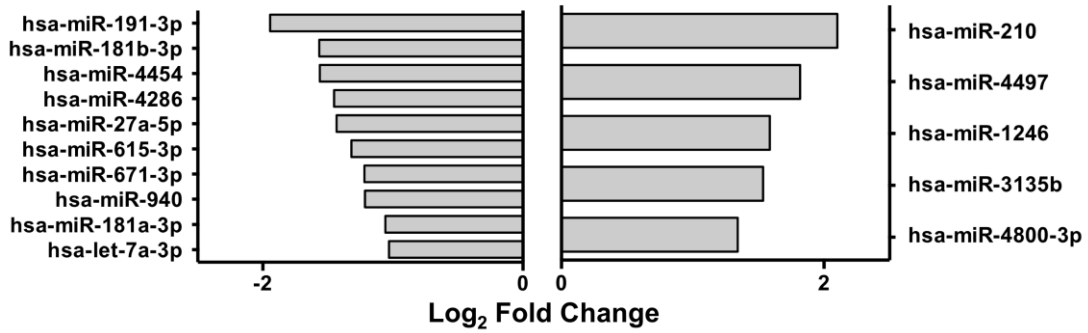

Figure 5.3: Top 15 repressed and induced miRNAs in hypoxic vs. normoxic KSHV-infected BCBL-1 cells. Bars below and above the y-axis show the 15 most abundant miRNAs repressed and induced, respectively, in hypoxia compared to normoxia in BCBL-1 cells. Data were considered significant when $P \leq 0.05$, an average miR count of 10 or more across all replicates (i.e. threshold of miR counts sum higher than 60).

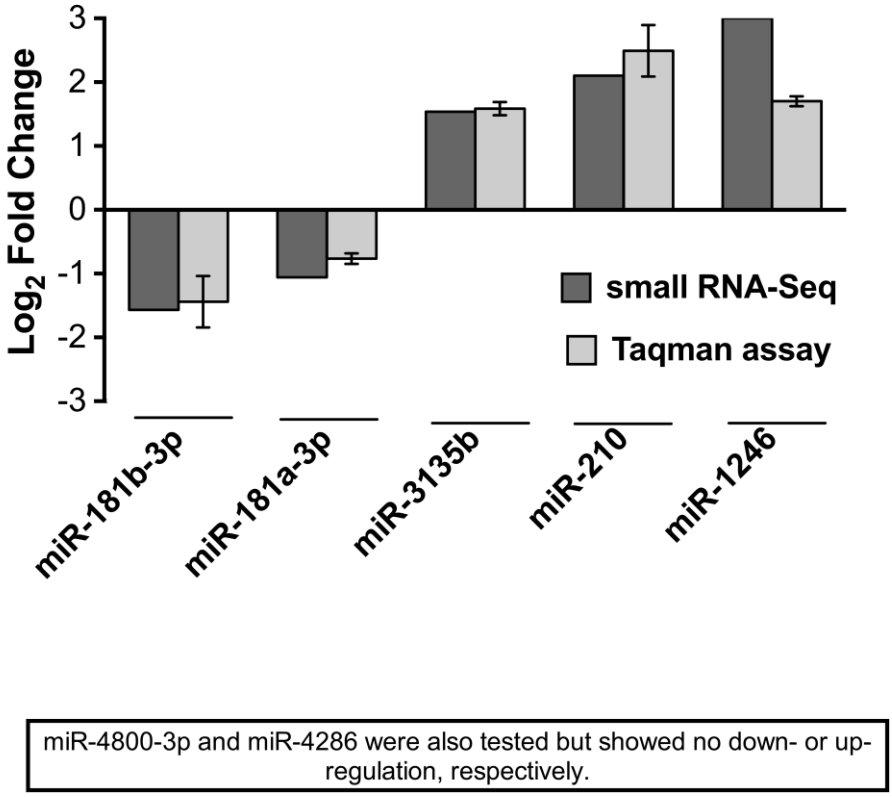

Figure 5.4: Validation of differential expression of miRNAs by Taqman assay.

Data represent the average log_2-transformed fold change of expression between hypoxic vs. normoxic BCBL-1 cells. Expression levels of mature miRNAs were evaluated using the comparative Ct methods (2-deltaCt). Transcript levels of RNU43 were used for sample normalisation. Results from the Taqman assays are shown in grey, and results from the small RNA-Seq are shown in black. Bars depict the mean of 3 independent experiments; error bars reflect the standard deviation of the log_2 ratios for Taqman assays. All the changes are significant ($P \leq 0.05$).

5.3 mRNA-Seq allows for cross-comparison with miRNA target prediction

5.3.1 mRNA-Seq differential analysis confirms hypoxic induction

In parallel, the relative expression of mRNAs in hypoxic compared to normoxic BCBL-1 cells (n=3) was determined by RNA-Seq and analysed by Cufflinks analysis. A total of 287 mRNAs were found significantly dysregulated ($P \leq 0.05$, FC $\leq$-2 or $\geq$2; **Figure 5.5**, top left and right sectors). The 287 mRNAs were comprised of 143 repressed and 144 induced mRNAs by hypoxia. Several known HIF-1 target genes were significantly up-regulated, including CA9, PLOD2, TXNIP, and PGK1 (Kaluz et al. 2009; Gilkes et al. 2013; Baker et al. 2008; Semenza et al. 1994). In addition, HIF-1α has been reported to induce histone demythylase KDM3A, also known as JMJD1A (Beyer et al. 2008), and it was up-regulated 1.8 $\log_2$ FC by hypoxia in BCBL-1 cells (P= $8x10^{-7}$ and FDR= $3.9x10^{-3}$). Interestingly, KDM3A in turn enhances hypoxic gene expression and tumour growth by regulating adrenomedullin (ADM) and growth and differentiation factor 15 (GDF15) (Krieg et al. 2010).

The top 15 molecular networks dysregulated by hypoxia in BCBL-1 cells were identified using Ingenuity Pathway analysis (IPA) (**Figure 5.6**). They were comprised of a number of signalling pathways expected to be altered by hypoxia. For instance, glycolysis, gluconeogenesis, sucrose degradation. androgen signalling, interleukin-1 signalling, HIF-1α signalling, chemokine receptor CCR5 signalling, chemokine signalling, and atherosclerosis signalling have been previously associated with hypoxia (Park et al. 2006; Robin, Murphy, and Theodore 1984; Pison et al. 1995; Hempel, Monick, and Hunninghake 1996; Bosco et al. 2004; Schioppa et al. 2003; Hultén and Levin 2009). Of

note, all of the genes that overlap with glycolysis, gluconeogenesis and sucrose degradation are up-regulated (in red in **Figure 5.6**) supporting the utilisation of glucose during hypoxia. This is consistent with what would be observed when cells are put in hypoxia.

5.3.2 Validation of differential expression in hypoxic BCBL-1 cells using qRT-PCR and Taqman assays

To assess the level of hypoxic induction in BCBL-1 cells, quantitative real time PCR was carried out to determine the expression fold change of VEGF, a well-known HIF-1α target (Forsythe et al. 1996). Although VEGF was not significantly up-regulated by hypoxia in the mRNA-Seq (1.1 $\log_2$ FC, P = 0.09, in hypoxia vs. normoxia BCBL-1 cells), VEGF mRNA levels increased 2 fold (P = 0.003) as assessed by qRT-PCR upon hypoxia exposure, confirming HIF-1α induction in BCBL-1 cells (**Figure 5.7**).

In BCBL-1 cells, H19-MIR675 is the most significantly dysregulated mRNAs under hypoxia (5.0 $\log_2$ FC, $P = 6\text{x}10^{-9}$, and FDR = $1\text{x}10^{-4}$). Of note, it was also found up-regulated by hypoxia in SLKK cells. H19-MIR675 is a non-coding RNA that has been previously shown to be induced by hypoxia (Matouk et al. 2007), and to up-regulate human IL-6 (Ayesh et al. 2002), which plays a role in angiogenesis. It also encodes miR-675 and miR-675*. Taqman assays were undertaken to determine whether or not these miRNAs were up-regulated in hypoxic BCBL-1 cells. In BCBL-1 cells, miR-675 expression shows a significant increase (3 fold; **Figure 5.8**). Like in the SLKK cells, the other miRNA arm, miR-675*, did not change upon hypoxia exposure.

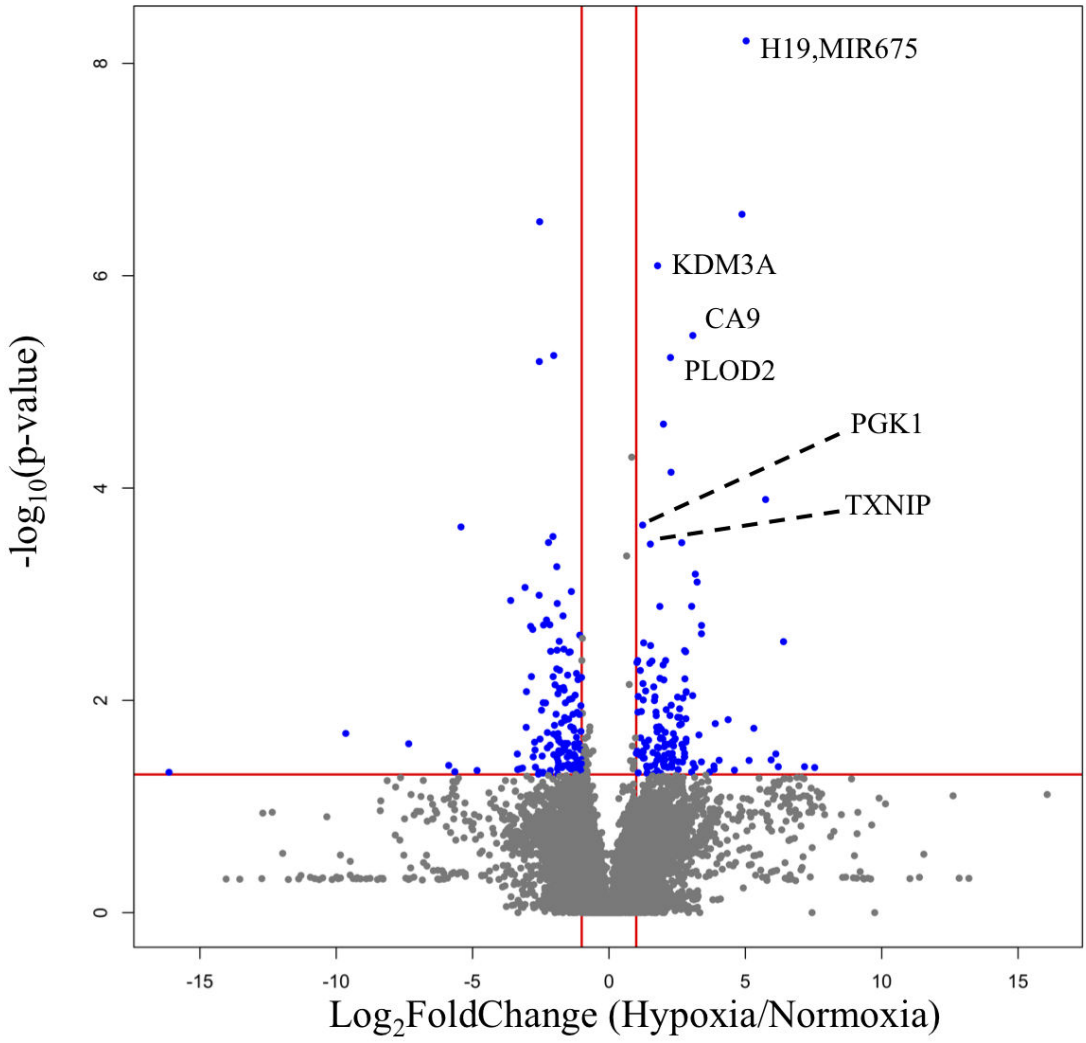

Figure 5.5: Volcano plot of mRNA differential expression in hypoxic vs. normoxic BCBL-1 cells. The plot is depicted as in **Figure 5.1**, with vertical and horizontal red lines similarly representing the thresholds of a fold change of 2 or -2, and of a *P*-value of 0.05, respectively. Labelled mRNAs are known HIF-1 target genes, found significantly up-regulated in this study.

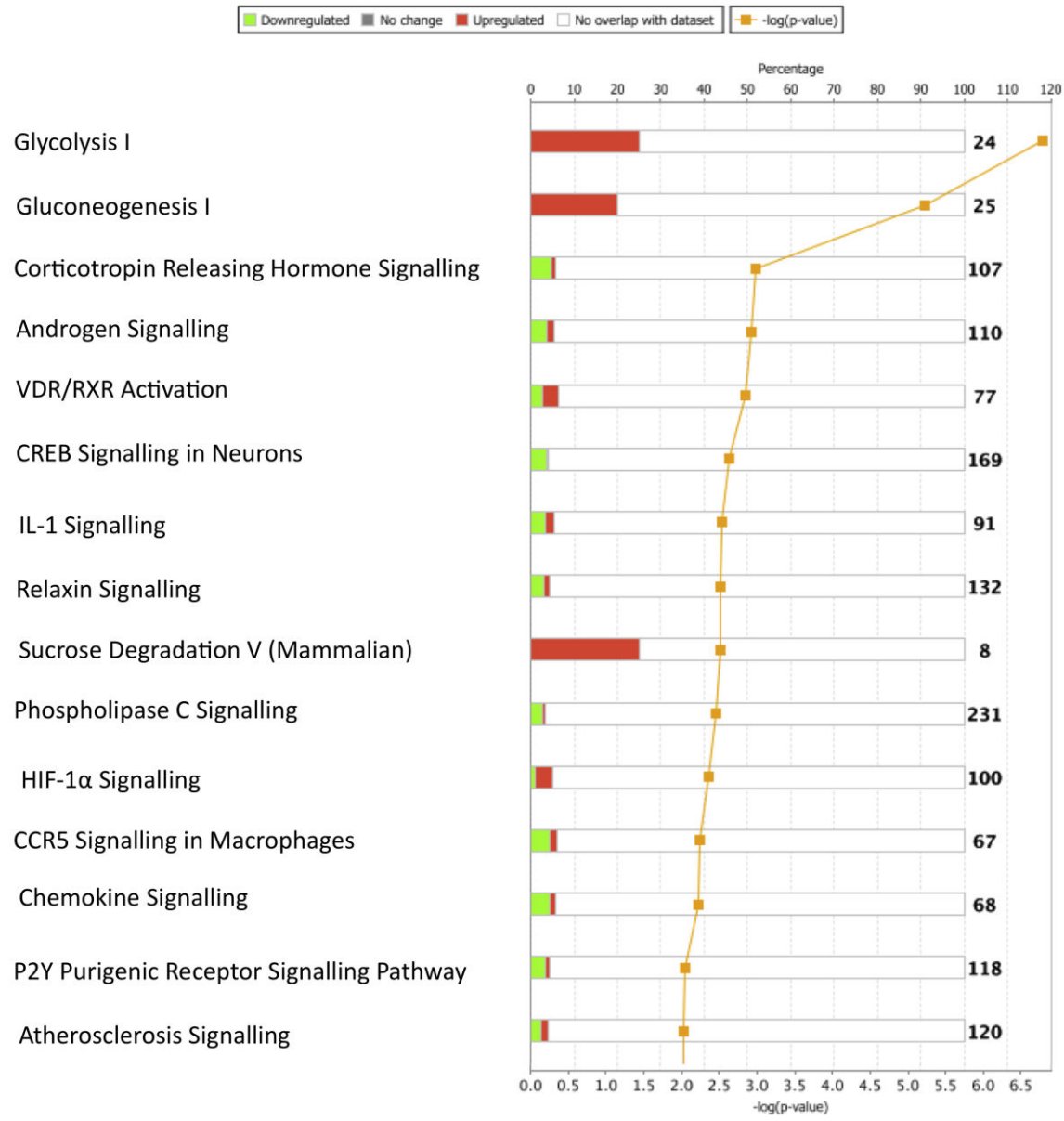

Figure 5.6: Top 15 pathways altered by hypoxia in BCBL-1 cells. A list of differentially expressed mRNAs in BCBL-1 cells was used for Ingenuity Pathway Analysis. The 25 pathways that were most significantly altered by hypoxia are presented here. The yellow line reflects the significance ($P \leq 0.05$ corresponds to $-\log(P\text{-value}) \geq 1.3$). For any given pathway, the percentage of down-regulated and up-regulated genes are depicted in green and red, respectively. The total number of genes in each pathway is indicated in bold on the right hand side.

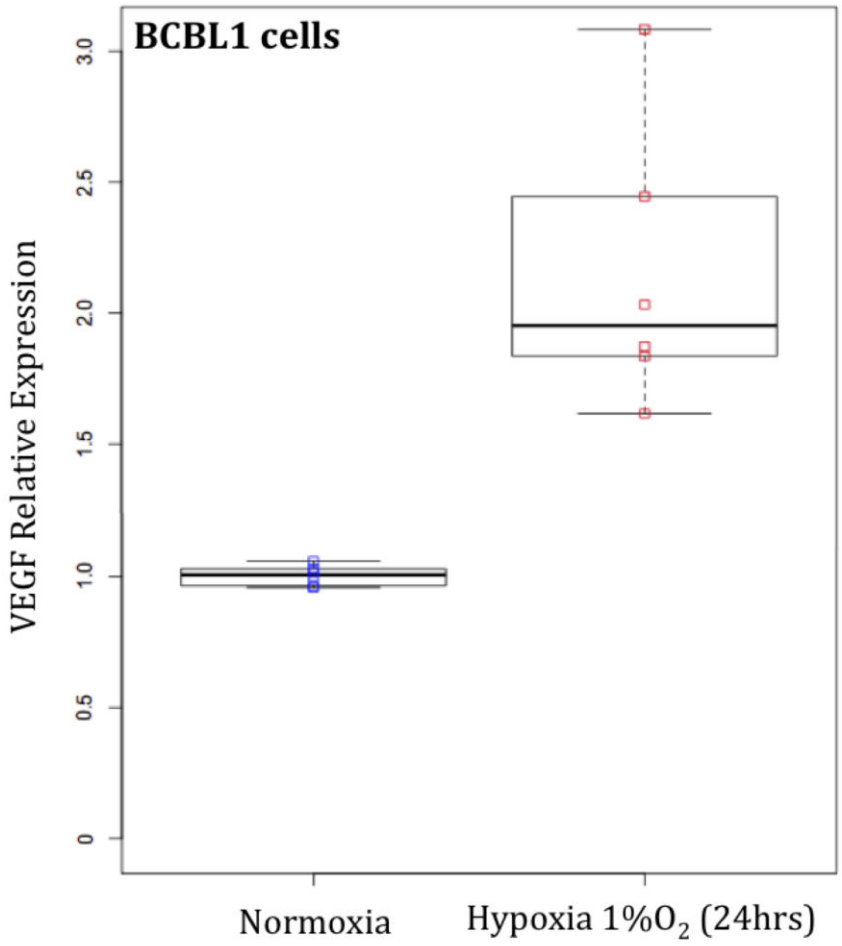

Figure 5.7: VEGF differential expression in hypoxic vs. normoxic BCBL-1 cells. This plot represents the fold difference in VEGF expression between hypoxia and normoxia in BCBL-1 cells, measured by qRT-PCR (n=6). Hypoxic samples were normalised to normoxic samples. This plot was generated using the R software programme. The rectangular box shows the interquartile range (IQR), from the 1st quartile (25th percentile) to the 3rd quartile (75th percentile). It includes the 2nd quartile (median) of VEGF relative expression change. The whiskers correspond to the minimum and maximum values.

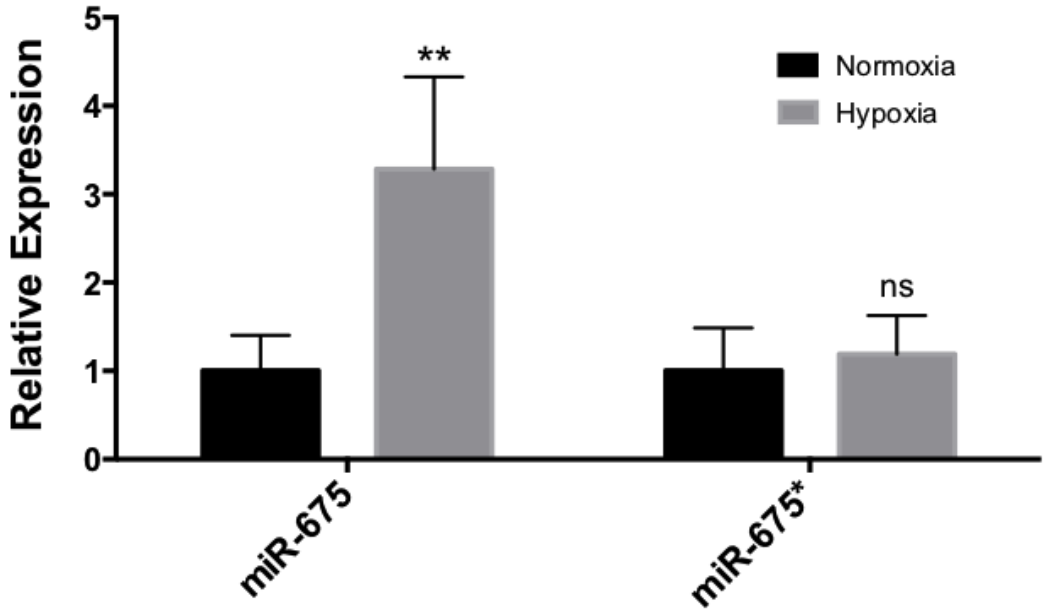

Figure 5.8: Expression levels of H19-derived miRNAs in BCBL-1 cells under hypoxia and normoxia. Expression levels of miR-675 and miR-675* were quantified by Taqman assays 24hrs after exposure to 1% O_2 in comparison to 24% O_2. Gene expression values were normalised to housekeeping snoRNA RNU43. Shown are mean and standard deviation (n=6). The changes observed were significant (**, $P \leq 0.01$) for miR-675, and not significant (ns; $P > 0.05$) for miR-675*.

5.3.3 Integrated miRNA-mRNA analysis in hypoxic and normoxic BCBL-1 cells

Small RNA-Seq analysis results were combined with mRNA-Seq data to predict miRNA-mRNA pairs that were concordantly differentially expressed in hypoxia. A summary of the different steps of the Ingenuity microRNA Target Filter process is shown in **Figure 5.9**. Target prediction using the 91 differentially expressed miRNAs in hypoxia vs. normoxia BCBL-1 cells ($P \leq 0.05$, FC ≤ -2 or ≥ 2 and miR count ≥ 1) yielded 13,998 potential mRNA targets from 73 miRNAs with known targeting information. Comparing those 13,998 putative targets to the list of hypoxia regulated genes from the mRNA-Seq, a total of 167 mRNAs overlapped. Of these, a majority (110) was inversely expressed as compared to the miRNA(s) targeting them, consistent with the hypothesis that some of the changes in mRNAs are due to miRNA regulation. The list of paired miRNA-mRNA targets was further reduced to 27 miRNAs targeting 45 mRNAs, using a stringent confidence filter (high confidence predictions or experimentally observed targets) and this is illustrated in **Table 5.1**. Of these 45miRNAs, several have been described in the literature as miRNA targets. For instance, miR-4458, which has the same seed sequence as let-7a-5p (GAGGUAG), is known to target IFIT5. miR-4458 was down-regulated by hypoxia in BCBL-1 (-8.6 $\log_2$ FC), while IFIT5 was up-regulated (1.7 $\log_2$ FC). This data provide evidence that the changes at the miRNA level are in at least some instances affecting known miRNA targets in BCBL-1 cells and helps dissect the role of differentially expressed miRNA/mRNA pairs in KSHV pathogenesis.

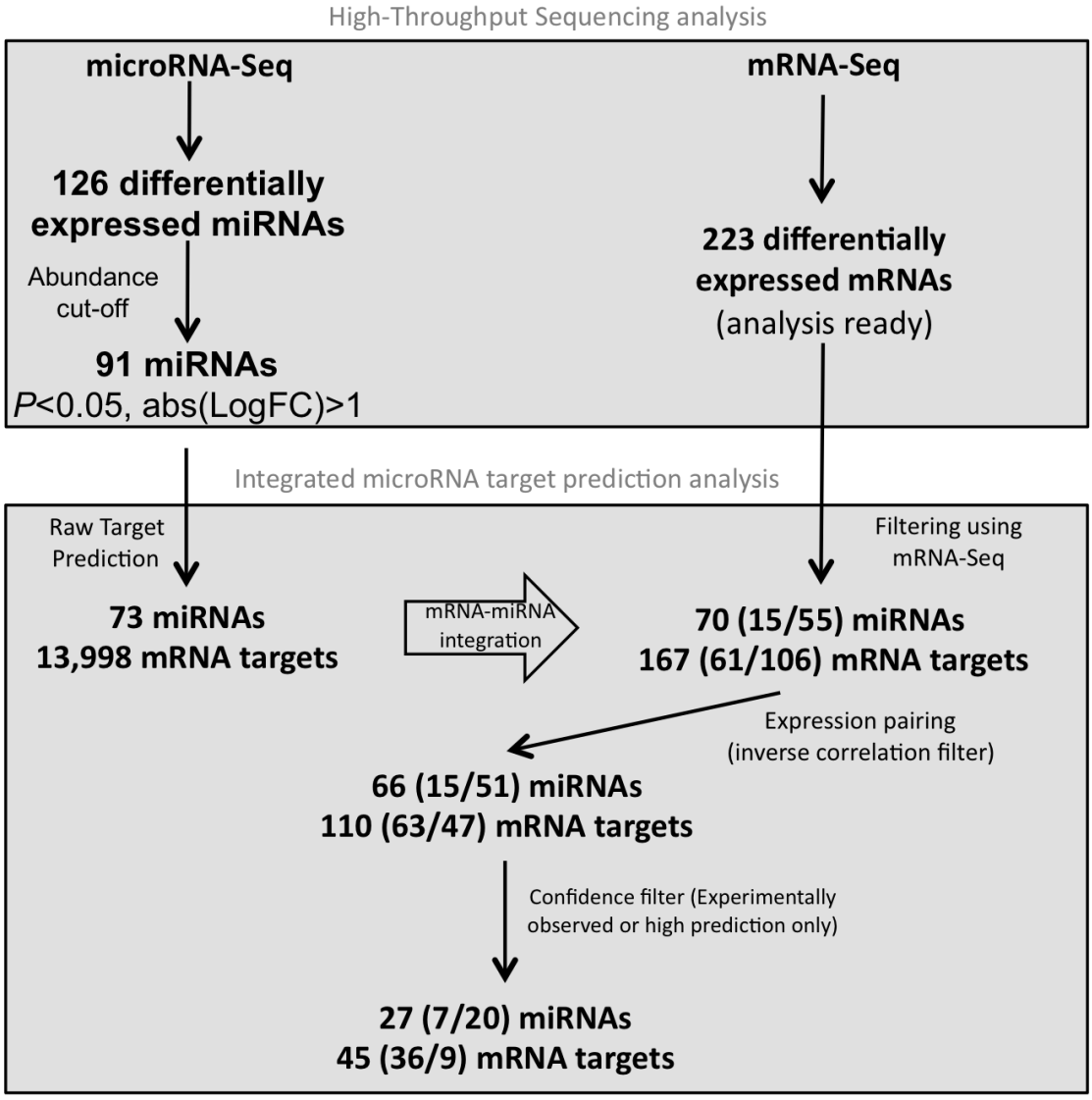

Figure 5.9: Workflow of integrated miRNA-mRNA association analysis using IPA. This experimental workflow shows the various filters used to associate miRNA-Seq and mRNA-Seq data from hypoxic and normoxic BCBL-1 cells. Numbers are presented as Total differentially expressed miRNAs or mRNAs (Up-regulated/Down-regulated).

miRNA	Log_2 Fold Change	# Target genes	Top 5 target genes
Up-regulated miRNAs/Down-regulated targets			
hsa-miR-410	7.6	1	PRUNE2
hsa-miR-1224-5p	2.4	1	NAA50
hsa-miR-4497	1.8	1	KCNA
hsa-miR-3135b	1.5	3	METTL8, PRR11, TRPM7
hsa-miR-1233-3p	1.5	3	CCR2, TRPM7, VOPP1
hsa-miR-5706	1.2	1	CCR2
hsa-miR-4421	1.2	1	SRSF1
Down-regulated miRNAs/Up-regulated targets			
hsa-miR-4458	-8.6	7	SKIDA1, CBFA2T3, DPYSL3, RORC, **IFIT5**
hsa-miR-139-5p	-7.8	5	DDIT4, JUN, SYT14, ENC1, PEG10
hsa-miR-3917	-7.6	2	PDGFA. JUN
hsa-miR-4665-5p	-7.4	4	COL8A2, ELFN2, BNIP3L, PKM
hsa-miR-3691-3p	-6.7	2	NEDD9, E2F7
hsa-miR-217	-3.6	1	TTC30A
hsa-miR-4419b	-2.6	1	GPI
hsa-miR-3201	-2.5	1	BNIP3L
hsa-miR-3187-5p	-2.4	4	RORC, PLOD1, GPI, PKM
hsa-miR-1271-5p	-2.3	8	REPS2, CBFA2T3, PLOD2, TSPAN9, TFRC
hsa-miR-486-3p	-2.3	3	TSPAN9, TXNIP, S100A10
hsa-miR-4758-3p	-2.0	1	PGK1
hsa-miR-1255b-5p	-1.6	1	MAOA
hsa-miR-939-5p	-1.6	1	ENC1
hsa-miR-4259	-1.4	1	REPS2
hsa-miR-5095	-1.3	3	MAOA, SLC2A3, PLEKHA2

hsa-miR-940	-1.2	1	PFKFB3
hsa-miR-548b-3p	-1.1	2	NEDD9, SLC2A3
hsa-miR-1343	-1.0	4	C19orf35, DDIT4, ITGA5, IFIT5
hsa-miR-5010-5p	-1.0	1	HK2

Table 5.1: Ingenuity analysis predicts inversely correlated miRNA-mRNA target pairs. Using lists of differentially expressed miRNAs and mRNAs as input for the Ingenuity Pathway Analysis (IPA), it was found that 27 differentially expressed miRNAs target 45 mRNAs (high confidence and experimentally observed results). Only mRNAs and miRNAs with opposite differential expression are shown in this table. Columns identify the miRNA name, its log-transformed expression fold change between hypoxic and normoxic BCBL-1 cells, the number of identified targets, and the five or less most differentially expressed targets. In bold are miRNAs and mRNA targets that have been previously reported in the literature.

5.4 Similarities and differences in the hypoxic response of BCBL-1 cells and SLKK cells

5.4.1 Comparative miRNA expression profiling analysis

The SLKK and BCBL-1 cells were assessed for similarity and differences in their response to hypoxia. Looking at miRNAs induced by hypoxia, of the 34 up-regulated HRMs in SLKK cells, only one overlapped with the 24 up-regulated HRMs in BCBL-1 cells, namely, miR-210 (**Figure 5.10**). miR-210 is a well-described hypoxia-regulated miRNA in a variety of cell types (for a review, see Huang, Le, and Giaccia 2010). Both SLKK and BCBL-1 cells showed miR-210 up-regulation when exposed to hypoxia. miR-210 expression increased 4 fold in BCBL-1 cells and 7 fold in SLKK cells. Interestingly, as pointed out previously miR-210 is also up-regulated (3 fold) in SLK cells infected with KSHV even in normoxia, demonstrating that KSHV and hypoxia induce similar changes. miR-210 regulates many aspects of the hypoxic pathway by affecting angiogenesis via target genes such as the receptor tyrosine kinase ligand EFNA3 and PTP1B, and by regulating mitochondrial metabolism through repression of iron-sulphur (Fe-S) cluster scaffold protein homolog ISCU. Of note, it was speculated that miR-210 may be associated with the Warburg effect, a metabolic alteration under which cancer cells consume glucose and lactic acid even when oxygen is readily available (X. Huang and Zuo 2014; Xin Huang, Le, and Giaccia 2010). It has been reported that KSHV induces the Warburg effect; this may serve to enhance survival of latently infected cells under a variety of conditions (Delgado et al. 2010). Because miR-210 is elevated in various cancer types, in KSHV-infected compared to uninfected cells (SLKK vs. SLK), and in hypoxic environment of either infected or uninfected cells, it is

plausible that this multifaceted regulator could also play a role in the KSHV-induction of the Warburg effect.

Of the miRNAs down-regulated by hypoxia, a total of nine miRNAs overlapped between KSHV-positive BCBL-1 and SLKK cells. These included miR-3159, 3201, 4664-3p, 4687-3p, 5095, 548ah-3p, 548e, 6514-5p, and 1271-5p (**Figure 5.11**). Interestingly, these have not been previously reported as regulated by hypoxia and therefore may require KSHV infection to lead to their down-regulation.

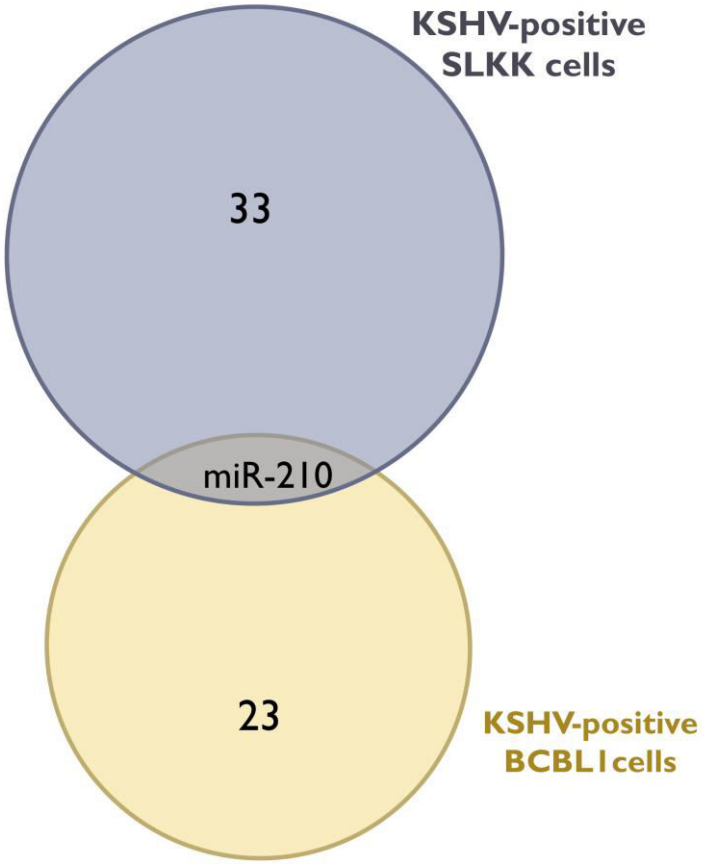

Figure 5.10: Venn diagram showing the overlap of miRNAs up-regulated by hypoxia between BCBL-1 and SLKK infected cells.

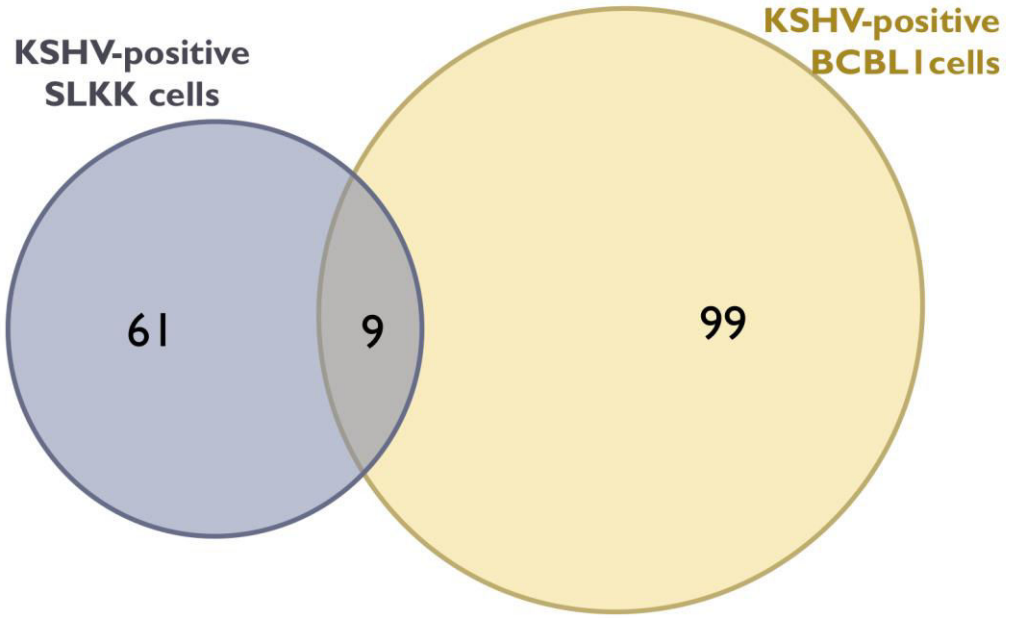

Figure 5.11: Venn diagram showing the overlap of miRNAs down-regulated by hypoxia between BCBL-1 and SLKK infected cells. Nine down-regulated HRMs: hsa-miR-3159, hsa-miR-3201, hsa-miR-4664-3p, hsa-miR-4687-3p, hsa-miR-5095, hsa-miR-548ah-3p, hsa-miR-548e, hsa-miR-6514-5p, and hsa-miR-1271-5p.

5.4.2 Comparative mRNA expression profiling analysis

With regards to hypoxic regulation of mRNAs, 236 identifiable genes were dysregulated upon hypoxia exposure in BCBL-1 cells, while 268 were altered in SLKK cells. A total of 15 mRNAs were similarly dysregulated in both cell lines. Of note, those 15 genes were all up-regulated in hypoxia. In other words, there were no similarly down-regulated genes (**Figure 5.12**). Analysis of these 15 genes revealed that 14 are known HIF target genes: ALDOC, BNIP3L, CA9, DDIT4, H19-MIR675, HK2, MIR210HG, P4HA2, PGK1, PFKFB4, PLOD2, PPFIA4, SLC2A1 (also known as GLUT1), and TXNIP (Baker et al. 2008; Gilkes et al. 2013; Bellot et al. 2009; Kaluz et al. 2009; Matouk et al. 2007; Wang et al. 2005; Hayashi et al. 2004; Mathupala, Rempel, and Pedersen 2001; Jean, Rich, and Joyce-Brady 2006). The up-regulation of the remaining mRNA (LOC154761) by hypoxia has previously been reported to occur in both astrocytes and HeLa cells (Mense et al. 2006). However, LOC154761 is a pseudogene and it is unknown if it plays a role in the cellular response to hypoxia.

The induction of the above mRNAs occurred in cells exposed to hypoxia regardless of them being infected or not. This demonstrates that KSHV does not interfere with the HIF up-regulation of these genes, but in fact might favour the hypoxic response.

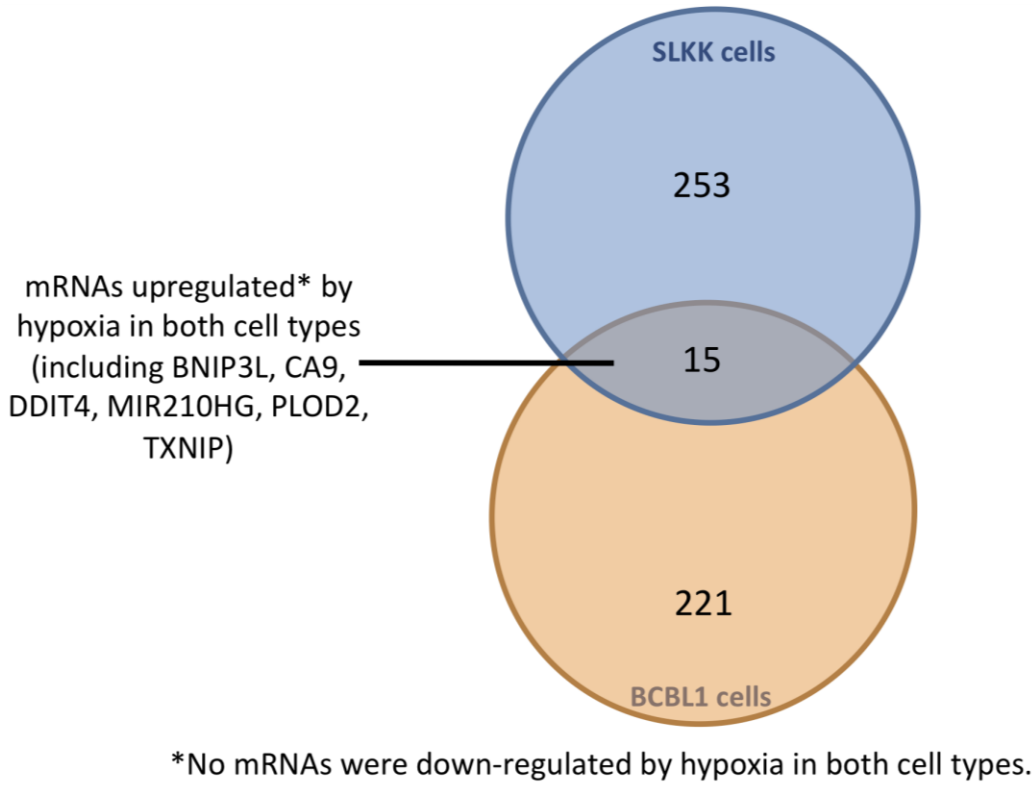

Figure 5.12: Venn diagram showing the overlap of hypoxia inducible genes between KSHV-positive BCBL-1 and SLKK cells.

5.5 Conclusions and future directions

In 2001, for the first time, a link between hypoxia and KSHV was described in a well-established PEL model, BCBL-1 cells (Davis 2001). Thanks to the advancements of next-generation sequencing technologies, it has now become possible to evaluate the overall effects of oxygen deprivation on both mRNA and miRNA cellular expressions in BCBL-1 cells. This chapter presents the results of such analysis, as well as the inverse correlation between the expression profiles of miRNA and mRNAs.

It was found that most miRNAs (83%) changing upon hypoxic stress in BCBL-1 cells were down-regulated. Interestingly, the same observation was made in **Chapter 4** for KSHV-positive SLKK cells under hypoxia. Ten miRNAs overlapped between the two infected cell lines. However, miR-210 was the only up-regulated miRNA in common, with a 4 fold and a 7 fold increase in BCBL-1 and SLKK cells (hypoxia vs. normoxia), respectively. Such differences between the two cells lines could be due to cell type differences (B-cells vs. epithelial cells) or the use of recombinant rKSHV.219 virus in SLKK cells vs. wild type KSHV in BCBL-1 cells.

In addition, RNA-Seq and qRT-PCR assays revealed that a number of known hypoxia-inducible genes were up-regulated in BCBL-1 cells. For instance, VEGF, KDM3A (JMJD1A), CA9, PLOD2, TXNIP and PGK1 were all significantly induced under hypoxic stress in the PEL cell model. This provides evidence that KSHV-infected BCBL-1 cells undergo cellular alterations in response to the absence of oxygen. These alterations include glycolysis enhancement in order to maintain a balance of energy, and

angiogenesis, which may indirectly fuel KSHV-infected cell growth. Finally, by integrating both miRNA and mRNA datasets, it was learned that 27 HRMs were inversely correlated to 45 hypoxia-regulated mRNAs. This analysis has helped pinpoint which mRNA changes are consistent with miRNA differential expression in hypoxia.

6

Assessing the response of KSHV miRNAs to external stimuli

More than a decade ago, the first virally encoded miRNAs were identified in EBV, KSHV's closest relative among human herpesviruses. Since then, many more viruses, including KSHV, have been shown to encode their own miRNAs. Viral miRNAs regulate important host biological processes such as cell survival, angiogenesis, proliferation and even the immune response, and on-going studies are investigating their other potential functions and targets. Given their involvement in viral biology, pathogenesis and tumourigenesis, it is of interest to understand what might regulate viral miRNA expression. Like cellular miRNAs, viral miRNAs could respond to external stimuli such as hypoxia, pathogen infection, oxidative stress, radiation, UV, etc. However, the effect of these stimuli on viral miRNA expression is poorly characterised. This chapter describes the effects of hypoxia, oxidative stress and the immunomodulatory drug pomalidomide on KSHV miRNAs.

6.1 Introduction

In 2004, Epstein Barr Virus (EBV) was the first virus shown to encode viral miRNAs (Pfeffer et al. 2004), and this was shortly followed by KSHV (Cai et al. 2005; Samols et al. 2005; Pfeffer et al. 2005). More than 140 virally encoded miRNAs have since then been identified. The vast majority belong to three main virus families: Adenoviridae, Herpesviridae, and Polyomaviridae. Virally encoded miRNAs have been shown to target either host cellular genes to optimise infection, or viral genes to fine-tune the expression of KSHV mRNAs.

Viral miRNAs affect targets that are involved in the regulation of latency, control of the immune response, and oncogenesis. For example, EBV miRNA miR-BART-2 has been shown to target EBV DNA polymerase BALF5, in order to control viral replication (Barth et al. 2008). Similarly, Hussain et al. reported that an insect virus-encoded miRNA regulates viral replication by targeting HvAv DNA polymerase I (Hussain, Taft, and Asgari 2008).

Viral miRNAs rely on the host cellular machinery to be generated. However, viral factors may also specifically regulate viral miRNA processing. The exact regulatory mechanisms by which viral miRNA expression is controlled are currently unknown. One can hypothesise that the regulation of cellular viral miRNAs is similar to that for cellular miRNAs. For instance, since global cellular miRNA expression has been shown to change upon hypoxia exposure (Kulshreshtha et al. 2007) and oxidative stress (Simone et al. 2009), viral miRNA expression might also be altered under such stresses. Therefore, this chapter is investigating the effects of external stimuli such as hypoxia, oxidative stress and drug treatment on KSHV miRNAs.

6.2 Effects of hypoxic stress on viral miRNAs

Although KSHV only encodes for 25 mature miRNAs through 12 pre-miRNAs, they have been found to make up a significant fraction of the total mature miRNA pool in PEL cells (Gottwein et al., 2011; Lin et al., 2010; Umbach & Cullen, 2009). Here, the effects of 1% oxygen on the viral miRNA expression of infected cells, SLKK and BCBL-1, were assessed by miRNA-Seq and Taqman assays.

6.2.1 KSHV miRNA response to hypoxia in SLKK cells

6.2.1.1 Distribution of viral miRNAs in normoxic SLKK cells by miRNA-Seq

Cellular and viral miRNA expression in KSHV latently infected SLKK cells was analysed by deep sequencing. It was observed that a sizable fraction (~9%) of miRNA reads in SLKK cells were of KSHV origin (**Figure 6.1**). The distribution of the different KSHV miRNAs in normoxic SLKK cells (**Table 6.1**) was generally similar to that of the PEL cell lines BC-1, BC-3 and BCBL-1 as reported previously (Gottwein et al. 2011). For example, in SLKK cells, KSHV-miR-K12-4-3p and 8-3p comprise a similar proportion of KSHV miRNAs as in PEL cells (~26% and ~13%, respectively). However, there were some differences; KSHV-miR-K12-6-3p was expressed at a lower level (2%), and KSHV-miR-K12-10a-3p was expressed at a higher level (40.5%) in SLKK cells compared with PEL cells (20-43% and <1%, respectively).

It should be noted that substantial differences in KSHV miRNA distribution were previously observed even within the same cell type although the reason for these difference is unclear (B-cells, i.e. BC-1, BC-3 and BCBL-1) (Gottwein et al., 2011; Lin et al. 2010). It is therefore not unexpected to observe similarities but also dissimilarities between the SLKK viral miRNA profile and that of PEL cells.

Of note, the most abundant KSHV miRNA in normoxic SLKK cells, miR-K12-10a, is known to target TWEAKR (TNFRSF12A) (Abend et al. 2010), which was significantly repressed in SLKK vs. SLK cells (-2.0 $\log_2$ FC and FDR = 0.001). Another KSHV miRNA, miR-K12-11, down-regulates a translational regulator of interleukin 6, C/BEPβ (Boss et al. 2011), which was also decreased in SLKK compared to SLK cells (-1.3 $\log_2$ FC and FDR = 0.016). These changes in the cellular target genes is consistent with the high expression of the viral miRNAs in infected cells.

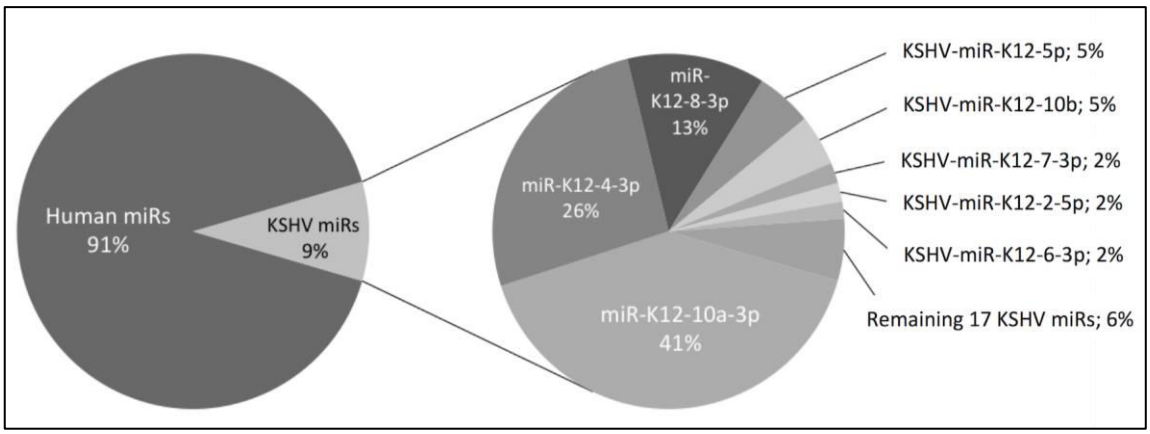

Figure 6.1: Relative abundance of human and KSHV-encoded miRNAs in normoxic SLKK cells. The expression levels of KSHV miRNAs are shown as the percentage of the total of viral miRNA reads. Data are the mean of sequenced samples from three independent experiments. Percentages have been rounded to the closest digit. For a detailed breakdown, see **Table 6.1**.

KSHV miRNA	Count	Percentage of KSHV
KSHV-miR-K12-10a-3p	405,293	40.53%
KSHV-miR-K12-4-3p	261,969	26.20%
KSHV-miR-K12-8-3p	126,885	12.69%
KSHV-miR-K12-3-5p	51,448	5.14%
KSHV-miR-K12-10b	46,503	4.65%
KSHV-miR-K12-7-3p	18,871	1.89%
KSHV-miR-K12-2-5p	17,029	1.70%
KSHV-miR-K12-6-3p	154,08	1.54%
KSHV-miR-K12-11-3p	14,417	1.44%
KSHV-miR-K12-12-5p	11,199	1.12%
KSHV-miR-K12-4-5p	10,389	1.04%
KSHV-miR-K12-6-5p	5,124	0.51%
KSHV-miR-K12-3-3p	3251	0.33%
KSHV-miR-K12-12-3p	2,938	0.29%
KSHV-miR-K12-1-5p	2,789	0.28%
KSHV-miR-K12-5-3p	2,657	0.27%
KSHV-miR-K12-9-3p	1,568	0.16%
KSHV-miR-K12-8-5p	962	0.10%
KSHV-miR-K12-9-5p	562	0.06%
KSHV-miR-K12-7-5p	401	0.04%
KSHV-miR-K12-2-3p	182	0.02%
KSHV-miR-K12-10a-5p	139	0.01%
KSHV-miR-K12-1-3p	7	0.00%
KSHV-miR-K12-5-5p	3	0.00%
KSHV-miR-K12-11-5p	5	0.00%

Table 6.1: KSHV miRNA distribution in normoxic SLKK cells. This table shows the read count and percentage representation of 25 mature KSHV miRNAs expressed in SLKK cells.

6.2.1.2 Comparison of the KSHV miRNA profiles between hypoxic and normoxic SLKK cells

The viral miRNA profile of SLKK cells under hypoxia (1% O_2 for 24hrs) was assessed using miRNA-Seq data, and compared to that of normoxic SLKK cells. Hypoxia did not affect the overall fraction of viral miRNA (~9%) as compared to the total miRNA read count (**Table 6.2**), nor did hypoxia change the relative expression of individual KSHV miRNAs (**Figure 6.2** and **Table 6.3**). In order to validate these findings, Taqman assays were undertaken to assess the expression of the four most abundant miRNAs in SLKK cells. These included miR-K12-10a-3p, a KSHV miRNA under the Kaposin promoter expressed both during the latent and lytic phases, and three other miRNAs, miR-K12-4-3p, miR-K12-8-3p and miR-K12-3-5p, expressed only during latency. Moreover, Taqman assays quantified the expression of four additional KSHV miRNAs that are less abundant in SLKK cells (miR-K12-1-5p, miR-K12-2-5p, miR-K12-6-3p, and miR-K12-11-3p). It was observed that none of these eight KSHV miRNAs showed a significant change in expression between normoxia and hypoxia in SLKK cells (**Figure 6.3**). These results suggest that while cellular miRNAs such as miR-210 are dramatically affected by hypoxia, viral miRNAs are not. These results also indicate that KSHV miRNAs may not be HIF-regulated as none of the eight tested miRNAs responded to hypoxia.

SLKK	Aligned miRNA reads			Percentage of aligned KSHV miRNA reads vs. Total
	Total	Human	KSHV	
Normoxia A	1,101,677	954,226	147,451	13.4%
Normoxia B	1,684,493	1,558,250	126,243	7.5%
Normoxia C	691,718	641,567	50,151	7.3%
Average Normoxia	**1,159,296**	**1,051,348**	**107,948**	**9.4%**
Hypoxia A	3,232,670	2,955,249	277,421	8.6%
Hypoxia B	661,448	575,814	85,634	12.3%
Hypoxia C	460,587	425,181	35,406	7.7%
Average Hypoxia	**1,451,568**	**1,318,748**	**132,820**	**9.7%**

Table 6.2: Read statistics for human and viral miRNAs expressed in hypoxic and normoxic SLKK cells. Three independent experiments are displayed (A, B and C). Columns identify the replicate number, the number of aligned miRNA reads per species or total, and the percentage of KSHV miRNA reads vs. the total number of aligned reads for each SLKK replicate and overall.

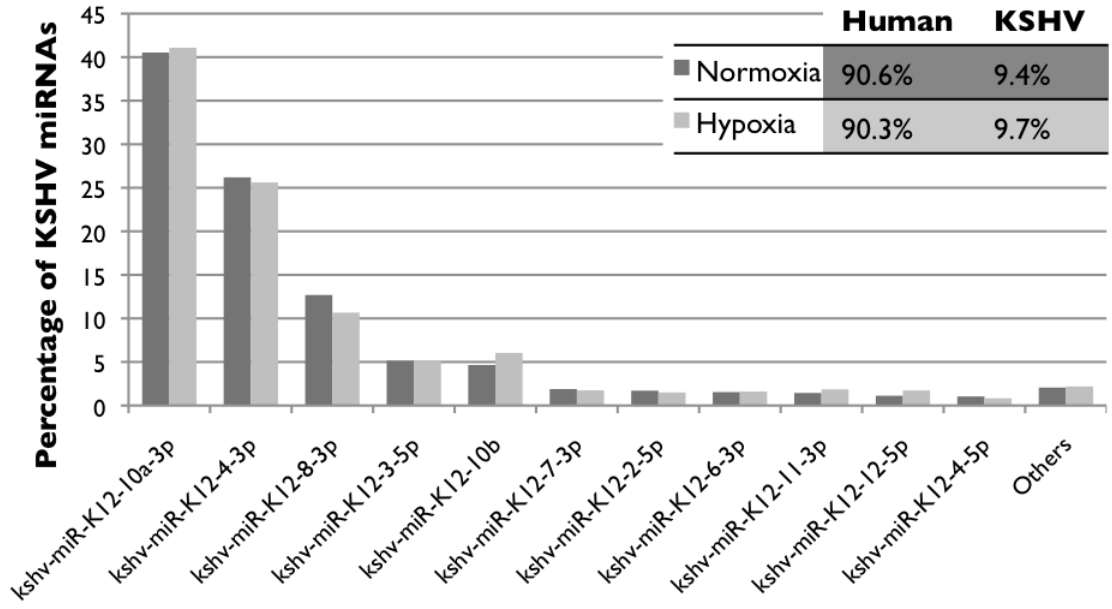

Figure 6.2: Percentage of KSHV miRNAs in hypoxic and normoxic SLKK cells. The expression levels of each viral miRNAs in SLKK cells are shown as the percentage of the total viral miRNA reads. For a detailed breakdown, see **Table 6.3**.

KSHV miRNA	Normoxic SLKK cells			Hypoxic SLKK cells		
	Count	Percentage of Total	Percentage of KSHV	Count	Percentage of Total	Percentage of KSHV
kshv-miR-K12-10a-3p	405,293	3.81	40.53	410,783	3.98	41.08
kshv-miR-K12-4-3p	261,969	2.46	26.20	256,130	2.48	25.61
kshv-miR-K12-8-3p	126,885	1.19	12.69	106,622	1.03	10.66
kshv-miR-K12-3-5p	51,448	0.48	6.05	51,753	0.50	5.18
kshv-miR-K12-10b	46,503	0.44	4.65	60,362	0.59	6.04
kshv-miR-K12-7-3p	18,871	0.18	1.89	17,393	0.17	1.74
kshv-miR-K12-2-5p	17,029	0.16	1.70	14,982	0.15	1.50
kshv-miR-K12-6-3p	15,408	0.14	1.54	16,016	0.16	1.60
kshv-miR-K12-11-3p	14,417	0.14	1.44	18,543	0.18	1.85
kshv-miR-K12-12-5p	11,199	0.11	1.12	17,288	0.17	1.73
kshv-miR-K12-4-5p	10,389	0.10	1.04	8,259	0.08	0.83
Others	20,588	0.19	2.06	21,871	0.21	2.19
kshv-miR-K12-6-5p	5,124	0.05	0.51	7,135	0.07	0.71
kshv-miR-K12-3-3p	3,251	0.03	0.33	1,527	0.01	0.15
kshv-miR-K12-12-3p	2,938	0.03	0.29	4,359	0.04	0.44
kshv-miR-K12-1-5p	2,789	0.03	0.28	1,820	0.02	0.18
kshv-miR-K12-5-3p	2,657	0.02	0.27	2,787	0.03	0.28

kshv-miR-K12-9-3p	1,568	0.01	0.16	1,257	0.01	0.13
kshv-miR-K12-8-5p	962	0.01	0.10	1,521	0.01	0.15
kshv-miR-K12-9-5p	562	0.01	0.06	772	0.01	0.08
kshv-miR-K12-7-5p	401	0.00	0.04	254	0.00	0.03
kshv-miR-K12-2-3p	182	0.00	0.02	197	0.00	0.02
kshv-miR-K12-10a-5p	139	0.00	0.01	218	0.00	0.02
kshv-miR-K12-1-3p	7	0.00	0.00	10	0.00	0.00
kshv-miR-K12-11-5p	5	0.00	0.00	1	0.00	0.00
kshv-miR-K12-5-5p	3	0.00	0.00	12	0.00	0.00

Table 6.3: Detailed analysis of KSHV miRNA read counts in hypoxic and normoxic SLKK cells. The average of three independent experiments for each condition is displayed. Columns identify each KSHV miRNA, its total miR count, its percentage as compared to either KSHV miR reads or the overall read number, in either normoxia or hypoxia. The top part illustrates KSHV miRNAs present in more than 1% of total KSHV reads. The rest is displayed under "Others". KSHV miRNAs in bold have been validated by Taqman assays (**Figure 6.3**).

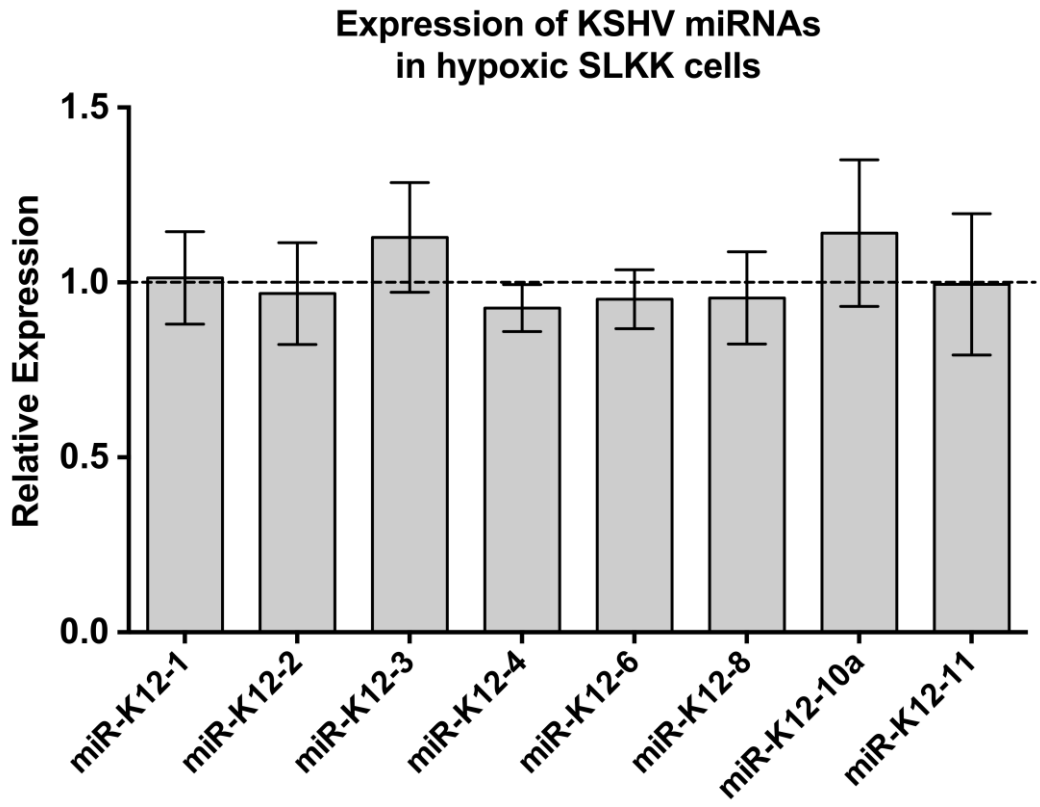

Figure 6.3: Taqman assays show a constant expression of KSHV miRNAs in hypoxic SLKK cells compared to normoxia. The dashed line corresponds to the normoxic levels. No significant change was observed.

6.2.2 KSHV miRNA response to hypoxia in BCBL-1 cells

In order to assess KSHV miRNA expression in both hypoxic and normoxic BCBL-1 cells, miRNA-Seq analysis was carried out in triplicate samples. In both conditions, it was observed that ~32% of the miRNA reads were of KSHV origin (**Table 6.4**). The result in normoxia is remarkably similar to a previous report showing that KSHV miRNAs made up ~30% of the total miRNA reads in normoxic BCBL-1 cells (Gottwein et al. 2011).

The relative abundance of various KSHV miRNAs in BCBL-1 cells was also analysed in both hypoxia and normoxia. The most highly expressed viral miRNAs in both hypoxia and normoxia were miR-K12-4-3p, miR-K12-8-3p, miR-K12-3-5p, miR-K12-11-3p, miR-K12-2-5p, and miR-K12-7-3p (**Figure 6.4**). Furthermore, like in SLKK cells, no significant change was observed between normoxic and hypoxia BCBL-1 cells (**Figure 6.4** and **Table 6.5**). This was confirmed by Taqman assays in both normoxia and hypoxia for nine of the KSHV miRNAs. These comprised the seven most abundant viral miRNAs (miR-K12-4-3p, miR-K12-8-3p, miR-K12-3-5p, miR-K12-11-3p, miR-K12-2-5p, miR-K12-7-3p, and miR-K12-10a-3p), as well as two less abundant KSHV miRNAs (miR-K12-1-5p and miR-K12-6-3p).

BCBL-1	Aligned miRNA reads			Percentage of aligned KSHV miRNA reads vs. Total
	Total	Human	KSHV	
Normoxia A	2,174,168	1,442,652	731,516	33.6%
Normoxia B	2,419,366	1,644,976	774,391	32.0%
Normoxia C	1,887,843	1,280,870	606,974	32.2%
Average Normoxia	**2,160,459**	**1,456,166**	**704,294**	**32.6%**
Hypoxia A	1,468,423	957,147	511,277	34.8%
Hypoxia B	760,771	552,847	207,924	27.3%
Hypoxia C	4,711,178	3,149,988	1,561,190	33.1%
Average Hypoxia	**2,313,457**	**1,553,327**	**760,130**	**31.8%**

Table 6.4: Read statistics for human and viral miRNAs expressed in hypoxic and normoxic BCBL-1 cells. Three independent experiments are displayed (A, B and C). Columns identify the replicate number, the number of aligned miRNA reads per species or total, and the percentage of KSHV miRNA reads vs. the total number of aligned reads for each BCBL-1 replicate and overall.

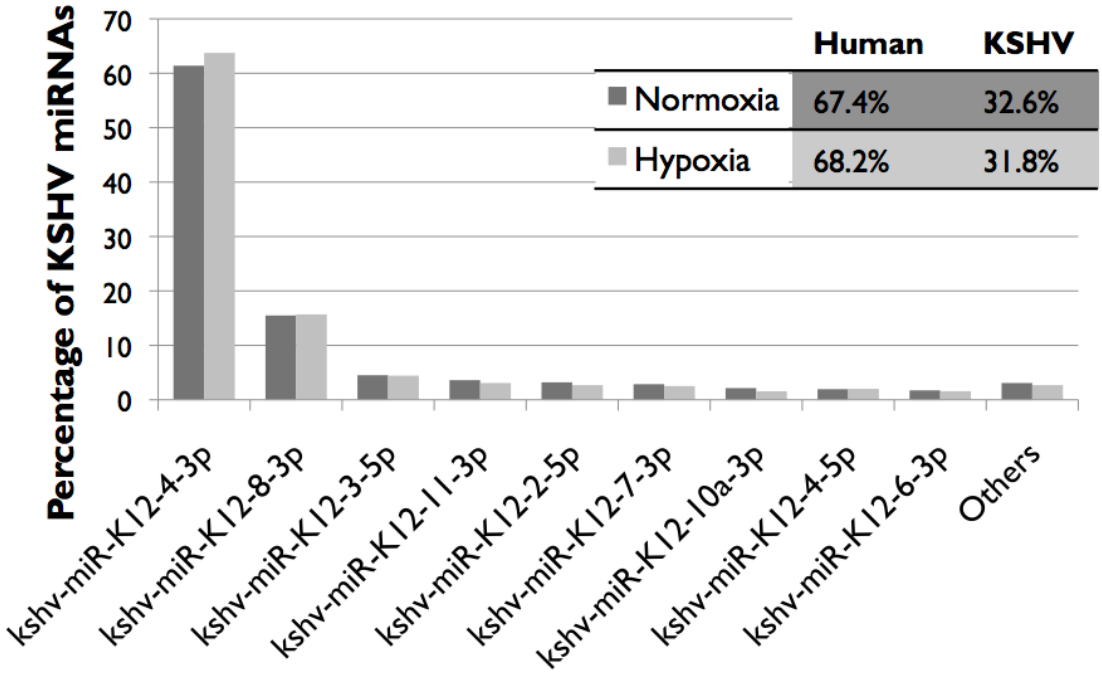

Figure 6.4: Percentage of KSHV miRNAs in hypoxic and normoxic BCBL-1 cells. The expression levels of each viral miRNAs in BCBL-1 cells are shown as the percentage of the total viral miRNA reads. Data are the average of sequenced BCBL-1 samples from three independent experiments. For a detailed breakdown, see **Table 6.5**.

KSHV miRNA	Normoxic BCBL-1 cells			Hypoxic BCBL-1 cells		
	Count	Percentage of Total	Percentage of KSHV	Count	Percentage of Total	Percentage of KSHV
kshv-miR-K12-4-3p	613,898	20.01	61.39	637,344	20.27	63.73
kshv-miR-K12-8-3p	154,885	5.05	15.49	156,913	4.99	15.69
kshv-miR-K12-3-5p	45,165	1.47	4.52	44,361	1.41	4.44
kshv-miR-K12-11-3p	36,117	1.18	3.61	30,831	0.98	3.08
kshv-miR-K12-2-5p	32,074	1.05	3.21	26,883	0.85	2.69
kshv-miR-K12-7-3p	28,695	0.94	2.87	25,244	0.80	2.52
kshv-miR-K12-10a-3p	21,504	0.70	2.15	15,586	0.50	1.56
kshv-miR-K12-4-5p	19,538	0.64	1.95	20,079	0.64	2.01
kshv-miR-K12-6-3p	17,314	0.56	1.73	15,821	0.50	1.58
Others	30,811	1.00	3.08	26,937	0.86	2.69
kshv-miR-K12-5-3p	8,395	0.27	0.84	9,629	0.31	0.96
kshv-miR-K12-6-5p	6,415	0.21	0.64	6,070	0.19	0.61
kshv-miR-K12-3-3p	3,922	0.13	0.39	2,148	0.07	0.21
kshv-miR-K12-9-3p	3,588	0.12	0.36	2,669	0.08	0.27
kshv-miR-K12-8-5p	1,757	0.06	0.18	1,241	0.04	0.12
kshv-miR-K12-9-5p	1,737	0.06	0.17	1,299	0.04	0.13
kshv-miR-K12-1-5p	1,591	0.05	0.16	1,048	0.03	0.10

kshv-miR-K12-10b	1,329	0.04	0.13	1,359	0.04	0.14
kshv-miR-K12-12-5p	991	0.03	0.10	719	0.02	0.07
kshv-miR-K12-7-5p	472	0.02	0.05	343	0.01	0.03
kshv-miR-K12-12-3p	275	0.01	0.03	176	0.01	0.02
kshv-miR-K12-2-3p	273	0.01	0.03	204	0.01	0.02
kshv-miR-K12-5-5p	31	0.00	0.00	18	0.00	0.00
kshv-miR-K12-1-3p	18	0.00	0.00	9	0.00	0.00
kshv-miR-K12-10a-5p	12	0.00	0.00	2	0.00	0.00
kshv-miR-K12-11-5p	5	0.00	0.00	1	0.00	0.00

Table 6.5: Detailed analysis of KSHV miRNA read counts in hypoxic and normoxic BCBL-1 cells. The average of three independent experiments for each condition is displayed. Columns identify each KSHV miRNA, its total miR count, its percentage as compared to either KSHV miR reads or the overall read number, in either normoxia or hypoxia. The top part illustrates KSHV miRNAs present in more than 1% of total KSHV reads. The rest is displayed under "Others". KSHV miRNAs in bold have been validated by Taqman assays (**Figure 6.5**).

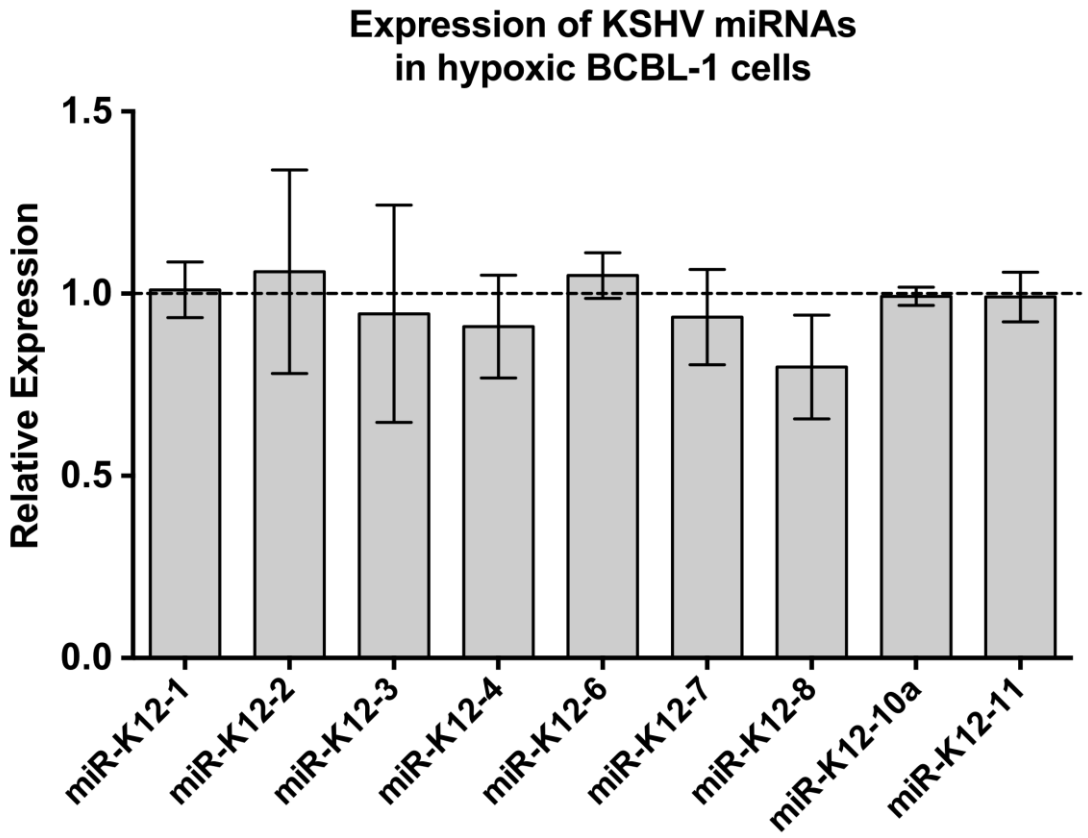

Figure 6.5: Taqman assays show a constant expression of KSHV miRNAs in hypoxic BCBL-1 cells compared to normoxia. The dashed line corresponds to the normoxic levels. No significant change was observed.

6.3 Effects of oxidative stress on viral miRNAs in BCBL-1 cells

All clinical forms of Kaposi's sarcoma have been associated with increased inflammation and oxidative stress (for reviews, see Ye et al. 2011; Purushothaman et al. 2015). Oxidative stress is known to generate ROS (reactive oxygen species) such as H_2O_2 (hydrogen peroxide) that can affect expression of KSHV-encoded genes. Indeed, oxidative stress was reported to promote reactivation of KSHV and induce cell death in PEL (BC-3 and BCBL-1 cells) (Li, Feng, and Sun 2011). Additionally, unpublished work from Davis et al. shows that H_2O_2–induced oxidative stress triggers an increase in LANA protein levels. Here, these results were reproduced in PEL cells, BCBL-1 and BC-3, after a 20hr-treatment of 25μM H_2O_2 (**Figure 6.6**).

Moreover, like hypoxic stress, oxidative stress is known to alter cellular miRNA expression (Simone et al. 2009; Xu et al. 2012). It was therefore hypothesised that the expression of KSHV encoded miRNAs might change upon H_2O_2 treatments. To address this, the expression of four viral miRNAs were analysed in the PEL cell line, BCBL-1, treated with 25μM H_2O_2 for 6hrs and 24hrs. These four miRNAs comprised miR-K12-10a-3p, which is under the Kaposin promoter, and 3 others that are under latency promoters – miR-K12-4-3p, miR-K12-6-3p, and miR-K12-11-3p. Although 24hr H_2O_2–treatments of BCBL-1 cells have been reproducibly shown to increase LANA levels, an additional 6hr time point was added since miRNAs are produced earlier than proteins in response to various treatments and have been shown to respond to environmental cues within hours. The results were normalised to untreated controls. It was found that H_2O_2–induced oxidative stress did not alter any of the four tested KSHV miRNAs at any time point (**Figure 6.7**). In addition, a time-course experiment was carried out for 6 different time points: 3hrs, 6hrs, 9hrs, 12hrs, 24hrs, and 48hrs. No differential expression for the

tested miRNAs was observed at any time point. This is similar to that seen following hypoxic treatments in BCBL-1 cells. This demonstrates that KSHV miRNA expression is kept under tight control regardless of cellular stresses such as oxidative stress or hypoxia.

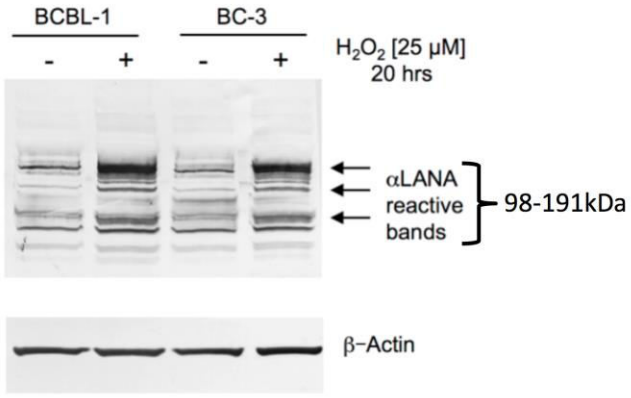

Figure 6.6: H_2O_2-induced oxidative stress increases LANA in B-cells. Western blot of nuclear extracts was stained for LANA protein.

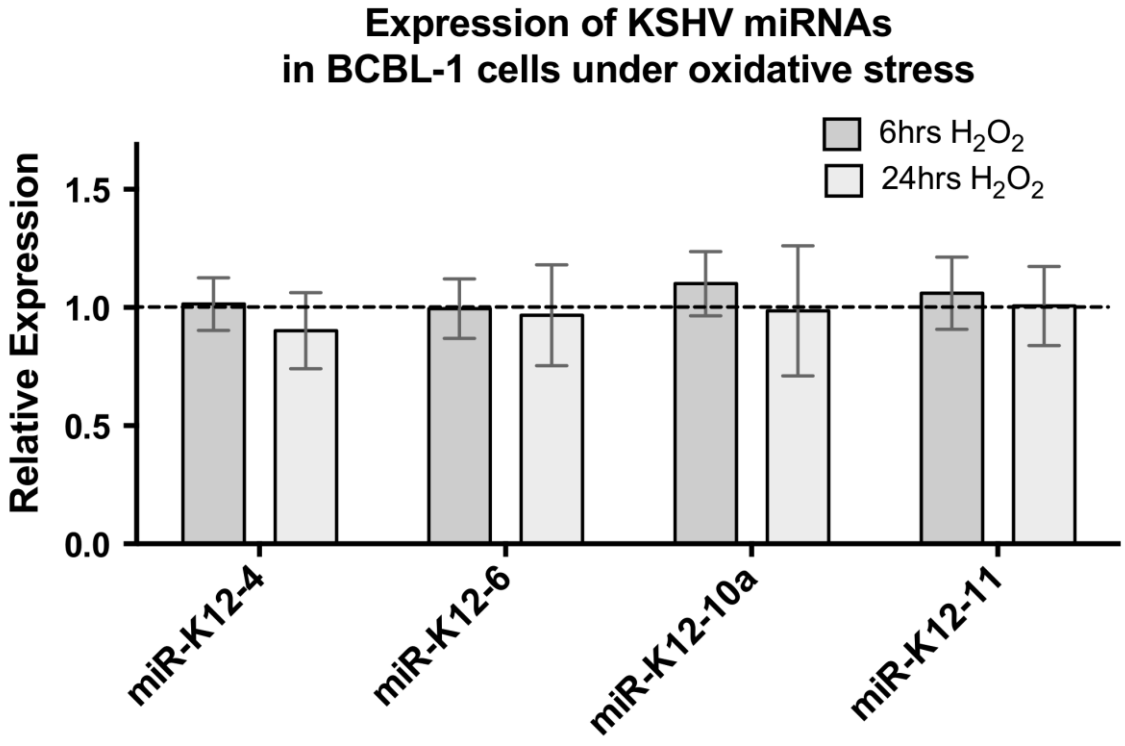

Figure 6.7: Taqman assays show a constant expression of KSHV miRNAs in BCBL-1 cells under oxidative stress as compared to controls. The dashed line corresponds to the untreated samples. No significant change was observed (n=3).

6.4 Effects of immunomodulatory drug Pomalidomide on viral miRNAs in BCBL-1 cells

Pomalidomide is an immunomodulatory drug recently approved by the FDA for the treatment of relapsed multiple myeloma (MM) (Chanan-Khan et al. 2013). Together with its sister compounds, lenalidomide and thalidomide, pomalidomide belongs to the IMiDs class of drugs, a novel group of anticancer and immunomodulatory agents. IMiDs have greatly improved the treatment of patients with MM and other hematologic diseases. They bind cereblon, a component of CUL4 E3 ubiquitin ligase, which down-regulates IRF4, a key feature of MM cell survival (Zhu, Kortuem, and Stewart 2013; Shaffer et al. 2008). Thus, the IMiDs mediate the inhibition of IRF4, therefore inducing MM cytotoxicity.

KSHV-infected cells have elevated levels of IRF4 and NF-κB, much like MM (Shaffer et al. 2008; Shaffer et al. 2009). These changes are known to be involved in maintaining cell viability and cell proliferation. Based in part on the activity of thalidomide in KS, the group of Dr. Robert Yarchoan at the NIH (Bethesda, USA) is conducting a clinical trial of pomalidomide in KS. Unpublished results from his laboratory at the HIV and AIDS Malignancy Branch, NCI, show that (i) pomalidomide down-regulates cellular proteins IRF4 and NF-κB in KSHV-infected cells, thereby interfering with cell proliferation; and (ii) at higher doses, pomalidomide prevents the down-regulation of MHC I hence blocking a mechanism for virus-induced immune evasion.

Here, the regulation of LANA was investigated in BCBL-1 cells treated with 10μM IMiDs for 48hrs. LANA protein levels decreased in BCBL-1 cells treated with 10μM pomalidomide (**Figure 6.8**). Lenalidomide treatment also triggered a clear decrease in

LANA protein levels. Thalidomide however did not show as strong of a down-regulation after treatment. Because LANA is a latent protein, its expression might be similar to that of KSHV miRNAs since the latter are expressed in latency. It was therefore postulated that KSHV miRNAs might be down-regulated by pomalidomide treatment in BCBL-1 cells. A total of 10 miRNAs were quantified by Taqman assay in BCBL-1 untreated cells, and pomalidomide treated cells (0.1μM, 1μM, 5μM, and 10μM). The 10 tested miRNAs included seven KSHV miRNAs (miR-K12-1-5p, miR-K12-2-5p, miR-K12-3-5p, miR-K12-4-3p, miR-K12-6-3p, miR-K12-7-3p and miR-K12-11-3p) as well as an additional three cellular miRNAs that are not known to be affected by IMiD drug treatments (miR-193b, miR-500, and let-7c). It was observed that pomalidomide at doses of 5μM and 10μM triggers a significant decrease in all tested KSHV miRNAs, but not in the control cellular miRNAs (**Figure 6.9**). Furthermore, pomalidomide at a dose of 1μM already starts showing a trend for down-regulation.

This is the first time that KSHV miRNAs have been shown to respond to drug treatment in a dose dependent manner. It would be of interest to determine the levels of known KSHV miRNA targets such as TWEAKR, targeted by miR-K12-11, to see if they are in turn up-regulated with pomalidomide treatment.

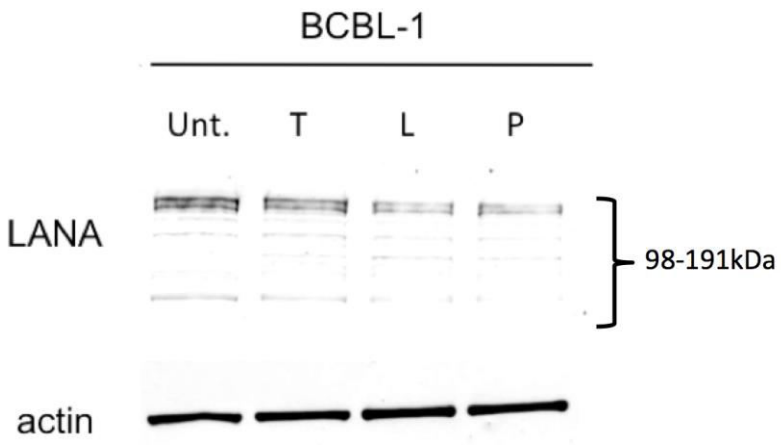

Figure 6.8: Effects of IMiD treatments on LANA in BCBL-1 cells. Western blot of nuclear extracts was stained for LANA protein. Actin was used at internal control. Unt.: Untreated BCBL-1 cells, T: 10μM Thalidomide, L: 10μM Lenalidomide, P: 10μM Pomalidomide.

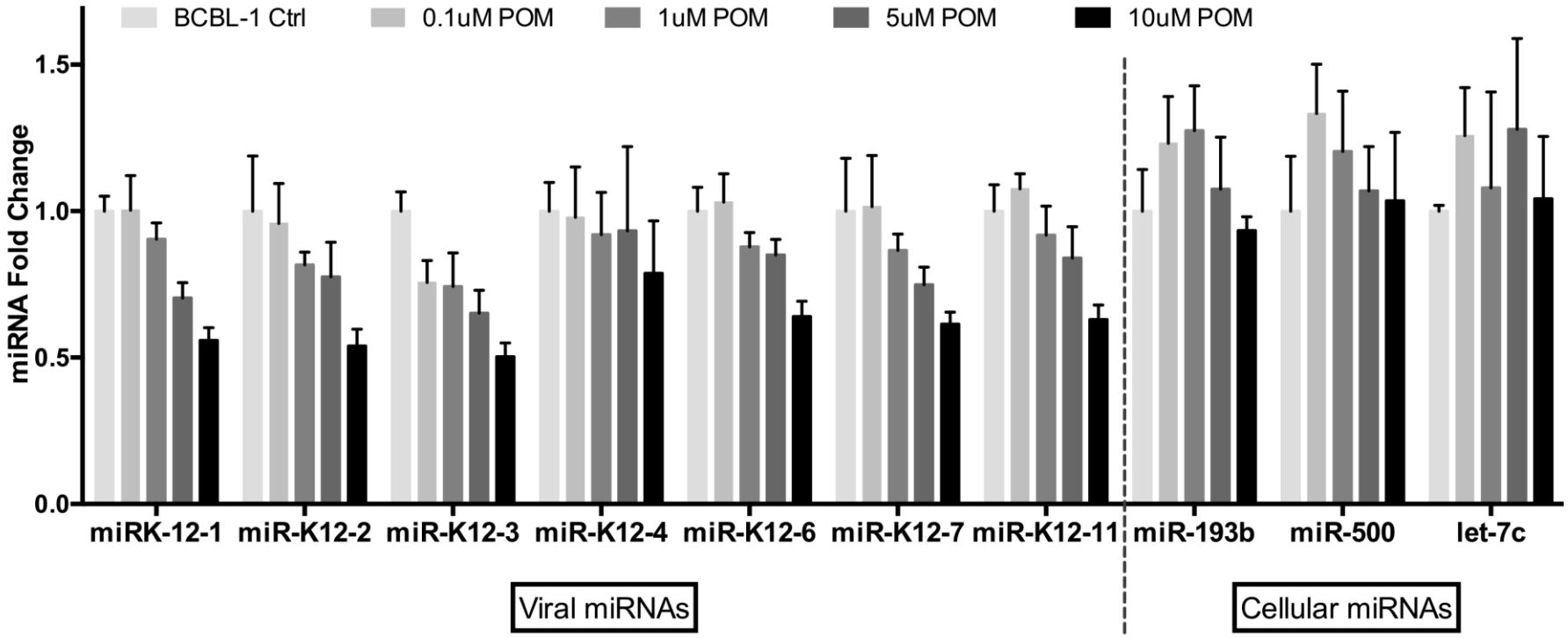

Figure 6.9: Dose response of KSHV miRNAs to pomalidomide treatment in BCBL-1 cells.

6.5 Conclusions and future directions

A decade after the first viral miRNAs was discovered, it is still unclear how the expression of these important viral repressors is regulated. KSHV encodes 12 pre-miRNAs, all of them being constitutively expressed in latency, but 2 of these are also expressed during lytic replication and are under a separate promoter. It has been shown that a slight increase could be seen for these 2 miRNAs (miR-K12-10 and miR-K12-12) when cells are undergoing lytic replication (Cullen 2011; Cai and Cullen 2006). Since it was found that hypoxia can dramatically affects cellular miRNA expression, the effects of hypoxia on viral miRNA expression were also investigated. In addition, the effects of oxidative stress and pomalidomide treatments on KSHV miRNA expression were addressed. Hypoxia and oxidative stress can induce a number of changes in KSHV genes expression. For example, LANA is up-regulated in cells treated with H_2O_2. Furthermore, hypoxia is known to up-regulate LANA and RTA (Davis 2001; Veeranna et al. 2012; Haque et al. 2003). However, neither hypoxic nor oxidative stress triggered a change in KSHV miRNA expression. Taken together, these results suggest that KSHV has evolved to constitutively express its own miRNAs, and still respond to microenvironmental stresses such as oxidative stress and hypoxia through changes in LANA and other viral genes.

Regarding pomalidomide treatment of BCBL-1 cell, the results were strikingly different. Not only did KSHV miRNA expression decrease in response to the immunomodulatory drug, but it did so in a dose-dependent manner. Remarkably, all tested miRNAs (miR-K12-1, -2, -3, -4, -6, -7, -11) were reduced ~50% at the strongest pomalidomide dose (10μM). By comparison, three control cellular miRNAs did not show any significant expression change under pomalidomide treatment, suggesting that pomalidomide only

affects viral miRNAs and does not interfere with the host cell machinery of small RNA silencing.

Publication arising from data presented in this Chapter:

Viollet, Coralie, David A. Davis, Martin Reczko, Joseph M. Ziegelbauer, Francesco Pezzella, Jiannis Ragoussis, and Robert Yarchoan. 2015. "Next-Generation Sequencing Analysis Reveals Differential Expression Profiles of MiRNA-mRNA Target Pairs in KSHV-Infected Cells." Plos One 10 (5): e0126439. doi:10.1371/journal.pone.0126439.

7

Summary and future directions

THIS thesis describes in great detail the changes in miRNA and mRNA expression that occur due to hypoxia, KSHV infection and a combination of the two. This was done to develop a deeper understanding of the interactive effects of hypoxic stress and KSHV infection on the cellular machinery. First, the SLK/SLKK cell system was chosen as a suitable cell model, to assess the effects of latent KSHV infection on cellular miRNA and mRNA expression (**Chapter 3**). Second, this system was used to determine the effects of hypoxic stress on cells and how oxygen deprivation compared to KSHV infection (**Chapter 4**). Third, KSHV-infected B-cells were utilised to gain a better understanding of the effects of hypoxia in primary effusion lymphoma (PEL), a KSHV-induced tumour (**Chapter 5**). Finally, a comprehensive analysis of the effects of external stimuli, such as oxidative stress, hypoxia and pomalidomide treatment was carried out on viral miRNAs in two KSHV-infected cell lines, BCBL-1 and SLKK (**Chapter 6**). This study is unique in that it is the first time an analysis of both mRNA and miRNA changes were evaluated in KSHV infection, allowing for an assessment of the potential

for the miRNA changes to affect their target mRNAs. By profiling both miRNA and mRNA expression in a variety of conditions and cell lines and performing validation and functional assays, the work presented in this thesis describes a multidisciplinary and detailed approach – the first of its kind – toward understanding the implications of microenvironmental changes such as oxygen deprivation in KSHV pathogenesis.

7.1 Summary of the contributions to the field of hypoxia and KSHV

Two KSHV cell models, SLK/SLKK and BCBL-1 cells, were used in this thesis to address hypoxic and KSHV regulation of miRNAs and mRNAs. The SLK/SLKK cell system was chosen for a variety of reasons: (i) SLK and SLKK cells are unique in the KSHV field as they provide the rare ability to directly compare latent KSHV-infected and uninfected cells, (ii) in SLKK cells, KSHV latency is under tight control, hence being a robust model for latency, rather than lytic replication (Arias et al. 2014) and (iii) since miRNAs and mRNAs are constitutively expressed at varying abundance levels depending on the cell type, the use of the same cell line with and without infection (i.e. KSHV-positive and -negative SLK cells) is key when dealing with deep sequencing studies as it minimises the fluctuations in genetic background, thereby decreasing the false positive rate in differentially expressed hits.

However, these factors do not necessarily make SLK/SLKK the *best* model for studying KSHV infection and hypoxia. KSHV-positive BCBL-1 cells are suspension cells of a KSHV tumour, PEL. They are particularly relevant for the study of oxygen deprivation as PEL often occurs in effusion in the pleural space, a region of low oxygen tension (Dobyns 1999). In this thesis, BCBL-1 cells were used not only for hypoxia exposure, but also oxidative stress and pomalidomide treatment.

As a general note, very few deep sequencing studies have been conducted on hypoxia combining both mRNA and miRNA profiles (Camps et al. 2014), and none related to KSHV infection. Here, SLK, SLKK and BCBL-1 cells in hypoxic and normoxic conditions were surveyed for both mRNA and miRNA expression profiles, providing a wealth of information and an invaluable platform unprecedented in the KSHV field.

The effects of KSHV infection on miRNAs and mRNAs in SLK and SLKK triplicate samples were investigated in **Chapter 3**. In general, there were significantly more down- than up-regulated miRNAs and more than a third of the down-regulated miRNAs were located within 50kb of each other, in the same miRNA cluster. Using miRNA transfection assays, it was subsequently found that a number of differentially expressed miRNAs in the SLK/SLKK system were associated with inverse changes in the target mRNAs that were predicted by the dual mRNA-miRNA-Seq analysis. By carrying out the analysis on cells from three separate experiments, it was possible to have high confidence in the findings and avoid high rates of false-positive or false-negative hits.

Chapter 4 described how the same cell model, SLK/SLKK, behaved under hypoxic stress. It was demonstrated that, similar to KSHV infection, the majority of the dysregulated miRNAs were down-regulated by hypoxia. Additionally, a remarkable third of the total number of genes altered under hypoxia exposure were similarly changed in cell latently infected with KSHV, suggesting that, to some degree, KSHV infection triggers similar signalling pathways to that of hypoxia.

Using the BCBL-1 cell model, the effects of hypoxia on cellular mRNA and miRNA expression were studied. As discussed at the end of **Chapter 5**, much like the SLKK hypoxic study, miRNAs were repressed under hypoxic stress and only one miRNA was similarly up-regulated between the two KSHV-infected cell lines.

In **Chapter 6**, the differential expression of viral miRNAs from hypoxic and normoxic SLKK and BCBL-1 cells were investigated by miRNA-Seq and/or individual Taqman assays. Viral miRNA expression remained unchanged between normoxia and hypoxia in both cell lines. Also, oxidative stress did not affect the tested KSHV miRNAs in BCBL-1 cells. However, pomalidomide, an immunomodulatory drug presently in clinical trial for the treatment of KS and being considered for PEL, dose dependently reduced the levels of the tested KSHV miRNAs in BCBL-1 cells.

Important results and potential future experiments will be hereafter discussed for each of the above stated findings.

7.2 Insights toward the effects of KSHV infection on host miRNA-mRNA target pairs

Although much research has been dedicated to studying the effects of KSHV infection on host cells, the work described in **Chapter 3** is the first to establish differential expression profiles for both miRNAs and mRNAs and is now published in PLoS One (Viollet et al. 2015). Indeed, the deep sequencing studies presented in this thesis allowed for the cross-comparison between the two datasets and enabled the identification of miRNA-mRNA target pairs affected by KSHV infection within the same cells. By comparing the SLK and SLKK miRNA expression profiles, it was found that the majority (~73%) of the cellular miRNAs that were significantly altered by KSHV infection were down-regulated. Of note, more than a third (~38%) of these repressed miRNAs were encoded by miRNA genes located in the 14q32 miRNA cluster. Interestingly, the down-regulation of this particular miRNA cluster has been previously identified in PEL and linked to cancer development, demonstrating a similarity between

viral and non-viral cancers (Lucon et al. 2013; Thayanithy, Sarver, et al. 2012; Thayanithy, Park, et al. 2012). However, it was found that the down-regulation of the 14q32 miRNAs was not due to a deletion of genomic DNA in SLKK cells, in constrast to the previous studies in PEL cells (Luan et al. 2010). Further studies should investigate whether this miRNA down-regulation is due to post-transcriptional and/or epigenetic mechanisms.

Moreover, validations assays (Taqman) independently confirmed the differential expression of nine miRNAs seen significantly dysregulated based on miRNA-Seq in the SLK/SLKK system (five down-regulated and four up-regulated miRNAs). Additionally, two miRNAs, miR-224-5p and miR-409-3p, were found similarly affected in *de novo* infected cells, suggesting that some of the changes observed under KSHV latency could also occur soon after *de novo* infection. However, it remains unknown to what extent the miRNAs seen differentially expressed in newly infected cells differ or overlap to those altered in latently infected cells. The idea could be taken further by conducting miRNA-Seq analysis on *de novo* infected SLK cells to determine the overlap between miRNAs altered by latent and *de novo* KSHV infection.

Finally, the relative expression of three miRNAs as well as their targets (FGB and RDX for miR-409-3p, MDM2 for miR-409-5p, and CASP2 and LIF for miR-708-5p) was verified either in SLK and SLKK cells, or in cells transfected by miRNA mimics. In all cases, the expression of the tested miRNAs decreased the expression of their target mRNA(s). These transfection assays also identified two novel mRNA targets not previously reported: LIF for miR-708-5p and MDM2 for miR-409-5p. These results support the hypothesis that changes in miRNAs are driving at least some of the observed mRNA changes. However, it is not expected that the differential expression of *all* mRNAs will be solely or directly the result of miRNA silencing. A number of other

factors may also affect cellular mRNAs in KSHV-infected cells. These include KSHV proteins that can have both direct or indirect effects on cellular genes, and the host defence response to viral infection. Although some of the miRNA-mRNA target pairs have been validated by Taqman assays, further analysis of novel target mRNAs identified in this study should be done using techniques such as CLIP (crosslinking and immunoprecipitation) in SLKK cells. This would allow for the co-immunoprecipitation of miRNA-containing ribonucleoprotein complexes (miRNPs) and their target mRNAs, thereby determining the entire targetome of miRNAs in living cells and confirming which changes correlates on a global scale. Such work has been done in PEL cells (Gottwein et al. 2011), but not in SLKK cells.

7.3 Evaluation of the interplay between KSHV infection and the hypoxic response

A central finding presented in this thesis is that there are striking similarities between the cellular response to hypoxia and the cellular response to KSHV infection. As discussed at the end of **Chapter 4**, KSHV infection is known to increase HIF levels in normoxia (Carroll et al. 2006; Shin et al. 2008), and HIFs can also induce a number of KSHV genes (Haque et al. 2003; Veeranna et al. 2012). This suggests that certain signalling pathways or regulatory networks are related between the hypoxic pathway and KSHV infection. Results presented in this thesis support this hypothesis and demonstrate that about a third (~30%) of the genes seen differentially expressed under hypoxia were similarly up- or down-regulated by KSHV latent infection. Interestingly, some of these genes (BIRC3, NEAT1, and ITGAV) are known to play independent roles in hypoxia and/or viral infection. For instance, baculoviral IAP repeat containing 3 (BIRC3), also

known as cellular inhibitor of apoptosis 2 (cIAP-2), has been previously shown to be up-regulated by hypoxia (Hu et al. 2003). In addition, KSHV protein K15 also up-regulates BIRC3 (Brinkmann et al. 2007), which suggest that this up-regulation might occur through HIF-dependent mechanisms. BIRC3 inhibits apoptosis by interfering with the activation of caspases, which is an important factor in both KSHV infection and hypoxia (Bertrand et al. 2008; Deveraux et al. 1998; Roy 1997). Here, BIRC3 was found induced in both hypoxic vs. normoxic SLK cells, and in infected vs. uninfected SLK cells. Further work involving viability and transfection assays could determine whether or not the up-regulation of BIRC3 by KSHV is induced through hypoxic pathways to provide a survival advantage to KHSV-infected cells. These parallels between hypoxia and KSHV infection are interesting to highlight as they demonstrate both the relevance of hypoxia in KSHV pathogenesis and the usefulness of this mRNA sequencing study. If validated, targeting BIRC3 may be a useful strategy in specifically killing KSHV-infected cells and cancer cells.

Regarding the miRNA response to hypoxia, as compared to KSHV infection, the majority of the dysregulated miRNAs were repressed in both (~88% by hypoxia and ~73% by KSHV infection). However, miR-210 was found up-regulated by both hypoxia and KSHV latent infection using independent Taqman validation assays. miR-210 is directly up-regulated by HIF and has been shown to be up-regulated in a variety of cell lines exposed to hypoxia (Chan et al. 2012). Interestingly, this is the first time that a HIF-inducible miRNA was validated as induced in KSHV-infected cells, compared to uninfected cells, in normoxic conditions. It is also known that miR-210 mediates the down-regulation of ISCU, a mitochondrial iron sulphur scaffold protein involved in cellular metabolism (Favaro et al. 2010). Of note, inhibition of ISCU by miR-210 in MCF7 cells has been shown to lead to a shift to glycolysis, an enhanced cell survival

rate, and an increased iron uptake required for cell growth (Favaro et al. 2010). Such changes could favour KSHV infected cells in a similar manner. Further study will be necessary to determine whether HIF-1 and/or HIF-2 are required for the up-regulation of miR-210 in infected SLKK cells. For example, lentiviral vectors encoding shRNAs to HIF-1 and HIF-2 mRNAs could be used to artificially reduce these mRNA levels in SLKK cells, which would help decipher these regulatory mechanisms.

7.4 Understanding the regulatory mechanisms behind hypoxic stress in BCBL-1 cells

A number of studies of the effects of hypoxia, including three research articles from Dr. Yarchoan's laboratory (Davis 2001; Haque et al. 2003; Veeranna et al. 2012), have been conducted in KSHV-infected BCBL-1 cells. Although these studies provided the first insights into the biochemical interaction between hypoxia and KSHV, they addressed neither the regulatory effects of hypoxia on transcriptome-wide miRNAs, nor the global impact of hypoxia on mRNA expression. **Chapter 5** showed that combining miRNA-Seq and mRNA-Seq enabled not only the first compilation of a comprehensive list of miRNAs and mRNAs seen differentially expressed by hypoxia in KSHV-infected B-cells, but also the comparison with SLKK cells.

Using miRNA-Seq, it was demonstrated that ~83% of all dysregulated human miRNAs in BCBL-1 cells were decreased under hypoxic stress. This result is consistent with findings from **Chapter 4** showing that miRNAs in SLKK cells were globally (~88%) repressed by the absence of oxygen. Moreover, miR-210, a known hypoxia-inducible miRNA in many cell lines (Camps et al. 2008; Pulkkinen et al. 2008), was identified as the sole hypoxia-induced miRNA in common between BCBL-1 and SLKK cells,

consistent with its significant role in hypoxia. This also suggests it may have important effects in KSHV infection and the pathogenesis of KSHV-induced diseases. miR-210 was previously shown to be directly induced by HIF-1 and, to a lesser extent, HIF-2 (McCormick et al. 2013).

It would be of great interest to study the different impacts of HIFs on miR-210 in the context of KSHV infection, utilising BCBL-1 cells lines that have the HIF proteins (either HIF-1 or HIF-2) knocked down, and that are readily available in Dr. Yarchoan's laboratory. Since miR-210 is primarily induced by HIF-1, it could be hypothesised that a decrease in miR-210 levels in BCBL-1 cells transduced with lentiviral vectors encoding for HIF-1 shRNAs compared to scramble shRNA may be observed in both normoxia and hypoxia. However, it has been observed that PEL lines have low levels of detectable HIF-2 mRNA and protein expression even in hypoxia. Therefore, miR-210 expression might be expected to only be slightly reduced when HIF-2 mRNA is knocked-down in normoxic and hypoxic BCBL-1 cells. In fact, initial experiments were undertaken shortly before the submission of this thesis, supporting this hypothesis (**Figure 7.1**). Although these results would require further validation, this encourages further research involving miR-210 and KSHV-infected B-cells.

In addition, the up-regulation of hypoxia-inducible genes in BCBL-1 cells such as VEGF, KDM3A (JMJD1A), CA9, PLOD2, TXNIP and PGK1 was described in **Chapter 5**. For example, the HIF-target gene VEGF, vascular endothelial growth factor, is known to promote angiogenesis, which is a characteristic feature of KSHV-induced neoplasms. VEGF is currently a target for anti-angiogenic treatments of KS and inhibition of angiogenesis has been shown to normalise the tumour vasculature (Folkman 2007; Uldrick et al. 2012). Furthermore, the inhibition of histone demethylase KDM3A, another gene found up-regulated in hypoxic BCBL-1 cells, can decrease

tumour growth and angiogenesis by itself, and when used in combination with the anti-VEGF monoclonal antibody bevacizumab, it can also improve the overall outcome of the treatment (Osawa et al. 2013). Of note, phosphoglycerate kinase 1 (PGK1), which was also up-regulated in BCBL-1 cells under hypoxia, is a key gene in the glycolytic pathway and is instrumental in the shift to glycolysis under hypoxia (Semenza 2003; Gao et al. 2004). Taken together, this suggests that the dysregulation of these genes under hypoxia may indirectly fuel KSHV-infected cell growth, and enhance glycolysis in order to maintain energy balance. Some of these genes should be investigated as potential novel therapeutic treatments of KSHV-associated diseases.

As a general comment regarding hypoxic *in vitro* experiments, it is worth mentioning that using growth media containing high glucose concentrations (4.5g/L, 25mM) such as DMEM is standard in tissue culture. However, these glucose conditions may differ from those in cells *in vivo* where glucose concentrations range from 1mM to 5mM. Indeed, hypoxia is known to induce the use of glucose for energy production; therefore studying the effects of hypoxia in high glucose conditions could potentially bias the results and differ from lower glucose conditions. Similarly, using oxygen concentration of 1% O_2 in a hypoxic chamber may or may not be similar to tumour environment *in vivo* – hence the use for clinical follow-up validations and the development of models that are physiologically relevant.

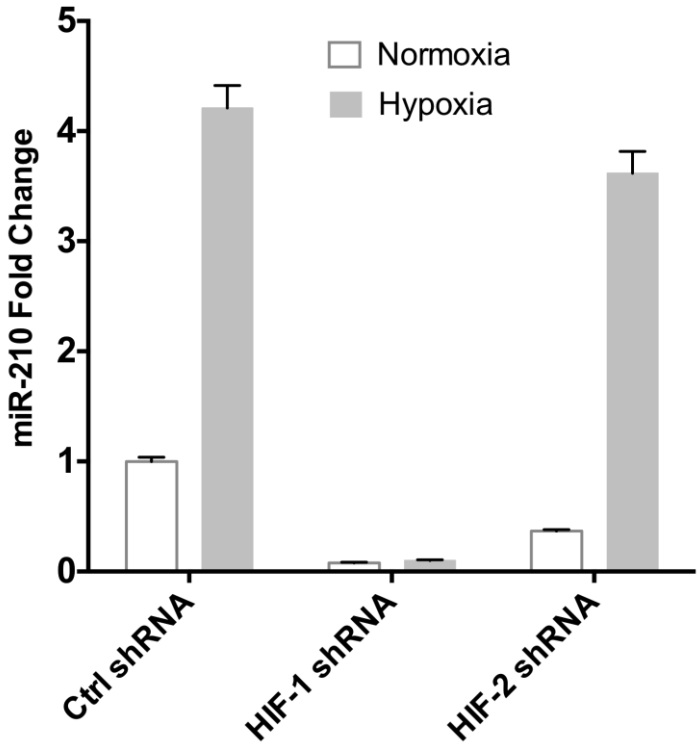

Figure 7.1: miR-210 expression in BCBL-1 cells in the absence and presence of either HIF-1 or HIF-2 mRNAs using Taqman assays.

Ctrl shRNA: BCBL-1 cells transducted with lentiviral vectors encoding for a scramble shRNA. HIF-1 shRNA: BCBL-1 cells transducted with lentiviral vector encoding for HIF-1 shRNA. HIF-2 shRNA: BCBL-1 cells transducted with lentiviral vector encoding for HIF-2 shRNA. This intial experiment was conducted once (n=1).

7.5 KSHV miRNA expression in response to microenvironmental stresses and pomalidomide drug treatment

The biogenesis of cellular miRNAs is relatively well characterised. Key proteins such as RNA polymerase II, Drosha, DGCR8, Dicer, and Argonaute all play an important role in the production and the excision of mature miRNAs, as well as the actual silencing of their respective target mRNAs (for a review, see Bartel, Lee, and Feinbaum 2004). Any changes in these central proteins will result in a global lower efficiency of miRNA biogenesis, hence impairing the translation inhibition of the targets. Additionally, it is known that many stresses such as cancer, hypoxia, oxidative stress, UV radiation and viral infection can greatly perturb cellular miRNA expression (Thulasingam et al. 2011; Nallamshetty, Chan, and Loscalzo 2013; Fu et al. 2014; Zheng and Wang 2015; Jansson and Lund 2012; Syed et al. 2013). For viral miRNAs however, besides the fact that they are transcribed and generated using the host cellular machinery, not much is known about their expression following different types of environmental stresses or exposure to drugs.

To address this, the effects of environmental stresses or drug treatment on viral miRNAs were described in **Chapter 6**. It has been previously reported that KSHV miRNAs are largely unaffected by TPA treatment, an inducer of lytic replication (Cai et al. 2005; Pfeffer et al. 2005). However, most KSHV miRNAs are encoded alongside latent KSHV genes, and it was somewhat surprising that neither hypoxic nor oxidative stresses affected KSHV miRNA expression. All in all, these results indicate that KSHV miRNAs are constitutively expressed and under very tight control.

Unlike environmental stresses, treatment of BCBL-1 cells with pomalidomide led to a global decrease in KSHV miRNA expression. Pomalidomide is a drug currently used in clinical trial for patients with KS. Since the decrease in viral miRNAs was seen for all tested KSHV miRNAs, it suggests that pomalidomide was affecting the constitutive expression of viral miRNAs in latency rather than targeting specific KSHV miRNAs.

Therefore, these results indicate that pomalidomide is affecting either a cellular or viral protein that is involved in globally regulating KSHV miRNA biogenesis. Further work should investigate how pomalidomide is reducing global KSHV miRNA expression, but not cellular miRNAs. The drug should also be tested in another system such as EBV-infected cells to see whether EBV-encoded miRNAs are also decreased upon pomalidomide treatment.

Finally, it is known that pomalidomide down-regulates cellular levels of IRF4 and NF-κB (Zhu, Kortuem, and Stewart 2013; Chanan-Khan et al. 2013) and inhibits the down-regulation of MHC I, a protein whose expression is required for immune surveillance (unpublished data, Yarchoan lab). Further studies should address whether these inhibitory processes lead to the decrease in KSHV miRNAs, or conversely whether the pomalidomide-mediated decrease in viral miRNAs causes the observed cellular effects on IRF4, NF-κB and MHC I.

7.6 Concluding remarks

The main goals of this dissertation were (i) to determine the effect of KSHV infection on cellular miRNA expression and correlate these changes with those occurring at the mRNA level, (ii) to evaluate the effects of hypoxia on cellular and viral miRNA

expression, and (iii) to understand how the cellular response to hypoxia changes in the context of KSHV infection.

Through this analysis, it was shown that (i) KSHV infection drastically altered the expression of some miRNA-mRNA target pairs that may play a significant role in KSHV pathobiology, (ii) hypoxia dramatically changed both cellular mRNAs and miRNAs – but not viral miRNAs – in KSHV-infected cells, (iii) miR-210, a miRNA involved in hypoxia and cancer, was increased by both hypoxia and KSHV infection and the down-regulation of its target genes may play a role in the development of KSHV-associated diseases, and (iv) the cellular gene expression (mRNA) responses to hypoxia and KSHV infection were found to be similar. These findings suggest that KSHV infection and hypoxia work in concert to promote biological processes such as cellular proliferation, which can play a significant role in KSHV pathogenesis.

Throughout this study, many pairs of inversely correlated miRNAs and target mRNAs were identified and some were also validated. However, it should be noted that the importance of miRNAs in KSHV-associated malignancies is *not* restricted to their ability to target one individual gene, but rather their overall influence on signalling pathways and biological networks of genes. Therefore, the results presented here offer novel insights into the pathogenesis of KSHV and the effects of hypoxia on the development of KSHV-associated diseases. This work has opened up new avenues for the discovery of novel miRNA- or mRNA-based therapeutic targets to treat KSHV-related malignancies.

8

Appendix: Figure permissions

SOME figures and tables in this thesis were reproduced from other sources, for which detailed copyright and permissions information is listed below.

Figure 1.1: MicroRNA biogenesis and activity.

Reference (Kim 2005). Kim, V. N. (2005). MicroRNA biogenesis: coordinated cropping and dicing. *Nature Reviews. Molecular Cell Biology*, *6*(5), 376–85. doi:10.1038/nrm1644

License obtained through Rightstlink/Macmillan Publishers Ltd: License # 3603710281500.

Figure1.3: Possible mechanisms of miRNA target regulation.

Reference (Carthew & Sontheimer 2009). Carthew, R. W., & Sontheimer, E. J. (2009). Origins and Mechanisms of miRNAs and siRNAs. *Cell*, *136*(4), 642–55. doi:10.1016/j.cell.2009.01.035

License obtained through Rightstlink/Elsevier: License # 3603750512146.

Figure 1.4: Representation of HIF regulation under hypoxic and normoxic conditions.

Reference (George & Kaelin 2003). George, D. J., & Kaelin, W. G. (2003). The von Hippel-Lindau protein, vascular endothelial growth factor, and kidney cancer. *The New England Journal of Medicine*, *349*(5), 419–21. doi:10.1056/NEJMp030061

Reproduced with permission from (George & Kaelin 2003), Copyright Massachusetts Medical Society, Publisher of the New England Journal of Medicine.

Figure 1.5: Tumour physiology under hypoxia versus normoxia.

Reference (J M Brown & Giaccia 1998). Brown, J. M., & Giaccia, A. J. (1998). The Unique Physiology of Solid Tumors : Opportunities (and Problems) for Cancer Therapy. *Cancer Research*, *58*(7), 1408–1416. Retrieved from http://www.ncbi.nlm.nih.gov/pubmed/9537241

License obtained through Rightstlink/AACR: License # 3603780657851.

Figure 1.6: Seroprevalence of KSHV.

Reference (Mesri et al. 2010). Mesri, E. A., Cesarman, E., & Boshoff, C. (2010). Kaposi's sarcoma and its associated herpesvirus. *Nature Reviews. Cancer*, *10*(10), 707–19. doi:10.1038/nrc2888

License obtained through Rightstlink/Macmillan Publishers Ltd: License # 3603781182476.

Figure 1.7: KSHV Genome.

Reference (Coscoy 2007). Coscoy, L. (2007). Immune evasion by Kaposi's sarcoma-associated herpesvirus. *Nature Reviews. Immunology*, *7*(5), 391–401. doi:10.1038/nri2076

License obtained through Rightstlink/Macmillan Publishers Ltd: License # 3603790159563.

Figure 1.9: Development of KSHV-related malignancy under microenvironmental stress.

Reference (Cai et al. 2010). Cai, Q., Verma, S. C., Lu, J., & Robertson, E. S. (2010). Molecular biology of Kaposi's sarcoma-associated herpesvirus and related oncogenesis. *Advances in Virus Research*, *78*, 87–142. doi:10.1016/B978-0-12-385032-4.00003-3

License obtained through Rightstlink/Elsevier: License # 3603801104833.

Table 1.3: Putative functions and targets of KSHV miRNAs.

Reference (Qin 2012). Qin, Z., Jakymiw, A., Findlay, V., & Parsons, C. (2012). KSHV-Encoded MicroRNAs: Lessons for Viral Cancer Pathogenesis and Emerging Concepts. *International Journal of Cell Biology*, *2012*, 603961. doi:10.1155/2012/603961

9

Bibliography

Abend, Johanna R, Dhivya Ramalingam, Philippe Kieffer-Kwon, Thomas S Uldrick, Robert Yarchoan, and Joseph M Ziegelbauer. 2012. “Kaposi’s Sarcoma-Associated Herpesvirus microRNAs Target IRAK1 and MYD88, Two Components of the Toll-like Receptor/interleukin-1R Signaling Cascade, to Reduce Inflammatory-Cytokine Expression.” *Journal of Virology* 86 (21): 11663–74. doi:10.1128/JVI.01147-12.

Abend, Johanna R, Thomas Uldrick, and Joseph M Ziegelbauer. 2010. “Regulation of Tumor Necrosis Factor-like Weak Inducer of Apoptosis Receptor Protein (TWEAKR) Expression by Kaposi’s Sarcoma-Associated Herpesvirus microRNA Prevents TWEAK-Induced Apoptosis and Inflammatory Cytokine Expression.” *Journal of Virology* 84 (23): 12139–51. doi:10.1128/JVI.00884-10.

Akula, S M, N P Pramod, F Z Wang, and B Chandran. 2001. “Human Herpesvirus 8 Envelope-Associated Glycoprotein B Interacts with Heparan Sulfate-like Moieties.” *Virology* 284 (2): 235–49. doi:10.1006/viro.2001.0921.

Akula, S M, F Z Wang, J Vieira, and B Chandran. 2001. “Human Herpesvirus 8 Interaction with Target Cells Involves Heparan Sulfate.” *Virology* 282 (2): 245–55. doi:10.1006/viro.2000.0851.

Akula, Shaw M, Pramod P Naranatt, Neelam-Sharma Walia, Fu-Zhang Wang, Barbara Fegley, and Bala Chandran. 2003. “Kaposi’s Sarcoma-Associated Herpesvirus (human Herpesvirus 8) Infection of Human Fibroblast Cells Occurs through Endocytosis.” *Journal of Virology* 77 (14): 7978–90. http://www.pubmedcentral.nih.gov/articlerender.fcgi?artid=161913&tool=pmcentrez&rendertype=abstract.

Albini, A, I Paglieri, G Orengo, S Carlone, M G Aluigi, R DeMarchi, C Matteucci, et al. 1997. “The Beta-Core Fragment of Human Chorionic Gonadotrophin Inhibits Growth of Kaposi’s Sarcoma-Derived Cells and a New Immortalized Kaposi's Sarcoma Cell Line.” *AIDS (London, England)* 11 (6): 713–21. http://www.ncbi.nlm.nih.gov/pubmed/9143602.

Angst, E, S Sibold, C Tiffon, R Weimann, B Gloor, D Candinas, and D Stroka. 2006. "Cellular Differentiation Determines the Expression of the Hypoxia-Inducible Protein NDRG1 in Pancreatic Cancer." *British Journal of Cancer* 95 (3): 307–13. doi:10.1038/sj.bjc.6603256.

Antman, K, and Y Chang. 2000. "Kaposi's Sarcoma." *The New England Journal of Medicine* 342 (14): 1027–38. doi:10.1056/NEJM200004063421407.

Aoki, Y, R Yarchoan, J Braun, A Iwamoto, and G Tosato. 2000. "Viral and Cellular Cytokines in AIDS-Related Malignant Lymphomatous Effusions." *Blood* 96 (4). American Society of Hematology: 1599–1601. http://www.bloodjournal.org/content/96/4/1599.abstract.

Aoki, Yoshiyasu, Elaine S Jaffe, Yuan Chang, Karen Jones, Julie Teruya-feldstein, Patrick S Moore, By Yoshiyasu Aoki, and Giovanna Tosato. 2011. "Angiogenesis and Hematopoiesis Induced by Kaposi's Sarcoma-Associated Herpesvirus-Encoded Interleukin-6." *Blood*, 4034–43.

Arias, Carolina, Ben Weisburd, Noam Stern-Ginossar, Alexandre Mercier, Alexis S Madrid, Priya Bellare, Meghan Holdorf, Jonathan S Weissman, and Don Ganem. 2014. "KSHV 2.0: A Comprehensive Annotation of the Kaposi's Sarcoma-Associated Herpesvirus Genome Using next-Generation Sequencing Reveals Novel Genomic and Functional Features." Edited by Dirk P. Dittmer. *PLoS Pathogens* 10 (1). Public Library of Science: e1003847. doi:10.1371/journal.ppat.1003847.

Arvanitakis, L, EA Mesri, RG Nador, JW Said, AS Asch, DM Knowles, and E Cesarman. 1996. "Establishment and Characterization of a Primary Effusion (body Cavity- Based) Lymphoma Cell Line (BC-3) Harboring Kaposi's Sarcoma-Associated Herpesvirus (KSHV/HHV-8) in the Absence of Epstein-Barr Virus." *Blood* 88 (7): 2648–54. http://bloodjournal.hematologylibrary.org/cgi/content/abstract/88/7/2648.

Ayesh, Suhail, Imad Matouk, Tamar Schneider, Patricia Ohana, Morris Laster, Wasif Al-Sharef, Nathan de-Groot, and Abraham Hochberg. 2002. "Possible Physiological Role of H19 RNA." *Molecular Carcinogenesis* 35 (2): 63–74. doi:10.1002/mc.10075.

Baker, Amanda F, Mei Y Koh, Ryan R Williams, Brian James, Huamin Wang, Wendy R Tate, Alfred Gallegos, Daniel D Von Hoff, Haiyong Han, and Garth Powis. 2008. "Identification of Thioredoxin-Interacting Protein 1 as a Hypoxia-Inducible Factor 1alpha-Induced Gene in Pancreatic Cancer." *Pancreas* 36 (2): 178–86. doi:10.1097/MPA.0b013e31815929fe.

Ballestas, M E, P A Chatis, and K M Kaye. 1999. "Efficient Persistence of Extrachromosomal KSHV DNA Mediated by Latency-Associated Nuclear Antigen." *Science (New York, N.Y.)* 284 (5414): 641–44. http://www.ncbi.nlm.nih.gov/pubmed/10213686.

Barbera, Andrew J, Jayanth V Chodaparambil, Brenna Kelley-Clarke, Karolin Luger, and Kenneth M Kaye. 2006. "Kaposi's Sarcoma-Associated Herpesvirus LANA

Hitches a Ride on the Chromosome." *Cell Cycle (Georgetown, Tex.)* 5 (10): 1048–52. http://www.ncbi.nlm.nih.gov/pubmed/16721045.

Bartel, David P, Rosalind Lee, and Rhonda Feinbaum. 2004. "MicroRNAs : Genomics , Biogenesis, Mechanism, and Function." *Cell* 116 (2): 281–97. http://www.ncbi.nlm.nih.gov/pubmed/14744438.

Barth, Stephanie, Thorsten Pfuhl, Alfredo Mamiani, Claudia Ehses, Klaus Roemer, Elisabeth Kremmer, Christoph Jäker, Julia Höck, Gunter Meister, and Friedrich A Grässer. 2008. "Epstein-Barr Virus-Encoded microRNA miR-BART2 down-Regulates the Viral DNA Polymerase BALF5." *Nucleic Acids Research* 36 (2): 666–75. doi:10.1093/nar/gkm1080.

Behm-Ansmant, Isabelle, Jan Rehwinkel, Tobias Doerks, Alexander Stark, Peer Bork, and Elisa Izaurralde. 2006. "mRNA Degradation by miRNAs and GW182 Requires Both CCR4:NOT Deadenylase and DCP1:DCP2 Decapping Complexes." *Genes & Development* 20 (14): 1885–98. doi:10.1101/gad.1424106.

Bellare, Priya, and Don Ganem. 2009. "Regulation of KSHV Lytic Switch Protein Expression by a Virus-Encoded microRNA: An Evolutionary Adaptation That Fine-Tunes Lytic Reactivation." *Cell Host & Microbe* 6 (6). Elsevier: 570–75. doi:10.1016/j.chom.2009.11.008.

Bellot, Grégory, Raquel Garcia-Medina, Pierre Gounon, Johanna Chiche, Danièle Roux, Jacques Pouysségur, and Nathalie M Mazure. 2009. "Hypoxia-Induced Autophagy Is Mediated through Hypoxia-Inducible Factor Induction of BNIP3 and BNIP3L via Their BH3 Domains." *Molecular and Cellular Biology* 29 (10): 2570–81. doi:10.1128/MCB.00166-09.

Bennasser, Yamina, Christine Chable-Bessia, Robinson Triboulet, Derrick Gibbings, Carole Gwizdek, Catherine Dargemont, Eric J Kremer, Olivier Voinnet, and Monsef Benkirane. 2011. "Competition for XPO5 Binding between Dicer mRNA, Pre-miRNA and Viral RNA Regulates Human Dicer Levels." *Nature Structural & Molecular Biology* 18 (3). Nature Publishing Group, a division of Macmillan Publishers Limited. All Rights Reserved. 323–27. doi:10.1038/nsmb.1987.

Beral, V, T A Peterman, R L Berkelman, and H W Jaffe. 1990. "Kaposi's Sarcoma among Persons with AIDS: A Sexually Transmitted Infection?" *Lancet* 335 (8682): 123–28. http://www.ncbi.nlm.nih.gov/pubmed/1967430.

Bertrand, Mathieu J.M., Snezana Milutinovic, Kathleen M. Dickson, Wai Chi Ho, Alain Boudreault, Jon Durkin, John W. Gillard, James B. Jaquith, Stephen J. Morris, and Philip A. Barker. 2008. "cIAP1 and cIAP2 Facilitate Cancer Cell Survival by Functioning as E3 Ligases That Promote RIP1 Ubiquitination." *Molecular Cell* 30 (6): 689–700. doi:10.1016/j.molcel.2008.05.014.

Beyaert, R, K Heyninck, and S Van Huffel. 2000. "A20 and A20-Binding Proteins as Cellular Inhibitors of Nuclear Factor-Kappa B-Dependent Gene Expression and Apoptosis." *Biochemical Pharmacology* 60 (8): 1143–51. http://www.ncbi.nlm.nih.gov/pubmed/11007952.

Beyer, Sophie, Malene Maag Kristensen, Kim Steen Jensen, Jens Vilstrup Johansen, and Peter Staller. 2008. "The Histone Demethylases JMJD1A and JMJD2B Are Transcriptional Targets of Hypoxia-Inducible Factor HIF." *The Journal of Biological Chemistry* 283 (52): 36542–52. doi:10.1074/jbc.M804578200.

Blick, C, A Ramachandran, S Wigfield, R McCormick, A Jubb, F M Buffa, H Turley, et al. 2013. "Hypoxia Regulates FGFR3 Expression via HIF-1α and miR-100 and Contributes to Cell Survival in Non-Muscle Invasive Bladder Cancer." *British Journal of Cancer* 109 (1). Cancer Research UK: 50–59. doi:10.1038/bjc.2013.240.

Bosco, M. C., M. Puppo, C. Santangelo, L. Anfosso, U. Pfeffer, P. Fardin, F. Battaglia, and L. Varesio. 2006. "Hypoxia Modifies the Transcriptome of Primary Human Monocytes: Modulation of Novel Immune-Related Genes and Identification Of CC-Chemokine Ligand 20 as a New Hypoxia-Inducible Gene." *The Journal of Immunology* 177 (3). American Association of Immunologists: 1941–55. doi:10.4049/jimmunol.177.3.1941.

Bosco, Maria Carla, Gioia Reffo, Maura Puppo, and Luigi Varesio. 2004. "Hypoxia Inhibits the Expression of the CCR5 Chemokine Receptor in Macrophages." *Cellular Immunology* 228 (1): 1–7. doi:10.1016/j.cellimm.2004.03.006.

Boss, Isaac W, Peter E Nadeau, Jeffrey R Abbott, Yajie Yang, Ayalew Mergia, and Rolf Renne. 2011. "A Kaposi's Sarcoma-Associated Herpesvirus-Encoded Ortholog of microRNA miR-155 Induces Human Splenic B-Cell Expansion in NOD/LtSz-Scid IL2Rγnull Mice." *Journal of Virology* 85 (19): 9877–86. doi:10.1128/JVI.05558-11.

Boulanger, Emmanuelle, Renan Duprez, Eric Delabesse, Jean Gabarre, Elizabeth Macintyre, and Antoine Gessain. 2005. "Mono/oligoclonal Pattern of Kaposi Sarcoma-Associated Herpesvirus (KSHV/HHV-8) Episomes in Primary Effusion Lymphoma Cells." *International Journal of Cancer. Journal International Du Cancer* 115 (4): 511–18. doi:10.1002/ijc.20926.

Boulanger, Emmanuelle, Laurence Gérard, Jean Gabarre, Jean-Michel Molina, Christophe Rapp, Jean-François Abino, Jacques Cadranel, Sylvie Chevret, and Eric Oksenhendler. 2005. "Prognostic Factors and Outcome of Human Herpesvirus 8-Associated Primary Effusion Lymphoma in Patients with AIDS." *Journal of Clinical Oncology : Official Journal of the American Society of Clinical Oncology* 23 (19): 4372–80. doi:10.1200/JCO.2005.07.084.

Brennecke, Julius, David R Hipfner, Alexander Stark, Robert B Russell, and Stephen M Cohen. 2003. "Bantam Encodes a Developmentally Regulated microRNA That Controls Cell Proliferation and Regulates the Proapoptotic Gene Hid in Drosophila." *Cell* 113 (1): 25–36. http://www.ncbi.nlm.nih.gov/pubmed/12679032.

Brinkmann, Melanie M, Marcel Pietrek, Oliver Dittrich-Breiholz, Michael Kracht, and Thomas F Schulz. 2007. "Modulation of Host Gene Expression by the K15 Protein of Kaposi's Sarcoma-Associated Herpesvirus." *Journal of Virology* 81 (1): 42–58. doi:10.1128/JVI.00648-06.

Brooks, Christopher L, and Wei Gu. 2006. "p53 Ubiquitination: Mdm2 and Beyond." *Molecular Cell* 21 (3): 307–15. doi:10.1016/j.molcel.2006.01.020.

Brown, J Martin, and Amato J Giaccia. 1998. "The Unique Physiology of Solid Tumors : Opportunities (and Problems) for Cancer Therapy." *Cancer Research* 58 (7): 1408–16. http://www.ncbi.nlm.nih.gov/pubmed/9537241.

Bruning, Ulrike, Luca Cerone, Zoltan Neufeld, Susan F Fitzpatrick, Alex Cheong, Carsten C Scholz, David A Simpson, et al. 2011. "MicroRNA-155 Promotes Resolution of Hypoxia-Inducible Factor 1alpha Activity during Prolonged Hypoxia." *Molecular and Cellular Biology* 31 (19): 4087–96. doi:10.1128/MCB.01276-10.

Cai, Qiliang, Ke Lan, Subhash C Verma, Huaxin Si, Doug Lin, and Erle S Robertson. 2006. "Kaposi's Sarcoma-Associated Herpesvirus Latent Protein LANA Interacts with HIF-1 Alpha to Upregulate RTA Expression during Hypoxia: Latency Control under Low Oxygen Conditions." *Journal of Virology* 80 (16): 7965–75. doi:10.1128/JVI.00689-06.

Cai, Qiliang, Masanao Murakami, Huaxin Si, and Erle S Robertson. 2007. "A Potential Alpha-Helix Motif in the Amino Terminus of LANA Encoded by Kaposi's Sarcoma-Associated Herpesvirus Is Critical for Nuclear Accumulation of HIF-1alpha in Normoxia." *Journal of Virology* 81 (19): 10413–23. doi:10.1128/JVI.00611-07.

Cai, Qiliang, Suhbash C Verma, Jie Lu, and Erle S Robertson. 2010. "Molecular Biology of Kaposi's Sarcoma-Associated Herpesvirus and Related Oncogenesis." *Advances in Virus Research* 78 (January): 87–142. doi:10.1016/B978-0-12-385032-4.00003-3.

Cai, Xuezhong, and Bryan R Cullen. 2006. "Transcriptional Origin of Kaposi's Sarcoma-Associated Herpesvirus microRNAs." *Journal of Virology* 80 (5): 2234–42. doi:10.1128/JVI.80.5.2234-2242.2006.

Cai, Xuezhong, Shihua Lu, Zhihong Zhang, Carlos M Gonzalez, Blossom Damania, and Bryan R Cullen. 2005. "Kaposi's Sarcoma-Associated Herpesvirus Expresses an Array of Viral microRNAs in Latently Infected Cells." *Proceedings of the National Academy of Sciences of the United States of America* 102 (15): 5570–75. doi:10.1073/pnas.0408192102.

Calin, George Adrian, Cinzia Sevignani, Calin Dan Dumitru, Terry Hyslop, Evan Noch, Sai Yendamuri, Masayoshi Shimizu, et al. 2004. "Human microRNA Genes Are Frequently Located at Fragile Sites and Genomic Regions Involved in Cancers." *Proceedings of the National Academy of Sciences of the United States of America* 101 (9): 2999–3004. doi:10.1073/pnas.0307323101.

Camps, Carme, Francesca M Buffa, Stefano Colella, John Moore, Christos Sotiriou, Helen Sheldon, Adrian L Harris, Jonathan M Gleadle, and Jiannis Ragoussis. 2008. "Hsa-miR-210 Is Induced by Hypoxia and Is an Independent Prognostic Factor in Breast Cancer." *Clinical Cancer Research : An Official Journal of the American*

Association for Cancer Research 14 (5): 1340–48. doi:10.1158/1078-0432.CCR-07-1755.

Camps, Carme, Harpreet K Saini, David R Mole, Hani Choudhry, Martin Reczko, José Afonso Guerra-Assunção, Ya-Min Tian, et al. 2014. "Integrated Analysis of microRNA and mRNA Expression and Association with HIF Binding Reveals the Complexity of microRNA Expression Regulation under Hypoxia." *Molecular Cancer* 13 (January): 28. doi:10.1186/1476-4598-13-28.

Caro, J. 2001. "Hypoxia Regulation of Gene Transcription." *High Altitude Medicine & Biology* 2 (2): 145–54. doi:10.1089/152702901750265251.

Carroll, Patrick A, Elizabeth Brazeau, and Michael Lagunoff. 2004. "Kaposi's Sarcoma-Associated Herpesvirus Infection of Blood Endothelial Cells Induces Lymphatic Differentiation." *Virology* 328 (1): 7–18. doi:10.1016/j.virol.2004.07.008.

Carroll, Patrick a, Heidi L Kenerson, Raymond S Yeung, and Michael Lagunoff. 2006. "Latent Kaposi's Sarcoma-Associated Herpesvirus Infection of Endothelial Cells Activates Hypoxia-Induced Factors." *Journal of Virology* 80 (21): 10802–12. doi:10.1128/JVI.00673-06.

Cartee, Todd V, Kellie J White, Marvin Newton-West, and Robert A Swerlick. 2012. "Hypoxia and Hypoxia Mimetics Inhibit TNF-Dependent VCAM1 Induction in the 5A32 Endothelial Cell Line via a Hypoxia Inducible Factor Dependent Mechanism." *Journal of Dermatological Science* 65 (2): 86–94. doi:10.1016/j.jdermsci.2011.10.003.

Carthew, Richard W, and Erik J Sontheimer. 2009. "Origins and Mechanisms of miRNAs and siRNAs." *Cell* 136 (4): 642–55. doi:10.1016/j.cell.2009.01.035.

Cascio, Sandra, Aleco D'Andrea, Rita Ferla, Eva Surmacz, Eliana Gulotta, Valeria Amodeo, Viviana Bazan, Nicola Gebbia, and Antonio Russo. 2010. "miR-20b Modulates VEGF Expression by Targeting HIF-1 Alpha and STAT3 in MCF-7 Breast Cancer Cells." *Journal of Cellular Physiology* 224 (1): 242–49. doi:10.1002/jcp.22126.

Castaño-Rodríguez, Natalia, Nadeem O Kaakoush, Khean-Lee Goh, Kwong Ming Fock, and Hazel M Mitchell. 2014. "The NOD-like Receptor Signalling Pathway in Helicobacter Pylori Infection and Related Gastric Cancer: A Case-Control Study and Gene Expression Analyses." *PloS One* 9 (6): e98899. doi:10.1371/journal.pone.0098899.

Catrina Ene, Ana Maria, Ioana Borze, Mohamed Guled, Mariana Costache, Gayle Leen, Maria Sajin, Elena Ionica, Aura Chitu, and Sakari Knuutila. 2014. "MicroRNA Expression Profiles in Kaposi's Sarcoma." *Pathology Oncology Research : POR* 20 (1): 153–59. doi:10.1007/s12253-013-9678-1.

Cattelan, A M, M L Calabrò, P Gasperini, S M Aversa, M Zanchetta, F Meneghetti, A De Rossi, and L Chieco-Bianchi. 2001. "Acquired Immunodeficiency Syndrome-Related Kaposi's Sarcoma Regression after Highly Active Antiretroviral Therapy:

Biologic Correlates of Clinical Outcome." *Journal of the National Cancer Institute. Monographs*, no. 28 (January): 44–49. http://www.ncbi.nlm.nih.gov/pubmed/11158206.

Cesarman, E, Y Chang, P S Moore, J W Said, and D M Knowles. 1995. "Kaposi's Sarcoma-Associated Herpesvirus-like DNA Sequences in AIDS-Related Body-Cavity-Based Lymphomas." *The New England Journal of Medicine* 332 (18): 1186–91. doi:10.1056/NEJM199505043321802.

Chakraborty, Sayan, Mohanan Valiya Veettil, Virginie Bottero, and Bala Chandran. 2012. "Kaposi's Sarcoma-Associated Herpesvirus Interacts with EphrinA2 Receptor to Amplify Signaling Essential for Productive Infection." *Proceedings of the National Academy of Sciences of the United States of America* 109 (19): E1163–72. doi:10.1073/pnas.1119592109.

Chan, Stephen Y, Ying-Yi Zhang, Craig Hemann, Christopher E Mahoney, Jay L Zweier, and Joseph Loscalzo. 2009. "MicroRNA-210 Controls Mitochondrial Metabolism during Hypoxia by Repressing the Iron-Sulfur Cluster Assembly Proteins ISCU1/2." *Cell Metabolism* 10 (4): 273–84. doi:10.1016/j.cmet.2009.08.015.

Chan, Yuk C, Jaideep Banerjee, Sang Yong Choi, and Chandan K Sen. 2012. "miR-210: The Master Hypoxamir." *Microcirculation (New York, N.Y. : 1994)* 19 (3): 215–23. doi:10.1111/j.1549-8719.2011.00154.x.

Chan, Yuk Cheung, Savita Khanna, Sashwati Roy, and Chandan K Sen. 2011. "miR-200b Targets Ets-1 and Is down-Regulated by Hypoxia to Induce Angiogenic Response of Endothelial Cells." *The Journal of Biological Chemistry* 286 (3): 2047–56. doi:10.1074/jbc.M110.158790.

Chanan-Khan, A A, A Swaika, A Paulus, S K Kumar, J R Mikhael, S V Rajkumar, A Dispenzieri, and M Q Lacy. 2013. "Pomalidomide: The New Immunomodulatory Agent for the Treatment of Multiple Myeloma." *Blood Cancer Journal* 3 (January). Macmillan Publishers Limited: e143. doi:10.1038/bcj.2013.38.

Chang, Qing, Igor Jurisica, Trevor Do, and David W Hedley. 2011. "Hypoxia Predicts Aggressive Growth and Spontaneous Metastasis Formation from Orthotopically Grown Primary Xenografts of Human Pancreatic Cancer." *Cancer Research* 71 (8): 3110–20. doi:10.1158/0008-5472.CAN-10-4049.

Chang, Ting-Yu, Yu-Hsuan Wu, Cheng-Chung Cheng, and Hsei-Wei Wang. 2011. "Differentially Regulated Splice Variants and Systems Biology Analysis of Kaposi's Sarcoma-Associated Herpesvirus-Infected Lymphatic Endothelial Cells." *Nucleic Acids Research* 39 (16): 6970–85. doi:10.1093/nar/gkr405.

Chang, Y, E Cesarman, M. S Pessin, F Lee, J Culpepper, D. M Knowles, and P. S Moore. 1994. "Identification of Herpesvirus-like DNA Sequences in AIDS-Associated Kaposi's Sarcoma." *Science* 266 (5192): 1865–69. doi:10.1126/science.7997879.

Chen, Baosheng, D Michael Nelson, and Yoel Sadovsky. 2006. "N-Myc down-Regulated Gene 1 Modulates the Response of Term Human Trophoblasts to Hypoxic Injury." *The Journal of Biological Chemistry* 281 (5): 2764–72. doi:10.1074/jbc.M507330200.

Chen, Chang-Zheng, Ling Li, Harvey F Lodish, and David P Bartel. 2004. "MicroRNAs Modulate Hematopoietic Lineage Differentiation." *Science (New York, N.Y.)* 303 (5654): 83–86. doi:10.1126/science.1091903.

Chen, X, M Hamon, Z Deng, M Centola, R Sood, K Taylor, D L Kastner, and N Fischel-Ghodsian. 1999. "Identification and Characterization of a Zinc Finger Gene (ZNF213) from 16p13.3." *Biochimica et Biophysica Acta* 1444 (2): 218–30. http://www.ncbi.nlm.nih.gov/pubmed/10023065.

Chen, Yi-Bin, Aliyah Rahemtullah, and Ephraim Hochberg. 2007. "Primary Effusion Lymphoma." *The Oncologist* 12 (5): 569–76. doi:10.1634/theoncologist.12-5-569.

Chen, Zhe, Huazong Zeng, Yong Guo, Pei Liu, Hui Pan, Anmei Deng, and Jian Hu. 2010. "miRNA-145 Inhibits Non-Small Cell Lung Cancer Cell Proliferation by Targeting c-Myc." *Journal of Experimental & Clinical Cancer Research : CR* 29 (January): 151. doi:10.1186/1756-9966-29-151.

Chendrimada, Thimmaiah P, Richard I Gregory, Easwari Kumaraswamy, Jessica Norman, Neil Cooch, Kazuko Nishikura, and Ramin Shiekhattar. 2005. "TRBP Recruits the Dicer Complex to Ago2 for microRNA Processing and Gene Silencing." *Nature* 436 (7051). Macmillian Magazines Ltd. 740–44. doi:10.1038/nature03868.

Cheng, Yunhui, Ping Zhu, Jian Yang, Xiaojun Liu, Shimin Dong, Xiaobin Wang, Bao Chun, Jian Zhuang, and Chunxiang Zhang. 2010. "Ischaemic Preconditioning-Regulated miR-21 Protects Heart against Ischaemia/reperfusion Injury via Anti-Apoptosis through Its Target PDCD4." *Cardiovascular Research* 87 (3): 431–39. doi:10.1093/cvr/cvq082.

Cho, William C S, Andrew S C Chow, and Joseph S K Au. 2011. "MiR-145 Inhibits Cell Proliferation of Human Lung Adenocarcinoma by Targeting EGFR and NUDT1." *RNA Biology* 8 (1): 125–31. http://www.ncbi.nlm.nih.gov/pubmed/21289483.

Choudhry, H, A Albukhari, M Morotti, S Hider, D Moralli, J Smythies, J Schödel, et al. 2014. "Tumor Hypoxia Induces Nuclear Paraspeckle Formation through HIF-2α Dependent Transcriptional Activation of NEAT1 Leading to Cancer Cell Survival." *Oncogene*, November. doi:10.1038/onc.2014.378.

Choudhuri, Supratim. 2010. "Small Noncoding RNAs: Biogenesis, Function, and Emerging Significance in Toxicology." *Journal of Biochemical and Molecular Toxicology* 24 (3): 195–216. doi:10.1002/jbt.20325.

Cicchillitti, Lucia, Valeria Di Stefano, Eleonora Isaia, Luca Crimaldi, Pasquale Fasanaro, Valeria Ambrosino, Annalisa Antonini, et al. 2012. "Hypoxia-Inducible

Factor 1-A Induces miR-210 in Normoxic Differentiating Myoblasts." *The Journal of Biological Chemistry* 287 (53): 44761–71. doi:10.1074/jbc.M112.421255.

Cloutier, Nathalie, and Louis Flamand. 2010. "Kaposi Sarcoma-Associated Herpesvirus Latency-Associated Nuclear Antigen Inhibits Interferon (IFN) Beta Expression by Competing with IFN Regulatory Factor-3 for Binding to IFNB Promoter." *The Journal of Biological Chemistry* 285 (10): 7208–21. doi:10.1074/jbc.M109.018838.

Coscoy, Laurent. 2007. "Immune Evasion by Kaposi's Sarcoma-Associated Herpesvirus." *Nature Reviews. Immunology* 7 (5): 391–401. doi:10.1038/nri2076.

Crosby, Meredith E, Ritu Kulshreshtha, Mircea Ivan, and Peter M Glazer. 2009. "MicroRNA Regulation of DNA Repair Gene Expression in Hypoxic Stress." *Cancer Research* 69 (3): 1221–29. doi:10.1158/0008-5472.CAN-08-2516.

Cullen, Bryan R. 2011. "Viruses and microRNAs: RISCy Interactions with Serious Consequences." *Genes & Development* 25 (18): 1881–94. doi:10.1101/gad.17352611.

Cuninghame, Sean, Robert Jackson, and Ingeborg Zehbe. 2014. "Hypoxia-Inducible Factor 1 and Its Role in Viral Carcinogenesis." *Virology* 456-457 (May): 370–83. doi:10.1016/j.virol.2014.02.027.

Daniels, Sarah I, Erin E Soule, Katharine S Davidoff, John G Bernbaum, Duosha Hu, Kenji Maeda, Stephen J Stahl, et al. 2014. "Activation of Virus Uptake through Induction of Macropinocytosis with a Novel Polymerizing Peptide." *FASEB Journal : Official Publication of the Federation of American Societies for Experimental Biology* 28 (1): 106–16. doi:10.1096/fj.13-238113.

Davis, D. A. 2001. "Hypoxia Induces Lytic Replication of Kaposi Sarcoma-Associated Herpesvirus." *Blood* 97 (10): 3244–50. doi:10.1182/blood.V97.10.3244.

Davis, David A., Rachel W. Humphrey, Fonda M. Newcomb, Thomas R. O'Brien, James J. Goedert, Stephen E. Straus, and Robert Yarchoan. 1997. "Detection of Serum Antibodies to a Kaposi's Sarcoma-Associated Herpesvirus-Specific Peptide." *The Journal of Infectious Diseases* 175 (5): 1071–79. doi:10.1086/516444.

Dejean, E, M H Renalier, M Foisseau, X Agirre, N Joseph, G R de Paiva, T Al Saati, et al. 2011. "Hypoxia-microRNA-16 Downregulation Induces VEGF Expression in Anaplastic Lymphoma Kinase (ALK)-Positive Anaplastic Large-Cell Lymphomas." *Leukemia* 25 (12): 1882–90. doi:10.1038/leu.2011.168.

Delgado, Tracie, Patrick A Carroll, Almira S Punjabi, Daciana Margineantu, David M Hockenbery, and Michael Lagunoff. 2010. "Induction of the Warburg Effect by Kaposi's Sarcoma Herpesvirus Is Required for the Maintenance of Latently Infected Endothelial Cells." *Proceedings of the National Academy of Sciences of the United States of America* 107 (23): 10696–701. doi:10.1073/pnas.1004882107.

Deveraux, Q L, N Roy, H R Stennicke, T Van Arsdale, Q Zhou, S M Srinivasula, E S Alnemri, G S Salvesen, and J C Reed. 1998. "IAPs Block Apoptotic Events Induced by Caspase-8 and Cytochrome c by Direct Inhibition of Distinct Caspases." *The EMBO Journal* 17 (8): 2215–23. doi:10.1093/emboj/17.8.2215.

Dezube, Bruce J, Maria Zambela, David R Sage, Jian-Feng Wang, and Joyce D Fingeroth. 2002. "Characterization of Kaposi Sarcoma-Associated Herpesvirus/human Herpesvirus-8 Infection of Human Vascular Endothelial Cells: Early Events." *Blood* 100 (3): 888–96. http://www.ncbi.nlm.nih.gov/pubmed/12130499.

Ding, Yong-Bin, Guo-Yu Chen, Jian-Guo Xia, Xi-Wei Zang, Hong-Yu Yang, and Li Yang. 2003. "Association of VCAM-1 Overexpression with Oncogenesis, Tumor Angiogenesis and Metastasis of Gastric Carcinoma." *World Journal of Gastroenterology : WJG* 9 (7): 1409–14. http://www.ncbi.nlm.nih.gov/pubmed/12854131.

Dobyns, E L. 1999. "Pleural Effusions and Hypoxemia." *Critical Care Medicine* 27 (3): 472. http://www.ncbi.nlm.nih.gov/pubmed/10199520.

Dorner, Marcus, Franziska Zucol, Davide Alessi, Stephan K Haerle, Walter Bossart, Markus Weber, Rahel Byland, et al. 2010. "beta1 Integrin Expression Increases Susceptibility of Memory B Cells to Epstein-Barr Virus Infection." *Journal of Virology* 84 (13): 6667–77. doi:10.1128/JVI.02675-09.

Drexler, H G, C C Uphoff, G Gaidano, and A Carbone. 1998. "Lymphoma Cell Lines: In Vitro Models for the Study of HHV-8+ Primary Effusion Lymphomas (body Cavity-Based Lymphomas)." *Leukemia* 12 (10). Nature Publishing Group: 1507–17. doi:10.1038/sj.leu.2401160.

Dudek, Katarzyna A, Jérôme E Lafont, Aida Martinez-Sanchez, and Christopher L Murphy. 2010. "Type II Collagen Expression Is Regulated by Tissue-Specific miR-675 in Human Articular Chondrocytes." *The Journal of Biological Chemistry* 285 (32): 24381–87. doi:10.1074/jbc.M110.111328.

Dyson, Ossie F, Telisha L Oxendine, Khalief E Hamden, Patrick W Ford, and Shaw M Akula. 2008. "Differential Regulation of the Attachment of Kaposi's Sarcoma-Associated Herpesvirus (KSHV)-Infected Human B Cells to Extracellular Matrix by KSHV-Encoded gB and Cellular alphaV Integrins." *Cellular Microbiology* 10 (7): 1546–58. doi:10.1111/j.1462-5822.2008.01149.x.

Engels, Eric A, Robert J Biggar, Vickie A Marshall, Michael A Walters, Christine J Gamache, Denise Whitby, and James J Goedert. 2003. "Detection and Quantification of Kaposi's Sarcoma-Associated Herpesvirus to Predict AIDS-Associated Kaposi's Sarcoma." *AIDS (London, England)* 17 (12): 1847–51. doi:10.1097/01.aids.0000076275.54156.08.

Epstein, M A. 2001. "Reflections on Epstein-Barr Virus: Some Recently Resolved Old Uncertainties." *The Journal of Infection* 43 (2): 111–15. doi:10.1053/jinf.2001.0898.

Erler, Janine T, Kevin L Bennewith, Thomas R Cox, Georgina Lang, Demelza Bird, Albert Koong, Quynh-Thu Le, and Amato J Giaccia. 2009. "Hypoxia-Induced Lysyl Oxidase Is a Critical Mediator of Bone Marrow Cell Recruitment to Form the Premetastatic Niche." *Cancer Cell* 15 (1). Elsevier: 35–44. doi:10.1016/j.ccr.2008.11.012.

Erler, Janine T, Christopher J Cawthorne, Kaye J Williams, Marianne Koritzinsky, Bradley G Wouters, Clare Wilson, Crispin Miller, Costas Demonacos, Ian J Stratford, and Caroline Dive. 2004. "Hypoxia-Mediated Down-Regulation of Bid and Bax in Tumors Occurs via Hypoxia-Inducible Factor 1-Dependent and -Independent Mechanisms and Contributes to Drug Resistance." *Society* 24 (7): 2875–89. doi:10.1128/MCB.24.7.2875.

Evellin, Sandrine, Federico Galvagni, Alessio Zippo, Francesco Neri, Maurizio Orlandini, Danny Incarnato, Daniela Dettori, et al. 2013. "FOSL1 Controls the Assembly of Endothelial Cells into Capillary Tubes by Direct Repression of Av and β3 Integrin Transcription." *Molecular and Cellular Biology* 33 (6): 1198–1209. doi:10.1128/MCB.01054-12.

Fasanaro, Pasquale, Yuri D'Alessandra, Valeria Di Stefano, Roberta Melchionna, Sveva Romani, Giulio Pompilio, Maurizio C Capogrossi, and Fabio Martelli. 2008. "MicroRNA-210 Modulates Endothelial Cell Response to Hypoxia and Inhibits the Receptor Tyrosine Kinase Ligand Ephrin-A3." *The Journal of Biological Chemistry* 283 (23): 15878–83. doi:10.1074/jbc.M800731200.

Favaro, Elena, Anassuya Ramachandran, Robert McCormick, Harriet Gee, Christine Blancher, Meredith Crosby, Cecilia Devlin, et al. 2010. "MicroRNA-210 Regulates Mitochondrial Free Radical Response to Hypoxia and Krebs Cycle in Cancer Cells by Targeting Iron Sulfur Cluster Protein ISCU." *PloS One* 5 (4): e10345. doi:10.1371/journal.pone.0010345.

Fernández-Martínez, Ana Belén, María Isabel Arenas Jiménez, Irene Sánchez Hernández, María Laura García-Bermejo, Victoria Moreno Manzano, Elia Aguado Fraile, and Francisco Javier de Lucio-Cazaña. 2011. "Mutual Regulation of Hypoxic and Retinoic Acid Related Signalling in Tubular Proximal Cells." *The International Journal of Biochemistry & Cell Biology* 43 (8): 1198–1207. doi:10.1016/j.biocel.2011.04.013.

Folkman, Judah. 2007. "Angiogenesis: An Organizing Principle for Drug Discovery?" *Nature Reviews. Drug Discovery* 6 (4). Nature Publishing Group: 273–86. doi:10.1038/nrd2115.

Forsythe, JA, BH Jiang, NV Iyer, F Agani, SW Leung, RD Koos, and GL Semenza. 1996. "Activation of Vascular Endothelial Growth Factor Gene Transcription by Hypoxia-Inducible Factor 1." *Mol. Cell. Biol.* 16 (9): 4604–13. http://mcb.asm.org/content/16/9/4604.abstract.

Fort, Alexandre, Christelle Borel, Eugenia Migliavacca, Stylianos E Antonarakis, Richard J Fish, and Marguerite Neerman-Arbez. 2010. "Regulation of Fibrinogen

Production by microRNAs." *Blood* 116 (14): 2608–15. doi:10.1182/blood-2010-02-268011.

Frankel, Lisa B, Nanna R Christoffersen, Anders Jacobsen, Morten Lindow, Anders Krogh, and Anders H Lund. 2008. "Programmed Cell Death 4 (PDCD4) Is an Important Functional Target of the microRNA miR-21 in Breast Cancer Cells." *The Journal of Biological Chemistry* 283 (2): 1026–33. doi:10.1074/jbc.M707224200.

Friborg, J, W Kong, M O Hottiger, and G J Nabel. 1999. "p53 Inhibition by the LANA Protein of KSHV Protects against Cell Death." *Nature* 402 (6764): 889–94. doi:10.1038/47266.

Friedman, Robin C, Kyle Kai-how Farh, Christopher B Burge, and David P Bartel. 2009. "Most Mammalian mRNAs Are Conserved Targets of microRNAs." *Genome Research* 19 (1): 92–105. doi:10.1101/gr.082701.108.

Fu, Miao, Yan Gao, Qiuju Zhou, Qi Zhang, Ying Peng, Kegang Tian, Jinhua Wang, and Xiaoqun Zheng. 2014. "Human Cytomegalovirus Latent Infection Alters the Expression of Cellular and Viral microRNA." *Gene* 536 (2): 272–78. doi:10.1016/j.gene.2013.12.012.

Fujimuro, Masahiro, Frederick Y Wu, Colette ApRhys, Henry Kajumbula, David B Young, Gary S Hayward, and S Diane Hayward. 2003. "A Novel Viral Mechanism for Dysregulation of Beta-Catenin in Kaposi's Sarcoma-Associated Herpesvirus Latency." *Nature Medicine* 9 (3): 300–306. doi:10.1038/nm829.

Fujita, Shuji, Taiji Ito, Taketoshi Mizutani, Shigeru Minoguchi, Nobutake Yamamichi, Kouhei Sakurai, and Hideo Iba. 2008. "miR-21 Gene Expression Triggered by AP-1 Is Sustained through a Double-Negative Feedback Mechanism." *Journal of Molecular Biology* 378 (3): 492–504. doi:10.1016/j.jmb.2008.03.015.

Gabalski, E C, M Adam, H Pinto, J M Brown, D A Bloch, and D J Terris. 1998. "Pretreatment and Midtreatment Measurement of Oxygen Tension Levels in Head and Neck Cancers." *The Laryngoscope* 108 (12): 1856–60. http://www.ncbi.nlm.nih.gov/pubmed/9851504.

Ganem, Don. 2007. "KSHV-Induced Oncogenesis". Cambridge University Press. http://www.ncbi.nlm.nih.gov/books/NBK47373/.

Gao, Jie, Désirée Schatton, Paola Martinelli, Henriette Hansen, David Pla-Martin, Esther Barth, Christian Becker, et al. 2014. "CLUH Regulates Mitochondrial Biogenesis by Binding mRNAs of Nuclear-Encoded Mitochondrial Proteins." *The Journal of Cell Biology* 207 (2): 213–23. doi:10.1083/jcb.201403129.

Gao, Lin, Rebeca Mejías, Miriam Echevarría, and José López-Barneo. 2004. "Induction of the Glucose-6-Phosphate Dehydrogenase Gene Expression by Chronic Hypoxia in PC12 Cells." *FEBS Letters* 569 (1-3): 256–60. doi:10.1016/j.febslet.2004.06.004.

Garrigues, H Jacques, Yelena E Rubinchikova, C Michael Dipersio, and Timothy M Rose. 2008. "Integrin alphaVbeta3 Binds to the RGD Motif of Glycoprotein B of

Kaposi's Sarcoma-Associated Herpesvirus and Functions as an RGD-Dependent Entry Receptor." *Journal of Virology* 82 (3): 1570–80. doi:10.1128/JVI.01673-07.

Gasperini, Paola, Georgina Espigol-Frigole, Peter J McCormick, Ombretta Salvucci, Dragan Maric, Thomas S Uldrick, Mark N Polizzotto, Robert Yarchoan, and Giovanna Tosato. 2012. "Kaposi Sarcoma Herpesvirus Promotes Endothelial-to-Mesenchymal Transition through Notch-Dependent Signaling." *Cancer Research* 72 (5): 1157–69. doi:10.1158/0008-5472.CAN-11-3067.

George, Daniel J, and William G Kaelin. 2003. "The von Hippel-Lindau Protein, Vascular Endothelial Growth Factor, and Kidney Cancer." *The New England Journal of Medicine* 349 (5): 419–21. doi:10.1056/NEJMp030061.

Gilkes, Daniele M, Saumendra Bajpai, Pallavi Chaturvedi, Denis Wirtz, and Gregg L Semenza. 2013. "Hypoxia-Inducible Factor 1 (HIF-1) Promotes Extracellular Matrix Remodeling under Hypoxic Conditions by Inducing P4HA1, P4HA2, and PLOD2 Expression in Fibroblasts." *The Journal of Biological Chemistry* 288 (15): 10819–29. doi:10.1074/jbc.M112.442939.

Godshalk, Sirie E, Sumita Bhaduri-McIntosh, and Frank J Slack. 2008. "Epstein-Barr Virus-Mediated Dysregulation of Human microRNA Expression." *Cell Cycle (Georgetown, Tex.)* 7 (22): 3595–3600. http://www.ncbi.nlm.nih.gov/pubmed/19001862.

Gorospe, Myriam, Kumiko Tominaga, Xue Wu, Michael Fähling, and Mircea Ivan. 2011. "Post-Transcriptional Control of the Hypoxic Response by RNA-Binding Proteins and MicroRNAs." *Frontiers in Molecular Neuroscience* 4 (July): 7. doi:10.3389/fnmol.2011.00007.

Gottwein, Eva, David L Corcoran, Neelanjan Mukherjee, Rebecca L Skalsky, Markus Hafner, Jeffrey D Nusbaum, Priscilla Shamulailatpam, et al. 2011. "Viral microRNA Targetome of KSHV-Infected Primary Effusion Lymphoma Cell Lines." *Cell Host & Microbe* 10 (5): 515–26. doi:10.1016/j.chom.2011.09.012.

Gottwein, Eva, and Bryan R Cullen. 2008. "Viral and Cellular microRNAs as Determinants of Viral Pathogenesis and Immunity." *Cell Host & Microbe* 3 (6): 375–87. doi:10.1016/j.chom.2008.05.002.

Gottwein, Eva, Neelanjan Mukherjee, Christoph Sachse, Corina Frenzel, William H Majoros, Jen-Tsan A Chi, Ravi Braich, et al. 2007. "A Viral microRNA Functions as an Orthologue of Cellular miR-155." *Nature* 450 (7172): 1096–99. doi:10.1038/nature05992.

Grandadam, M, N Dupin, V Calvez, I Gorin, L Blum, S Kernbaum, D Sicard, et al. 1997. "Exacerbations of Clinical Symptoms in Human Immunodeficiency Virus Type 1-Infected Patients with Multicentric Castleman's Disease Are Associated with a High Increase in Kaposi's Sarcoma Herpesvirus DNA Load in Peripheral Blood Mononuclear Cells." *The Journal of Infectious Diseases* 175 (5): 1198–1201. http://www.ncbi.nlm.nih.gov/pubmed/9129085.

Greene, Whitney, Kurt Kuhne, Fengchun Ye, Jiguo Chen, Fuchun Zhou, Xiufen Lei, and Shou-Jiang Gao. 2007. "Molecular Biology of KSHV in Relation to AIDS-Associated Oncogenesis." *Cancer Treatment and Research* 133 (July): 69–127. doi:10.1016/j.bbi.2008.05.010.

Guasparri, Ilaria, Shannon A Keller, and Ethel Cesarman. 2004. "KSHV vFLIP Is Essential for the Survival of Infected Lymphoma Cells." *The Journal of Experimental Medicine* 199 (7): 993–1003. doi:10.1084/jem.20031467.

Guo, K, G Searfoss, D Krolikowski, M Pagnoni, C Franks, K Clark, K T Yu, M Jaye, and Y Ivashchenko. 2001. "Hypoxia Induces the Expression of the pro-Apoptotic Gene BNIP3." *Cell Death and Differentiation* 8 (4): 367–76. doi:10.1038/sj.cdd.4400810.

Hahn, Alexander S, Johanna K Kaufmann, Effi Wies, Elisabeth Naschberger, Julia Panteleev-Ivlev, Katharina Schmidt, Angela Holzer, et al. 2012. "The Ephrin Receptor Tyrosine Kinase A2 Is a Cellular Receptor for Kaposi's Sarcoma–associated Herpesvirus." *Nature Medicine* 18 (6): 961–66. doi:10.1038/nm.2805.

Haque, Muzammel, David A Davis, Victoria Wang, Isabelle Widmer, and Robert Yarchoan. 2003. "Kaposi ' S Sarcoma-Associated Herpesvirus (Human Herpesvirus 8) Contains Hypoxia Response Elements : Relevance to Lytic Induction by Hypoxia." *Cancer* 77 (12): 6761–68. doi:10.1128/JVI.77.12.6761.

Haque, Muzammel, Victoria Wang, David A Davis, Zhi-Ming Zheng, and Robert Yarchoan. 2006. "Genetic Organization and Hypoxic Activation of the Kaposi's Sarcoma-Associated Herpesvirus ORF34-37 Gene Cluster." *Journal of Virology* 80 (14): 7037–51. doi:10.1128/JVI.00553-06.

Harris, Adrian L. 2002. "Hypoxia--a Key Regulatory Factor in Tumour Growth." *Nature Reviews. Cancer* 2 (1): 38–47. doi:10.1038/nrc704.

Hayashi, Masami, Masahiro Sakata, Takashi Takeda, Toshiya Yamamoto, Yoko Okamoto, Kenjiro Sawada, Akiko Kimura, et al. 2004. "Induction of Glucose Transporter 1 Expression through Hypoxia-Inducible Factor 1alpha under Hypoxic Conditions in Trophoblast-Derived Cells." *The Journal of Endocrinology* 183 (1): 145–54. doi:10.1677/joe.1.05599.

Hempel, S L, M M Monick, and G W Hunninghake. 1996. "Effect of Hypoxia on Release of IL-1 and TNF by Human Alveolar Macrophages." *American Journal of Respiratory Cell and Molecular Biology* 14 (2): 170–76. doi:10.1165/ajrcmb.14.2.8630267.

Herdegen, T., and J.D. Leah. 1998. "Inducible and Constitutive Transcription Factors in the Mammalian Nervous System: Control of Gene Expression by Jun, Fos and Krox, and CREB/ATF Proteins." *Brain Research Reviews* 28 (3): 370–490. doi:10.1016/S0165-0173(98)00018-6.

Herndier, B G, A Werner, P Arnstein, N W Abbey, F Demartis, R L Cohen, M A Shuman, and J A Levy. 1994. "Characterization of a Human Kaposi's Sarcoma Cell

Line That Induces Angiogenic Tumors in Animals." *AIDS (London, England)* 8 (5): 575–81. http://www.ncbi.nlm.nih.gov/pubmed/7520247.

Höckel, M, and P Vaupel. 2001. "Tumor Hypoxia: Definitions and Current Clinical, Biologic, and Molecular Aspects." *Journal of the National Cancer Institute* 93 (4): 266–76. http://www.ncbi.nlm.nih.gov/pubmed/11181773.

Hu, C.-J., L.-Y. Wang, L. A. Chodosh, B. Keith, and M. C. Simon. 2003. "Differential Roles of Hypoxia-Inducible Factor 1 (HIF-1) and HIF-2 in Hypoxic Gene Regulation." *Molecular and Cellular Biology* 23 (24): 9361–74. doi:10.1128/MCB.23.24.9361-9374.2003.

Huang, X., and J. Zuo. 2014. "Emerging Roles of miR-210 and Other Non-Coding RNAs in the Hypoxic Response." *Acta Biochimica et Biophysica Sinica* 46 (3): 220–32. doi:10.1093/abbs/gmt141.

Huang, Xin, Lianghao Ding, Kevin L Bennewith, Ricky T Tong, Scott M Welford, K Kian Ang, Michael Story, Quynh-Thu Le, and Amato J Giaccia. 2009. "Hypoxia-Inducible Mir-210 Regulates Normoxic Gene Expression Involved in Tumor Initiation." *Molecular Cell* 35 (6): 856–67. doi:10.1016/j.molcel.2009.09.006.

Huang, Xin, Quynh-Thu Le, and Amato J Giaccia. 2010. "MiR-210--Micromanager of the Hypoxia Pathway." *Trends in Molecular Medicine* 16 (5): 230–37. doi:10.1016/j.molmed.2010.03.004.

Hultén, Lillemor Mattsson, and Max Levin. 2009. "The Role of Hypoxia in Atherosclerosis." *Current Opinion in Lipidology* 20 (5): 409–14. doi:10.1097/MOL.0b013e3283307be8.

Hussain, Mazhar, Ryan J Taft, and Sassan Asgari. 2008. "An Insect Virus-Encoded microRNA Regulates Viral Replication." *Journal of Virology* 82 (18): 9164–70. doi:10.1128/JVI.01109-08.

Jang, Ji-Young, Young-Sin Lee, Yoon-Kyung Jeon, Kyoungbun Lee, Ja-June Jang, and Chul-Woo Kim. 2013. "ANT2 Suppression by shRNA Restores miR-636 Expression, Thereby Downregulating Ras and Inhibiting Tumorigenesis of Hepatocellular Carcinoma." *Experimental & Molecular Medicine* 45 (January). KSBMB. e3. doi:10.1038/emm.2013.1.

Jansson, Martin D, and Anders H Lund. 2012. "MicroRNA and Cancer." *Molecular Oncology* 6 (6): 590–610. doi:10.1016/j.molonc.2012.09.006.

Jean, Jyh-Chang, Celeste B Rich, and Martin Joyce-Brady. 2006. "Hypoxia Results in an HIF-1-Dependent Induction of Brain-Specific Aldolase C in Lung Epithelial Cells." *American Journal of Physiology. Lung Cellular and Molecular Physiology* 291 (5): L950–6. doi:10.1152/ajplung.00087.2006.

Jian, Pan, Zhao Wen Li, Tao Yan Fang, Wang Jian, Zhou Zhuan, Liao Xin Mei, Wu Shui Yan, and Ni Jian. 2011. "Retinoic Acid Induces HL-60 Cell Differentiation via

the Upregulation of miR-663." *Journal of Hematology & Oncology* 4 (January): 20. doi:10.1186/1756-8722-4-20.

Judde, J G, V Lacoste, J Brière, E Kassa-Kelembho, E Clyti, P Couppié, C Buchrieser, M Tulliez, J Morvan, and A Gessain. 2000. "Monoclonality or Oligoclonality of Human Herpesvirus 8 Terminal Repeat Sequences in Kaposi's Sarcoma and Other Diseases." *Journal of the National Cancer Institute* 92 (9): 729–36. http://www.ncbi.nlm.nih.gov/pubmed/10793109.

Kaaya, E E, C Parravicini, C Ordonez, R Gendelman, E Berti, R C Gallo, and P Biberfeld. 1995. "Heterogeneity of Spindle Cells in Kaposi's Sarcoma: Comparison of Cells in Lesions and in Culture." *Journal of Acquired Immune Deficiency Syndromes and Human Retrovirology : Official Publication of the International Retrovirology Association* 10 (3): 295–305. http://www.ncbi.nlm.nih.gov/pubmed/7552491.

Kaleeba, Johnan A R, and Edward A Berger. 2006. "Kaposi's Sarcoma-Associated Herpesvirus Fusion-Entry Receptor: Cystine Transporter xCT." *Science (New York, N.Y.)* 311 (5769): 1921–24. doi:10.1126/science.1120878.

Kaluz, Stefan, Milota Kaluzová, Shu-Yuan Liao, Michael Lerman, and Eric J Stanbridge. 2009. "Transcriptional Control of the Tumor- and Hypoxia-Marker Carbonic Anhydrase 9: A One Transcription Factor (HIF-1) Show?" *Biochimica et Biophysica Acta* 1795 (2): 162–72. doi:10.1016/j.bbcan.2009.01.001.

Katano, H, Y Sato, T Kurata, S Mori, and T Sata. 2000. "Expression and Localization of Human Herpesvirus 8-Encoded Proteins in Primary Effusion Lymphoma, Kaposi's Sarcoma, and Multicentric Castleman's Disease." *Virology* 269 (2): 335–44. doi:10.1006/viro.2000.0196.

Keller, Shannon A, Denise Hernandez-Hopkins, Jelena Vider, Vladimir Ponomarev, Elizabeth Hyjek, Elaine J Schattner, and Ethel Cesarman. 2006. "NF-kappaB Is Essential for the Progression of KSHV- and EBV-Infected Lymphomas in Vivo." *Blood* 107 (8): 3295–3302. doi:10.1182/blood-2005-07-2730.

Kim, V Narry. 2005. "MicroRNA Biogenesis: Coordinated Cropping and Dicing." *Nature Reviews. Molecular Cell Biology* 6 (5): 376–85. doi:10.1038/nrm1644.

Kioi, Mitomu, Hannes Vogel, Geoffrey Schultz, Robert M Hoffman, Griffith R Harsh, and J Martin Brown. 2010. "Inhibition of Vasculogenesis , but Not Angiogenesis, Prevents the Recurrence of Glioblastoma after Irradiation in Mice" 120 (3). doi:10.1172/JCI40283DS1.

Kozomara, Ana, and Sam Griffiths-Jones. 2011. "miRBase: Integrating microRNA Annotation and Deep-Sequencing Data." *Nucleic Acids Research* 39 (Database issue): D152–7. doi:10.1093/nar/gkq1027.

Krieg, Adam J, Erinn B Rankin, Denise Chan, Olga Razorenova, Sully Fernandez, and Amato J Giaccia. 2010. "Regulation of the Histone Demethylase JMJD1A by

Hypoxia-Inducible Factor 1 Alpha Enhances Hypoxic Gene Expression and Tumor Growth." *Molecular and Cellular Biology* 30 (1): 344–53. doi:10.1128/MCB.00444-09.

Kulshreshtha, Ritu, Manuela Ferracin, Sylwia E Wojcik, Ramiro Garzon, Hansjuerg Alder, Francisco J Agosto-Perez, Ramana Davuluri, et al. 2007. "A microRNA Signature of Hypoxia." *Molecular and Cellular Biology* 27 (5): 1859–67. doi:10.1128/MCB.01395-06.

Kumar, Madhu S, Jun Lu, Kim L Mercer, Todd R Golub, and Tyler Jacks. 2007. "Impaired microRNA Processing Enhances Cellular Transformation and Tumorigenesis." *Nature Genetics* 39 (5): 673–77. doi:10.1038/ng2003.

Kyotani, Yoji, Hiroyo Ota, Asako Itaya-Hironaka, Akiyo Yamauchi, Sumiyo Sakuramoto-Tsuchida, Jing Zhao, Kentaro Ozawa, et al. 2013. "Intermittent Hypoxia Induces the Proliferation of Rat Vascular Smooth Muscle Cell with the Increases in Epidermal Growth Factor Family and erbB2 Receptor." *Experimental Cell Research* 319 (19): 3042–50. doi:10.1016/j.yexcr.2013.08.014.

Laderoute, K. R., J. M. Calaoagan, C. Gustafson-Brown, A. M. Knapp, G.-C. Li, H. L. Mendonca, H. E. Ryan, Z. Wang, and R. S. Johnson. 2002. "The Response of c-Jun/AP-1 to Chronic Hypoxia Is Hypoxia-Inducible Factor 1 Dependent." *Molecular and Cellular Biology* 22 (8): 2515–23. doi:10.1128/MCB.22.8.2515-2523.2002.

Lagos, Dimitrios, Gabriel Pollara, Stephen Henderson, Fiona Gratrix, Martin Fabani, Richard S B Milne, Frances Gotch, and Chris Boshoff. 2010. "miR-132 Regulates Antiviral Innate Immunity through Suppression of the p300 Transcriptional Co-Activator." *Nature Cell Biology* 12 (5): 513–19. doi:10.1038/ncb2054.

Lagos-Quintana, M, R Rauhut, W Lendeckel, and T Tuschl. 2001. "Identification of Novel Genes Coding for Small Expressed RNAs." *Science (New York, N.Y.)* 294 (5543): 853–58. doi:10.1126/science.1064921.

Lan, Ke, Daniel A Kuppers, Subhash C Verma, and Erle S Robertson. 2004. "Kaposi's Sarcoma-Associated Herpesvirus-Encoded Latency-Associated Nuclear Antigen Inhibits Lytic Replication by Targeting Rta: A Potential Mechanism for Virus-Mediated Control of Latency." *Journal of Virology* 78 (12): 6585–94. doi:10.1128/JVI.78.12.6585-6594.2004.

Lau, N C, L P Lim, E G Weinstein, and D P Bartel. 2001. "An Abundant Class of Tiny RNAs with Probable Regulatory Roles in Caenorhabditis Elegans." *Science (New York, N.Y.)* 294 (5543): 858–62. doi:10.1126/science.1065062.

Law, Alice Y S, and Chris K C Wong. 2010a. "Stanniocalcin-2 Is a HIF-1 Target Gene That Promotes Cell Proliferation in Hypoxia." *Experimental Cell Research* 316 (3): 466–76. doi:10.1016/j.yexcr.2009.09.018.

Law, Alice Y S, and Chris K C Wong. 2010b. "Stanniocalcin-2 Promotes Epithelial-Mesenchymal Transition and Invasiveness in Hypoxic Human Ovarian Cancer Cells." *Experimental Cell Research* 316 (20): 3425–34. doi:10.1016/j.yexcr.2010.06.026.

Lee, R C, R L Feinbaum, and V Ambros. 1993. "The C. Elegans Heterochronic Gene Lin-4 Encodes Small RNAs with Antisense Complementarity to Lin-14." *Cell* 75 (5): 843–54. http://www.ncbi.nlm.nih.gov/pubmed/8252621.

Li, Xudong, Jiaying Feng, and Ren Sun. 2011. "Oxidative Stress Induces Reactivation of Kaposi's Sarcoma-Associated Herpesvirus and Death of Primary Effusion Lymphoma Cells." *Journal of Virology* 85 (2): 715–24. doi:10.1128/JVI.01742-10.

Li, Zesong, Jiezhong Chen, Kwok Wah Chan, Liang Qiao, and Benjamin C Y Wong. 2011. "A Possible Role of cIAP2 in Helicobacter Pylori-Associated Gastric Cancer." *Cancer Letters* 313 (2): 192–200. doi:10.1016/j.canlet.2011.09.007.

Liao, Debbie, and Randall S Johnson. 2007. "Hypoxia: A Key Regulator of Angiogenesis in Cancer." *Cancer Metastasis Reviews* 26 (2): 281–90. doi:10.1007/s10555-007-9066-y.

Lim, Lee P, Margaret E Glasner, Soraya Yekta, Christopher B Burge, and David P Bartel. 2003. "Vertebrate microRNA Genes." *Science (New York, N.Y.)* 299 (5612): 1540. doi:10.1126/science.1080372.

Lin, Xianzhi, Deguang Liang, Zhiheng He, Qiang Deng, Erle S Robertson, and Ke Lan. 2011. "miR-K12-7-5p Encoded by Kaposi's Sarcoma-Associated Herpesvirus Stabilizes the Latent State by Targeting Viral ORF50/RTA." *PloS One* 6 (1): e16224. doi:10.1371/journal.pone.0016224.

Livak, K J, and T D Schmittgen. 2001. "Analysis of Relative Gene Expression Data Using Real-Time Quantitative PCR and the 2(-Delta Delta C(T)) Method." *Methods (San Diego, Calif.)* 25 (4): 402–8. doi:10.1006/meth.2001.1262.

Long, E, M Ilie, V Hofman, K Havet, E Selva, C Butori, J P Lacour, A M Nelson, G Cathomas, and P Hofman. 2009. "LANA-1, Bcl-2, Mcl-1 and HIF-1alpha Protein Expression in HIV-Associated Kaposi Sarcoma." *Virchows Archiv : An International Journal of Pathology* 455 (2): 159–70. doi:10.1007/s00428-009-0791-1.

Lu, Chih-Chung, Zhonghan Li, Chia-Ying Chu, Jiaying Feng, Jun Feng, Ren Sun, and Tariq M Rana. 2010. "MicroRNAs Encoded by Kaposi's Sarcoma-Associated Herpesvirus Regulate Viral Life Cycle." *EMBO Reports* 11 (10). Nature Publishing Group: 784–90. doi:10.1038/embor.2010.132.

Lu, Chun, Yi Zeng, Zan Huang, Li Huang, Chao Qian, Guixia Tang, and Di Qin. 2005. "Human Herpesvirus 6 Activates Lytic Cycle Replication of Kaposi's Sarcoma-Associated Herpesvirus." *The American Journal of Pathology* 166 (1): 173–83. doi:10.1016/S0002-9440(10)62242-0.

Lu, Fang, Kevin Tsai, Horng-Shen Chen, Priyankara Wikramasinghe, Ramana V Davuluri, Louise Showe, John Domsic, Ronen Marmorstein, and Paul M Lieberman. 2012. "Identification of Host-Chromosome Binding Sites and Candidate Gene Targets for Kaposi's Sarcoma-Associated Herpesvirus LANA." *Journal of Virology* 86 (10): 5752–62. doi:10.1128/JVI.07216-11.

Lu, Fang, Andreas Weidmer, Chang-Gong Liu, Stefano Volinia, Carlo M Croce, and Paul M Lieberman. 2008. "Epstein-Barr Virus-Induced miR-155 Attenuates NF-kappaB Signaling and Stabilizes Latent Virus Persistence." *Journal of Virology* 82 (21): 10436–43. doi:10.1128/JVI.00752-08.

Lu, Jun, Gad Getz, Eric A Miska, Ezequiel Alvarez-Saavedra, Justin Lamb, David Peck, Alejandro Sweet-Cordero, et al. 2005. "MicroRNA Expression Profiles Classify Human Cancers." *Nature* 435 (7043). Nature Publishing Group: 834–38. http://www.ncbi.nlm.nih.gov/pubmed/15944708.

Luan, Shi-Lu, Emmanuelle Boulanger, Hongtao Ye, Estelle Chanudet, Nicola Johnson, Rifat A Hamoudi, Chris M Bacon, et al. 2010. "Primary Effusion Lymphoma: Genomic Profiling Revealed Amplification of SELPLG and CORO1C Encoding for Proteins Important for Cell Migration." *The Journal of Pathology* 222 (2): 166–79. doi:10.1002/path.2752.

Lucon, Danielle Ribeiro, Cristiane de Souza Rocha, Rogerio Bastos Craveiro, Dagmar Dilloo, Izilda A Cardinalli, Denise Pontes Cavalcanti, Simone Dos Santos Aguiar, Claudia Maurer-Morelli, and Jose Andres Yunes. 2013. "Downregulation of 14q32 microRNAs in Primary Human Desmoplastic Medulloblastoma." *Frontiers in Oncology* 3 (January): 254. doi:10.3389/fonc.2013.00254.

Mandrekar, Shweta, Qingguang Jiang, C Y Daniel Lee, Jessica Koenigsknecht-Talboo, David M Holtzman, and Gary E Landreth. 2009. "Microglia Mediate the Clearance of Soluble Abeta through Fluid Phase Macropinocytosis." *The Journal of Neuroscience : The Official Journal of the Society for Neuroscience* 29 (13): 4252–62. doi:10.1523/JNEUROSCI.5572-08.2009.

Maréchal, V, M C Prevost, C Petit, E Perret, J M Heard, and O Schwartz. 2001. "Human Immunodeficiency Virus Type 1 Entry into Macrophages Mediated by Macropinocytosis." *Journal of Virology* 75 (22): 11166–77. doi:10.1128/JVI.75.22.11166-11177.2001.

Marshall, Vickie, Thomas Parks, Rachel Bagni, Cheng Dian Wang, Mark A Samols, Jianhong Hu, Kathleen M Wyvil, et al. 2007. "Conservation of Virally Encoded microRNAs in Kaposi Sarcoma--Associated Herpesvirus in Primary Effusion Lymphoma Cell Lines and in Patients with Kaposi Sarcoma or Multicentric Castleman Disease." *The Journal of Infectious Diseases* 195 (5): 645–59. doi:10.1086/511434.

Mathupala, S P, A Rempel, and P L Pedersen. 2001. "Glucose Catabolism in Cancer Cells: Identification and Characterization of a Marked Activation Response of the Type II Hexokinase Gene to Hypoxic Conditions." *The Journal of Biological Chemistry* 276 (46): 43407–12. doi:10.1074/jbc.M108181200.

Matouk, Imad J, Nathan DeGroot, Shaul Mezan, Suhail Ayesh, Rasha Abu-lail, Abraham Hochberg, and Eithan Galun. 2007. "The H19 Non-Coding RNA Is Essential for Human Tumor Growth." *PloS One* 2 (9): e845. doi:10.1371/journal.pone.0000845.

Matsumura, Satoko, Linda M Persson, LaiYee Wong, and Angus C Wilson. 2010. "The Latency-Associated Nuclear Antigen Interacts with MeCP2 and Nucleosomes through Separate Domains." *Journal of Virology* 84 (5): 2318–30. doi:10.1128/JVI.01097-09.

Maxwell, P J, R Gallagher, A Seaton, C Wilson, P Scullin, J Pettigrew, I J Stratford, K J Williams, P G Johnston, and D J J Waugh. 2007. "HIF-1 and NF-kappaB-Mediated Upregulation of CXCR1 and CXCR2 Expression Promotes Cell Survival in Hypoxic Prostate Cancer Cells." *Oncogene* 26 (52). Nature Publishing Group: 7333–45. doi:10.1038/sj.onc.1210536.

Mazumdar, Jolly, W Timothy O'Brien, Randall S Johnson, Joseph C LaManna, Juan C Chavez, Peter S Klein, and M Celeste Simon. 2010. "O2 Regulates Stem Cells through Wnt/β-Catenin Signalling." *Nature Cell Biology* 12 (10). Nature Publishing Group, a division of Macmillan Publishers Limited. All Rights Reserved. 1007–13. doi:10.1038/ncb2102.

McCarthy, Davis J, Yunshun Chen, and Gordon K Smyth. 2012. "Differential Expression Analysis of Multifactor RNA-Seq Experiments with Respect to Biological Variation." *Nucleic Acids Research* 40 (10): 4288–97. doi:10.1093/nar/gks042.

McCormick, R I, C Blick, J Ragoussis, J Schoedel, D R Mole, A C Young, P J Selby, R E Banks, and A L Harris. 2013. "miR-210 Is a Target of Hypoxia-Inducible Factors 1 and 2 in Renal Cancer, Regulates ISCU and Correlates with Good Prognosis." *British Journal of Cancer* 108 (5): 1133–42. doi:10.1038/bjc.2013.56.

Meijer, Hedda A, Ewan M Smith, and Martin Bushell. 2014. "Regulation of miRNA Strand Selection: Follow the Leader?" *Biochemical Society Transactions* 42 (4): 1135–40. doi:10.1042/BST20140142.

Mense, S M, A Sengupta, M Zhou, C Lan, G Bentsman, D J Volsky, and L Zhang. 2006. "Gene Expression Profiling Reveals the Profound Upregulation of Hypoxia-Responsive Genes in Primary Human Astrocytes." *Physiological Genomics* 25 (3): 435–49. doi:10.1152/physiolgenomics.00315.2005.

Mesri, Enrique A, Ethel Cesarman, and Chris Boshoff. 2010. "Kaposi's Sarcoma and Its Associated Herpesvirus." *Nature Reviews. Cancer* 10 (10). Nature Publishing Group, a division of Macmillan Publishers Limited. All Rights Reserved. 707–19. doi:10.1038/nrc2888.

Moeller, Benjamin J, Yiting Cao, Chuan Y Li, and Mark W Dewhirst. 2004. "Radiation Activates HIF-1 to Regulate Vascular Radiosensitivity in Tumors: Role of Reoxygenation, Free Radicals, and Stress Granules." *Cancer Cell* 5 (5): 429–41. http://www.ncbi.nlm.nih.gov/pubmed/15144951.

Moore, Patrick S. 2007. "KSHV Manipulation of the Cell Cycle and Apoptosis". Cambridge University Press. http://www.ncbi.nlm.nih.gov/books/NBK47432/.

Nachmani, Daphna, Noam Stern-Ginossar, Ronit Sarid, and Ofer Mandelboim. 2009. "Diverse Herpesvirus microRNAs Target the Stress-Induced Immune Ligand MICB to Escape Recognition by Natural Killer Cells." *Cell Host & Microbe* 5 (4). Elsevier Ltd: 376–85. doi:10.1016/j.chom.2009.03.003.

Nakamura, S, S. Salahuddin, P Biberfeld, B Ensoli, P. Markham, F Wong-Staal, and R. Gallo. 1988. "Kaposi's Sarcoma Cells: Long-Term Culture with Growth Factor from Retrovirus-Infected CD4+ T Cells." *Science* 242 (4877): 426–30. doi:10.1126/science.3262925.

Nakano, Daisuke, Tetsuya Hayashi, Naoko Tazawa, Chika Yamashita, Sakiko Inamoto, Nobuaki Okuda, Tatsuhiko Mori, et al. 2005. "Chronic Hypoxia Accelerates the Progression of Atherosclerosis in Apolipoprotein E-Knockout Mice." *Hypertension Research : Official Journal of the Japanese Society of Hypertension* 28 (10): 837–45. doi:10.1291/hypres.28.837.

Nallamshetty, Shriram, Stephen Y Chan, and Joseph Loscalzo. 2013. "Hypoxia: A Master Regulator of microRNA Biogenesis and Activity." *Free Radical Biology & Medicine* 64 (September): 20–30. doi:10.1016/j.freeradbiomed.2013.05.022.

Natsuizaka, Mitsuteru, Seiji Naganuma, Shingo Kagawa, Shinya Ohashi, Azal Ahmadi, Harry Subramanian, Sanders Chang, et al. 2012. "Hypoxia Induces IGFBP3 in Esophageal Squamous Cancer Cells through HIF-1α-Mediated mRNA Transcription and Continuous Protein Synthesis." *FASEB Journal : Official Publication of the Federation of American Societies for Experimental Biology* 26 (6): 2620–30. doi:10.1096/fj.11-198598.

Neipel, F, J C Albrecht, and B Fleckenstein. 1998. "Human Herpesvirus 8--the First Human Rhadinovirus." *Journal of the National Cancer Institute. Monographs*, no. 23 (January): 73–77. http://www.ncbi.nlm.nih.gov/pubmed/9709307.

Nishimura, K, K Ueda, S Sakakibara, K Ishikawa, J Chen, T Okuno, and K Yamanishi. 2001. "Functional Analysis of Kaposi's Sarcoma-Associated Herpesvirus RTA in an RTA-Depressed Cell Line." *Journal of Human Virology* 4 (6): 296–305. http://www.ncbi.nlm.nih.gov/pubmed/12082396.

O'Hara, Andrea J, Ling Wang, Bruce J Dezube, William J Harrington, Blossom Damania, and Dirk P Dittmer. 2009. "Tumor Suppressor microRNAs Are Underrepresented in Primary Effusion Lymphoma and Kaposi Sarcoma." *Blood* 113 (23): 5938–41. doi:10.1182/blood-2008-09-179168.

Olbryt, Magdalena, Anna Habryka, Sebastian Student, Michał Jarząb, Tomasz Tyszkiewicz, and Katarzyna Marta Lisowska. 2014. "Global Gene Expression Profiling in Three Tumor Cell Lines Subjected to Experimental Cycling and Chronic Hypoxia." *PloS One* 9 (8): e105104. doi:10.1371/journal.pone.0105104.

Osawa, Tsuyoshi, Rika Tsuchida, Masashi Muramatsu, Teppei Shimamura, Feng Wang, Jun-ichi Suehiro, Yasuharu Kanki, et al. 2013. "Inhibition of Histone Demethylase JMJD1A Improves Anti-Angiogenic Therapy and Reduces Tumor-Associated Macrophages." *Cancer Research* 73 (10): 3019–28. doi:10.1158/0008-5472.CAN-12-3231.

Park, Soo-Yeon, Yun-Jeong Kim, Allen C Gao, James L Mohler, Sergio A Onate, Alejandro A Hidalgo, Clement Ip, Eun-Mi Park, Sun Young Yoon, and Young-Mee Park. 2006. "Hypoxia Increases Androgen Receptor Activity in Prostate Cancer Cells." *Cancer Research* 66 (10): 5121–29. doi:10.1158/0008-5472.CAN-05-1341.

Parravicini, C, B Chandran, M Corbellino, E Berti, M Paulli, P S Moore, and Y Chang. 2000. "Differential Viral Protein Expression in Kaposi's Sarcoma-Associated Herpesvirus-Infected Diseases: Kaposi's Sarcoma, Primary Effusion Lymphoma, and Multicentric Castleman's Disease." *The American Journal of Pathology* 156 (3): 743–49. doi:10.1016/S0002-9440(10)64940-1.

Parravicini, C, M Corbellino, M Paulli, U Magrini, M Lazzarino, P S Moore, and Y Chang. 1997. "Expression of a Virus-Derived Cytokine, KSHV vIL-6, in HIV-Seronegative Castleman's Disease." *The American Journal of Pathology* 151 (6): 1517–22. http://www.pubmedcentral.nih.gov/articlerender.fcgi?artid=1858372&tool=pmcentrez&rendertype=abstract.

Pasquinelli, A E, B J Reinhart, F Slack, M Q Martindale, M I Kuroda, B Maller, D C Hayward, et al. 2000. "Conservation of the Sequence and Temporal Expression of Let-7 Heterochronic Regulatory RNA." *Nature* 408 (6808). Macmillian Magazines Ltd. 86–89. doi:10.1038/35040556.

Pfeffer, Sébastien, Alain Sewer, Mariana Lagos-quintana, Robert Sheridan, Chris Sander, Friedrich A Grässer, Linda F Van Dyk, et al. 2005. "Identification of microRNAs of the Herpesvirus Family." *Nature Methods* 2 (4): 269–76. doi:10.1038/NMETH746.

Pfeffer, Sébastien, Mihaela Zavolan, Friedrich a Grässer, Minchen Chien, James J Russo, Jingyue Ju, Bino John, et al. 2004. "Identification of Virus-Encoded microRNAs." *Science (New York, N.Y.)* 304 (5671): 734–36. doi:10.1126/science.1096781.

Pison, C M, C Chauvin, E Fontaine, F Catelloni, C Keriel, B Paramelle, and X M Leverve. 1995. "Mechanism of Gluconeogenesis Inhibition in Rat Hepatocytes Isolated after in Vivo Hypoxia." *The American Journal of Physiology* 268 (5 Pt 1): E965–73. http://www.ncbi.nlm.nih.gov/pubmed/7762652.

Pocock, Roger. 2011. "Invited Review: Decoding the microRNA Response to Hypoxia." *Pflügers Archiv : European Journal of Physiology* 461 (3): 307–15. doi:10.1007/s00424-010-0910-5.

Pulkkinen, Kati, Tarja Malm, Mikko Turunen, Jari Koistinaho, and Seppo Ylä-Herttuala. 2008. "Hypoxia Induces microRNA miR-210 in Vitro and in Vivo Ephrin-A3 and

Neuronal Pentraxin 1 Are Potentially Regulated by miR-210." *FEBS Letters* 582 (16): 2397–2401. doi:10.1016/j.febslet.2008.05.048.

Punjabi, Almira S, Patrick A Carroll, Lei Chen, and Michael Lagunoff. 2007. "Persistent Activation of STAT3 by Latent Kaposi's Sarcoma-Associated Herpesvirus Infection of Endothelial Cells." *Journal of Virology* 81 (5): 2449–58. doi:10.1128/JVI.01769-06.

Purushothaman, Pravinkumar, Timsy Uppal, and Subhash C Verma. 2015. "Molecular Biology of KSHV Lytic Reactivation." *Viruses* 7 (1): 116–53. doi:10.3390/v7010116.

Qin, Zhiqiang, Eduardo Freitas, Roger Sullivan, Sarumathi Mohan, Rocky Bacelieri, Drake Branch, Margaret Romano, et al. 2010. "Upregulation of xCT by KSHV-Encoded microRNAs Facilitates KSHV Dissemination and Persistence in an Environment of Oxidative Stress." *PLoS Pathogens* 6 (1): e1000742. doi:10.1371/journal.ppat.1000742.

Qin, Zhiqiang, Andrew Jakymiw, Victoria Findlay, and Chris Parsons. 2012. "KSHV-Encoded MicroRNAs: Lessons for Viral Cancer Pathogenesis and Emerging Concepts." *International Journal of Cell Biology* 2012 (January): 603961. doi:10.1155/2012/603961.

Qu, Yanhua, Hongwei Zhao, Naijian Han, Guangyu Zhou, Gang Song, Bin Gao, Shilin Tian, et al. 2013. "Ground Tit Genome Reveals Avian Adaptation to Living at High Altitudes in the Tibetan Plateau." *Nature Communications* 4 (January). Nature Publishing Group: 2071. doi:10.1038/ncomms3071.

Raghu, Hari, Neelam Sharma-Walia, Mohanan Valiya Veettil, Sathish Sadagopan, and Bala Chandran. 2009. "Kaposi's Sarcoma-Associated Herpesvirus Utilizes an Actin Polymerization-Dependent Macropinocytic Pathway to Enter Human Dermal Microvascular Endothelial and Human Umbilical Vein Endothelial Cells." *Journal of Virology* 83 (10): 4895–4911. doi:10.1128/JVI.02498-08.

Rainbow, L, G M Platt, G R Simpson, R Sarid, S J Gao, H Stoiber, C S Herrington, P S Moore, and T F Schulz. 1997. "The 222- to 234-Kilodalton Latent Nuclear Protein (LNA) of Kaposi's Sarcoma-Associated Herpesvirus (human Herpesvirus 8) Is Encoded by orf73 and Is a Component of the Latency-Associated Nuclear Antigen." *Journal of Virology* 71 (8): 5915–21. http://www.pubmedcentral.nih.gov/articlerender.fcgi?artid=191847&tool=pmcentrez&rendertype=abstract.

Rajashekhar, G, A Loganath, A C Roy, S S Chong, and Y C Wong. 2005. "Hypoxia up-Regulated Angiogenin and down-Regulated Vascular Cell Adhesion Molecule-1 Expression and Secretion in Human Placental Trophoblasts." *Journal of the Society for Gynecologic Investigation* 12 (5): 310–19. doi:10.1016/j.jsgi.2005.02.010.

Reinhart, B J, F J Slack, M Basson, A E Pasquinelli, J C Bettinger, A E Rougvie, H R Horvitz, and G Ruvkun. 2000. "The 21-Nucleotide Let-7 RNA Regulates

Developmental Timing in Caenorhabditis Elegans." *Nature* 403 (6772): 901–6. doi:10.1038/35002607.

Renne, R, W Zhong, B Herndier, M McGrath, N Abbey, D Kedes, and D Ganem. 1996. "Lytic Growth of Kaposi's Sarcoma-Associated Herpesvirus (human Herpesvirus 8) in Culture." *Nature Medicine* 2 (3): 342–46. http://www.ncbi.nlm.nih.gov/pubmed/8612236.

Renne, Rolf, Weidong Zhong, Brian Herndier, Michael Mcgrath, Nancy Abbey, Dean Kedes, and Don Ganem. 1996. "Lytic Growth of Kaposi's Sarcoma–associated Herpesvirus (human Herpesvirus 8) in Culture." *Nature Medicine* 2 (3): 342–46. doi:10.1038/nm0396-342.

Robin, E D, B J Murphy, and J Theodore. 1984. "Coordinate Regulation of Glycolysis by Hypoxia in Mammalian Cells." *Journal of Cellular Physiology* 118 (3): 287–90. doi:10.1002/jcp.1041180311.

Rossetto, Cyprian C, and Gregory Pari. 2012. "KSHV PAN RNA Associates with Demethylases UTX and JMJD3 to Activate Lytic Replication through a Physical Interaction with the Virus Genome." *PLoS Pathogens* 8 (5): e1002680. doi:10.1371/journal.ppat.1002680.

Roth, W K, S Werner, W Risau, K Remberger, and P H Hofschneider. 1988. "Cultured, AIDS-Related Kaposi's Sarcoma Cells Express Endothelial Cell Markers and Are Weakly Malignant in Vitro." *International Journal of Cancer. Journal International Du Cancer* 42 (5): 767–73. http://www.ncbi.nlm.nih.gov/pubmed/3141299.

Roy, N. 1997. "The c-IAP-1 and c-IAP-2 Proteins Are Direct Inhibitors of Specific Caspases." *The EMBO Journal* 16 (23): 6914–25. doi:10.1093/emboj/16.23.6914.

Rumble, Stephen M, Phil Lacroute, Adrian V Dalca, Marc Fiume, Arend Sidow, and Michael Brudno. 2009. "SHRiMP: Accurate Mapping of Short Color-Space Reads." *PLoS Computational Biology* 5 (5): e1000386. doi:10.1371/journal.pcbi.1000386.

Rupaimoole, Rajesha, Sherry Y Wu, Sunila Pradeep, Cristina Ivan, Chad V Pecot, Kshipra M Gharpure, Archana S Nagaraja, et al. 2014. "Hypoxia-Mediated Downregulation of miRNA Biogenesis Promotes Tumour Progression." *Nature Communications* 5 (January). Nature Publishing Group: 5202. doi:10.1038/ncomms6202.

Samols, Mark A, Jianhong Hu, Rebecca L Skalsky, and Rolf Renne. 2005. "Cloning and Identification of a microRNA Cluster within the Latency-Associated Region of Kaposi's Sarcoma-Associated Herpesvirus." *Journal of Virology* 79 (14): 9301–5. doi:10.1128/JVI.79.14.9301-9305.2005.

Samols, Mark a, Rebecca L Skalsky, Ann M Maldonado, Alberto Riva, M Cecilia Lopez, Henry V Baker, and Rolf Renne. 2007. "Identification of Cellular Genes Targeted by KSHV-Encoded microRNAs." *PLoS Pathogens* 3 (5): e65. doi:10.1371/journal.ppat.0030065.

Schioppa, Tiziana, Badarch Uranchimeg, Alessandra Saccani, Subhra K Biswas, Andrea Doni, Annamaria Rapisarda, Sergio Bernasconi, et al. 2003. "Regulation of the Chemokine Receptor CXCR4 by Hypoxia." *The Journal of Experimental Medicine* 198 (9): 1391–1402. doi:10.1084/jem.20030267.

Schulz, T F. 1999. "Epidemiology of Kaposi's Sarcoma-Associated Herpesvirus/human Herpesvirus 8." *Advances in Cancer Research* 76 (January): 121–60. http://www.ncbi.nlm.nih.gov/pubmed/10218100.

Semenza, G L. 2010. "Defining the Role of Hypoxia-Inducible Factor 1 in Cancer Biology and Therapeutics." *Oncogene* 29 (5): 625–34. doi:10.1038/onc.2009.441.

Semenza, G L, P H Roth, H M Fang, and G L Wang. 1994. "Transcriptional Regulation of Genes Encoding Glycolytic Enzymes by Hypoxia-Inducible Factor 1." *The Journal of Biological Chemistry* 269 (38): 23757–63. http://www.ncbi.nlm.nih.gov/pubmed/8089148.

Semenza, Gregg L. 2003. "Targeting HIF-1 for Cancer Therapy." *Nature Reviews. Cancer* 3 (10): 721–32. doi:10.1038/nrc1187.

Semenza, Gregg L. 2004. "Intratumoral Hypoxia, Radiation Resistance, and HIF-1." *Cancer Cell* 5 (5): 405–6. http://www.ncbi.nlm.nih.gov/pubmed/15144945.

Semenza, Gregg L. 2007. "Hypoxia-Inducible Factor 1 (HIF-1) Pathway." *Science's STKE : Signal Transduction Knowledge Environment* 2007 (407): cm8. doi:10.1126/stke.4072007cm8.

Semenza, Gregg L. 2012. "Hypoxia-Inducible Factors: Mediators of Cancer Progression and Targets for Cancer Therapy." *Trends in Pharmacological Sciences* 33 (4): 207–14. doi:10.1016/j.tips.2012.01.005.

Shaffer, Arthur L, N C Tolga Emre, Laurence Lamy, Vu N Ngo, George Wright, Wenming Xiao, John Powell, et al. 2008. "IRF4 Addiction in Multiple Myeloma." *Nature* 454 (7201): 226–31. doi:10.1038/nature07064.

Shaffer, Arthur L, N C Tolga Emre, Paul B Romesser, and Louis M Staudt. 2009. "IRF4: Immunity. Malignancy! Therapy?" *Clinical Cancer Research : An Official Journal of the American Association for Cancer Research* 15 (9): 2954–61. doi:10.1158/1078-0432.CCR-08-1845.

Shalinsky, D R, D B McNamara, and K C Agrawal. 1989. "Modulation of Prostaglandin Biosynthesis in Hypoxic Murine Mammary Adenocarcinoma Cells by Misonidazole." *Cancer Research* 49 (14): 3853–56. http://www.ncbi.nlm.nih.gov/pubmed/2736527.

Shannon, Aoife M, David J Bouchier-Hayes, Claire M Condron, and Deirdre Toomey. 2003. "Tumour Hypoxia, Chemotherapeutic Resistance and Hypoxia-Related Therapies." *Cancer Treatment Reviews* 29 (4): 297–307. doi:10.1016/S0305-7372(03)00003-3.

Shin, Young C, Chul-Hyun Joo, Michaela U Gack, Hye-Ra Lee, and Jae U Jung. 2008. "Kaposi's Sarcoma-Associated Herpesvirus Viral IFN Regulatory Factor 3 Stabilizes Hypoxia-Inducible Factor-1 Alpha to Induce Vascular Endothelial Growth Factor Expression." *Cancer Research* 68 (6): 1751–59. doi:10.1158/0008-5472.CAN-07-2766.

Shinohara, Hirohiko, Masaya Fukushi, Masaya Higuchi, Masayasu Oie, Osamu Hoshi, Tatsuo Ushiki, Jun-Ichi Hayashi, and Masahiro Fujii. 2002. "Chromosome Binding Site of Latency-Associated Nuclear Antigen of Kaposi's Sarcoma-Associated Herpesvirus Is Essential for Persistent Episome Maintenance and Is Functionally Replaced by Histone H1." *Journal of Virology* 76 (24): 12917–24. http://www.pubmedcentral.nih.gov/articlerender.fcgi?artid=136661&tool=pmcentrez&rendertype=abstract.

Shu, Weiguo, Yue Qin Jiang, Min Min Lu, and Edward E Morrisey. 2002. "Wnt7b Regulates Mesenchymal Proliferation and Vascular Development in the Lung." *Development (Cambridge, England)* 129 (20): 4831–42. http://www.ncbi.nlm.nih.gov/pubmed/12361974.

Simmons, Steven O. 2009. "Hypoxia Response: A Model Toxicity Pathway for High-Throughput Screening." *Toxicological Sciences : An Official Journal of the Society of Toxicology* 112 (1): 1–3. doi:10.1093/toxsci/kfp193.

Simone, Nicole L, Benjamin P Soule, David Ly, Anthony D Saleh, Jason E Savage, William Degraff, John Cook, Curtis C Harris, David Gius, and James B Mitchell. 2009. "Ionizing Radiation-Induced Oxidative Stress Alters miRNA Expression." *PloS One* 4 (7): e6377. doi:10.1371/journal.pone.0006377.

Sodhi, Akrit, Silvia Montaner, Vyomesh Patel, Muriel Zohar, Carlos Bais, Enrique A. Mesri, and J. Silvio Gutkind. 2000. "The Kaposi's Sarcoma-Associated Herpes Virus G Protein-Coupled Receptor Up-Regulates Vascular Endothelial Growth Factor Expression and Secretion through Mitogen-Activated Protein Kinase and p38 Pathways Acting on Hypoxia-Inducible Factor 1{{alpha}}." *Cancer Res.* 60 (17): 4873–80. http://cancerres.aacrjournals.org/content/60/17/4873.abstract?ijkey=433e767293df862c3e7a4ace9085d1b85110ce11&keytype2=tf_ipsecsha.

Song, G, H Jia, H Xu, W Liu, H Zhu, S Li, J Shi, Z Li, J He, and Z Chen. 2014. "Studying the Association of microRNA-210 Level with Chronic Hepatitis B Progression." *Journal of Viral Hepatitis* 21 (4). Wiley Subscription Services, Inc., A Wiley Company: 272–80. doi:10.1111/jvh.12138.

Song, Moon Jung, Hongyu Deng, and Ren Sun. 2003. "Comparative Study of Regulation of RTA-Responsive Genes in Kaposi's Sarcoma-Associated Herpesvirus/human Herpesvirus 8." *Journal of Virology* 77 (17): 9451–62. http://www.pubmedcentral.nih.gov/articlerender.fcgi?artid=187374&tool=pmcentrez&rendertype=abstract.

Song, Tao, Xu Zhang, Lei Zhang, Jun Dong, Wei Cai, Jiangping Gao, and Baofa Hong. 2013. "miR-708 Promotes the Development of Bladder Carcinoma via Direct

Repression of Caspase-2." *Journal of Cancer Research and Clinical Oncology* 139 (7): 1189–98. doi:10.1007/s00432-013-1392-6.

Sowter, H M, P J Ratcliffe, P Watson, A H Greenberg, and A L Harris. 2001. "HIF-1-Dependent Regulation of Hypoxic Induction of the Cell Death Factors BNIP3 and NIX in Human Tumors." *Cancer Research* 61 (18): 6669–73. http://www.ncbi.nlm.nih.gov/pubmed/11559532.

Spear, Patricia G, and Richard Longnecker. 2003. "Herpesvirus Entry: An Update." *Journal of Virology* 77 (19): 10179–85. http://www.pubmedcentral.nih.gov/articlerender.fcgi?artid=228481&tool=pmcentrez&rendertype=abstract.

Staskus, Katherine A., Ren Sun, George Miller, Paul Racz, Anthony Jaslowski, Craig Metroka, Helena Brett-Smith, and Ashley T. Haase. 1999. "Cellular Tropism and Viral Interleukin-6 Expression Distinguish Human Herpesvirus 8 Involvement in Kaposi's Sarcoma, Primary Effusion Lymphoma, and Multicentric Castleman's Disease." *J. Virol.* 73 (5): 4181–87. http://jvi.asm.org/content/73/5/4181?ijkey=1c919e0a923497288db008a434720f685c962a07&keytype2=tf_ipsecsha.

Sternbach, G, and J Varon. 1995. "Moritz Kaposi: Idiopathic Pigmented Sarcoma of the Skin." *The Journal of Emergency Medicine* 13 (5): 671–74. http://www.ncbi.nlm.nih.gov/pubmed/8530789.

Stommel, Jayne M, and Geoffrey M Wahl. 2005. "A New Twist in the Feedback Loop: Stress-Activated MDM2 Destabilization Is Required for p53 Activation." *Cell Cycle (Georgetown, Tex.)* 4 (3): 411–17. http://www.ncbi.nlm.nih.gov/pubmed/15684615.

Stürzl, Michael, Dominika Gaus, Wilhelm G Dirks, Don Ganem, and Ramona Jochmann. 2013. "Kaposi's Sarcoma-Derived Cell Line SLK Is Not of Endothelial Origin, but Is a Contaminant from a Known Renal Carcinoma Cell Line." *International Journal of Cancer. Journal International Du Cancer* 132 (8): 1954–58. doi:10.1002/ijc.27849.

Subramanian, Aravind, Pablo Tamayo, Vamsi K Mootha, Sayan Mukherjee, Benjamin L Ebert, Michael A Gillette, Amanda Paulovich, et al. 2005. "Gene Set Enrichment Analysis: A Knowledge-Based Approach for Interpreting Genome-Wide Expression Profiles." *Proceedings of the National Academy of Sciences of the United States of America* 102 (43): 15545–50. doi:10.1073/pnas.0506580102.

Sun, R, S F Lin, L Gradoville, and G Miller. 1996. "Polyadenylylated Nuclear RNA Encoded by Kaposi Sarcoma-Associated Herpesvirus." *Proceedings of the National Academy of Sciences of the United States of America* 93 (21): 11883–88. http://www.pubmedcentral.nih.gov/articlerender.fcgi?artid=38153&tool=pmcentrez&rendertype=abstract.

Suzuma, K, H Takagi, A Otani, and Y Honda. 1998. "Hypoxia and Vascular Endothelial Growth Factor Stimulate Angiogenic Integrin Expression in Bovine Retinal

Microvascular Endothelial Cells." *Investigative Ophthalmology & Visual Science* 39 (6): 1028–35. http://www.ncbi.nlm.nih.gov/pubmed/9579483.

Syed, Deeba N, Mohammad Imran Khan, Maria Shabbir, and Hasan Mukhtar. 2013. "MicroRNAs in Skin Response to UV Radiation." *Current Drug Targets* 14 (10): 1128–34. http://www.pubmedcentral.nih.gov/articlerender.fcgi?artid=3985496&tool=pmcentrez&rendertype=abstract.

Taganov, Konstantin D, Mark P Boldin, Kuang-Jung Chang, and David Baltimore. 2006. "NF-kappaB-Dependent Induction of microRNA miR-146, an Inhibitor Targeted to Signaling Proteins of Innate Immune Responses." *Proceedings of the National Academy of Sciences of the United States of America* 103 (33): 12481–86. doi:10.1073/pnas.0605298103.

Thayanithy, Venugopal, ChangWon Park, Aaron L Sarver, Reena V Kartha, Derek M Korpela, Ashley J Graef, Clifford J Steer, Jaime F Modiano, and Subbaya Subramanian. 2012. "Combinatorial Treatment of DNA and Chromatin-Modifying Drugs Cause Cell Death in Human and Canine Osteosarcoma Cell Lines." *PloS One* 7 (9): e43720. doi:10.1371/journal.pone.0043720.

Thayanithy, Venugopal, Aaron L Sarver, Reena V Kartha, Lihua Li, Andrea Y Angstadt, Matthew Breen, Clifford J Steer, Jaime F Modiano, and Subbaya Subramanian. 2012. "Perturbation of 14q32 miRNAs-cMYC Gene Network in Osteosarcoma." *Bone* 50 (1): 171–81. doi:10.1016/j.bone.2011.10.012.

Thiery, Jean Paul, Hervé Acloque, Ruby Y J Huang, and M Angela Nieto. 2009. "Epithelial-Mesenchymal Transitions in Development and Disease." *Cell* 139 (5): 871–90. doi:10.1016/j.cell.2009.11.007.

Thompson, Matthew P, and Razelle Kurzrock. 2004. "Epstein-Barr Virus and Cancer." *Clinical Cancer Research : An Official Journal of the American Association for Cancer Research* 10 (3): 803–21. http://www.ncbi.nlm.nih.gov/pubmed/14871955.

Thulasingam, Sivasubramani, Chandirasegaran Massilamany, Arunakumar Gangaplara, Hongjiu Dai, Shahlo Yarbaeva, Sakthivel Subramaniam, Jean-Jack Riethoven, James Eudy, Marjorie Lou, and Jay Reddy. 2011. "miR-27b*, an Oxidative Stress-Responsive microRNA Modulates Nuclear Factor-kB Pathway in RAW 264.7 Cells." *Molecular and Cellular Biochemistry* 352 (1-2): 181–88. doi:10.1007/s11010-011-0752-2.

Tong, Wing-Hang, and Tracey A Rouault. 2006. "Functions of Mitochondrial ISCU and Cytosolic ISCU in Mammalian Iron-Sulfur Cluster Biogenesis and Iron Homeostasis." *Cell Metabolism* 3 (3): 199–210. doi:10.1016/j.cmet.2006.02.003.

Trapnell, Cole, Lior Pachter, and Steven L Salzberg. 2009. "TopHat: Discovering Splice Junctions with RNA-Seq." *Bioinformatics (Oxford, England)* 25 (9): 1105–11. doi:10.1093/bioinformatics/btp120.

Trapnell, Cole, Brian A Williams, Geo Pertea, Ali Mortazavi, Gordon Kwan, Marijke J van Baren, Steven L Salzberg, Barbara J Wold, and Lior Pachter. 2010. "Transcript Assembly and Quantification by RNA-Seq Reveals Unannotated Transcripts and Isoform Switching during Cell Differentiation." *Nature Biotechnology* 28 (5): 511–15. doi:10.1038/nbt.1621.

Ubbink, D T, I I Tulevski, D den Hartog, M J Koelemay, D A Legemate, and M J Jacobs. 1997. "The Value of Non-Invasive Techniques for the Assessment of Critical Limb Ischaemia." *European Journal of Vascular and Endovascular Surgery : The Official Journal of the European Society for Vascular Surgery* 13 (3): 296–300. http://www.ncbi.nlm.nih.gov/pubmed/9129603.

Ueda, Keiji, Eriko Ohsaki, Kazushi Nakano, and Xin Zheng. 2011. "Characterization of Kaposi's Sarcoma-Associated Herpesvirus-Related Lymphomas by DNA Microarray Analysis." *Leukemia Research and Treatment* 2011 (January): 726964. doi:10.4061/2011/726964.

Uldrick, Thomas S, Victoria Wang, Deirdre O'Mahony, Karen Aleman, Kathleen M Wyvill, Vickie Marshall, Seth M Steinberg, et al. 2010. "An Interleukin-6-Related Systemic Inflammatory Syndrome in Patients Co-Infected with Kaposi Sarcoma-Associated Herpesvirus and HIV but without Multicentric Castleman Disease." *Clinical Infectious Diseases : An Official Publication of the Infectious Diseases Society of America* 51 (3): 350–58. doi:10.1086/654798.

Uldrick, Thomas S, Kathleen M Wyvill, Pallavi Kumar, Deirdre O'Mahony, Wendy Bernstein, Karen Aleman, Mark N Polizzotto, et al. 2012. "Phase II Study of Bevacizumab in Patients with HIV-Associated Kaposi's Sarcoma Receiving Antiretroviral Therapy." *Journal of Clinical Oncology : Official Journal of the American Society of Clinical Oncology* 30 (13): 1476–83. doi:10.1200/JCO.2011.39.6853.

Umbach, Jennifer L., and Bryan R. Cullen. 2009. "In-Depth Analysis of Kaposi's Sarcoma-Associated Herpesvirus MicroRNA Expression Provides Insights into the Mammalian MicroRNA-Processing Machinery." *Journal of Virology* 84 (2): 695–703. doi:10.1128/JVI.02013-09.

Van der Flier, Arjan, Kwabena Badu-Nkansah, Charles A Whittaker, Denise Crowley, Roderick T Bronson, Adam Lacy-Hulbert, and Richard O Hynes. 2010. "Endothelial alpha5 and Alphav Integrins Cooperate in Remodeling of the Vasculature during Development." *Development (Cambridge, England)* 137 (14): 2439–49. doi:10.1242/dev.049551.

Veeranna, Ravindra P, Muzammel Haque, David A Davis, Min Yang, and Robert Yarchoan. 2012. "Kaposi's Sarcoma-Associated Herpesvirus Latency-Associated Nuclear Antigen Induction by Hypoxia and Hypoxia-Inducible Factors." *Journal of Virology* 86 (2): 1097–1108. doi:10.1128/JVI.05167-11.

Verde, Pasquale, Laura Casalino, Francesco Talotta, Moshe Yaniv, and Jonathan B. Weitzman. 2014. "Deciphering AP-1 Function in Tumorigenesis: Fra-Ternizing on

Target Promoters." *Cell Cycle* 6 (21). Taylor & Francis: 2633–39. doi:10.4161/cc.6.21.4850.

Vieira, J, P O'Hearn, L Kimball, B Chandran, and L Corey. 2001. "Activation of Kaposi's Sarcoma-Associated Herpesvirus (human Herpesvirus 8) Lytic Replication by Human Cytomegalovirus." *Journal of Virology* 75 (3): 1378–86. doi:10.1128/JVI.75.3.1378-1386.2001.

Vieira, Jeffrey, and Patricia M O'Hearn. 2004. "Use of the Red Fluorescent Protein as a Marker of Kaposi's Sarcoma-Associated Herpesvirus Lytic Gene Expression." *Virology* 325 (2): 225–40. doi:10.1016/j.virol.2004.03.049.

Viollet, Coralie, David A. Davis, Martin Reczko, Joseph M. Ziegelbauer, Francesco Pezzella, Jiannis Ragoussis, and Robert Yarchoan. 2015. "Next-Generation Sequencing Analysis Reveals Differential Expression Profiles of MiRNA-mRNA Target Pairs in KSHV-Infected Cells." *Plos One* 10 (5): e0126439. doi:10.1371/journal.pone.0126439.

Wang, L. 2004. "The Kaposi's Sarcoma-Associated Herpesvirus (KSHV/HHV-8) K1 Protein Induces Expression of Angiogenic and Invasion Factors." *Cancer Research* 64 (8): 2774–81. doi:10.1158/0008-5472.CAN-03-3653.

Wang, Victoria, David A Davis, Muzammel Haque, L Eric Huang, and Robert Yarchoan. 2005. "Differential Gene Up-Regulation by Hypoxia-Inducible Factor-1 A and Hypoxia-Inducible Factor-2 A in HEK293T Cells", no. 12: 3299–3307.

Warburg, O. 1956. "On Respiratory Impairment in Cancer Cells." *Science (New York, N.Y.)* 124 (3215): 269–70. http://www.ncbi.nlm.nih.gov/pubmed/13351639.

Weeks, B S, M E Klotman, S Dhawan, M Kibbey, J Rappaport, H K Kleinman, K M Yamada, and P E Klotman. 1991. "HIV-1 Infection of Human T Lymphocytes Results in Enhanced Alpha 5 Beta 1 Integrin Expression." *The Journal of Cell Biology* 114 (4): 847–53. http://www.pubmedcentral.nih.gov/articlerender.fcgi?artid=2289886&tool=pmcentrez&rendertype=abstract.

Werth, Nadine, Christiane Beerlage, Christian Rosenberger, Amir S Yazdi, Markus Edelmann, Amro Amr, Wanja Bernhardt, et al. 2010. "Activation of Hypoxia Inducible Factor 1 Is a General Phenomenon in Infections with Human Pathogens." *PloS One* 5 (7): e11576. doi:10.1371/journal.pone.0011576.

Wierzbicka-Patynowski, Iwona, and Jean E Schwarzbauer. 2003. "The Ins and Outs of Fibronectin Matrix Assembly." *Journal of Cell Science* 116 (Pt 16): 3269–76. doi:10.1242/jcs.00670.

Wilkinson, John, Alethea Cope, Jas Gill, Dimitra Bourboulia, Peter Hayes, Nesrina Imami, Toru Kubo, et al. 2002. "Identification of Kaposi's Sarcoma-Associated Herpesvirus (KSHV)-Specific Cytotoxic T-Lymphocyte Epitopes and Evaluation of Reconstitution of KSHV-Specific Responses in Human Immunodeficiency Virus

Type 1-Infected Patients Receiving Highly Active Antiretr." *Journal of Virology* 76 (6): 2634–40. http://www.pubmedcentral.nih.gov/articlerender.fcgi?artid=135964&tool=pmcentrez&rendertype=abstract.

Wojtowicz, Woj M, Michael Farzan, John L Joyal, Kara Carter, Gregory J Babcock, David I Israel, Joseph Sodroski, and Tajib Mirzabekov. 2002. "Stimulation of Enveloped Virus Infection by Beta-Amyloid Fibrils." *The Journal of Biological Chemistry* 277 (38): 35019–24. doi:10.1074/jbc.M203518200.

Wu, Connie, Jessica So, Brandi N Davis-Dusenbery, Hank H Qi, Donald B Bloch, Yang Shi, Giorgio Lagna, and Akiko Hata. 2011. "Hypoxia Potentiates microRNA-Mediated Gene Silencing through Posttranslational Modification of Argonaute2." *Molecular and Cellular Biology* 31 (23): 4760–74. doi:10.1128/MCB.05776-11.

Wu, Xiu-Juan, Xiong-Ming Pu, Zong-Feng Zhao, Ya-Nan Zhao, Xiao-Jing Kang, Wei-Dong Wu, Yun-Min Zou, et al. 2014. "The Expression Profiles of microRNAs in Kaposi's Sarcoma." *Tumour Biology : The Journal of the International Society for Oncodevelopmental Biology and Medicine*, October. doi:10.1007/s13277-014-2626-1.

Wu, Yu-Hsuan, Tzu-Fang Hu, Yu-Chieh Chen, Ya-Ni Tsai, Yuan-Hau Tsai, Cheng-Chung Cheng, and Hsei-Wei Wang. 2011. "The Manipulation of miRNA-Gene Regulatory Networks by KSHV Induces Endothelial Cell Motility." *Blood* 118 (10): 2896–2905. doi:10.1182/blood-2011-01-330589.

Xiang, Michael, Nicolai J Birkbak, Vida Vafaizadeh, Sarah R Walker, Jennifer E Yeh, Suhu Liu, Yasmin Kroll, et al. 2014. "STAT3 Induction of miR-146b Forms a Feedback Loop to Inhibit the NF-κB to IL-6 Signaling Axis and STAT3-Driven Cancer Phenotypes." *Science Signaling* 7 (310): ra11. doi:10.1126/scisignal.2004497.

Xu, Shunjiang, Rui Zhang, Jingya Niu, Dongsheng Cui, Bing Xie, Binggui Zhang, Kang Lu, Wenjun Yu, Xueyi Wang, and Qingfu Zhang. 2012. "Oxidative Stress Mediated-Alterations of the microRNA Expression Profile in Mouse Hippocampal Neurons." *International Journal of Molecular Sciences* 13 (12): 16945–60. doi:10.3390/ijms131216945.

Yang, Wei, Ting Sun, Jianping Cao, Fenju Liu, Ye Tian, and Wei Zhu. 2012. "Downregulation of miR-210 Expression Inhibits Proliferation, Induces Apoptosis and Enhances Radiosensitivity in Hypoxic Human Hepatoma Cells in Vitro." *Experimental Cell Research* 318 (8): 944–54. doi:10.1016/j.yexcr.2012.02.010.

Ye, Fengchun, Xiufen Lei, and Shou-Jiang Gao. 2011. "Mechanisms of Kaposi's Sarcoma-Associated Herpesvirus Latency and Reactivation." *Advances in Virology* 2011 (January). doi:10.1155/2011/193860.

Yotnda, Patricia, Danli Wu, and Anna May Swanson. 2010. "Hypoxic Tumors and Their Effect on Immune Cells and Cancer Therapy." *Methods in Molecular Biology*,

Methods in Molecular Biology, 651 (January). Totowa, NJ: Humana Press: 1–29. doi:10.1007/978-1-60761-786-0.

Zhang, Guang-ling, Yi-xuan Li, Shu-qi Zheng, Min Liu, Xin Li, and Hua Tang. 2010. "Suppression of Hepatitis B Virus Replication by microRNA-199a-3p and microRNA-210." *Antiviral Research* 88 (2): 169–75. doi:10.1016/j.antiviral.2010.08.008.

Zhang, Jufeng, Xia Luo, Huiming Li, Ling Deng, and Ying Wang. 2014. "Genome-Wide Uncovering of STAT3-Mediated miRNA Expression Profiles in Colorectal Cancer Cell Lines." *BioMed Research International* 2014 (January): 187105. doi:10.1155/2014/187105.

Zhang, Ping, Kam-Meng Tchou-Wong, and Max Costa. 2007. "Egr-1 Mediates Hypoxia-Inducible Transcription of the NDRG1 Gene through an Overlapping Egr-1/Sp1 Binding Site in the Promoter." *Cancer Research* 67 (19): 9125–33. doi:10.1158/0008-5472.CAN-07-1525.

Zhang, Qi, Xueli Bai, Wei Chen, Tao Ma, Qida Hu, Chao Liang, Shangzhi Xie, et al. 2013. "Wnt/β-Catenin Signaling Enhances Hypoxia-Induced Epithelial-Mesenchymal Transition in Hepatocellular Carcinoma via Crosstalk with Hif-1α Signaling." *Carcinogenesis* 34 (5): 962–73. doi:10.1093/carcin/bgt027.

Zhang, Quan, Chia-Yen Chen, Venkat S R K Yedavalli, and Kuan-Teh Jeang. 2013. "NEAT1 Long Noncoding RNA and Paraspeckle Bodies Modulate HIV-1 Posttranscriptional Expression." *mBio* 4 (1): e00596–12. doi:10.1128/mBio.00596-12.

Zheng, B, L Liang, S Huang, R Zha, L Liu, D Jia, Q Tian, et al. 2012. "MicroRNA-409 Suppresses Tumour Cell Invasion and Metastasis by Directly Targeting Radixin in Gastric Cancers." *Oncogene* 31 (42). Macmillan Publishers Limited: 4509–16. doi:10.1038/onc.2011.581.

Zheng, Zhi-Ming, and Xiaohong Wang. 2015. "Regulation of Cellular miRNA Expression by Human Papillomaviruses." *Biochimica et Biophysica Acta* 1809 (11-12): 668–77. Accessed April 13. doi:10.1016/j.bbagrm.2011.05.005.

Zhu, Yuan Xiao, K Martin Kortuem, and A Keith Stewart. 2013. "Molecular Mechanism of Action of Immune-Modulatory Drugs Thalidomide, Lenalidomide and Pomalidomide in Multiple Myeloma." *Leukemia & Lymphoma* 54 (4): 683–87. doi:10.3109/10428194.2012.728597.

Ziegelbauer, Joseph M, Christopher S Sullivan, and Don Ganem. 2009. "Tandem Array-Based Expression Screens Identify Host mRNA Targets of Virus-Encoded microRNAs." *Nature Genetics* 41 (1): 130–34. doi:10.1038/ng.266.